NEUROMAGNETIC INVESTIGATIONS OF FUNCTIONAL ORGANISATION WITHIN HUMAN VISUAL CORTEX

FIONA CATHERINE FYLAN

Doctor of Philosophy

THE UNIVERSITY OF ASTON IN BIRMINGHAM

September 1995

The University of Aston in Birmingham

Neuromagnetic Investigations of Functional Organisation Within Human Visual Cortex

Fiona Catherine Fylan

Doctor of Philosophy
1995

This thesis describes a series of experimental investigations into the functional organisation of human visual cortex using neuromagnetometry. This technique combines good spatial and temporal resolution enabling identification of the location and temporal response characteristics of cortical neurones within alert humans. To activate different neuronal populations and cortical areas a range of stimuli were used, the parameters of which were selected to match the known physiological properties of primate cortical neurones. In one series of experiments the evoked magnetic response was recorded to isoluminant red/green gratings. Co-registration of signal and magnetic resonance image data indicated a contribution to the response from visual areas V1, V2 and V4. To investigate the spatio-temporal characteristics of neurones within area V1 the evoked response was recorded for a range of stimulus spatial and temporal frequencies. The response to isoluminant red/green gratings was dominated by a major component which was found to have bandpass spatial frequency tuning with a peak at 1-2 cycles/degree, falling to the level of the noise at 6-8 cycles/degree. The temporal frequency tuning characteristics of the response showed bimodal sensitivity with peaks at 0-1Hz and 4Hz. In a further series of experiments the luminance evoked response was recorded to red/black, yellow/black and achromatic gratings and in all cases was found to be more complex than the isoluminant chromatic response, comprising up to three distinct components. The major response peak showed bandpass spatial frequency tuning characteristics, peaking at 6-8 cycles/degree, falling to the level of the noise at 12-16 cycles/degree. The results provide evidence to suggest that within area V1 the same neuronal population encodes both chromatic and luminance information and has spatial frequency tuning properties consistent with single-opponent cells. Furthermore, the results indicate that cells within area V1 encode chromatic motion information over a wide range of temporal frequencies with temporal response characteristics suggestive of the existence of a sub-population of cells sensitive to high temporal frequencies.

Key Words: *neuromagnetometry, chromatic visual evoked response, spatio-temporal, V1, V4.*

ACKNOWLEDGEMENTS

Within the Aston clinical neurophysiology unit there is tremendous team of people whose help and support have made this thesis possible. Sincere thanks goes to all my subjects who sat for many hours and heard patiently "just one more run" on innumerable occasions. I am indebted to Krish Singh who wrote the SMEG analysis software which is used extensively throughout this thesis, Ian Holliday who helped with the stimulus software and Gareth Barnes who wrote the data aquisition program. Many thanks to Steve Anderson, Ian and Krish for reading through seemingly endless draft chapters and papers. I would like to acknowledge the Dr Hadwen Trust for Humane Research who provided the original funding for my post. Finally, I would like to thank my supervisor, Graham Harding, whose support and enthusiasm initiated and maintained the MEG program at Aston.

INDEX

List of Figures and Tables

CHAPTER 1

INTRODUCTION

This thesis describes a series of experimental investigations into the functional organisation of the human visual system. Initial clues to the functional organisation of the human brain were provided by observations that damage to localised cortical areas resulted in specific deficits. For example, Broca identified an area in the left frontal lobe whose damage resulted in aphasia. This concept of functional segregation was extended to incorporate the observation that cortex comprising primary sensory areas were further divided into functional subunits. In the sensory and motor areas this takes the form of the homunculus. In visual cortex, details of cortical retinopy was gained by Holmes (1918) from examining World War I patients with cerebral gunshot wounds. Following observations of patients with selective achromtopsia (Verrey, 1988, Damasio et al., 1980) and akinetopsia (Zihl et al., 1983), it became apparent that what had been termed visual association areas were also functionally segregated. Tremendous advances have since been made in understanding the organisational principles of the visual system. Information has been gained from a wide range of sources, including studies of single cell electrophysiology in monkey, direct stimulation of alert human cortex during surgery, examination of callosal connections within human cortex at post-mortem and from human psychophysical measurements. Recently, the introduction of magnetic resonance imaging (MRI) has provided the scientific community with detailed knowledge of the anatomy of the alert human cortex. The next requirement is to link this anatomical knowledge with the physiological response properties of neurones within discrete cortical regions. This is known as functional imaging.

There are currently four main functional imaging techniques; magnetometry (MEG), electroencephalography (EEG), positron emission tomography (PET) and functional MRI (fMRI). MEG records the magnetic field generated by cortical neurones and as such provides a direct measure of activity within those neurones. Detailed investigation of the response properties of cell populations can be obtained within the same subject. Cortical localisation is achieved by applying an inverse solution to the data in order to identify the region of cortex generating the response. This information is then co-registered with MRI data. The temporal resolution of MEG is a few milliseconds and the spatial resolution is limited by the number and size of the

magnetometer coils, the accuracy of the model used in the inverse solution and the accuracy with which MEG and MRI information can be co-registered, typically 5mm.

Similarly, EEG detects the electrical field generated by cortical neurones and as such provides a direct measure of their activity. The temporal resolution of EEG is also a few milliseconds but due to differences in the electrical and magnetic field dependence on conductivity, the spatial resolution of EEG is generally not as good as that of MEG.

In contrast, both PET and fMRI reflect changes in neural activity by detecting changes in cerebral metabolism. PET involves the introduction of a radioactive tracer into the body, and by detecting local increases in the concentration of the tracer, changes in regional cerebral blood flow (rCBF) are determined and thus areas of increased cortical activity are deduced. The half-life of the tracer is short, hence the duration in which measurements can be made is restricted. Furthermore, the procedure is not without risk so that the number of scans that can be undertaken on an individual is very low. Similarly, fMRI detects the blood oxygenation-level-dependent (BOLD) within an active neural population. While no radioactive substance is administered, due to the cost of the equipment, MRI research facilities are often shared with clinical facilities, resulting in restricted measurement time.

Both these techniques are based on a subtraction paradigm in which the active areas are identified by subtracting baseline levels from those measured during a stimulus presentation. The changes take place over several seconds and even minutes so that the temporal resolution of these techniques is poor. Furthermore, the changes measured must be used to infer changes in cerebral metabolism so that PET and fMRI provide only indirect evidence of neuronal activity. The signal to noise ratio obtained for both techniques is often so low as to require averaging across subjects. Due to often marked differences in individual cortical anatomy, this approach is inherently inaccurate.

Hence these considerations result in MEG being the optimal technique for locating and characterising the spatial and temporal properties of neurones within functionally discrete regions of human visual cortex.

This thesis is divided into two parts. Section A examines the foundation of magnetometry, the visual system and visual evoked responses. The principles of MEG will be will further explored in Chapter 2. The mechanisms giving rise to the recorded signals will be investigated and MEG will be compared with the more traditional

technique of EEG. Finally, details of the Aston MEG facility used for the experiments described in this thesis will be given. The concept of functional imaging is based on the assumption that the human visual cortex is functionally segregated, i.e. within the cortex there are areas that are specialised for the analysis of particular attributes of the visual scene. Chapter 3 describes the anatomy and physiology of the visual pathway and examines the evidence for functional segregation within the pathway and within visual cortex. By combining what is known of the functional properties of the visual system and previous studies of the visual evoked response, described in Chapter 4, a set of stimuli will be devised in order to characterise the spatio-temporal frequency properties of units within discrete regions of the human visual cortex.

Section B of the thesis describes the experimental work performed. Chapter 5 will record the visual evoked magnetic response to isoluminant chromatic stimulation and thus isolate a discrete neuronal population. The cortical location of these cells will be determined by co-registering this information with MRI data. The spatial frequency tuning characteristics of these cells will be examined in Chapter 6 and compared with those measures obtained psychophysically and from single cell studies in macaque. Chapter 7 will establish the temporal frequency tuning properties of these cells and in this way examine the contribution of chromatic information to the perception of motion. The evoked response to luminance stimulation will be recorded in Chapter 8 and the spatial frequency tuning of luminance sensitive cells will be compared with that of chromatic sensitive cells. Finally, higher cortical processing of chromatic information will be investigated and the location and temporal sequence of cells within extrastriate areas V2 and V4 will be examined.

Hence this thesis will localise and characterise the spatio-temporal properties of cells within human visual cortex. The results will be compared with data obtained from single cell electrophysiology and from psychophysical measures and the uses of MEG will be discussed in relation to other investigative techniques.

CHAPTER 2

PRINCIPLES OF MAGNETOMETRY

2.1 Introduction

Magnetometry is a relatively new discipline, with the first measurements of biomagnetic activity made in the 1960's (Baule and McFee, 1963; Cohen, 1968). The QRS complex of the magnetocardiogram was recorded using an induction coil, thus confirming the possibility of recording the magnetic fields associated with bioelectric events. In contrast, measurements of the electric potential arising from bioelectric events have been established as a recording technique since the beginning of the twentieth century. In part, this time difference between the onset of electrical and magnetic recording techniques was due to the increased technical difficulties involved in magnetic recordings. The introduction of the superconducting quantum interference device, or SQUID, (Zimmerman et al., 1970) and the gradiometer (Opfer et al., 1974) provided an increase in sensitivity, facilitating recordings of the magnetocardiogram, or MCG (Cohen et al., 1970), spontaneous alpha activity (Cohen, 1972) and visual evoked response (Brenner et al., 1975). Further improvements have been made with the advent of electromagnetically shielded rooms, enabling recordings to be made in the urban environment without excessive noise intrusion.

Since the initial measurements, the field of biomagnetism has greatly expanded and has succeeded in measuring both spontaneous and evoked activity. Several important findings have been made, for example the non-invasive verification that human auditory cortex is organised tonotopically, with the neuronal generators being located progressively deeper with increasing frequency (Romani et al., 1982; Pantev et al., 1988). Magnetometry has proved to be of tremendous value in the investigation of the foetal MCG (FMCG). Less affected than ECG by sources some distance from the sensors, such as the maternal MCG, the FMCG can be clearly seen when recording from above the maternal abdomen (Dunajski and Peters, 1995). Furthermore, the FECG is often unrecordable during the 28th-32nd week gestational age due to the insulating vernix caseosa layer which forms at this stage in pregnancy whereas the FMCG can be monitored throughout pregnancy, providing an indication of foetal well-being from the 13th week of gestation (Dunajski and Peters, 1995).

Until the mid 1980's almost all magnetometry investigations were confined to single

channel systems. The advent of multichannel devices has provided a number of advantages including simultaneous measurement of a large region of interest and the corresponding decrease in the duration of the investigation. This has opened the way for magnetometry to move into the clinical setting and it is being used successfully in the localisation of epileptogenic regions (Modena et al., 1982; Stefan et al., 1990). One of the most recent developments in magnetometry is the co-registration of source localisation data and MRI information. This enables precise anatomical identification of regions generating the surface recorded activity. This has several applications. In the clinical setting, the identification of somatosensory and motor cortex prior to neurosurgery allows the surgeon to, as far as possible, avoid these regions during surgery (Gallen et al., 1995). The technique is also of considerable value in the research setting, enabling the localisation of cortical areas responding to specific stimuli.

Hence since its introduction, magnetometry has moved from a phenomenological state to one which offers important advantages in the investigation of the human brain, heart and lungs. This chapter will examine the neural basis of the external biomagnetic field and the instrumentation used to record biomagnetic signals. A comparison of MEG and EEG will be made in terms of recording techniques and inverse solutions, with the emphasis being on neuromagnetic applications. Finally, the Aston MEG facility used for this research will be described.

2.2 Neural basis of biomagnetic recordings

The basis of all bioelectric events is the nerve action potential and post-synaptic potential. Action potentials communicate sensory information along a neurone and post-synaptic potentials arise from communication with adjacent neurones via the synapse. This neural communication utilises electrical current flow formed by the exchange of sodium and potassium ions between active cells and their surroundings. In the resting state the neurone contains a high concentration of potassium ions and a low concentration of sodium ions which results in a resting potential of -70mV. When stimulated the permeability of the cell membrane to sodium ions is increased and the intracellular potential increases from its resting state of -70mV to +30mV. This depolarisation causes current flow away from the depolarised region in both directions and an outward current flow through the membrane into the extracellular space back to the origin of the depolarisation. This activity takes place over a duration of about 1ms.

The membrane permeability then changes again causing the outflow of potassium ions and repolarisation, with the return to the resting potential. The region then enters an inactive refractory period during which it cannot be depolarised. Meanwhile, the current flow causes the adjacent region of the neurone to depolarise so that the action potential self-propogates along the axon. As the preceding region of the axon is in the refractory period, the excitation travels in the forward direction. This is shown in Figure 2.1.

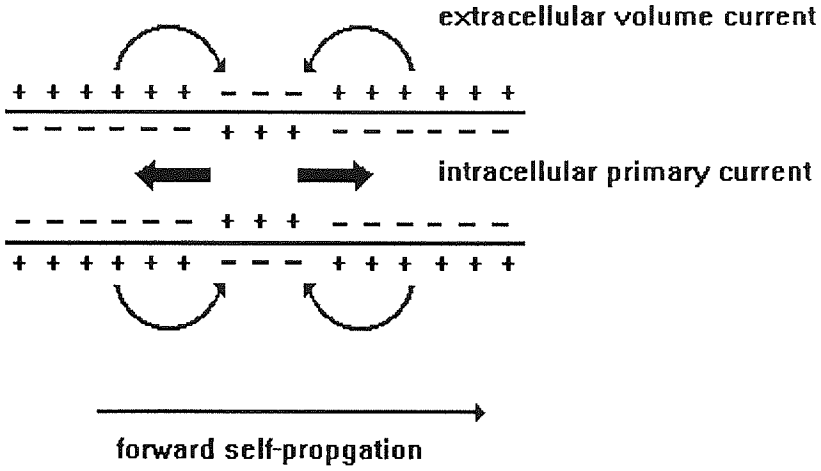

Figure 2.1 Current flow during an action potential.

The postsynaptic activity is similar but acts over a longer time scale. When an action potential reaches a synapse, neurotransmitters are released which diffuse across the synaptic cleft and produce a potential called a post-synaptic potential. The current distribution lasts for tens of milliseconds although the repolarisation process is not sufficiently synchronous across neurones to be macroscopically detectable (Pizzella and Romani, 1990). This is shown in Figure 2.2.

The current produced by neuronal events can be described as a current dipole **Q**. As described above, due to the differences in the depolarisation and repolarisation process, the action potential and postsynaptic potential give rise to different current patterns. That associated with an action potential is of two oppositely oriented dipoles separated by a few milliseconds while the post-synaptic potential can be considered as a single current dipole.

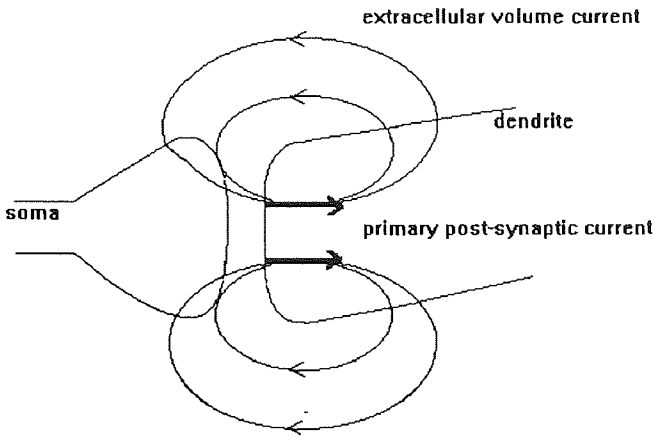

Figure 2.2 Current flow during a postsynaptic potential. Modified from Pizella and Romani (1990).

Post-synaptic excitation occurs in two cortical cell types; open and closed configuration. Closed cells, for example stellate cells, have short, spherically symmetric dendritic trees which result in cancellation of the electromagnetic field. However open cells, for example pyramidal cells, have a single elongated dendrite. The post-synaptic potential travels along the dendrite thus resulting in a long current dipole and thus a large dipole moment which is not cancelled by adjacent dendrites of the same cell. It is therefore the open cell type which is likely to generate the externally recorded electromagnetic field. Of the open cells the pyramidal cell is considered most likely to give rise to the surface-recorded electromagnetic field (Okada, 1983a). Pyramidal cells are large, extending through many of the cortical layers and they occur regularly throughout the cortex, aligned parallel to one another and perpendicular to the cortical surface (Okada, 1983a). It is therefore possible to consider excitation within a number of these cells as a dipole sheet with dipole moment perpendicular to the cortical surface.

The magnetic field generated in this way is approximately 0.002fT for a pyramidal cell (Pizella and Romani, 1990). Such a single event would not be measurable outside the vicinity of the cell, hence the magnetic field recorded during biomagnetic measurements does not reflect the activity of a single neurone. If the neurones are closely spaced and oriented in the same direction, as is the case for pyramidal cells (Hubel, 1988), the principle of superposition implies that simultaneous activation of these cells will produce a current that sums to provide a field of sufficient magnitude to be detected outside the head. The resultant magnetic field may then be considered

as a single current dipole. More than fifty thousand neurones must be simultaneously active to produce a magnetic field of approximately 100fT; a typical field strength evoked by a sensory stimulus (Pizella and Romani, 1990). Hence action potentials, which occur over a time period of only 1ms, are less likely to overlap temporally than postsynaptic potentials which have a duration of approximately 17ms (Vvedensky et al., 1985). Temporal summation effects therefore make it more likely that postsynaptic potentials underlie the external magnetic field (Kaufman and Williamson, 1980). Furthermore, the action potential, modelled as a pair of oppositely oriented dipoles or a quadrupole, falls off as the cube of the distance from the origin to the measuring point (Hämäläinen et al., 1993). The postsynaptic potential, however, is more accurately modelled as a current dipole, falling off as the square of the distance between source and point of measurement. Hence some distance from the neurones, the external field will be dominated by the postsynaptic potentials. Empirical support for this is provided by measurement of the direct cortical response (Barth, 1991).

The neuronal currents associated with postsynaptic events can be divided into intracellular currents and extracellular volume currents. As shown in Figure 2.2 the volume currents are passive and act to complete the loop of ionic transfer. When considering the sphere model of the head, only intracellular currents contribute towards the external magnetic field (Hari et al., 1980; Hari and Ilmoniemi, 1986). The extracellular volume currents cancel and do not generate a magnetic field outside the head (Swinney and Wikswo, 1980; Okada, 1983a).

2.3 Characteristics and models of the neuromagnetic field

Section 2.2 describes how neuronal activation leads to intracellular and extracellular currents to flow in banks of aligned cells. Intracellular currents, detectable outside the head are the primary current, while extracellular currents are passive volume currents. Associated with every current flow is a magnetic field and it can readily be shown that electric and magnetic fields are interdependent with an orientation between them of 90 degrees. Hence the current flow arising from neuronal activation will produce a magnetic field outside the head. Calculating the magnetic field produced by a particular current distribution is known as the forward problem.

The initial point in the calculation of this magnetic field is Maxwell's equations with the appropriate equation being:

$$\text{curl } \mathbf{B} = \mu \mathbf{J} \qquad \text{equation 2.1}$$

where $\mathbf{B}$ = magnetic field
μ = permeability
$\mathbf{J}$ = current density

The solution is given by the Biot Savart law

$$\mathbf{B}(\mathbf{r}) = \frac{\mu}{4\pi} \int \frac{\mathbf{J}(\mathbf{r}') \wedge \mathbf{R}}{R^3} d\tau \qquad \text{equation 2.2}$$

where $\mathbf{r}$ = point of measurement $\quad \mathbf{R} = \mathbf{r} - \mathbf{r}'$
$\mathbf{r}'$ = position of source $\quad \tau$ = volume

Now as seen is section 2.2, the current source density $\mathbf{J}$ is comprised of primary and volume currents, $\mathbf{J}p$ and $\mathbf{J}v$.

$$\mathbf{J}(\mathbf{r}') = \mathbf{J}p(\mathbf{r}') + \mathbf{J}v(\mathbf{r}') \qquad \text{equation 2.3}$$

and

$$\mathbf{J}v(\mathbf{r}') = -\sigma(\mathbf{r}')\nabla V \qquad \text{equation 2.4}$$

where σ = conductivity and V = scalar potential

Substituting equation 2.3 and 2.4 into 2.2

$$\mathbf{B}(\mathbf{r}) = \frac{\mu}{4\pi} \int \frac{\mathbf{J}p(\mathbf{r}') \wedge \mathbf{R}}{R^3} d\tau - \frac{\mu\sigma}{4\pi} \int \frac{\nabla V \wedge \mathbf{R}}{R^3} d\tau \qquad \text{equation 2.4}$$

Hence the the external magnetic field comprises two parts, the first is not affected by changes in conductivity and reflects the physiologically relevant primary currents $\mathbf{J}p$ only. The second part, however, retains σ and is therefore affected by changes in conductivity.

The task of magnetometry is to measure the magnetic field outside the head and to use this information to infer the cortical sources that produced that magnetic field distribution. This is known as the inverse problem. The inverse problem is intrinsically

ill-posed as its stability is threatened by noise and due to the principle of superposition its solution lacks uniqueness (Lorrain et al., 1988). This can result in several source geometries producing identical measurements, hence external constraints to the problem must be imposed. These include both models of the head and the source. Several models of the head have been used, the simplest of which is the homogeneous conducting sphere. The primary current can then be modelled by a current dipole **Q**.

There are several source models that can also be used to constrain the inverse solution. The most commonly used model is the current dipole as cortical pyramidal cells are well approximated by a current dipole (Okada, 1983a; Carelli and Pizella, 1992). The equivalent current dipole refers to what may be a number of simultaneously active neurones confined to a small region of cortical tissue whose net effect can be described as a single current dipole. (Kaufman and Williamson, 1986). Hence

$$\mathbf{B}(\mathbf{r}) = \frac{\mu}{4\pi} \mathbf{Q}(\mathbf{r}') \wedge \frac{\mathbf{R}}{R^3} - \frac{\mu\sigma}{4\pi} \int V(r)\mathbf{n}(r) \wedge \frac{\mathbf{R}}{R^3} dS \qquad \text{equation 2.5}$$

where $\mathbf{n}(r)$ is the normal to the surface and dS is the surface integral (Crowly and Budiman, 1989).

For a dipole in a homogeneous conducting sphere, this reduces to (Sarvas, 1987).

$$\mathbf{B}(\mathbf{r}) = \frac{\mu}{4\pi F^2} \left(F\, \mathbf{Q} \wedge \mathbf{r}' - \mathbf{Q} \wedge \mathbf{r}' \cdot \mathbf{r}\, \nabla F \right) \qquad \text{equation 2.6}$$

where $F = R\,(rR + r^2 - \mathbf{r}' \cdot \mathbf{r})$

However, the head is not truly a homogeneous conductor with the ventricles, skull and scalp all producing regions of inhomogeneity. A more realistic model of the head is the spherically symmetric head model. This model assumes the head to be radially anisotropic and considers a series of concentric spheres, each with differing conductivities, with the conductivity within each sphere constant. Here, $\nabla\sigma$ is non-zero only at the boundaries of different conductivity regions. Hence only at the boundaries do the volume currents contribute to the external magnetic field. However, in a spherically symmetric model, these volume currents do not contribute to the radial components of the external magnetic field. Thus the spherical model results in the radial components of the external magnetic field being sensitive only to primary currents. Therefore, while the homogeneous conducting sphere provides a

convenient, simple model for MEG (Grynszpan and Geslowitz, 1973; Cuffin and Cohen, 1977), changes in conductivity must be considered for EEG.

A consequence of the geometry of either of these models is that no external magnetic field arises from the radial components of dipoles within the sphere (Grynszpan and Geslowitz, 1973; Ducla-Soares, 1989). This is evident from equation 2.6; when the source is radial, $\mathbf{Q} \wedge \mathbf{r}'=0$. The non-uniqueness of the problem is therefore increased as the addition of any radial component to the solution would not produce a change in the external magnetic field. However, with approximately two thirds of primary sensory areas located within the fissures, thus tangential to the surface, this does not pose a major problem for MEG (Williamson et al., 1991).

The equivalent current dipole is characterised by three position parameters, one of orientation and one of strength. The maximum likelihood estimate of the equivalent current dipole parameters can be found by least squares fitting (Hämäläinen et al., 1993). In the moving dipole model, the source is assumed to be non-static so that its location, orientation and strength can vary in time. Fits are commonly performed at each millisecond time instant. An alternative to the equivalent current dipole model are multidipole models (Scherg, 1984). To find the multidipole solutions, dipole locations and orientations are fitted in an iterative procedure. The number of degrees of freedom can be reduced by fixing the locations or orientations of the dipoles, which may be achieved by analysis of the MRI. Temporal constraints may also be applied (Scherg and Berg, 1991). A further method of inverse solution is the minimum norm estimate which assumes the current to be distributed throughout the head. A set of linear equations are set up and the solution is the one with the smallest overall amplitude which can describe the observed signals. This method has been used in the analysis of visual evoked magnetic response data (Ahlfors et al., 1992) and it is a useful technique when the extent of activated cortex is unknown (Hämäläinen et al., 1993). A fourth approach is a continuous probabilistic one which assumes the probability distribution of current is gaussian and by finding the expectation value of the current density, the most probable solution consistent with the measured activity is found (Ioannides et al., 1989). A comprehensive review of several of the more commonly used inverse solutions is given by Hämäläinen et al. (1993).

2.4 Biomagnetic Instrumentation

The magnetic field outside the head evoked from a sensory stimulus is in the order of 10^{-13}T which is considerably smaller than the earth's magnetic field at $\approx 5 \times 10^{-5}$T or power lines of, for example, 10^{-7}T. Noise sources are prevalent, being found in electrical motors, power lines, moving cars, radio frequency fields, computers and other laboratory equipment, including the display monitor used during visual evoked response measurement. Further artefacts may arise from movement of the subject and any magnetic hooks or zips on their clothing. Hence an efficient method of sensing tiny magnetic fields arising from the brain without them being saturated by the relatively huge environmental noise must be employed. Although measurements of the magnetic field have been made using induction coils (Cohen, 1968) the small magnitude of the magnetic field arising from spontaneous and evoked neural activity result in only SQUID magnetometers having sufficient sensitivity to routinely measure the neuromagnetic field.

The magnetometer comprises a detection coil which senses changes in the external magnetic field and transforms them into currents. The input coil transforms the resulting current into magnetic flux to be applied to the SQUID sensor. SQUID electronics transform the applied flux into a room temperature output voltage. The SQUID thus acts as a highly sensitive amplifier and forms the basis of biomagnetic measurements.

The operating principle of the SQUID is based on the Josephson junction (Josephson, 1962) in which electrons can tunnel through resistive barriers, or weak links, between two superconducting regions. At superconducting temperatures, electrons become associated in pairs and can be described by the same wave function (Bardeen et al., 1957). In a closed ring superconductor, the ring circumference must be equal to an integral number of wavelengths and this wavelength varies with the amount of magnetic flux incident on the ring. Therefore the enclosed flux is quantised. If an external magnetic field is applied, a shielding current will flow to prevent a change in flux in the ring. If a weak link is introduced into the ring the shielding current will flow through this link, thus increasing the energy of the superconducting state. This increase in energy makes the shielding ineffective, allowing one flux quantum to enter. The link then reverts to the original current state and the process is repeated periodically as the applied magnetic field is increased. The current flow in the weak link can be monitored and this provides a measure of the applied magnetic field. Alternatively, a coil wrapped around the SQUID applies a feedback current which is inductively coupled back to the SQUID loop to null the applied signal flux. The feedback current is thus a direct measure of the flux applied to the SQUID and is

therefore proportional to the external magnetic field.

The SQUID thus consists of a superconducting ring separated by one (rf SQUID) or two (dc SQUID) Josephson junctions. Rf SQUIDs are biased by an rf alternating current and dc SQUIDs by a direct current. The simpler fabrication of the rf SQUID made it more popular at the beginning of the 1980s but it is less sensitive than the dc SQUID and with multichannel systems, there can be problems with interference between channels (Carelli and Pizella, 1992). A fuller description of both rf and dc SQUIDs and their operating principles is provided by Romani et al. (1982), Fagaly (1990) and Kaufman and Williamson (1980).

The operating temperature of the SQUIDs must be kept below Tc, the critical temperature at which there exists sufficient energy to destroy superconductivity. Tc for niobium, a common SQUID material, is 9.3K which results in the SQUID operating temperature being maintained below 9.3K. Hence the SQUID must be kept cool within a bath of liquid helium which has a temperature of 4.7K.

Although the SQUID can be used to sense magnetic fields directly, a more practical arrangement is provided by a superconducting detecting coil, coupled to the SQUID by means of an input coil. This configuration is known as a flux transporter and in its simplest form, coupled to the SQUID it is known as a magnetometer. It will respond to any magnetic field whose flux is incident upon the detecting coil, including that from the earth's field, power lines and electronic equipment. However, the geometry of the detection coil can be manipulated to make it insensitive to relatively uniform fields while retaining full sensitivity to fields produced by nearby sources. By having two coaxial detecting coils, wound in opposite directions and separated by a distance known as the baseline, a field produced by a distant source approximates a uniform field and induces almost the same current in the two coils and will therefore cancel. A nearby source, however, will produce a flux that is larger in the nearer coil, resulting in a net current. This design is known as a first order gradiometer. Two gradiometers can be combined to form a second order gradiometer which, in addition to rejecting spatially uniform fields, is also insensitive to fields with spatially uniform gradients. The different types of detection coils are shown in Figure 2.3.

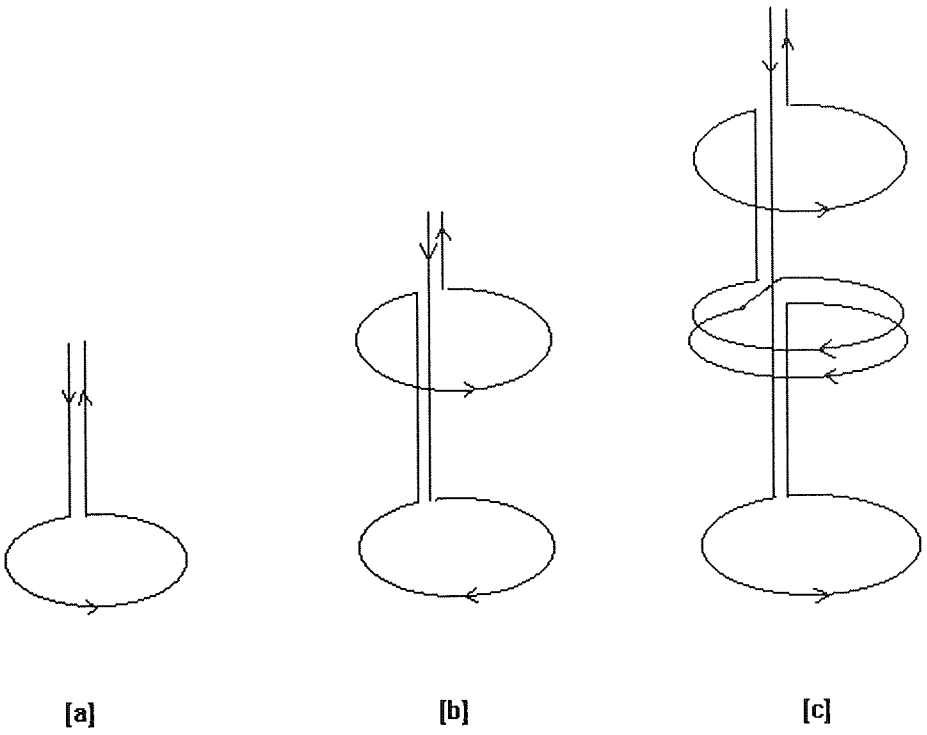

Figure 2.3: Various designs of detection coils: (a) magnetometer; (b) first order gradiometer; (c) second order gradiometer.

In addition to axial gradiometers, there is also a planar design which is sensitive to the field tangential to the surface. Planar gradiometers are more affected by noise than axial gradiometers, although they are more efficient at discriminating multiple sources (Erné and Romani, 1985). However, the field distribution measured by a planar gradiometer lacks symmetry (Romani and Pizella, 1990) so the position and orientation of the underlying cortical generator of the recorded activity is less intuitively determined.

Despite the noise reduction properties of gradiometers, there are frequently residual noise problems. To counter this it is possible to incorporate additional reference magnetometers into the system to measure the ambient noise in three orthogonal directions. The common mode disturbances of the gradiometers can then be removed to provide electronic noise cancellation (Matlashov et al., 1989).

2.5 Multichannel Systems

Until the mid 1980's, almost all magnetometry investigations were confined to single channel systems. The advent of multichannel devices provided a number of advantages. Simultaneous measurement of a large region of cerebral activity reduced the time of the investigation, making clinical recording more feasible. Measurement of spontaneous activity was facilitated and the topographic mapping and source localisation of spontaneous events such as spike activity was enabled. However, simultaneous measurements are meaningless unless the relative sensitivity of all the SQUIDs is known and compensated for. Hence multichannel devices must be accurately calibrated. Further problems arise from the possibility of crosstalk between the channels and additional shielding may therefore be required.

Large numbers of recording channels may also result in problems due to the physical dimensions of the larger dewar, resulting in a number of SQUIDs being positioned some distance away from the surface of the scalp. This can be reduced by the use of a curved dewar bottom but it is difficult to devise a curvature that will be suitable for all subjects to be tested. In addition, the curved bottom may limit the applications of the system to head recordings as the curved base renders the dewar unsuitable for cardiac or thoracic measurements.

2.6 Averaging and Filtering

Biomagnetic signals tend to be of low field strength and it is therefore necessary to find methods to extract them from background noise. For repeatable events, for example evoked responses, summing a number of events and averaging the result provides a simple and effective method of improving the signal-to-noise ratio (SNR). White noise which is not time-locked to the stimulus will thus be reduced, providing an improvement in the SNR of $\sqrt{N}$ where N is the number of averaged recording epochs. However, this assumes that neuronal events are perfectly reproducible and this is not always the case (Regan, 1989). Factors such as fatigue, attention and fixation affect the response and these will influence the effectiveness of averaging.

For spontaneous phenomena, averaging is not applicable and alternative methods of improving the signal to noise ratio must be found. Electronic noise cancellation, can

be applied and further noise reduction can be achieved by frequency filtering to remove signals which lie outside the frequency range of interest.

2.7 Shielded Rooms

One of the simplest and most effective methods of noise cancellation is to use an electromagnetically shielded room. The first dedicated shielded enclosure was made from three ferromagnetic layers and two aluminium layers (Cohen et al., 1970) This design utilises both eddy-current and ferromagnetic shielding and results in a shielding factor of 100dB above 10Hz. The design of shielded rooms has remained similar, providing both eddy-current shielding and ferromagnetic shielding. The eddy-current shielding effect is determined by the skin depth, λ, of the material, i.e. the distance travelled by an electromagnetic wave at which it is attenuated by a factor of 1/e. The skin depth is given by:

$$\lambda = \sqrt{(\rho/\pi\mu f)} \qquad \text{equation 2.7}$$

where ρ = resistivity μ = permeability f = frequency

Hence equation 2.7 shows that skin depth is proportional to the resistivity of the material and inversely proportional to the frequency of the magnetic field. Eddy-current shielding is often achieved by layers of aluminium; the low resisitivity of aluminium results in a low skin depth which provides high attenuation of electromagnetic waves. The shielding is most effective at high frequencies. At low frequencies the thickness of the shielding material would be have to be extremely large, exceeding 1m to provide sufficient eddy current shielding (Fagaly, 1990). Hence ferromagnetic shielding provided by layers of μ-metal is also used. This high permeability material channels the external magnetic flux around the exterior of the chamber (Fagaly, 1990). However, shielded rooms can themselves introduce noise problems as their interior can act a resonant cavity, a particular problem if external rf is carried into the interior by cables. Cables must therefore be shielded and if necessary, earthed (Hämäläinen et al., 1993).

2.8 Comparison of MEG and EEG

Both MEG and EEG arise from fluctuations in the resting membrane potential of the dendrites of cortical neurones (Okada, 1983a). In this respect the two techniques are

equivalent, yet there are a number of similarities and differences between them which are discussed below.

2.8.1 Temporal Resolution

Both MEG and EEG have a temporal resolution of less than a millisecond, with their exact resolution being determined by the analogue to digital converters and filters used in processing the recorded activity. Other functional imaging techniques such as PET and fMRI have temporal resolution of a few minutes and seconds respectively. EEG and MEG are therefore the only techniques available to study the pattern of activation between the different cortical areas.

2.8.2 Spatial Resolution

There have been several studies comparing the spatial resolution of MEG to that of EEG. MEG is sensitive to the intracellular current summed across many neurones while it is the extracellular volume currents which are conducted to the scalp that are measured in EEG. EEG is more sensitive to changes in conductivity than MEG and is therefore affected by conditions that alter the conductivity in regions of the brain, for example space occupying lesions. MEG will be less affected by these conditions and hence is intrinsically more accurate when localising cortical events. Nevertheless, flux reversal phenomena have been observed in MEG recordings from cases in which the conductivities of inhomogeneous regions have changed with pathological conditions (Ueno and Iramina, 1990). Hence for EEG localisations, it is necessary to use accurate models of the brain, skull and scalp. Simple models of uniform conductivity and spherical shell models have been proposed but modelling errors can nevertheless produce errors in dipole localisation of 10mm (Cohen et al, 1991). Localisation accuracy studies have also been performed with MEG and suggest an accuracy of 3mm in spheres and model skulls (Yamamoto et al., 1988).

A comparison of the localisation accuracy of MEG and EEG was made by Cohen et al. (1991) who compared the techniques using implanted depth electrodes in human subjects undergoing pre-surgical investigations for epilepsy. By passing currents through these depth electrodes it was possible to appraise the accuracy with which MEG and EEG could in practice locate the artificial current dipoles. Cohen reported that the error in locating the currents dipoles was 8mm for MEG and 10mm for EEG and thus concluded that MEG offered no significant localisation advantage over EEG. However, the methodology of the study has been criticised (Hämäläinen, 1993). Twice the number of epochs were recorded for EEG than for MEG and only a single channel magnetometer was employed in the study, which measured from sixteen

positions over the scalp as opposed to sixteen electrodes simultaneously recording the EEG. Of the twelve implanted dipoles, ten were radial, thus disadvantaging MEG which is relatively insensitive to radial field components. For the two tangential dipoles the MEG localisation error was 5.5mm. Hence for tangential current dipoles, the results indicate that MEG is more accurate than EEG. However, it should be considered that for cortical generators located on gyri, the accuracy of MEG localisation will drop.

The spatiotemporal resolution accuracies of MEG and EEG in relation to other recording techniques are shown in Figure 2.4. It can be seen that MEG has spatial resolution comparable or better than PET and fMRI but far exceeds them in temporal resolution. MEG is thus the only technique which offers sufficient spatial and temporal resolution for the investigation of the relationship between different cortical areas. PET and SPECT suffer from the further disadvantage that due to the isotopes involved, recordings cannot be made frequently.

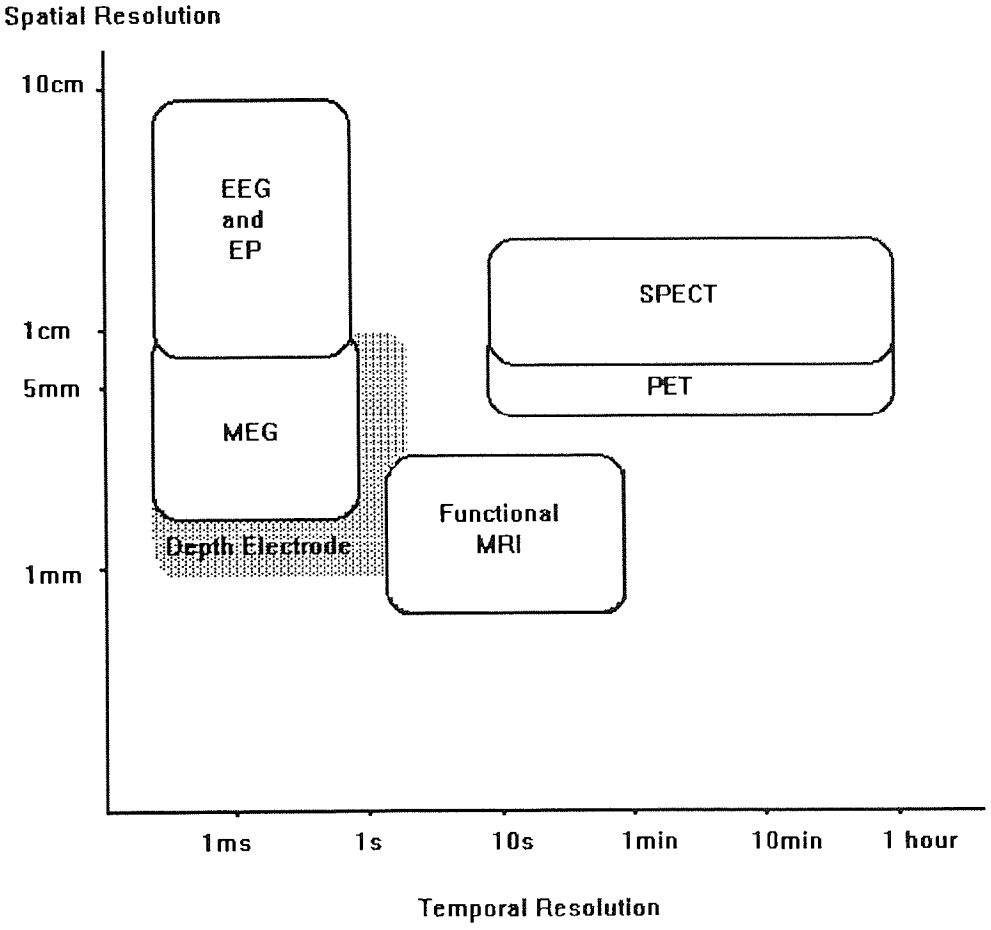

Figure 2.4 The spatiotemporal accuracy of imaging techniques. Redrawn from Harding (1993).

2.8.4 Radial and tangential current dipole components

EEG records the volume conducted currents from the scalp surface and is thus sensitive to all components of the underlying source generator. MEG, however, is sensitive only to the tangential components of the source (Grynszpan and Geslowitz, 1973). On first consideration this would seem to be a disadvantage for MEG but due to the convoluted nature of the human cerebral cortex, some 66% of primary sensory areas lie within fissures and as such are tangential to the surface of the scalp (Williamson et al., 1991). Hence MEG's insensitivity to radial source components may provide an advantage in the ability to discriminate tangential and radial source geometries when used in conjunction with EEG.

2.8.5 Reference

MEG provides a measure of the magnetic field arising from a cortical generator and as such measures the absolute value of a number of points in that field. EEG, however, measures the voltage at points on the scalp and must therefore measure that voltage with reference to another point. EEG cannot therefore provide an unbiased measure of the activity at a certain point on the scalp but is always affected by the choice of reference. This results in, for example, the VEP being contaminated with frontal negativity when an Fz reference is used (Hobley, 1988). One of the major problems faced by EEG, particularly by evoked potentials, has thus been to find an inactive reference. MEG does not suffer from this disadvantage and as such is preferable when recordings are to be used for topographic analysis and source localisation.

2.8.6 Contact

A difference perhaps most obvious to the subject is that EEG involves the application of electrodes to the surface of the scalp, commonly by glue or tape. During a MEG investigation, however, the subject is merely seated with the area of interest positioned under the base of the dewar. In addition to the rapidity of the investigation, considered in the next section, MEG readily permits repositioning of the recording sensors if the exact position of interest is uncertain. During an EEG investigation removing and reapplying the electrodes to record from a slightly different position would take a considerable amount of time. However, the contactlessness of MEG also poses a number of problems in that the subject should not move during the investigation and all the measurements required must be performed in the same recording session to ensure identical measuring positions are achieved for each experiment. Fortunately, these problems can be overcome by the use of a bite bar which fixes the subject's head in position during the recording and enables the same recording position to be returned to

in between breaks. This is the method used at Aston and is described in more detail in section 2.9.

2.8.7 Duration of Investigation

Due to the contactless nature of MEG, the recording session is significantly shorter than equivalent measurements made of EEG. The application of 20 electrodes takes in the region of 30 minutes and there are frequently problems in achieving sufficiently low electrode impedance. As mentioned in the previous section, if an adjustment in recording position is required this can be instantly achieved with MEG while moving all the electrodes takes a discouragingly long time. Hence the rapidity with which measurements can be achieved offers a significant advantage for MEG.

2.8.8 Low Frequency Cutoff

With the introduction of the dc SQUID, MEG is able to record frequencies down to dc. While EEG can come close to this level, it retains a low frequency cutoff and is limited by problems of maintaining a stable electrode potential. Hence MEG is more readily able to study phenomena such as spreading depression in migraine (Barkley et al., 1995).

2.8.9 Cost

The final difference between MEG and EEG is in the cost of equipment. Whereas an EEG laboratory would cost in the region of £30,000 for an EEG and evoked potential facility the equivalent MEG cost would be at least four times that amount. In addition, a shielded room may be necessary if the laboratory is to be in an urban environment. There is also the running cost of liquid helium to keep the SQUIDs superconducting, at approximately £200 per month. Hence although MEG has several advantages over EEG, the investment required for a MEG system places the technique out of the reach of many clinical and research centres.

2.9 The Aston MEG Facility

Developed over 1992-1995 the Aston MEG facility arose as a collaboration between Aston University and the Institute of Radio Engineering and Electronics in Moscow.

It comprises 19 independent dc SQUIDs of second order axial gradiometer design (Matlashov et al., 1989). The gradiometers, which are balanced to an accuracy of 0.1%, use niobium wire on a graphite former, connected to thin film niobium dc SQUIDs. The channels have a diameter of 15mm and baseline 50mm and are positioned in a hexagonal array of spacing 29mm and a total diameter of 140mm. Shielding is provided by a layer of mylar. In addition there is a vector magnetometer which monitors ambient noise in three orthogonal directions. The channels are housed in a fibreglass dewar as shown in Figure 2.5.

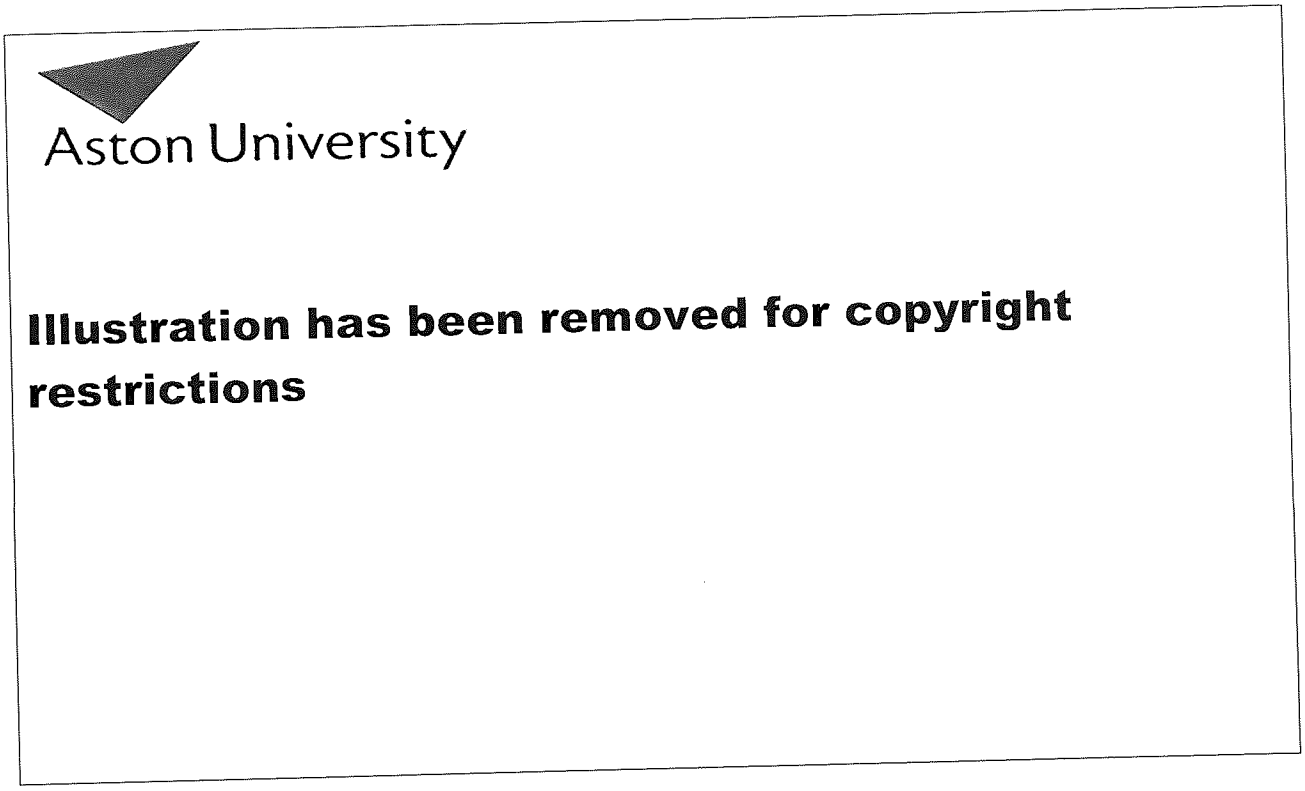

Figure 2.5 The Aston dewar design. From Matlashov et al. (1993)

The dewar is of flat bottomed design, enabling both neuromagnetic and cardiac measurements. The capacity is 12 litres and the evaporation rate is 2.2 litres/day which results in refilling with liquid helium every 3-4 days. This is achieved via a fill port incorporated into channel 18. The pre-amplified signals are filtered, typically at a bandwidth of 0-106Hz and then sampled with 16 bit accuracy. Further noise reduction is provided by a real time adaptive filtering algorithm which aims to remove all correlation between the gradiometer signals and those from the vector magnetometer (Barnes, 1995). The vector magnetometer is housed within channel 19.

The dewar is held in place in a wooden gantry which enables the dewar to be moved and rotated freely. Once in position beneath the dewar, the subject's position is maintained by means of a bite bar. This comprises the subject's dental impression mounted on a plastic frame which is held in place by a wooden platform. It also enables the subject to move around in between experimental recording runs and return to exactly the same position beneath the dewar at the start of each run.

All magnetic measurements take place in an electromagnetically shielded room which consists of two layers of aluminium and one of mu metal. To reduce magnetic noise, the stimulus display is housed outside the shielded room and is viewed by a system of front silvered mirrors. The subject looks down at the mirrors, thus exposing the occipital area to the base of the dewar.

Visual stimuli are generated using a Cambridge Research Systems VSG2/2 grating generator and are displayed on an Eizo Flexscan T560i colour monitor with 14 bit luminance resolution at a frame rate of 100Hz. The chromaticity co-ordinates of the display are r_x=0.625, r_y=0.340, g_x=0.280, g_y=0.595, b_x=0.155, b_y=0.070. Luminance is measured with a Minolta photometer and the gamma corrected display is linear over the display range used ($r>0.995$). The stimulus triggers the acquisition program to record an epoch. All epochs are saved individually, and averaging, filtering and noise rejection can be performed both on and off line. The system configuration is shown in Figure 2.6.

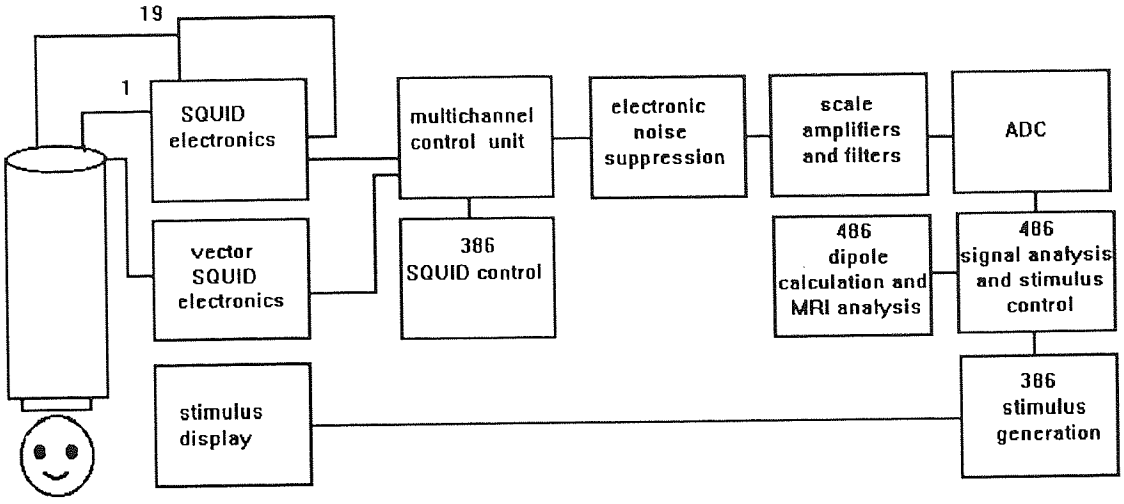

Figure 2.5 System configuration of the Aston MEG facility

2.10 Co-registration of MEG and MRI information

The ultimate aim of magnetometry is to localise an area of active cortex and to be able to superimpose this area with an image of the cortex, for example to localise the active area on an MRI. To do this it is necessary to use a common co-ordinate system for the MRI and MEG so that the two types of information can be combined. At Aston this is achieved by digitising the position of the subject's bite bar using a Polhemus 3D space tracker. During the MRI the subject wears the bite bar fitted with vitamin pill markers so that the activity recorded from the MEG can readily be superimposed on the MRI information. In this way the inaccuracies associated with converting the co-ordinates to the Tailerach system are avoided.

2.11 Methods of Analysis

The method of analysis used in this research is that of a single equivalent current dipole in a conducting sphere as this is both mathematically tractable and physiologically meaningful (Romani and Pizella, 1990). Although it is not suggested that a single source can account for all the activity over the entire recording epoch, single dipole analysis is effective when examining the source of activity at a particular time instant. The time of analysis is determined by maxima in the global field power which is defined as the sum-of-squares of the gradiometer output at each time instant. An iterative

procedure is employed with an initial approximation of the dipole's position, orientation and strength being made and the forward solution being calculated from that approximation. The dipole fitting procedure is a non-linear minimisation of the χ^2 value with respect to the dipole's position and orientation where

$$\chi^2(t) = \sum_{i=1}^{\text{detectors}} \left(\mathbf{B}_{\text{theoretical}}(t)_i - \mathbf{B}_{\text{measured}}(t)_i \right)^2 / \sigma_i^2$$

and σ_i^2 is the measured field standard deviation.

The correlation co-efficient for the minimised χ^2 dipole position is then calculated and dipoles with a correlation co-efficient of less than 0.95 are rejected as non-significant. The gammaQ value and the χ^2 statistic are also used to determine if the dipole fit is significant. GammaQ (Press et al., 1992) gives the probability that the calculated value of χ^2 was obtained by chance and therefore provides a quantitative measure for the goodness of fit of the recorded response to a single dipole model. An acceptable fit is that of gammaQ > 0.001 and a $\chi^2 \approx$ the number of degrees of freedom (Press et al., 1992) where (degrees of freedom) = (number of channels - 5). As the goodness of fits improves gammaQ $\rightarrow$ 1 and $\chi^2 \rightarrow 0$. These statistics must be interpreted with care, however, as if modelling is performed at a point at which the signal is weak it is likely that χ^2 will be low and hence gammaQ will be spuriously high. In this case the correlation co-efficient is unlikely to be greater than 0.95 so it is essential to assess the suitability of the dipole model using a combination of all three measures. This typically leaves one or more time intervals during the response for which the solution is both significant and stable. In addition, Monte-Carlo error analyses are then performed for the power peaks within the significant time intervals to assess the stability of the solutions with respect to noise (Medvick et al., 1990). This procedure randomly adds noise to the theoretical solution and establishes a spatial confidence limit for the dipole localisation. The 95% confidence region is then superimposed on the subjects' MRI to provide the cortical localisation for the neuronal generator of the recorded activity and an indication of the accuracy of that localisation. For stimuli near threshold (for example Chapters 6 and 7) the evoked response may not reach significance. Measures of latency and field strength are made at the appropriate peak of the global field power, determined by comparison with suprathreshold responses, but Monte-Carlo simulations are not performed.

2.12 Summary

The origin of the magnetic field recorded outside the head is the primary current arising from postsynaptic currents in cortical pyramidal cells. Unlike EEG, MEG is unaffected by volume currents and is independent of changes in conductivity within the head. This results in better spatial resolution. Further advantages include the lack of a reference point and the contactless nature and therefore rapidity of the investigation. The source model used is an equivalent current dipole in a conducting sphere and the position, orientation and strength of the dipole generator is calculated. Monte-Carlo analysis provides a confidence region for the source location and this can be coregistered with MRI data to provide three dimensional localisation of the volume of cortex activated.

CHAPTER 3

THE VISUAL SYSTEM

3.1 Introduction

The majority of what is known of the human visual system has been based upon studies of non-humans, for example cat and monkey. This approach can provide valuable insight into the functioning of the human visual system as the organisation, particularly in macaque, is thought to be similar to that in humans (DeValois et al., 1974). Nevertheless, it is often difficult to establish that the same underlying organisation exists in monkey and human and it is therefore important to consider that what is learnt of non-human visual organsiation may not strictly parallel the functioning of human systems. The lack of direct knowledge of human visual cortex is beginning to be countered by a number of relatively new investigative techniques such as fMRI and PET. In addition, metabolically active regions can be investigated by examining post-mortem tissues for an endogenous mitochondrial enzyme, cytochrome oxidase. Hence although this chapter out of necessity draws on primate literature, where available, corroborating human studies will be introduced.

3.2 The Retina

The retina forms the initial input area of the visual process. It serves to collect incoming light information and to transform it into a coded neural message that can be transmitted to the visual cortex. There are two types of receptors in the retina, rods and cones. The numbers of the two are not equal; in primates there are 6.5 million cones and 120 million rods (Kolb, 1991). The retina comprises ten layers of cell bodies and synaptic connections as shown in Figure 3.1 and the entire structure is approximately one quarter of a millimeter thick. There are four morphologically distinct regions within the primate retina (Polyak, 1941). The first of these, the optic disk, is situated in the inferior nasal field. It forms the point of exit of the optic nerve fibres and as such contains no nerve cells, receptors or pigment epithelium. The second of these regions is the macula which is a circular area containing a high density of ganglion cells. In humans it occupies 6mm in diameter and covers 15-20 degrees of visual field. The fovea forms the third region and is situated at the centre of the macula where the retina

Figure 3.1. The human retina From Kaplan et al. (1990)

is at its thinnest. Its diameter is 1.5mm and it covers 5 degrees of visual field. The final region, the peripheral retina, lies beyond the macula.

These different retinal regions possess different distributions of receptors. In humans, cones have maximal density in the fovea of approximately $162x10^3/mm^2$ which falls off with eccentricity (Curcio et al., 1987). Rods are absent from the fovea, becoming maximal at 5mm (18 degrees) from the centre of the fovea where their density rises to $160x10^3/mm^2$ before falling again in the periphery (Kolb, 1991). The ratio of rods to cones changes with eccentricity, being 1 rod: 2 cones at the macular periphery and changing to 1 cone: 3-4 rods in the periphery.

The normal human retina contains a single type of rod and three types of cones. Rods become saturated at luminances above 120-300 cd/m^2 (Aguilar and Stiles, 1954) and therefore do not contribute to visual perception at luminances above this value. The cones are distinguished on the basis of spectral absorbance and it is this difference in response as a function of wavelength that enables the perception of colour. L cones are sensitive to long wavelengths and absorb maximally at 558nm, which lies in the red portion of the spectrum. M cones are sensitive to medium wavelengths, absorbing maximally at 531nm, corresponding to green. The third type, S cones, respond optimally to short wavelengths of 420nm which lies within the blue (Gouras, 1984; Bowmaker et al., 1980). The L and M cones form a hexagonal array which is disrupted by the S cones which do not fit into this regular pattern (Kolb, 1991). The S cones are less frequent than the L and M cones, forming only 8% of the total cone population (Anhelt et al., 1987).

Although the cones are maximally hyperpolarised by a certain wavelength they respond only to the number of quanta absorbed and not to the energy (inversely proportional to wavelength) of the photons. Hence once absorbed, a long wavelength photon produces the same effect as a short wavelength photon; only the rate of absorbtion is signalled. This is called the principle of univariance (Naka and Rushton, 1966) and it results in a single cone being unable to distinguish the wavelength of the photon it absorbed. It is only by comparison of different cone activities that chromatic discrimination can occur.

There exist a number of different cell types within the retina, present in the different layers which are discussed below.

3.2.1 Bipolar cells

Bipolar cells are situated in the outer plexiform layer. There are nine different types of bipolar cells in the human retina, one subserving the rods and eight the cones (Kolb, 1991). The commonest human bipolar cells are the diffuse and midget types which are subdivided into flat or invaginating on the basis of their contact with the cone pedicle. The diffuse flat and diffuse invaginating bipolar cells contact 5-7 central retina cones or 12-14 peripheral cones. In contrast, the flat midget and invaginating midget bipolar cells each contact a single cone. Thus foveal cones provide input to two types of midget bipolar cells and two types of diffuse bipolar cells (Kolb, 1991). Three further types of cone bipolars, the wide field or giant bipolars, are less commonly observed (Kolb, 1991). They connect with as many as 15-20 different cones (Mariani, 1984b)

and little is known about them. The final cone bipolar cell is thought to be specific for the S cones (Mariani, 1984a). The type of bipolar synapse determines whether the bipolar connects to an on-centre or off-centre ganglion cell (Nelson and Kolb, 1983).

3.2.2 Horizontal cells

Situated in the outer nuclear layer, horizontal cells have complicated synapses in the outer plexiform layer (Kolb, 1970; 1979). There are three types of horizontal cells in the human retina HI, HII and HIII (Linberg et al., 1987). HI contact L and M cones with a small number of S connections, HII cells contact mainly S cones and HIII contact only L and M cones (Kolb et al., 1989). This cone related division has led to suggestions that horizontal cells are related to retinal chromatic function (Kolb, 1991).

3.2.3 Amacrine cells

There are at least 25 different types of amacrine cells and these synapse in the inner plexiform layer. They are classified in terms of morphology and dendritic tree size and they synapse with bipolar cells and ganglion cells. Their functions include the linking of rod and cone pathways to allow rod signals to utilise the cone bipolar to ganglion pathways (Kolb, 1991).

3.2.4 Ganglion cells

Primate retinal ganglion cells form at least 20 different categories on the basis of morphological characteristics (Kolb, 1991), although there are three common types when distinguished by size, pathway and functional characteristics. The first, characterised by its large size, has been called parasol (Polyak. 1941), A (Levanthal et al., 1981), P alpha (Perry et al., 1984) and M (Kaplan and Shapley, 1986). These cells form 10% of the population (Perry et al., 1984), are large with thick axons and extensive dendritic fields. The second cell type, called midget, B, P beta or P cells, are small with fine axons and small dendritic fields. They comprise 80% of the cell population and as such are the most common in the primate retina. The third category of cells, forming the remaining 10% of the population, is thought to project to the superior colliculus and the pretectum and these cells are not M or P types and have been termed P gamma (Perry and Cowey, 1984).

In addition to morphological differences, M and P ganglion cells differ both in their connections to other retinal cells and in their later projection sites. M cells receive input from diffuse bipolar cells with each bipolar contacting up to 7 cones. Additional input may arise from giant bipolars which contact up to 20 cones, and the rod bipolars which contact 15-45 rods. P cells, however, receive input from 1 or 2 midget bipolars,

each of which contacts only 1 cone. M cells typically project to the two ventral magnocellular layers of the lateral geniculate nucleus (LGN) while P cells project to the 4 dorsal layers (Leventhal et al., 1981). Indeed, the M and P terminology for retinal ganglion cells (Kaplan and Shapley, 1986) relates to their projection targets rather than their morphology but this appears to correlate well with morphological classification.

M and P cells are both present throughout the retina apart from in the fovea, where the high cone density causes them to be displaced laterally. Ganglion cell density peaks at approximately 0.5mm from the fovea and declines in an exponential manner towards the periphery. This distribution is anisotropic, the cell density in the nasal retina being approximately 3 times that of the temporal retina and the cell density decrease being smaller along the nasal retina (Perry and Cowey, 1985). There may be a difference in the ratio of M and P cells with retinal location with it suggested that while the number of P cells decreases with eccentricity, M cell numbers may remain approximately constant. There have been a large number of estimates made of this P:M ratio, for example from 9:1 near the fovea to 7:3 in the periphery (De Monasterio, 1978), and from 40:1 near the fovea to 4:1 in the periphery (Connolly and Van Essen, 1984). This change was also found in the human retina, at 30:1 near the fovea and 3:1 in the periphery (Dacey and Peterson, 1992). However, not all studies have supported this change in ratio with eccentricity. Macaque data (Perry et al., 1984; Perry and Cowey, 1984) shows the proportion of P to M cells remaining approximately constant at 8:1 throughout the retina. By examining cortical projections, Livingstone and Hubel (1988b) found that while small changes in the P:M ratio with eccentricity could not be excluded, there was no evidence of large differences between fovea and periphery in the relative mapping densities of M and P cells.

3.2.5 Summary of rod and cone retinal connections

Several rods provide input to a single rod bipolar. The output of rod bipolars is not direct to ganglion cells but occurs via various amacrine cells. Cone circuitry has several differences, the first of which is that there are a number of different types of bipolar cells receiving input from the cones. The cone bipolars then synapse directly with ganglion cells providing a more direct pathway than for rods. Fewer cones converge on bipolar cells and only a relatively small number of bipolars converge on the ganglion cells. This is most marked in the foveal midget pathway in which each foveal cone connects to one on centre and one off centre bipolar cell which in turn connects with one on centre and one off centre ganglion cell (Kolb and DeKorver,

cones although they may retain their one to one relationship with the midget ganglion cells (Kolb, 1991).

3.3 Functional Characteristics of Retinal Ganglion Cells

As a consequence of the differing bipolar inputs to the M and P ganglion cells, a difference in receptive field size is immediately apparent. M cells, whose bipolars receive approximately 7 cone inputs, have large receptive fields while foveal P cell bipolars receive input from a single cone resulting in small recepive fields. However, this 1:1 cone to ganglion cell relationship may decrease in the periphery, resulting in larger receptive fields (Shapley and Perry, 1986; Kolb and DeKorver, 1988). The smaller receptive fields of the P ganglion cells suggest that the P midget system underlies the detection of high spatial frequencies and as such mediates the accuity of the visual system.

The larger receptive fields of magnocellular ganglion cells result in a higher contrast sensitivity than that of parvocellular ganglion cells. This was demonstrated in rhesus monkey by Kaplan and Shapley (1986) who showed that the M cell sensitivity to luminance contrast was 8-10 times that of P cells. Their result is shown in Figure 3.2 and this also demonstrates that although the contrast gain of M cells is higher, it saturates at 10-15% contrast, while that of P cells increases linearly.

Figure 3.2. Contrast sensitivity of M and P ganglion cells in rhesus monkey. From Kaplan et al. (1990)

Both M and P ganglion cells have two regions within their receptive fields, the centre and surround. One region is excitatory, causing depolarisation, called "on". The other is inhibitory, causing hyperpolarisation, called "off". Like bipolar cells, ganglion cells can be on- or off-centre, where "on" results in the cell centre being excited by light increments and inhibited by light decrements and "off" results in the cell centre being inhibited by light increments and excited by light decrements. Either the centre or the surround can be on but centre and surround are always of opposite polarity. However, it is not only light increments which are capable of carrying information but also light decrements (DeValois and DeValois, 1990). For example, an on-centre ganglion would depolarise to a light increment in the centre and also to a light decrement in the surround. An off-centre ganglion cell would depolarise to a light decrement in the centre and also to a light increment in the surround. These spatially co-extensive antagonistic receptive fields have the effect of enhancing the ganglion response to light edges or boundaries.

The centre-surround organisation of a ganglion cell receptive field is shown in Figure 3.3 and can be represented by a difference of gaussian (DOG) filter (Rodieck, 1965). This receptive field provides both spatial frequency and phase selectivity, as the optimal response occurs for a bar of light (or dark if it was an off centre ganglion cell) of the width of the receptive field centre, positioned over the centre. This type of linear cell has been compared to the X ganglion cells in cat (Enroth-Cugell and Robson, 1966). However, Enroth-Cugell and Robson (1966) found an additional cell type, termed Y, which was non-linear, responding to a stimulus anywhere in the receptive field. There is also evidence of this cell type in human in which the spatial phase is unimportant (Hubel and Wiesel, 1962). However, these do not comprise a large proportion of cells and the DOG provides a good model of receptive field structure at the early stages of the visual process.

A further consequence of the cone circuitry is that the M cells, which receive a relatively large number of mixed cone inputs, are not chromatically selelctive. However, the foveal midget pathway, with one cone input per ganglion cell, carries a single colour information in its receptive field centre and another in its surround and this provides the substrate for chromatic perception. Both these cell types have been identified in single cell experiments (Gouras, 1968) and while both are described as spatially opponent, only one was found to show chromatic opponency. This opponency is of two forms; L with M, and S with (L+M) so that the cell is red/green or blue/yellow with the centre being either on or off and the surround always of opposite polarity. Beyond the fovea, where two or three cones provide input to a

ganglion cell, it is uncertain as to whether the cones are of a single type and as such capable of transmitting colour information (Kolb, 1991). However, psychophysical evidence shows that chromatic discrimination occurs at eccentricities of 25 degrees (Nagy and Doyal, 1993) which indicates that up to this eccentricity, cone inputs are not all mixed.

Figure 3.3 Receptive field sensitivity of a centre-surround ganglion cell. From Hubel (1988)

These differing cone inputs to ganglion cells provide a further system of ganglion cell classification; that of spectral sensitivity. A number of different types have been identified showing differing degrees of centre-surround and spectral opponency (Gouras and Zrenner, 1981; Zrenner, 1983b). These are shown in Table 3.1 from macaque data (Gouras, 1991).

Cell type	Cone input to centre	Size of centre	Percentage ON centre	Percentage OFF centre
P colour-opponent	S	0.29°	2.4	0.8
P colour-opponent	M	0.06°	13.9	9.0
P colour-opponent	L	0.07°	19.9	12.3
P non colour-opponent	L and M	0.12°	17.2	12.5
M non colour-opponent	L and M	0.15°	7.6	4.4

Table 3.1: Proportions and spectral opponency of retinal ganglion cells

The chromatic opponency of cells shown in Table 3.1 does not restrict their response to chromatic stimuli; they also respond to achromatic stimuli of the appropriate spatial frequency. Indeed, the P foveal midget pathway is thought to respond to achromatic spatial frequencies of up to 40 cycles/degree (Derrington and Lennie, 1984). Hence colour opponent cells provide ambiguous information; their response could arise from chromatic or achromatic stimuli. However, their spatially opponent receptive field organisation results in different response characteristics for chromatic and luminance signals, with the response to luminance stimuli being bandpass and that to chromatic stimuli being lowpass. This characteristic is also true of cortical cells and for the visual system as a whole, as shown in the upper panel of Figure 3.4 for single cell recordings from macaque striate cortex (Thorell et al., 1984) and in the lower panel for psychophysical measures (Mullen, 1985).

This has led to the "double duty" hypothesis of P cells, in which both chromatic and luminance information are multiplexed and later recovered at the level of the cortex (Ingling and Martinez-Uriegas, 1985; Ingling, 1991). However, this theory has been questioned by Rodieck (1991) who suggests that the ability of colour opponent cells to carry chromatic and luminance information is incidental and their function lies solely in the conveyence of luminance signals. He proposes a distinct class of retinal ganglion cells, resembling Type II cells (Wiesel and Hubel, 1966, see section 3.5), which are responsible for conveying chromatic information. While these Type II cells have been described both in the retina and the LGN (Wiesel and Hubel, 1966; DeMonasterio and Gouras, 1975; DeMonasterio, 1978) it is uncertain as to whether their numbers could account for the resolution of the chromatic system, estimated at between 10-12 cycles/degree (Granger and Heurtley, 1973; Mullen, 1985) and 21 cycles/degree for foveal viewing conditions (Anderson et al., 1991).

From Table 3.1 it can be seen that on centre cells are more common than off centre in the ratio 3:2. (Gouras and Zrenner, 1981). These two cell types appear to act independently of one another, forming separate sampling mosaics (Wässle et al., 1983; Perry and Silveira, 1988). This suggests that retinal images are coded twice by these two different systems, firstly for light increments and secondly for light decrements. Support for this comes from Schiller et al. (1986) who found that blocking the on channel in monkeys resulted in the loss of the detection of light increments but not decrements.

Figure 3.4 Spatial frequency response chracteristics of cells within macaque area V1 (upper panel) and the human visual system measured psychophysically (lower panel) to chromatic and luminance stimulation. From Thorell et al. (1984) (upper) and Mullen (1985) (lower: □ represent isoluminant red/green gratings and o green/black gratings).

Table 3.1 also shows differences in receptive field size. S/(L+M) cells have larger receptive fields than L/M cells which implies that the S system has lower spatial resolution (Zrenner et al., 1990). The S system appears to have a number of additional differences which include a longer response latency and duration which limits its temporal resolution (Zrenner et al., 1990). This conclusion is supported by Zrenner and Gouras (1981) who showed flicker fusion occurs at a lower temporal frequency for S driven cells than for L/M driven cells.

Temporal characteristics also differ between M and P cells, with M cells being able to respond to faster temporal frequencies than P cells (Purpura et al., 1988; Derrington and Lennie, 1984). Indeed, the initial distinction between M and P cells was that of phasic and tonic (Gouras, 1968) although this should be viewed in the sense of M cells being unable to follow slow changes rather than P cells being unable to respond to rapid changes (Kaplan et al., 1990). In their study of LGN cells, Derrington and Lennie (1984) reported that the optimal temporal frequency of P cells was approximately 10Hz while that of M cells was closer to 20 Hz. However, while P cells are capable of responding to such high temporal frequencies, phase differences between centre and surround result in the cell summing input from centre and surround and the loss of chromatic opponency (Ingling and Martinez-Uriegas, 1985).

The different characteristics of M and P ganglion cells have led to suggestions that the two pathways subserve different functions. P conveys colour and form information while M carries motion and depth information (Livingstone and Hubel, 1988a). However at isoluminance, when it is assumed the M units are nulled, texture, motion and depth perception are compromised but not abolished (Logothetis et al., 1990). These results may in part be due to chromatic aberrations, or the introduction of luminance artefacts into the stimulus due to optical, accommodatitive or display factors. However, studies which selectively destroy the P or M pathway (Schiller, 1991; Merigan et al., 1991) also find the division of information between M and P is not absolute. They show that colour and high spatial frequency luminance information is conveyed by the P system but low spatial frequency luminance information is carried by both P and M systems. Similarly, both pathways convey form and depth perception but only P contributes to high spatial frequencies. Motion is capable of being conveyed by both pathways at lower temporal frequencies but the M pathway only was operative at high temporal frequencies. Recent psychophysical measures suggest that in peripheral retina, it is the P system that limits motion acuity at all temporal frequencies (Anderson et al., 1995). Hence these studies suggest that neither

pathway is solely responsible for form or motion perception but simply signal different but overlapping regions of spatio-temporal space.

3.4 The Geniculostriate and the Collicular Pathway

The geniculostriate pathway and the collicular pathway are shown in Figure 3.5. Although the geniculostriate pathway is undoubtedly the major pathway in the visual process, receiving some 90% of retinal projections, there exist a number of subcortical pathways which also send afferents to striate cortex. The principle subcortical pathway runs through the superior colliculus, via the pulvinar complex to layers 6 and 1 in striate cortex (Benevento and Fallon, 1975; Ogren and Hendrickson, 1977) and to extrastriate regions MT and PO (Ungerleider et al., 1983).

Figure 3.5. The geniculostriate and the collicular pathways

The pulvinar can be divided into three separate regions, two of which have complete topographic maps of the contralateral visual field (Peterson et al., 1985). The pulvinar has been shown to respond during stimulus selection and saliance (Robinson, 1993) and macaque reaction times to visual stimuli are increased following inactivation of the pulvinar (Peterson et al., 1987). In humans, thalamic damage produces increased reaction times to visual stimuli, especially in the presence of visual cues (Rafal and Posner, 1987). Further evidence for the attentional role of the pulvinar in humans comes from PET studies (LaBerge and Buchsbaum, 1990). In subjects making identification discriminations in the presence of varying attentional demands, there is an increase in thalamic activity under the conditions of greatest attentional demand. No corresponding activity increase was seen in the ipsilateral thalamus. Hence the pulvinar seems to be involved in some sort of visual selection mechanism and it has been suggested that it acts as an early centre for the generation of visual salience (Robinson, 1993).

However there remains some debate as to the functional significance of these subcortical pathways. The residual visual function in subjects with striate cortex lesions has been studied. Such lesions affect V2, V3, V4, V5 and also the subcortical regions that normally receive striate projections, for example the superior colliculus, the pulvinar and the LGN. Within the first three months following such lesions 99% of projection neurones are lost and the remainder project directly to extrastriate areas (Cowey and Stoerig, 1989). The residual function of the surviving neurones has been demonstrated and remaining M and P cells appear to function with decreased sensitivity of 0.3-1.5 log units. Wavelength discrimination remains but it is unclear as to whether this is true of form discrimination (Stoerig and Cowey, 1993). Despite this demonstrable visual function, subjects tend to have no conscious perception of vision. Hence remaining visual function has been termed "blindsight". Although some additional 20 subcortical projections have been described in monkey (Tigges and Tigges, 1985), little is known of their function.

3.5 The Lateral Geniculate Nucleus (LGN)

The LGN is a multilayered structure comprising six cellular layers divided by more sparsely populated interlaminae regions. The organisation of these layers is such that the two eyes project to separate layers and the magnocellular and parvocellular afferents are separated into different layers. The four dorsal layers receive projections

from parvocellular ganglions and the two ventral layers receive magnocellular projections (Perry et al., 1984). This is shown in Figure 3.6. The majority of LGN cells receive input from a single retinal ganglion cell, so that the LGN receptive field properties resemble those of their retinal inputs (Cleland et al., 1971; Lee et al., 1983). The spectral properties of LGN cells were described by Wiesel and Hubel (1966) who identified three cell types. Type I units have centre and surround of different spectral selectivity, producing a spatially and chromatically opponent cell. Type II were chromatically but not spatially opponent and Type III were spatially but not chromatically opponent. The property of on- or off-centre receptive field also appears to be maintained in the LGN and there are suggestions that the LGN segregates cells on the basis of this property (Schiller and Malpeli, 1978).

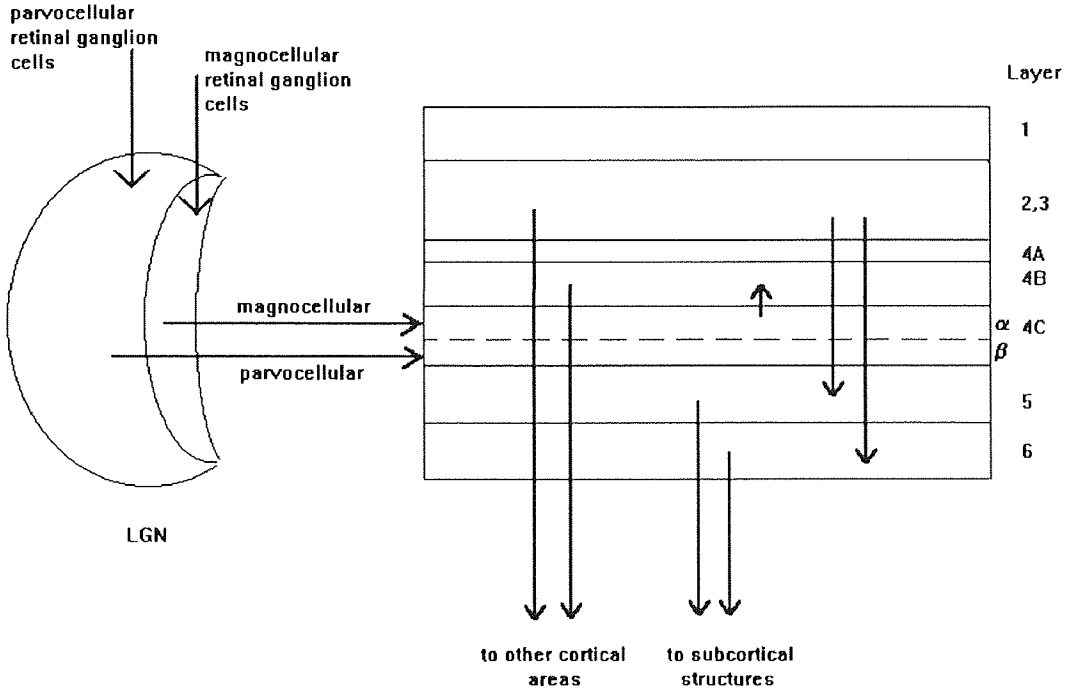

Figure 3.6. Projections and connections of area V1

In addition to the magnocellular and parvocellular layers there are reports of koniocellular or S cells which inhabit the interlaminae zones (Leventhal et al., 1981). These have very small cell bodies with large receptive fields and are thought to be wavelength selective, projecting to the blobs of striate cortex (Casagrande and DeBruyn, 1982). However, these small cells have only been described in cats, galago and more recently macaque (Hendry and Yoshioko, 1994) so their existence in human is uncertain.

Hence the LGN acts as a relay station between retina and cortex, retaining both receptive field properties and segregation of the different streams of information. However, its role is considerably more complex than this would suggest. This complexity becomes apparent when non-retinal inputs to the LGN are considered. V1 provides the major cortical input (Sherman and Koch, 1986; Robson, 1983; Swadlow, 1983) and this may provide more inputs than do retinal projections (Koch, 1987; Swadlow, 1983). The connections are topographic so that V1 cells representing a particular locus of the visual field project back to LGN cells representing the same region of visual space with independent modulation of magnocellular and parvocellular pathways (Lund et al., 1975). There may also be input to the LGN from the superior colliculus which is thought to be concentrated in the interlaminar regions and adjacent to magnocellular layers (Harting et al., 1978).

The effect of these non-retinal projections can be examined by the transfer ratio; the ratio of input synaptic cell potentials to LGN output. This is thought to be affected by global and specific mechanisms via the brainstem, superior colliculus and the cortex; see Casagrande and Norton (1990) for a review. These may provide a rapid, facilitatory action on the LGN which increases signal detectability. The retinotopic nature of links from cortex to LGN could act to increase the transfer ratio for a specific region of the visual field.

3.6 Striate Cortex

3.6.1 Anatomical organisation

The striate cortex, Brodman's area 17, V1, or the primary visual cortex was one of the first visual areas to be identified, in part due to its distinctive striations. It is a multi-layered structure with cells projecting from the LGN terminating in layer 4C and maintaining their M/P segregation; M cells in 4Cα and P in 4Cβ (Hubel and Wiesel, 1972). The activation of M and P recipient layers is not simultaneous, with 4Cα becoming active some 20ms prior to 4Cβ (Nowak et al., 1995; Givre et al., 1995). The two subdivisions of layer 4C in turn have different projection sites to the upper layers of V1. 4Cα sends its outputs to 4B while 4Cβ sends outputs to layers 2 and 3. All layers except 1, 4A and 4C have output fibres projecting both out of the cortex and locally, aiding the distribution of information throughout the cortical layers (Gilbert and Wiesel, 1979). Upper layers 2, 3 and 4B project to other cortical visual regions while deeper layers project to subcortical structures; layer 5 to the superior colliculus and layer 6 to the LGN (Hubel, 1988). Layers 5 and 6 also project to the upper

cortical layers 2,3 and 4 (Allison et al., 1995). This is summarised in Figure 3.6. The back projections are substantial in number with some 50% of layer 6 fibres sending projections back to the LGN. As described in section 3.5, the connections appear to be retinotopic so that projections return to the same layer of the LGN that provided the initial input. Parvocellular cells in layer 6 project to parvocellular layers of the LGN and magnocellular cells in layer 6 project to the magnocellular LGN (Lund et al., 1975). This feedback system continues past V1 with each of the areas to which V1 projects in turn sending connections back to V1.

It should be noted that the local connections within the cortex are relatively short, generally 1-2 mm (Hubel, 1988). As the striate cortex has topographical organisation, sharing or comparison of information enabled by local connections must therefore occur primarily for adjacent areas of the visual field. It can thus be concluded that the analysis performed by the primary visual cortex is limited and more global analyses must be performed at a higher stage of processing. However, there is certainly some degree of processing occurring in V1 as the cells receiving input from the LGN are not orientation selective (Hubel, 1988) yet in all other layers the cells show orientation selectivity arranged in a highly organised strucure. It has been suggested that the connections between layers 5 and 6 to layers 2, 3 and 4 provide an organised orientation tuned inhibition that sharpens the orientation tuning of cells in the upper cortical layers (Allison et al., 1995).

Within V1, staining for cytochrome oxidase has revealed a periodic, tangentially orientated pattern of heavily stained "blobs" separated by cytochrome oxidase sparse interblobs (Horton and Hubel, 1981; Horton, 1984). These blobs form columns approximately 0.2mm in diameter and are spaced 0.5mm apart (Hendrickson et al., 1981). They are most marked in layers 2 and 3 but are also faintly present in layers 5 and 6 (Livingstone and Hubel, 1984). Their absence in layer 4B indicates some form of functional segregation occurring, as magnocellular cells project to layer 4B and parvocellular to layers 2 and 3. Indeed, cells within these different regions have different response properties (Michael, 1987; Tootell et al., 1985; Livingstone and Hubel, 1982, 1984). Cells in layer 4B are orientation selective and show selectivity for direction of movement (Livingstone and Hubel, 1984). In the interblobs most cells are also orientation selective but not directionally selective (Livingstone and Hubel, 1984). While not wavelength selective, they do respond to correctly oriented colour borders, regardless of the relative brightness of the two colours. So colour information is utilised but wavelength selectivity is lost (Gouras and Kruger, 1979). Cells in the blobs, however, are not orientation selective but do show chromatic selectivity

(Livingstone and Hubel, 1988a). Hence within V1, segregation of M and P pathways is maintained and the P pathway appears to be divided into achromatic and chromatic selective regions. However, the segregation may not be complete. Several studies have reported M input into the blobs (Livingstone and Hubel, 1984; Tootell et al., 1988d). There is also evidence of communication between blob and interblob cells. Although no direct evidence of connections were found, cross-corellation studies of activity in blob and interblob cells suggest there may be connections between the two cell types (T'so and Gilbert, 1988).

3.6.2 Ocular dominance, orientation and spatial frequency columns.

The modular structure of the striate cortex was described by Hubel and Wiesel (1962, 1974) in cat and monkey microelectrode studies. With electrode penetrations perpendicular to the cortical surface, eye preference and orientation preference were found to remain roughly constant, forming a column through the cortex. This was interrupted by layer 4 which has no orientation selectivity. However, when the penetration was made parallel to the cortex a regular sequence of orientation shifts and changes in eye preference were noted, occurring independently of one another. The region of cortex containing all orientations at a particular position in the visual field was termed an orientation column and was found to be contained within the area of cortex favouring one eye; an ocular dominance column. These were arranged so that the cytochrome oxidase blobs lie in the centre of each ocular dominance column (Switkes et al., 1986). The region of cortex analysing both eyes at all orientations was termed a hypercolumn. The cycle was such that 180° was analysed within a 0.5mm strip of cortex and both eyes at all orientations within 1mm. This is summarised in Figure 3.7.

The periodicity of the ocular dominance columns can be explained by examining the pattern of horse-radish peroxidase staining (Hubel, 1988). This reveals that geniculate axons, which are monocular, terminate in 0.5mm wide synaptic clusters, separated by blank areas of 0.5mm. These blank areas are filled by axons from the opposite LGN which also form 0.5mm clusters. There are a number of horizontal and diagonal connections running for approximately 1mm which results in some smearing of the left eye versus right eye zones, so that a cell on the border of the zones may be binocular. This is confirmed by parallel penetrations of layers 5 and 6 and the upper layers which show smooth alternations between left and right eyes rather than the sharp transitions seen in layer 4C. Near the fovea the pattern becomes more complex and rather than

Figure 3.7. Organisation of ocular dominance and orientation columns. From Gouras (1991)

being arranged in regular slabs, the columns show irregular patterns of swirls (Hubel, 1988; Tootell et al., 1988a). The modular organisation has been confirmed in 2-DG studies (Hubel et al., 1978).

More recently, there has emerged evidence that spatial frequency selectivity may be arranged in a modular fashion in a manner similar to that of orientation. This appears to be the case in cats, with spatial frequency running perpendicular to orientation (Tootell at al., 1981). However, the organisation appears to be more complex in primates with the cytochrome oxidase blobs appearing to be related to spatial frequency (Tootell et al., 1988e). A visual stimulus containing all spatial frequencies at all orientations was found to produce a 2-DG pattern which was uniform. When the pattern was restricted to low spatial frequencies (1 cycle/degree) the 2-DG uptake pattern occured across the whole of the stimulated cortex but was confined to dots superimposed on the blobs. When a higher spatial frequency (4.5 cycles/degree) was used, the 2-DG uptake pattern varied with eccentricity.

Near the fovea, the uptake formed dots over the blobs. At an eccentricity of 3-5 degrees the uptake was evenly distributed in the blobs and interblobs. Further into the periphery, beyond 5 degrees, the uptake was arranged in an annular pattern surrounding the blobs as seen for high spatial frequencies in the fovea. This suggests that spatial frequency organisation is radial with low spatial frequencies being represented in the centre of the cortical modules, coinciding with the blobs, and the high spatial frequencies being represented increasingly radially out. The overall orientation and spatial frequency organisation may therefore be arranged spherically with orientation being represented angularly (θ) and spatial frequency arranged as distance radially outwards (r) (DeValois and DeValois, 1990). The changing patterns of 2-DG with eccentricity implies that spatial frequency selectivity changes with eccentricity, with cells in the fovea responding to higher spatial frequencies than those in the periphery. This is supported by primate electrophysiological and human psychophysical studies of acuity as a function of eccentricity, which show that acuity is highest in the fovea and falls off with eccentricity.

This spatial frequency model of the blobs contrasts with the chromatic function suggested by Livingstone and Hubel (1984). However, during their experiment low spatial frequency chromatic stimuli were used and according to the spatial frequncy model, this will always stimulate the blobs regardless of chromatic content (DeValois and DeValois, 1990). Indeed, high spatial frequency colour gratings (6.5 cycles/degree) activate cortical regions outside the blobs (Tootell, 1988c). However, above 4 cycles/degree, chromatic gratings can be severely contaminated by luminance modulations due to chromatic aberrations (Bradley et al., 1992). Hence this must be controlled for before it can be concluded that pure chromatic information activates areas of cortex outside the blobs. Indeed, Tootell et al. (1988c) noted that regardless

of spatial frequency, chromatic stimuli never produce 2-DG uptake confined to the interblobs. The same spatial frequency produces uptake which is shifted towards the blobs for chromatically modulated stimuli when compared with achromatically modulated stimuli (Tootell et al., 1988d). Hence the evidence would support a chromatic function for the blobs. However, the blobs also support a luminance mechanism, shown by 2-DG uptake at achromatic contrasts which activate only the magnocellular layer 4Cα (Tootell et al., 1988d) and by studies showing magnocellular input to the blobs (Livingstone and Hubel, 1984). Indeed, in their study of intracortical visual evoked potentials in macaque, Givre et al., (1995) did not find any evidence of chromatic sensitive cells being spatially confined. There is not, therefore, a clear segregation of luminance and chromatic function between blobs and interblobs in cortical area V1.

3.6.3 Physiological properties of striate cortex cells: simple and complex cells

Among the first descriptions of striate cortical cells was one which used a classification system based on receptive field properties (Hubel and Wiesel, 1959, 1962). The first cell type, termed simple, was categorised as having centres which showed an excitatory or inhibitory response to light increments and summation within the antagonistic excitatory and inhibitory regions. The second cell type, termed complex, was categorised by showing an absence of discrete excitatory and inhibitory subregions in the receptive field. A large excitatory response was produced by a bar of some fraction of the receptive field width with no response to a bar covering the entire receptive field although there was a response to such a bar anywhere within the receptive field. Both cell types showed orientation selectivity.

These two cell types form distinct categories, showing a bimodal distribution rather than a continuum (DeValois et al., 1982). Although the M/P division is commonly compared with the properties of X/Y cells in cat (Ingling and Martinez-Uriegas, 1985) it has been proposed that X and Y cell properties more closely resemble those of simple and complex cells (DeValois and DeValois, 1990). Hence in terms of cat cells (Enroth-Cugell and Robson, 1966) simple cells are similar to X cells, being restricted to a single spatial phase. Complex cells, however, resemble Y cells, with their response being phase insensitive. This lack of phase sensitivity leads to frequency doubling in which the cell fires in response to pattern luminance increases and decreases. Simple cells, however, are phase sensitive and produce only one response to a light cycle

Hubel and Wiesel (1965) describe a further cell type, called hypercomplex, as resembling complex cells except the length of an optimally orientated line was also a critical factor. This they described as end stopping. However, some hypercomplex cells resemble simple or complex cells in all but end stopping (Schiller et al., 1976) and simple and complex cells also show some degree of end stopping. Hence it has been suggested that hypercomplex cells, rather than forming a discrete category, are one extreme of a continuum of end stopping (DeValois and DeValois, 1990). Some cells also show side stopping, i.e. they will respond to a number of gratings but a further increase in grating number produces a response decrement (DeValois et al., 1985). So hypercomplex cells may have the property of inhibition around the whole receptive field (DeValois and DeValois, 1990).

Hubel and Wiesel (1962) hypothesised a hierarchical arrangement of LGN cells feeding into simple cells which in turn provided the input to complex cells which fed into hypercomplex cells. However, given the similarity of simple and complex cells to X and Y cells, which have a parallel organisation, it may be that there exists a degree of parallelism in primate cortex also. Indeed, both simple and complex cells receive a direct LGN input and X-like and Y-like geniculates feed into both simple and complex cortical cells (Bullier and Henry, 1979a,b,c). Further evidence for parallel processing is that 40% of cells in the main striate input layer 4C are complex (Gilbert, 1977). Indeed, some complex cells have properties not readily derived from a summation of simple cells, for example texture sensitivity (Hammond and MacKay, 1975).

With later work indicating a segregation of colour and orientation selective cells within V1 (Livingstone and Hubel, 1984), the observation of simple cells and not complex cells being colour selective (Thorell et al., 1984) would support this parallel processing model. Thorell's work further indicated that complex cells respond to higher spatial frequencies than simple cells and, in accordance with retinal receptive field properties, the majority of cells respond to both colour and luminance stimuli although complex cells are colour sensitive rather than selective. The spatial frequency tuning characteristics were found to be similar for luminance and chromatic stimuli and where a difference existed, cells were more broadly tuned and peaked at lower spatial frequencies for colour stimuli. Hence as shown in Figure 3.4, a summed population of cortical cells demonstrated lowpass characteristics for chromatic stimuli and bandpass for luminance. However, Thorell did not specify the regions of striate cortex in which the cells located so while of interest, their work is of limited use in interpreting cell functional segregation in V1.

3.6.4 Cells as spatial frequency filters

Both simple and complex cells have been described as responding optimally to bars and edges of specific orientations (Hubel and Wiesel, 1959,1962) and models of visual processing based on bar and edge detectors have been proposed (Lindsay and Norman, 1972). However, Campbell and Robson (1968) suggested that cells respond to a particular range of spatial frequencies, thus acting as a set of bandpass filters. This has been confirmed by two means of investigation; electrophysiological single cell recordings in primates and by psychophysical observations in humans.

Single cell recordings in macaque to gratings and checkerboards show that both simple and complex cells respond to the spatial frequency of a grating rather than the edges or the width (DeValois et al., 1979). As each cell is responsive to a particular orientation (Hubel and Wiesel, 1959, 1962), cortical cells can therefore be described as two dimensional spatial frequency filters. Different cells responding to the same region of space are tuned to different spatial frequencies and orientations.

Psychophysical evidence for multiple spatial frequency channels in humans comes from studies of spatial frequency specific adaptation, masking and sub-threshold summation. A group of spatial frequencies form a channel of a particular bandwidth. This bandwidth alters with spatial frequency, being narrower for high spatial frequencies (Blakemore et al., 1971, 1973; Anderson and Burr, 1985). There is mutual inhibition between the channels (DeValois, 1977b) and they are orientation specific (Blakemore and Nachmias, 1971). There is also evidence for chromatic spatial frequency channels and these are broader and flatter than the corresponding luminance channels (DeValois, 1978; DeValois and Switkes, 1983). Using a masking technique, Anderson and Burr (1985) showed that while there are multiple spatial frequency channels, there appears to be only two temporal frequency channels. The first, operative at a wide range of temporal frequencies, is bandpass, peaking at 7-13Hz. The second, which occurs at low temporal frequencies (<1Hz) is lowpass. More recently, there has been evidence for the existence of a third temporal frequency channel (Hess and Snowden, 1992).

Hence cortical cells appear to act as spatial frequency filters and when selectivity for orientation is considered, the cell can be thought of responding to a particular region of Fourier space (Robson, 1975; DeValois et al., 1977). Thus a hypercolumn could encode the Fourier spectrum of a region of the visual field (DeValois et al., 1979).

3.6.5 Retinotopic organisation of V1

The striate cortex receives projections only from the ipsilateral LGN so that the right visual field stimulates the left hemisphere and the left visual field stimulates the right hemisphere. The two halves of the visual field are not entirely separate, however, with the cortex representing the region of the vertical meridian being connected with the corresponding cortical regions of the opposite hemisphere through the corpus callosum (Myers, 1962). In macaque, the fovea projects to the most lateral region of the occipital pole, while more peripheral regions (up to 7°) move more medially. Beyond 7° the corresponding cortex is buried within the calcarine sulcus (Daniel and Witterage, 1961). In humans the entire structure has migrated medially so that only the central foveal projections remain on the exterior cortical surface. The area is defined by the white stria of Gennari (Holmes, 1918) and is bounded anteriorly by the junction of the inner parieto-occipital sulcus and the calcarine fissure. The extent of striate cortex is shown in Figure 3.8. The topographic organisation was described by Holmes (1918) who showed that projections from the LGN were retinotopically mapped onto the human striate cortex as shown in Figure 3.7. The upper visual field is represented on the lower bank of the calcarine sulcus and the lower visual field on the upper bank. The horizontal meridian is represented along the calcarine fissure and the vertical meridian runs along the perimeter of the striate cortex as shown in Figure 3.9.

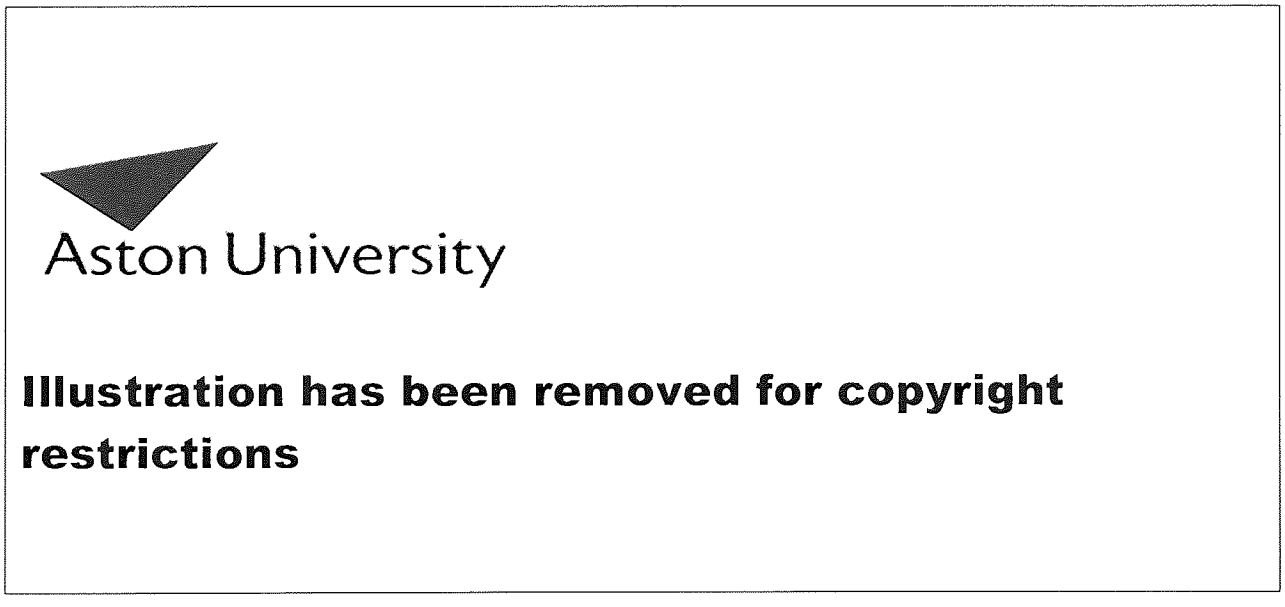

Figure 3.8 Medial section of the human visual cortex indicating the extent of striate cortex. From Zeki (1990).

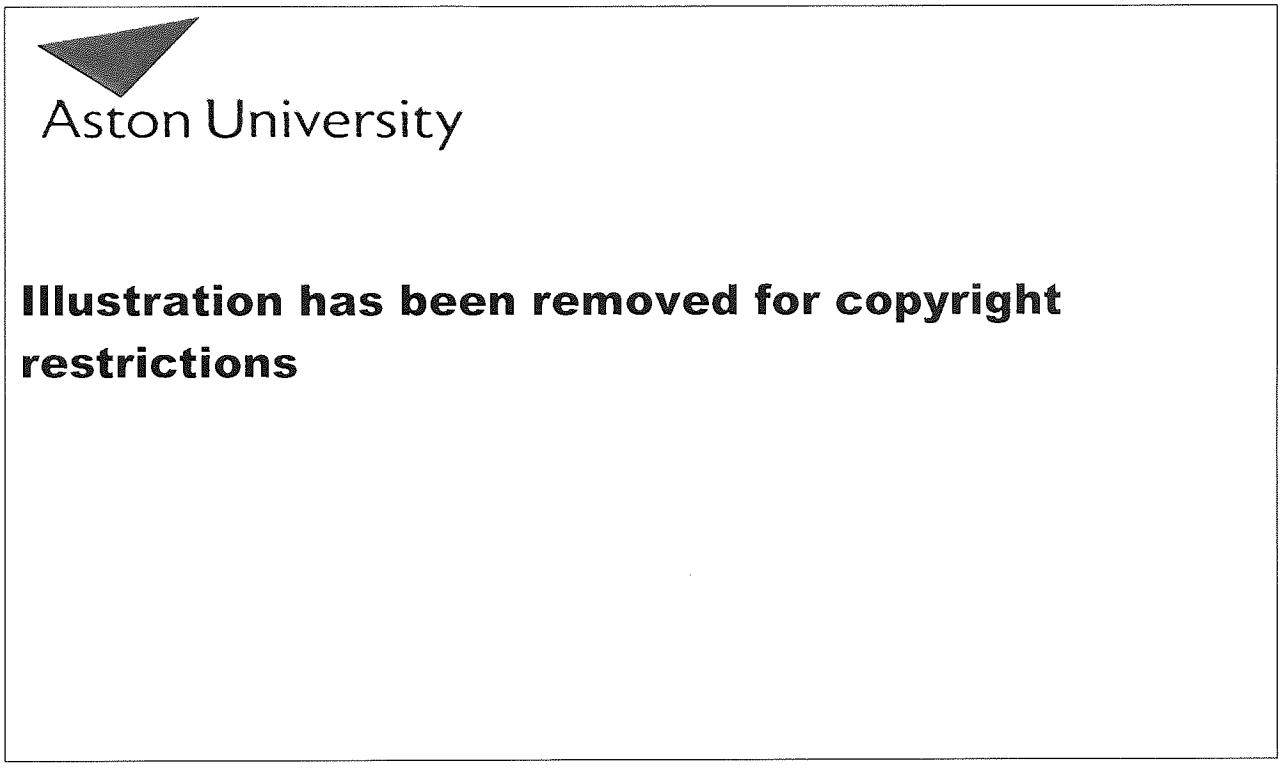

Figure 3.9 The Holmes map of human area V1 From Horton and Hoyt (1991).

Hence the striate cortex is organised in a retinotopic fashion, so that two adjacent points in the visual field are also adjacent in V1. This would appear to contradict the modular organisation of the striate cortex described in section 3.6.2 in which neighbouring cells deal with different orientations and spatial frequencies at the same position in the visual field. However, it is not known that the retinotopic organisation extends to such short cortical distances. Cortical modules are small with respect to the receptive field sizes of most cells and could correspond to a distance of 0.15° of visual angle (DeValois and DeValois, 1990). The model therefore allows the primate cortex to be divided into many cortical modules each processing information from a different position in the visual field with a considerable amount of overlap of receptive fields.

A simplified representation of striate cortex has been proposed in the cruciform model (Jeffreys and Axford, 1972a,b). This model divides the visual field into octants and

depicts each octant's projection onto the calcarine fissure. This is shown in Figure 3.10.

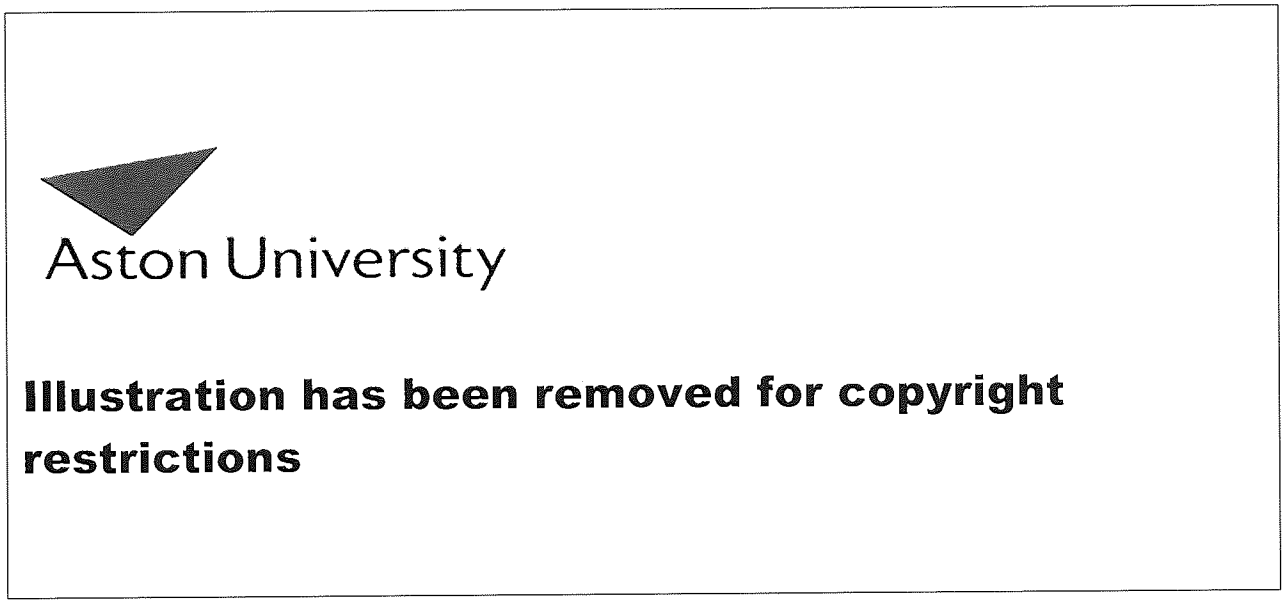

Figure 3.10 The cruciform model of striate cortex. cf calacarine fissure, lg lingual gyrus, cg cuneal gyrus. Redrawn from Jeffreys and Axford (1972).

Although the principle of retinotopic organisation and the Holmes map holds, there is a considerable amount of intersubject variability in the striate cortex. In their MRI study of V1, Clark et al. (1992) noted the extreme variability in the position, orientation and extent of V1. Stensaas et al. (1974) in a total of 52 hemispheres showed a three fold difference in the amount of striate cortex present and a four fold difference in the amount of cortex exposed. The striate area was also shown to have interhemispheric differences, only 2 out of 46 cases examined being symmetrical. The striate cortex was not always situated on the pole, in some cases being represented wholly around the calcarine fissure. These interhemispheric differences were confirmed in computed tomography studies (Le May and Kido, 1978) in which 71% of right handers had a parieto-occipital area wider on the left and only 9% on the right. The assymmetries were less marked in left handers, with 32% having a wider right occipital area, 34% being symmetrical and 34% having a wider left occipital area. The volume of the striate cortices is also often asymmetrical, with the right being greater in 77% of examined cases (Murphy, 1985).

3.6.6 Cortical magnification factor

The area of cortex allocated for processing information from different regions of the visual field is not equal, with a large proportion of both the LGN and striate cortex devoted to processing foveal information (Connolly and Van Essen, 1984; Perry and Cowey, 1985). This occurs to the exent that 42% of striate cortex is devoted to processing the central 5° of the visual field (Connolly and Van Essen, 1984). To quantatively describe this inhomogeneity the term cortical magnification factor was defined as the linear extent of visual cortex, in millimetres, devoted to each degree of visual field (Daniel and Witteridge, 1961). There have been various estimates of its magnitude in human, ranging from 4.5mm/deg to 25mm/deg at the fovea (Dobelle et al., 1979; Drasdo, 1991; Tolhurst and Ling, 1988). One explanation for less cortex being devoted to peripheral regions of the visual field is the increase in receptive field size with eccentricity in both ganglion cells (Piechl and Wassle, 1979) and cortical cells (Hubel and Wiesel, 1974b; Van Essen et al., 1984). The resulting uneven distribution of ganglion cells results in more cortex being devoted to processing the greater number of foveal ganglion cells. However, ganglion cells near the fovea are allocated between 3.3 and 5.9 times more cortex per cell than peripheral ganglion cells so that the cortical representation of the fovea is greater than that predicted from ganglion cell density (Azzopardi and Cowey, 1993).

3.7 Extrastriate cortex

In addition to striate cortex, several visual areas have been identified in monkey and in man. Brodmann's areas 18 and 19 have been shown to contain several visual areas: V2, V3, V4 and V5 (MT). These areas are characterised by stripes of callosal afferents bounding the representations of the vertical meridians which therefore provide useful anatomical markers both in monkey (Zeki, 1977, 1978a; Van Essen and Zeki, 1978) and in human (Clarke and Miklossy, 1990). However, the functional properties of these areas are less readily determined in human and our knowledge is based primarily on single cell recordings from these areas in monkey. Recent PET studies (Zeki et al., 1991) have shown some degree of functional specialisation in humans and there have been a small number of intracortical recordings in humans (Richer et al., 1991). Hence areas that until recently were all categorised as extrastriate are now beginning to be understood in more detail and the relationship between them is under investigation.

3.7.1 V2

Lying within area 18, V2 forms a horse-shoe shape around V1 in monkey (Zeki, 1969, 1978b) and in human (Clarke and Miklossy, 1990). Cytochrome oxidase studies indicate a modular organisation similar to that of V1 with 3 distinct regions being identified as thin, thick and pale cytochrome oxidase stripes (Tootell et al., 1983; Livingstone and Hubel, 1984, 1988a; Hubel and Livingstone, 1987). These regions correspond to non-orientated colour opponent cells, end stopped cells and cells responsive to binocular disparity (Hubel and Livingstone, 1987). The segregation of information in V1 is maintained in the connections to V2, with the non-oriented colour-responsive blob cells of V1 projecting to the thin stripes of V2 (Livingstone and Hubel, 1984; Hubel and Livingstone, 1985). Similarly, oriented non colour-opponent cells in V1 interblobs project to the pale stripes of V2 (Livingstone and Hubel, 1984) and layer 4B of V1 projects to the thick stripes of V2 (Livingstone and Hubel, 1987). V2 receives point to point projections from V1, hence like V1 there is retinotopic organisation but with dual representation of the horizontal meridian (Zeki, 1969) as shown in Figure 3.11. Although the cell properties of V2 resemble those of V1, some form of processing occurs here as cells in V2 but not V1 respond to illusory contours (Von der Haydt et al., 1984).

Figure 3.11 The representation of the horizontal and vertical meridians in areas V1 and V2. From Horton (1992).

3.7.3 V3

V3 corresponds to a horse-shoe shaped strip of cortex lateral to V2 bounded laterally by callosal afferents both in monkey (Zeki, 1978a) and in human (Clarke and Miklossy, 1990). The area is cyto- and myelo-architecturally inhomogeneous and has therefore been divided in monkeys into two subregions, dorsal V3 and ventral VP (Burkhalter and Van Essen, 1986). This difference is also apparent in humans; the upper part of human V3 cannot be architecturally distinguished from surrounding visual areas but lower V3, due to poor myelination, is readily distinguished (Clarke and Miklossy, 1990). This area has a more limited visual field than areas V1 and V2, responding only to the central 35-40 degrees of the contralateral visual field (Gattas et al., 1988). Representation of the upper and lower visual field is split so that the upper visual field is located ventrally and the lower visual field dorsally. The horizontal meridian is located adjacent to V2 and forms the posterior border with V2 while the anterior border represents the vertical meridian (Gattas et al., 1988) shown in Figure 3.11. V3 has a magnified representation of the central visual field with respect to the periphery with the size of its receptive fields increasing with eccentricity (Gattas et al., 1988). The response properties of V3 are not as well documented as the other visual areas considered here but are thought to include sensitivity to orientation, direction of motion and binocular disparity, with a small proportion being wavelength selective (Felleman and Van Essen, 1987; Desimone et al., 1985).

3.7.4 V4

V4 is a poorly myelinated area which in humans is thought to lie on the fusiform gyrus (Clarke and Miklossy, 1990). It receives projections from V2, both from the thin stripes and the pale stripes (De Yoe and Van Essen, 1985, 1988; Shipp and Zeki, 1985) and also from the magnocellular pathway (Ferrera et al., 1992). In turn, V4 sends projections out to inferotemporal cortex (area IT) (Mishkin, 1982). V4 has been reported to contain a high proportion of wavelength selective cells and has therefore been proposed to be the colour processing centre (Zeki, 1983a,b,c). This function has been supported in human by studies of patients who, following damage to the lingual and fusiform gyri, show signs of achromatopsia (Verrey, 1888; Damasio et al., 1980). Indeed, PET studies (Zeki et al., 1991) have shown an increase in metabolic activity in the fusiform and lingual gyri following exposure to a colour mondrian. However, V4 also contains neurones which are not chromatically sensitive but do respond to oriented textures and contours (Zeki, 1978; Schein et al., 1982). In monkey, lesions to V4 produce not only achromatopsia but also deficits in form perception and object recognition (Heywood and Cowey, 1987).

Like V3, V4 does not contain a representation of the whole visual field but is confined to the central 35-40 degrees (Gattas et al., 1988). A notable feature of V4 is its very large receptive fields and supressive surrounds (Desimone et al., 1985; Gattas et al., 1988). These receptive fields extend up to 30 degrees, including up to 16 degrees in the ipsilateral visual field and are up to 30 times larger than those of V1 (Van Essen and Zeki, 1978). This has led to the suggestion that V4 has a role in colour constancy (Zeki, 1993) Colour constancy is the ability of an observer to perceive the hue of an object while disregarding variations in its reflected wavelengths due to differing illumination conditions. However, this ability relies on having two or more adjacent objects for the illumination-independent hue perception to take place (Lennie and D'Zmura, 1988). It is thought that the large receptive fields of V4 enable a global analysis and subtraction of the illuminant thus enabling the observer to perceive the hue of the object rather than its reflected wavelengths.

3.7.5. V5

V5, also termed the middle temporal region (MT), is a heavily myelinated area which in humans is situated on the convexity of the occipito-temporal junction (Clarke and Miklossy, 1990). It receives topographically organised projections direct from layer 4B of V1 (DeYoe and Van Essen, 1985; Shipp and Zeki, 1985; Ungerleider and Mishkin, 1979) and also via the thick stripes of V2 (DeYoe and Van Essen, 1985). Recordings direct from this area suggest that it receives very few projections from the parvocellular pathway (Ferrera et al., 1992). V5 also receives projections from the collicular pathway (Cragg and Ainsworth, 1969; Ungerleider and Mishkin, 1979).

Within V5 there is a high proportion of directionally sensitive cells (Dubner and Zeki, 1971) which seem to be selective for velocity (Newsome et al., 1983) rather than temporal frequency, as in V1 (Foster et al., 1985). The preferred speeds of V5 cells are higher than those of cells in V1 (Van Essen, 1985). The underlying organisation of V5 appears to be on the basis of direction selectivity, with tangential electrode penetrations revealing gradual shifts in preferred direction and perpedicular penetrations revealing columns of cells with the same preferred direction of motion; its function has thus been linked to motion detection (Zeki, 1974). This has been supported by the destrucion of V5 in macaque resulting in the deficits in the perception of motion; lesions in V5 were found to result in deficits in eye movements which were suggestive of the underestimation of the speed of an object while eye movements to a stationary target were unaffected (Newsome et al., 1985a). This V5 motion function is supported by observations that in human, bilateral damage to the latero-tempero-

occipital cortex selectively disturbs motion perception (Zihl et al., 1983). Further evidence comes from direct stimulation of the medial parieto-occipital fissure in human consistently producing the perception of motion (Richer et al., 1991). In addition, PET studies in human show that following presentation of a moving stimulus there is an increase in metabolic activity in the parieto-occipital junction (Zeki et al., 1991). Indeed, V5 cells respond to moving stimuli in a different way to V1 cells, suggesting some form of additional processing occurring in this area. V5 units respond to the perceived direction of plaids as opposed to V1 units which respond to the direction of motion of the constituent grating components (Movshon et al., 1986). V5 has also been found to respond optimally to motion contrast, that is when the centre and surround of the receptive field detect motion in opposite directions. This is true both of owl monkey (Allman et al., 1985a) and macaque (Tanaka et al., 1986) and suggests a role for V5 in the perception of local motion; extracting the motion of an object from global motion induced by the viewers movement through the world (Maunsell and Newsome, 1987).

3.7.6. Hierarchical processing models

A number of models have been proposed which show the parallel processing of information by different areas. The initial stages are thought to be more sequential with information arriving in V1 and the majority of outputs being sent to V2 before being sent to the functionally different areas for higher processing. With cytochrome oxidase staining it is now known that this functional segregation is present in V1 with blobs, interblobs and layer 4B and in V2 with thin, thick and pale stripes. A higher segregation of information has been suggested (Mishkin et al., 1983) in the "where" and "what" pathways. This model proposes that information processed by V3 and V4 pertaining to form is sent to temporal areas for object indentification. Meanwhile, motion information processed by V5 is sent to parietal areas for object localisation. A schematic of information segregation between M and P cells and for functional segregation in the different visual areas is shown in Figure 3.12.

While this model provides an indication of the processes involved in visual analysis, the hierarchical approach is not entirely accurate. Intracortical investigation of V1 and V2 activation latencies have shown that there is simultaneous processing occurring in V1 and V2 (Nowak et al., 1995). Indeed the number of reciprocal connections between visual areas provide the basis of reverberatory loops (Salin et al., 1993) which may form an important part in the visual processing mechanism.

Figure 3.12 Hierarchical processing in the visual pathway. Redrawn from Gouras (1991)

3.8 Summary

Examination of the anatomy and physiology of the visual system has revealed that, at least initially, the organising principle is along the segregation of information on the grounds of spatial frequency, temporal frequency and chromaticity. There are two major pathways, M and P, wich project via the LGN to striate cortex. The M pathway transmits low spatial frequencies, high temporal frequencies, has high contrast sensitivity and as such is specialised for motion perception. The P pathway prefers low temporal frequencies and is divided into two, the first carries low spatial frequency chromatic information and the second high spatial frequency achromatic information.

The LGN maintains this segregation and it may act as a gain control mechanism, adjusting activity levels in different regions of visual space. The M and P pathways project to V1, where the segregation takes the form of blobs, interblobs and layer 4B. However, cross-correlation studies and inter-stream connections suggest the division between M and P may be blurred. The different regions of V1 project to the stripes,

interstripes and pale stripes of V2 and from there to various higher centres for functional processing. There are many interconnections however, with each of the areas to which V1 projects sending connections back.

The visual system therefore appears to be organised on the basis of selectivity for various attributes of the visual scene thus allowing the recording of activity from these funcionally selective areas and the following of patterns of spatio-temporal activation through the visual cortex.

CHAPTER 4

THE VISUAL EVOKED RESPONSE

4.1 Introduction

The visual evoked potential was first recorded by Adrian and Mathews (1934) who demonstrated a response over the occipital cortex following regular flashes of light from a car headlight. With the introduction of averaging techniques more detailed analysis of the response components became possible and the evoked response has been used both clinically, in testing the integrity of the visual pathway, and for research to investigate the response properties of the visual system. The measurement of the visual evoked magnetic response (VEMR) was not until 1975 when Brenner et al. reported the evoked magnetic response to pattern stimulation. Measurement of the VEP and VEMR suggest that both techniques are measuring the same sources (Spekreijse, 1991) and it is therefore appropriate to compare both electrical and magnetic recordings. Although MEG offers a number of advantages over the evoked potential, discussed in Chapter 2, the number of visual evoked magnetic response studies has been limited. However, the available literature will be reviewed and compared with evoked potential literature.

There are a number of methods commonly used to evoke a response from the visual system. The stimulus can consist of either a flash of light or a pattern, termed flash or pattern evoked response. If pattern stimulation is used, the pattern can be reversed, so that light becomes dark and dark becomes light or alternatively, the pattern can appear on the screen for a period of time before disappearing again. These two stimulation paradigms are called pattern reversal and pattern onset respectively. The pattern commonly consists of checkerboards or sinusoidal or square wave gratings. There are two fundamental modes of recording the visual evoked response. Transient stimulation records the response to slow stimulus presentation rates and this yields measures of amplitude and latency. Above a 4Hz stimulation rate the response approximates a sine wave, termed steady state (Harding, 1974), so that phase and amplitude provide the most pertinent measures. This chapter will concentrate upon pattern rather than flash evoked responses and transient rather than steady state stimulation. The morphology and origin of the evoked response will be considered together with the effect of varying stimulus parameters. The studies considered will be reviewed in terms of what they have revealed of the organisation of the visual system.

2.2 The Flash Evoked Response

A typical flash visual evoked response consists of a series of positive and negative peaks occurring between around 30ms and 220ms. The first is a negativity at 30ms, followed by a positivity at 55ms, a negativity at 75ms, a large, major positivity at around 110ms, a negativity at 140ms, a positivity at 175ms and finally, a negativity at around 220ms (Harding, 1974). This is shown in Figure 4.1. The first comprehensive morphological description of the response was provided by Ciganek (1961) who labelled the components as waves I to VII. There a number of different labelling schemes for flash evoked response; that used in this thesis is from Harding et al. (1995) as shown in Figure 4.1. The components of the flash evoked response show a great deal of intersubject variability, although the P2 component at 100-150ms is more consistent (Gastaut and Regis, 1965).

Figure 4.1 The flash visual evoked potential. Redrawn from Harding et al. (1995).

The topography of the flash response was studied in an attempt to determine the origin of the recorded signals. The response was divided into early and late waves with the initial components arising as early as 20-25ms (Cobb and Dawson, 1960). These early components were thought to arise either from the ERG (Allison et al., 1977), from subcortical centres (Harding and Rubenstein, 1981) or from striate cortex (Spekreijse

et al., 1977). However, due to removal of the occipital pole having little effect on the early component, a striate source was shown to be unlikely (Corletto et al., 1967). Subcortical centres, in particular the LGN were shown to be a more likely candidate than the ERG by Harding and Rubenstein (1981) and Harding and Dhanesha, (1986).

The subsequent components at 60-110ms are thought to arise from area 17 while the later components from areas 18 and 19 (Kraut et al., 1985). An investigation of the origins of the scalp recorded responses was provided by Ducati et al. (1988) who made intracortical measurements of the flash response in alert humans undergoing stereotactic surgery. They attributed the early flash response to activation of fast-conducting fibres from the peripheral regions of the retina producing activation of generators deep within the calcarine fissure. However, fast conducting magnocellular fibres are present throughout the entire retina (Kaplan and Shapley, 1986) so on the basis of retinal ganglion cell anatomy there is no reason why there should be selective activation of peripheral representations within striate cortex. The later components were found to be located within the cortex with the earlier P1 component having a more superficial generator than the larger, later P2. More detailed conclusions were provided by studies of the intracortical and scalp recorded response in macaque. Schroeder et al. (1991) was able to differentiate M and P input to layer 4C in V1 although no time differences between the two pathways were noted. In a similar study, Givre et al. (1994) showed that N40 arose from the depolarisation of stellate cells and thalamic axon terminals at the base of layer 4C of V1. P55 originated from layer 3, while P65 was due to hyperpolarisation of stellate cells in 4C. The additional response components were thought to arise from areas other than V1.

The flash visual evoked response has a high degree of intersubject variability. This, coupled with it being able to provide only a very crude luminance modulated stimulus lead to the development of patterned stimuli. Having both luminance modulation and spatial structure, checkerboards and gratings are able to probe in a more subtle manner, the organisation of the visual system.

4.3 Checkerboards versus Gratings

With the introduction of the pattern visual evoked response, both checks and gratings were commonly used. These different stimuli were based on two opposing theories of the organising principles of the visual system, that of edge detection (Hubel and

Wiesel, 1959, 1962) and of spatial frequency filters (Campbell and Robson, 1968). Checks and gratings have fundamentally different properties, which is revealed by examination of their Fourier spectra, shown in Figure 4.2. The grating has a simple spectrum with all power at one frequency and orientation. The checkerboard, however, has a relatively complex spectrum, containing many different spatial frequencies and orientations. The fundamental of the checkerboard is rotated 45° with respect to the gratings and its spatial frequency is $\sqrt{2}$ that of a grating of the same line width.

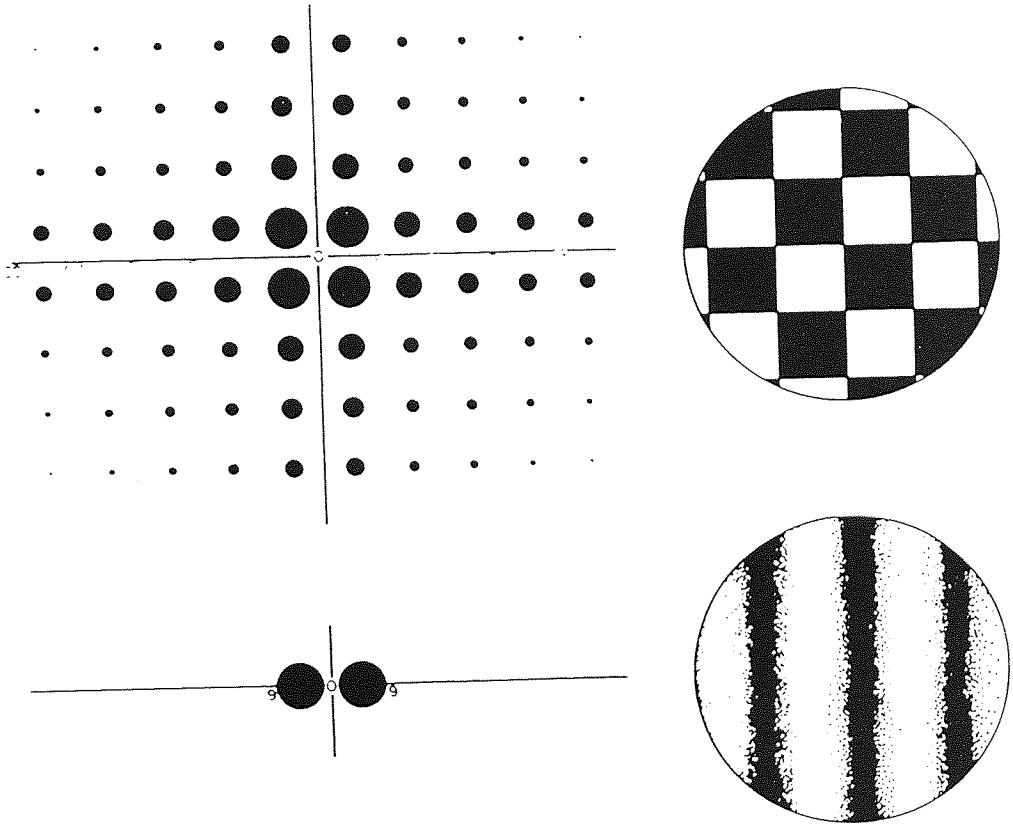

Figure 4.2 Fourier spectra of checkerboards and gratings. Radial distance from the origin represent component spatial frequency and azimuth represents orientation. Spot area indicates the component magnitude. Modified from Bodis-Wollner et al. (1986).

The responses of macaque striate cortex cells to checks and gratings were used to determine the encoding principle of the visual system (DeValois et al., 1979). Both

simple and complex cells were found to act as two dimensional spatial frequency filters with different cells responding to the same position in the visual field being tuned to different spatial frequencies and orientations. This would suggest that gratings provide the most pertinent mode of stimulation. However, the majority of studies, particularly those in the clinical setting, employ checkerboard stimuli. Checks, particularly when reversing, evoke a large response which is highly consistent both within and between subjects (Harding, 1991). Measures of latency and amplitude, particularly of the major P100 response to reversing checks, are used as a diagnostic tool in conditions such as optic neuritis and multiple sclerosis (Blumhardt, 1987). However, due to the multiple spatial frequency components of checks, they are unsuitable for use in testing the spatial frequency tuning characteristics of a response. Hence although the majority of literature is based upon the response to checkerboards, this research will employ only grating stimuli. Nevertheless, to consider the experimental results reported in this thesis in the context of previous research, a review of the response to checkerboard stimulation will be made.

4.4 The Pattern Reversal Visual Evoked Response

The pattern reversal response consists of a relatively simple triphasic morphology, comprising a negativity at around 75ms, termed the N75, a high amplitude positive component at around 100ms, the P100, and a negativity at approximately 145ms, the P145. This is shown in Figure 4.3. Of these, the P100 is the most consistent, showing a high degree of intra and inter-subject stability. It is this component which is primarily used in the clinical setting as its latency and amplitude provide a measure of the integrity of the visual pathway. Its clinical significance is discussed by Blumhardt (1987).

The topography of the reversal response to full field stimulation is straightforward, showing a P100 that is maximal at the midoccipital point. When half field stimulation is used, however, the topography becomes more complex, with the P100 response being recorded at the midline and ipsilaterally. Over the contralateral hemisphere, the response appears of lower amplitude and of opposite polarity and shows a different, more lateral distribution to that of the ipsilateral P100, with the major component, the N105, being of slightly longer latency (Blumhardt et al., 1977). This unexpected distribution became known as "paradoxical localisation" and gave rise to considerable debate as to the cortical origin of the recorded signals.

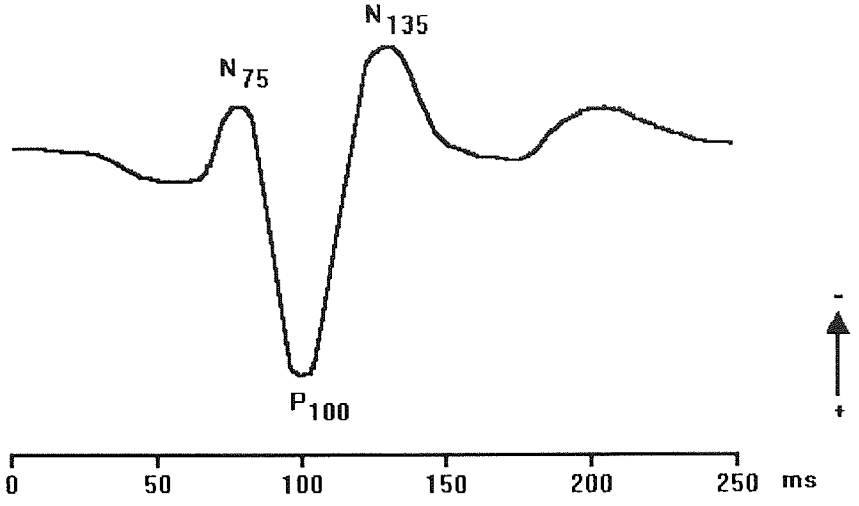

Figure 4.3 The pattern reversal visual evoked potential. Redrawn from Harding et al. (1995).

The independence of the ipsilateral P100 and the contralateral N105 was demonstrated by Blumhardt et al. (1977) who showed that occlusion of the central portion of a 16° half field resulted in marked reduction of the P100 while the N105 was enhanced. Reduction of the field size had an attenuating affect on the N105 to the extent that when the stimulus field was reduced to a 5° radius, the N105 was absent. It emerged that the full field response was a summation of the response to half field stimulation and that the full field midline maximum occurs due to this being the point of minimum cancellation between the ipsilateral positivity and contralateral negativity (Blumhardt and Halliday, 1979).

The contralateral hemisphere being the origin of the observed response was convincingly demonstrated by Blumhardt and Halliday (1979) who showed that hemispherectomy patients maintained the same ipsilateral scalp distribution as normal subjects. This was confirmed by Flanagan and Harding (1986) who, using a source derivation approach, demonstrated that while the source was maximal at the midline, the sink was always contralateral to the half field stimulated.

Indeed, this source configuration can explain the paradoxical distribution of the recorded response. If the response generators lie on the medial surface of the visual cortex, contralateral to the stimulated half field and are oriented perpendicular to the cortical surface this would result in an ipsilateral positivity and a contralateral negativity. When the foveal region of the stimulus is occluded the response is dominated by generators lying deeper within the calcarine fissure. This would result in the reduction of the P100 while the N105 would remain volume conducted through the contralateral cortex and thus appear unchanged, or due to decreased cancellation from the P100, appear augmented as observed experimentally (Blumhardt et al. 1977).

More precise localisation of the response generator was provided by Lehmann et al. (1982) who examined the P100 topography to stimulation of the right, left, lower and upper half fields, using two field sizes of 13° and 26°. For right and left half field stimulation the P100 peaked over the contralateral hemisphere for larger fields and moved more towards the midline for smaller fields. The dipole model used predicted a dipole in the contralateral hemisphere pointing towards the ipsilateral hemisphere. The smaller, 13° field produced a dipole that was angled more towards the midline. For upper and lower half fields the peak response occurred over the midline but was found to be more anterior and of a shorter latency for upper field stimulation. The dipole model predicted a midline dipole pointing down towards the occiput with the upper field dipole being located more anteriorly. The authors concluded that the results were suggestive of an extrastriate origin for the P100. This was supported by the work of Michael and Halliday (1971) and Halliday et al. (1977) who also predicted an extrastriate origin for the P100.

Their conclusions were challenged by Haimovic and Pedley (1982) who predicted that if the response were generated in striate as opposed to extrastriate cortex, patients with LGN or striate lesions would show attenuation or elimination of the P100 while patients with extrastriate lesions should have an intact P100. This was found to be the case, confirming that the P100 was generated in striate cortex, while the contralateral N105, which was absent in these patients, originated from extrastriate areas.

The striate origin of P100 was confirmed by intracortical recordings in macaque of the response to reversal of a square wave grating (Schroeder et al., 1991). N50, which corresponds to human N70, was thought to arise from the depolarisation of stellate cells in layer 4C of striate cortex. P60 (human P100) was considered likely to originate from the depolarisation of pyramidal cells in laminae 2 and 3. The later components were found to originate in extrastriate areas.

Of the limited work done on visual evoked magnetic responses, still less has concentrated on pattern reversal stimulation. The response is dominated by a major component occurring between 90 and 120ms, termed the P100m (Armstrong et al., 1991). Harding et al. (1991) examined the topographic distribution of the major component of the P100m, and the effect of check size using full field and half field stimulation. They found half field stimulation evoked responses which were maximal over the contralateral hemisphere, with the projected source pointing medially. For large check sizes (70') the full field response was shown to be the sum of the response to half field stimulation but some anomalies were noted for small check sizes. A dipole in a sphere source localisation technique was applied and it was found that the source lay close to the midline at depths varying between 2.0 and 5.5cm. Further work (Harding et al., 1992) found that dipole fits could be achieved for check sizes of 22' and 34' but it was not possible to fit a single dipole to a checkerboard pattern of 70'. Both left and right half field stimulation evoked a source in the contralateral hemisphere which pointed medially.

4.5 The Pattern Onset Visual Evoked Response

The morphology of the pattern onset response has been well documented. Initially described by Jeffreys and Axford (1972a,b) it is triphasic, consisting of a positive, negative, positive complex, the peaks of which are labelled C1, C2 and C3 respectively. These occur at approximately 75ms, 100ms and 150ms (Jeffreys, 1977). There are also reports of an additional component, termed C0 which occurs at around 60ms (Lesèvre and Joseph, 1979). This is shown in Figure 4.4. The onset and offset of the pattern do not evoke identical responses with the offset of the pattern evoking a response which is of opposite polarity (Spekreijse et al., 1973). In addition, altering the characteristics of the stimulus have different effects on the onset and offset responses. The check size of the pattern has a more profound effect on the onset response and decreasing the rate of change of contrast attenuates the offset response more than the onset (Kriss and Halliday, 1980). This review will concentrate on the onset response.

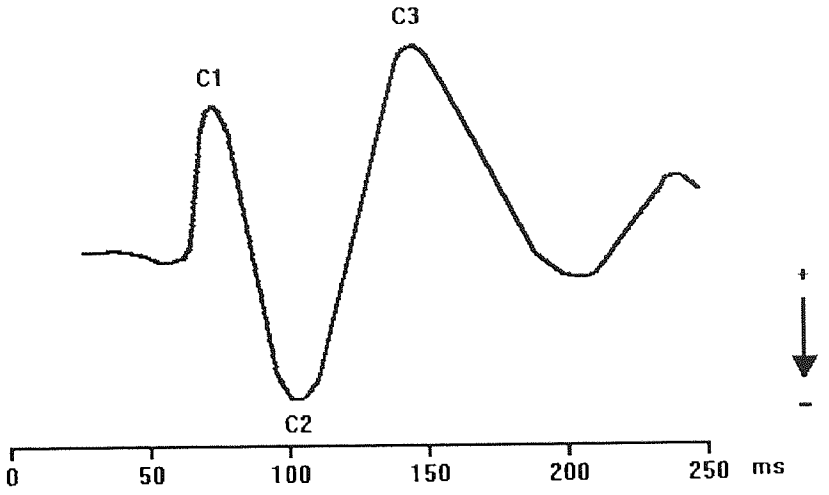

Figure 4.4 The pattern onset evoked potential. Redrawn from Harding et al. (1995).

The components comprising the onset response have been shown to possess different characteristics, with C1 being dependent on the contrast of the pattern and C2 and C3 being more sensitive to the contours of the pattern (Jeffreys, 1977). These differences in characteristics suggest that the components of the response may arise from different visual areas. Among the first to address this inverse problem were Jeffreys and Axford (1972 a,b) who analysed the pattern onset response with reference to the cruciform model of striate cortex. They assumed a dipolar response oriented perpendicular to the cortical surface, as shown in Figure 4.5.

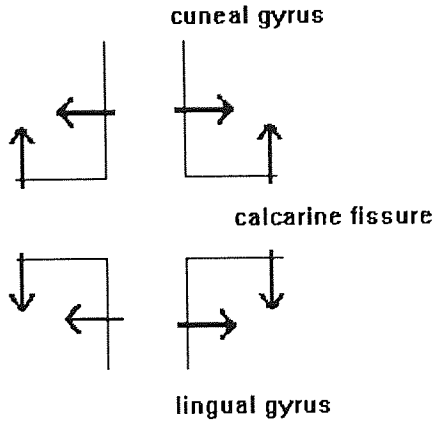

Figure 4.5 Location and orientation of dipole generators of the pattern onset response.

Hence a right half stimulation would produce a response in the left hemisphere with two horizontal and two vertical dipoles pointing laterally. Stimulation of the left hemifield would produce similarly oriented dipoles in the right hemisphere. The vertical dipoles cancel, resulting in two lateral sources pointing in opposite directions. Jeffreys and Axford (1972a) thus predicted the distribution of the evoked response and found that while the C1 component matched the predicted topography, the C2 component did not. They therefore concluded that C1 and C2 originate from areas 17 and 18 respectively.

This conclusion was supported by Darcey et al. (1980) who examined the pattern onset evoked potential to half field and quadrant stimualtion. Analysis of the C1 component found the equivalent current dipoles to be located within striate cortex. Upper and lower half fields required two dipoles to account for the results while left and right half fields required only a single dipole. Their results were thus consistent with a striate origin for C1.

A further theory was offered by Lesèvre and Joseph (1979) who suggested that topography consistent with the cruciform model could be generated by area 19. Indeed, they argued that area 19 was a more likely origin for C1 as the dipoles for upper and lower field stimulation had a separation too great to be contained within striate cortex. They therefore suggested an area 19 origin for C1 and area 18 for C2 while the earlier C0 was thought to arise from area 17. The authors noted, however, that each peak comprising the response need not result from a single, distinct dipole source but may reflect the simultaneous activity of several visual areas. Indeed, they showed that the generator of the C2 component is active at the time of the C1 peak. This was supported by Manahilov et al. (1992) who used Laplacian analysis to determine the origin and independence of the components of the pattern onset response. By altering the parameters of the stimulus and comparing the changes in the two components they concluded that the activity arose as a result of two dipole generators simultaneously active, one in area 17 and one in extrastriate areas. However, their stimulus employed full field presentation and simultaneous activation of opposing sources in both hemispheres may have contaminated the results.

A limitation of these studies is that they did not employ physiologically realistic models of the head, incorporating parameters such as the conductivity of the brain, skull and scalp and the relative thickness of these layers. As discussed in Chapter 2, such changes in conductivity have a significant effect on the source localisation of EEG

signals. Such a model was employed by Maier et al. (1987) who used principle component analysis to propose the spatial and temporal characteristics of the generators of the three pattern onset peaks. Using a three sphere algorithm they found that two dipoles could account for 95% of the response power with the remaining 5% attributed to noise. The first of these dipoles and that responsible for C1 was thought to lie in area 18 or 19 and the second to lie in area 17. The timecourse of the dipoles was thought to overlap with the first source occurring at 80-90ms and the second at 120-150ms. It was a combination of the activity of both dipoles which formed the C2 component which thus arose from both striate and extrastriate cortices.

These conclusions were supported by Ossenblok and Spekreijse (1991) who found that 90% of the response power could be attributed to two dipolar sources corresponding to C1 and C3. Both dipoles were located laterally and they concluded that C1 arises from area 18 and C3 from area 19. However, their stimulus was designed to minimise the presence of the C2 component and it is therefore possible that another source is required to describe the presence of C2.

In contrast, Butler et al. (1987), also using a three sphere algorithm, examined the C1 component as a function of stimulus position in the visual field. Although they only tentatively claim that their data is supportive of a striate origin for C1, the orientation shifts observed following stimulation of different regions of the visual field are as predicted by the cruciform model of striate cortex (Jeffreys and Axford, 1972a,b). Their study therefore provides clear support for an area 17 origin for C1.

Hence there is no consensus regarding the origins of the components comprising the pattern onset visual evoked potential. The differences in results between studies may be due to the different stimulus conditions or different recording positions used by different groups. Indeed, Darcey et al. (1980), recording from 40 electrode points, concluded that many of the differences reported in the literature could be explained by insufficient electrode numbers. The majority of the work in the area has been achieved using electrical evoked responses. Although there have been some studies of magnetic evoked responses these do not always yield conclusive results. Ahlfors et al. (1992) recorded the visual evoked magnetic field in response to octant checkerboards stimulating various foveal or parafoveal areas of the visual field. The sources were found to arise in the contralateral hemisphere but no systematic differences between the responses from upper and lower visual fields were noted. The results suggested the presence of at least two separate sources although no conclusions were drawn as to the origin of these dipole sources. This conclusion is supported by Spekreijse

(1991) who recorded both electrical and magnetic signals and found that there were two active sources contributing to the pattern onset response. The first of these was found to be predominantly radially oriented and originated from extrastriate areas. The second was found to be tangential and the observed retinotopic organisation was suggestive of a source in striate cortex.

Hence although there exists considerable uncertainty as to the origin of the components of both the evoked electrical and magnetic response, many of the studies appear to support a sequence of activation of visual areas that commences in V2 and then progresses to V1. This is a surprising feature of the response as cortical anatomy would suggest the order of activation being first V1 and then V2. Indeed, this has been shown to be the case in rhesus monkey, in which area 18 is activated some 15ms following the activation of V1 (Dagnelie, 1986). However, if the additional component C0 is considered and if this has a striate origin, as suggested by Lesèvre and Joseph (1979), then there is no conflicting sequencing of active areas. Examination of the responses reported by a number of authors (Butler et al., 1987; Maier et al., 1987) do indeed show some evidence of this early component. Being of very low amplitude and as such being difficult to extract from the noise it would not account for a significant proportion of power in the response and may thus be ignored by analysis techniques which fit the most powerful components of the recorded response.

4.6 Underlying Mechanisms of the Pattern Evoked Response

The two modes of stimulation, pattern onset and reversal have been shown to evoke signals of different spatio-temporal characteristics but which, nevertheless, originate in the same cortical areas, V1 and V2. There have been a number of attempts to determine the relationship between pattern onset and pattern reversal and to establish the functional characteristics of the mechanisms that give rise to the recorded signals,

Maier et al. (1987), although working primarily with pattern onset stimuli, suggested two principle components comprising the pattern evoked response. One of these he thought was present only in response to pattern onset stimulation but the other he thought was present in response to all stimulus types, including pattern reversal. The component was thought to arise from area 17 and was recorded maximally 2cm above the inion. When the stimulus was in the peripheral regions of the visual field the

response showed an ipsilateral positivity and a contralateral negativity.

Estévez and Spekreijse (1974) investigated the relationship between the response to pattern onset and reversal stimulation. They devised a set of stimuli that were intermediate between reversal and onset/offset modes of presentation. They concluded that the reversal response comprises an interaction between onset and offset responses but reflects mainly the offset component, being associated with an abrupt decrease in contrast with little sensitivity to the pattern itself.

Similar conclusions were reached by Kriss and Halliday (1980) who examined the topography of the responses recorded to pattern onset, offset and reversal using full fields and left, right, upper and lower half fields. The full field response appeared similar for all stimulus types but for the half field responses differences began to emerge. Although the scalp distribution recorded to pattern onset stimulation for left and right half fields was not in agreement with previous studies, they showed a consistent similarity between the topographies of the response recorded to offset and reversal modes of stimulation.

However, Skrandies et al. (1980) did not find such a similarity between offset and reversal. He suggested that the responses were not related, basing his conclusions on the differing latencies and topographies of the two recorded waveforms. Jeffreys (1977), however, supported the offset contribution and proposed that the reversal response is comprised of the C1 component of the onset response and the main positive offset component.

Kulikowski (1977b) analysed the responses to the onset and reversal of gratings in terms of pattern and movement sensitive mechanisms and examined their interaction. Using a technique of adaptation, he showed that reversal responses were not sensitive to the pattern of the stimulus and therefore proposed that the reversal response contains motion sensitive rather than pattern sensitive components. This was supported by Spekreijse (1985) who postulated that the response arises from motion onset and offset.

Hence although complete agreement has not been reached, the evidence presented by various groups tend to suggest that the reversal response signals sensitivity to the contrast of the pattern rather than its detail. There is also significant evidence to suggest that it reflects the activity of motion sensitive mechanisms. The onset response, however, is more likely to arise from mechanisms which are sensitive to the

pattern or form of the stimulus.

4.7 The Evoked Response to Grating Stimulation

The use of grating stimuli in evoked response investigations has been limited. The response to both grating onset and reversal is a sequence of two complexes termed N1-P1 and N2-P2 (Kulikowski, 1977a,b; Jones and Keck, 1978; Parker and Salzen, 1977; Plant et al., 1983). This is shown in Figure 4.6. The behaviour of these two complexes differs between onset and reversal presentation, however, with N2-P2 being considerably more marked following grating onset rather than reversal (Plant et al., 1983).

The spatial frequency tuning curves for the two stimulus modes are shown in Figure 4.7. The N1-P1 complex shows similar behaviour between onset and reversal modes of stimulation, although the amplitude is higher and peaks at higher spatial frequencies for onset. For both presentation modes N1 peaks at higher spatial frequencies than P1 which in turn peaks at higher spatial frequencies than P2 (Plant et al., 1983). This similarity for reversal and onset presentation was also found by Kulikowski (1977a,b) for low spatial frequency gratings and this was attributed to the stimulation of transient mechanisms. With the introduction of higher spatial frequencies this similarity is lost and Kulikowski suggests that this is due to the increasing activity of the pattern detection mechanisms responding to onset stimulation. This is consistent with Parker and Salzen's (1977) hypothesis that N1-P1 represents the transient system and N2-P2 the sustained system.

A third, earlier complex was noted by Jones and Keck (1978) who termed this N0-P0. This complex was found to saturate at low contrasts and was also attributed to the transient mechanism. A similar positive complex, termed P1a and P1b was described by Plant et al. (1983) which occurred at spatial frequencies below 2 cycles/degree in 7 of their 13 subjects.

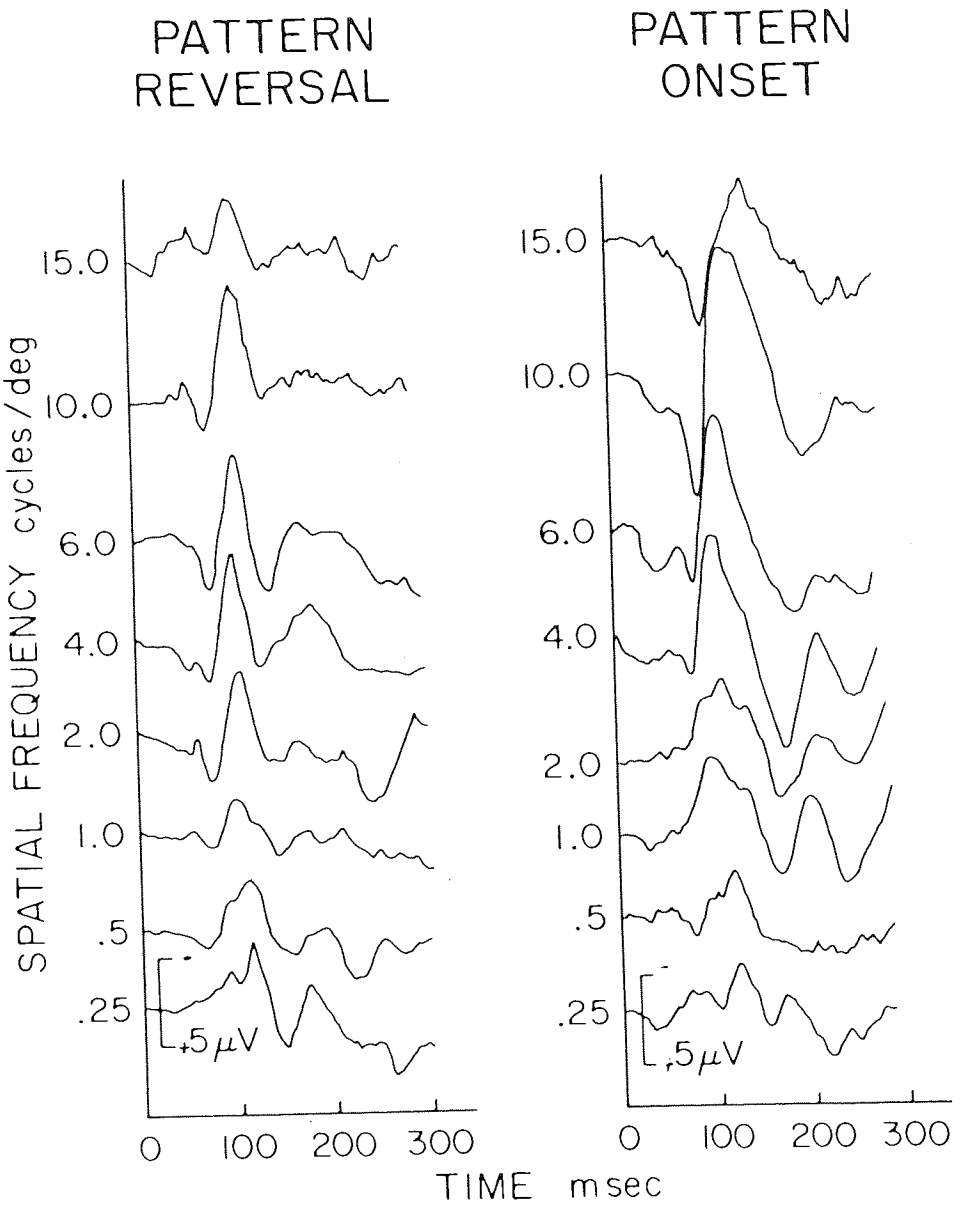

Figure 4.6 The gratings evoked response. Modified by Regan (1989) from Plant et al. (1983).

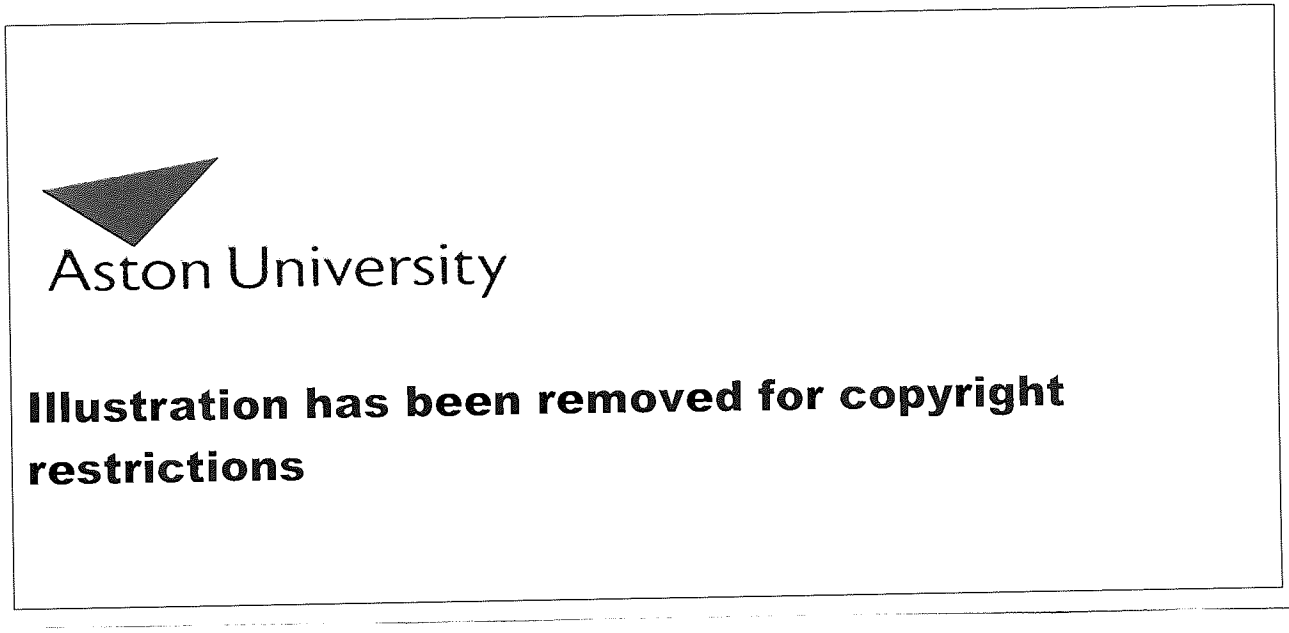

Figure 4.7 Spatio-temporal tuning characteristics of the N1-P1 and N2-P2 components of the grating evoked response. From Plant et al. (1983).

Cortical localisation of the components of the grating onset response was attempted by Aine et al. (1990). Single and two dipole models were used and the dipole position was coregistered with the MRI. Unsurprisingly, it was found that when full field stimulation was employed, a two dipole model, one dipole for each hemisphere, described more of the signal variance than a single dipole in either the left or the right hemispheres. Spatial frequencies of between 1 cycle/degree and 6 cycles/degree were used although comparison is difficult as the results from different subjects are shown for the different spatial frequencies. It was noted that the use of different spatial frequencies produced a change in the position of the dipole source although no systematic changes in dipole location were described. The results suggest that the earlier dipoles lies within striate cortex while the later components originate from extrastriate cortex.

4.8 The Effect of Stimulus Parameters on the Evoked Response

The comparison of results from different studies is complicated by the use of different stimulus parameters. Contrast, luminance, spatial frequency, field size and the position of the stimulus in the visual field all affect the response in various ways yet they are seldom similar in different experiments, making the interpretation of results between groups very difficult. This section will examine the effect of the above parameters on the latency, amplitude and distribution of the components of the pattern visual evoked response.

4.8.1 Contrast

There is general agreement within the literature that an increase in the contrast of the pattern produces a decrease in the latency and an increase in the amplitude of the response, to a certain saturation point. More specifically, Kurita-Tashima et al. (1991) found that the P100 pattern reversal component exhibited contrast saturation but that the N75 did not, suggesting different cortical generators for the two components. Similarly, Jeffreys (1977a,b) found that the thresholds and latencies of the components were dependent on contrast and this was more so for the C1 component of the onset response. None of the onset components were found to be dependent on the polarity of the pattern contrast (i.e. black on white or vice versa).

Similar effects of contrast were observed for the grating evoked response (Jones and Keck, 1978). The N1 component showed the most clear and consistent effect of contrast with an increase in amplitude and decrease in latency with contrasts up to 25% when saturation occurred. However, a single electrode pair was used, positioned at Oz and referred to O1. As the signal would have been recorded from both electrodes contamination of the results from reference activity may have occurred and obscured contrast effects on other components. For N1 to have shown such a clear change with spatial frequency it must be assumed its origin is away from the midline, resulting in the recorded signal being greater at one of the electrode sites.

The high sensitivity of the response to the contrast of the pattern was demonstrated by Kulikowski (1977a) who examined the correlation between the evoked response and psychophysical measures of grating detection. At low contrasts, the response consisted of two early and two late components. With decreasing contrast the early components were found to be more attenuated than the later ones, although this was not so for short stimulus durations when all the components were similarly reduced.

P150 was found to be highly correlated with the detection threshold, being distinguishable just above threshold. The responses to stimuli at detection threshold were averaged separately on the basis of whether the subject detected the stimulus. It was found that the detected stimuli produced clear responses, those for which the subject was uncertain produced less clear responses and the response to those stimuli which were not detected showed no distinguishable components. Examination of false positive detections eliminated the possibility of the response reflecting cognitive expectation. Thus the late components of the visual evoked response components correlate well with subjective threshold.

4.8.2 Luminance

The effect of luminance on the amplitude of the pattern reversal visual evoked response is minimal (Halliday, 1977). There is a small effect on the latency of the P100 component with a reduction in retinal illumination by a factor of 10 resulting in an increase in latency of 15ms (Halliday, 1977). The effect on the pattern onset response is similarly small although the response is reduced and delayed when luminance approaches threshold (Spekreijse et al., 1973). If the contrast is maintained at a fixed level, a reduction in luminance does not affect the amplitude of the response but the latency increases by approximately 30ms for a factor of 10 reduction in the luminance (Van der Tweel et al., 1979). A comparison of the VEP under photopic and scotopic conditions was made by Benedek et al. (1993). At scotopic levels, when the response reflects rod activation, both flash and pattern reversal stimulation produced similar responses. The amplitude was similar to the photopic pattern response but the latency was markedly longer. The topography of the response was noted to be different to the photopic VEP and this was attributed to the absence of a foveal response under scotopic conditions.

4.8.3 Spatial frequency and check size

In general, the literature tends to suggest that an increase in check size or decrease in spatial frequency will produce an increase in the amplitude of the response components, up to a maximum, when further increases will then cause a decrease in amplitude. For pattern reversal checkerboard stimuli, this maximum occurs at around 10-20' (Regan and Richards, 1971). This is also the case for the response to checkerboard onset but not for offset, which exhibits less variation with check size (Spekreijse et al., 1973). For gratings, this optimum spatial frequency is 4 cycles/degree for achromatic modulation (Jones and Keck, 1978). For chromatic gratings, the peak resonse has been reported as 4 cycles/degree (Murray et al., 1987) and 1-2 cycles/degree (Rabin et al., 1994). The situation is complicated by the

confounding effects of contrast and position in the visual field. A change in contrast affects the shape of the amplitude-check size curve (Spekreijse et al., 1973) and due to variations in receptive field sizes with eccentricity, larger field sizes and different areas in the visual field will provide different results (Meredith and Celesia, 1982). The decrease in optimum spatial frequency with increasing eccentricity for gratings was demonstrated by Parker and Salzen (1977) who found that the maximum N2-P2 amplitude was produced by a 6 cycles/degree stimulus for a 1° central field, 3 cycles/degree for a 3° field and 1 cycle/degree for a 1-3° annulus.

A comprehensive study of the effect of check size on both latency and amplitude of the main components of the pattern reversal response was made by Kurita-Tashima et al. (1991). They found that the latencies of the P100 and N145 components exhibited a curvilinear relationship with check size with the minimum occurring at around 35'. Both the latency and amplitude of the N75 component decreased linearly with the logarithm of the check size. Check size was found to modulate the latencies and amplitudes of each component separately, which would indicate different cortical generators for each component. The latency of the response to chromatic gratings was also found to increase with increasing spatial frequency, although for low spatial frequencies below 1-2 cycles/degree, the latency could show an increase (Rabin et al., 1994). Indeed, latency was found to be a more consistent measure than amplitude and Rabin et al. (1994) suggested that latency may be more indicative of response characteristics than amplitude. This is a valid point as although the amplitude of the evoked response may provide an indication of the number of units responding to a given stimulus, it is the latency that can reflect the processing time of a recorded component and can thus indicate the similarity of processing mechanisms of different recorded responses.

An explanation for the increase in latency with increasing spatial frequency was proposed by Kulikowski (1977a). He suggested that the effect may arise from the decrease in apparent contrast at high spatial frequencies due to the visual system's decreased sensitivity at higher spatial frequencies. When the increased threshold was controlled for, the effect of spatial frequency was found to be insignificant. However, this was only partly supported by Jakobson and Johansson (1992) who found that when contrast was held at a constant level, there was a strong effect of spatial frequency on latency. When the contrast was maintained at a fixed suprathreshold level, the effect on latency was diminished but a small increase in latency with spatial frequency persisted. By comparing the results with ERG latencies, it was concluded that the latency effects arose in the retino-cortical pathway.

Plant et al. (1983) found that the different components in the response behave differently to changes in the spatial frequency of sinusoidal gratings and do so independently of one another. Above 2 cycles/degree there was a monotonic increase in latency with spatial frequency and the amplitude of the N2-P2 complex was found to be sensitive to changes in spatial frequency. Below 1 cycle/degree onset and reversal stimuli produced similar changes. Above 1 cycle/degree the reversal response was found to be dominated by a positive component and the onset response by a negative component. Above 2 cycles/degree this negative onset component was of higher amplitude and peaked at a higher spatial frequency than the positive reversal component. For both modes of presentation the N1 peaked at higher spatial frequencies than the P1 which in turn peaked at higher spatial frequencies than the P2 component. Plant compared his results with those from checkerboard stimuli and concluded that N1 seemed to parallel the checkerboard onset C2 component, showing a similar increase in latency with decreasing check size. The amplitude of the response evoked by checks does not vary as much as that evoked by grating stimuli and this may be due to cortical cells responding to the spatial Fourier components of the checkerboard (DeValois et al., 1979) so cells tuned to higher spatial frequencies will also respond.

4.8.4 Field Size

There is an increase in the amplitude of the major components with increasing field size, in accordance with the increase in cortical area stimulated. Nesfield (1992) found no significant effect of field size on the amplitude or latency of the pattern reversal N145 component but the P100 amplitude was significantly decreased following central occlusion and decreased field size. Using sinusoidal gratings, Plant et al. (1983) demonstrated that for any spatial frequency, the amplitude of the response increased with increasing field size. Saturation occurred at a smaller field size for higher spatial frequencies. They noted that saturation occurred when the stimulus contained approximately 50 cycles. However, psychophysically measured contrast sensitivity is independent of field size and cycle number when ten or more cycles are displayed (Howell and Hess, 1978). This is consistent with reports of Rabin et al. (1994) that the amplitude but not the latency of the chromatic evoked response increases with increasing field size up to a saturation point of 20 degrees. The independence of latency on field size may indicate a constant mechanism responsible for detection of the stimulus, evidenced by the saturation of the contrast sensitivity at 4 cycles. The increase in amplitude may simply reflect increasing number of cells responding to a

more spatially extensive stimulus.

4.8.5 Position in the visual field

Due to cortical magnification, whether the fovea is stimulated or occluded has a profound effect on the amplitude of the response. However, when eccentricity is held constant, there remains a high degree of variation in both the amplitude and distribution of the response when different regions of the visual field are stimulated. Nesfield (1992) investigated the effect of the stimulus position in the visual field using pattern reversal stimulation. She found the amplitude of both the P100 and N145 were significantly decreased following upper half field compared with lower half field stimulation. Perhaps the most marked effect of stimulus position is on the distribution and polarity of the recorded response. The polarity of the major components are reversed between upper and lower half fields for both pattern reversal (Michael and Halliday, 1971) and pattern onset (Jeffreys, 1977, Lesèvre and Joseph, 1980) stimulation. This is in accord with the topographical representation of the visual field in the cortex. As described in Chapter 3, the upper visual field projects to the inferior surface of the calcarine fissure while the lower visual field projects to the superior surface. Such a difference in active cortical regions would result in the observed polarity shifts. Studies employing limited numbers of recording positions may find this orientation shift manifested in amplitude changes.

4.9 The Chromatic Evoked Response

The number of evoked response studies investigating the chromatic mechanism have been extremely limited. The chromatic response is usually recorded to isoluminant red/green gratings or checkerboards which may be reversing or onset-offset. The major finding is that the chromatic response is of opposite polarity to the achromatic response, being dominated by a negative component that peaks some 15-20ms later (Jeffreys, 1989; Murray et al., 1987; Crognale et al., 1992,1993; Rabin et al., 1994).

A major problem facing the recording of chromatic evoked responses is that of removing luminance artefacts from the display. Due to chromatic aberrations and display equipment alinearities a significant luminance artefact may appear and this is especially marked at high spatial frequencies (Bradley et al., 1992). However, the chromatic evoked response has been shown to arise from chromatic and not luminance mechanisms (Regan, 1973). The chromatic evoked response to low spatial frequency gratings has been shown to be robust and that the introduction of small luminance

artefacts into the stimulus due to variations in the subjective isoluminance point produce minimal effects on the recorded response (Crognale et al., 1992,1993; Rabin et al., 1994).

Regan (1973) used a system of mirrors to remove chromatic aberrations and demonstrated a polarity shift between upper and lower half fields using reversing checkerboards. Red/black, green/black and red/green checks all showed similar topography. A chromatic evoked response using checkerboard onset was demonstrated by Regan and Spekreijse (1974). Deuteranopes were shown to have a response to red/black and green/black checks but not red/green checks. Subjects with normal colour vision, however, showed a clear response to all three stimulus types. Again, the topography of the response was similar between isoluminant chromatic and monochromatic stimuli.

However, this topographical similarity between luminance and chromatic modulated stimuli was not supported by Murray et al. (1987). The effect of changing the ratio of red to green and thus the luminance in the stimulus was investigated using sinusoidal gratings. They found a polarity shift at isoluminance with the major component of the response at 120-140ms changing from positive for luminance modulated gratings to negative around the isoluminant point with no change in latency. This was most marked at 4 cycles/degree but the changes were not so clear for 1 cycle/degree gratings. The results contrast sharply with the those of Regan (1973) and this was ascribed to the use of gratings rather than checks. Indeed, Murray et al. (1987) also used checks of 15' and 30' and reported the change at isoluminance was not apparent. The majority of the study used a single recording electrode so changes in the topography of the response were not investigated. The results were attributed to selective activation of the parvocellular opponent mechanisms for isoluminant gratings.

A comprehensive investigation of the response to gratings of various positions within colour space was reported by Rabin et al. (1994). Like Murray et al. (1987) they found the chromatic response was of higher amplitude when onset stimulation was used rather than pattern reversal. This was attributed to reversal stimulation leading to adaptation of chromatic mechanisms. They found that while the luminance response was of low amplitude and variable, the response to gratings modulated along the L/M and S axis were robust. The chromatic response was dominated by a negativity at 120-140ms although the S modulated response peaked some 25-30ms later. The chromatic response was shown to have a bandpass spatial frequency tuning function, peaking at 1-2 cycles/degree with a high frequency cutoff of 5-10 cycles/degree.

Latency showed a bandpass function, with a slight tendency to increase for low spatial frequencies although the main increase was for high spatial frequencies, consistent with the decrease in chromatic contrast sensitivity for higher spatial frequencies (Mullen, 1985; Anderson et al., 1991). Temporal frequency tuning was also investigated using pattern reversal stimualtion. Amplitude was found to decrease slowly with increasing temporal frequency with a slight increase at 4.125Hz which was more marked for S cone stimulation. No explanation was offered for this effect.

However, this study made use of only a single recording electrode 1.5cm above the inion, referred to the earlobes. Such a limited recording area, typical of many VEP studies, cannot distinguish between a reduction in amplitude and a change in response topography. Descriptions are limited to the latency and amplitude of the recorded signal and do not discuss details of the response topography or its cortical origins. An exception to this, both in methodology and results, was a study of the response to homogenous, unpatterned colours (Paulus et al., 1988). The VEP was recorded to the appearance of a homogeneous colour which replaced a grey background. The topography of the evoked response to full and half field stimulation was shown to be similar to that following achromatic stimulation and the authors suggested a V1 source for the major component, the N87. However, the homogenous nature of the stimuli may have activated a different class of cells than would be activated following spatially structured stimuli. For example, the double-opponent cell would not be activated by such a diffuse coloured stimulus (see Chapter 2 for a discussion of cell types). Furthermore, the luminance of the coloured and grey screens were not accurately matched and it remains possible the results obtained were due to luminance modulations in the stimuli.

Such differences in chromatic and luminance modulated stimuli were noted in one of two subjects by Krauskopf et al. (1989) in a magnetic evoked response study. Both chromatic and luminance stimuli evoked triphasic responses although the latency of the response to achromatic stimulation peaked 10ms prior to that evoked following chromatic stimulation. One subject showed a 50 degree orientation shift of the dipole source following chromatic rather than luminance stimulation and they claim this provides evidence for spatially separate processing of chromatic and luminance information. However, the chromatic stimulus comprised red/black circles and thus combined chromatic and luminance information. The results cannot, therefore be attributed solely to the presence of chromatic information.

The clinical applications of chromatic VEPs was explored by Crognale et al. (1993)

who examined the changes in the morphology of the response as the stimulus passed through different regions in colour space. While achromatic modulated stimuli produced small, variable responses, those evoked by chromatic stimulation were of high amplitude. The response to S cone modulation showed longer latencies than to L and M cone stimulation. The latencies of the responses to different directions in colour space were found to change with colour-deficient observers. Latency changes were also noted along the S axis for subjects with diabetes. It was noted that small deviations from isoluminance produced little or no change in the VEP.

These studies demonstrate that the chromatic evoked response has morphology distinct from that of the luminance evoked response and that this is not due to chromatic aberrations. The studies have too limited a recording area to determine if this results from a different distribution of the same activity or if different mechanisms are responsible for the chromatic and luminance evoked responses. However, the change in latency that is consistently reported; the luminance evoked response peaking some 10-20ms prior to the the chromatic response, suggests that a different processing mechanism may underlie the two response types.

4.10 The Motion Evoked Response

Although it is assumed that pattern reversal stimulation activates motion sensitive mechanisms, very few studies specifically designed to record from motion sensitive areas have been reported. The motion VEP was recorded by Kuba and Zuzana (1992) who examined the effect of temporal frequency, position in the visual field and stimulus type; checkerboards versus random dots. The majority of their subjects displayed a dominant negativity, the N160, usually preceded by a positivity, the P105. With increasing temporal frequency the positivity became dominant and this was attributed to blurring of the stimulus at motion onset imitating the pattern offset response. Indeed, when an irregular structure, a random dot display, was used as a stimulus this positivity disappeared. Optimal stimulus conditions were found to be low contrast random dots at low luminance levels. Kuba and Zuzana concluded that the N160 is motion specific whereas the P105 is pattern dependent.

However, not all studies agree with these conclusions and the positivity has been described as the dominant component. Bach and Ullsrich (1994) examined the effect of the stimulus cycle on the relative contributions of these two components. Duty cycle was defined as the percentage of display time the stimulus was in motion and the

negativity was found to decrease significantly with an increase in duty cycle. This was attributed to adaptation effects.

A comprehensive study of motion evoked responses was that of Anderson et al. (in preparation). Using neuromagnetometry, they recorded a biphasic component at 166ms and 220ms. Co-registering the dipole solution with MRI data they were able to demonstrate that the response originated in an area in the minor sulcus immediately below the start of the ascending limb of the superior temporal sulcus. The area was shown to be selective for low spatial frequencies and a wide range of temporal frequencies and saturated at low contrasts. They concluded that this was the motion area MT (V5) and that it represented a stage of motion processing within the magnocellular pathway.

4.11 Summary

The evoked response studies described here have mapped in detail the morphology of the visual evoked response and the effect of various stimulus parameters. The use of a pattern onset stimulus appears to maximise differences in the evoked response following presentation of stimuli of different luminance and chromatic content. Hence this stimulus mode will be used for the experiments in this thesis. There has been considerable debate as to the cortical origin of these responses but agreement has yet to be reached. However, little attention has been paid to the implications of the activation of these cortical regions. Evoked response measurements are unique among techniques as they combine good spatial resolution with excellent temporal resolution. It should therefore be possible to map out the sequence of activation of different cortical regions. In this respect, previous studies have been of limited value in that they rely on response properties to infer the cortical location of a particular response component. With co-registration of signal information with MRI data it is now possible to identify with much more certainty the active cortical areas and their sequence in the visual process.

This thesis will explore the activity evoked by stimuli designed to selectively activate functional areas of visual cortex. Both response properties and MRI data will be used to determine the location, temporal sequence and spatio-temporal characteristics of the processing of a number of visual attributes including colour and the interaction of colour and motion.

CHAPTER 5

CORTICAL ORIGINS OF THE CHROMATIC EVOKED MAGNETIC RESPONSE

5.1 Introduction

In the human visual system, the segregation of information on a functional basis begins at the retina with two distinct streams of information, the magnocellular and parvocellular pathways (see Chapter 3 for a review). It has been proposed that the magnocellular channel transmits low spatial frequency and high temporal frequency information and its function has been linked with motion perception (Livingstone and Hubel, 1984; Derrington and Lennie, 1984; Livingstone and Hubel, 1988b; Merigan et al., 1991; Schiller, 1991; Van Essen et al., 1992). The parvocellular stream carries two types of information, both chromatic signals and luminance signals which are thought to form the substrate of colour and pattern perception respectively (Ingling and Martinez-Uriegas, 1985; Livingstone and Hubel, 1984; Derrington and Lennie, 1984; Livingstone and Hubel, 1988b; Merigan, 1990; Schiller, 1990; Van Essen et al., 1992). There remains some debate as to how both these information types are transmitted together while retaining their later separability. It has been proposed the information is multiplexed and extracted at the level of the cortex (Ingling and Martinez-Uriegas, 1985; Ingling, 1991). Alternatively, a separate non-spatially opponent Type II cell has been suggested as the carrier of chromatic information (Rodieck, 1991). Hence in some manner, both chromatic and luminance information are transmitted in the parvocellular channel, thus sharing a common pre cortical pathway.

Investigation of the primary processing of chromatic signals has been limited. Descriptions of the chromatic evoked response tend to concentrate on the amplitude and latency of the principle response peak rather than to characterise its distribution or to determine its cortical origins. The recorded response arising from chromatic mechanisms rather than luminance artefacts was demonstrated by Regan (1973). As discussed in the previous chapter, the chromatic evoked response has been noted to be of opposite polarity to the achromatic response and to peak some 15-20ms later (Murray et al., 1987; Jeffreys, 1989; Rabin et al., 1994). However, little additional characteristics of the response have been established. Although several studies have described the response topography (Darcey et al., 1980; Krauskopf et al., 1989)

red/black and green/black checks or gratings tend to be employed. As stimuli such as these contain both chromatic and luminance modulations, the results cannot be attributed solely to chromatic mechanisms.

This chapter therefore aims to investigate the evoked magnetic response to isoluminant chromatic stimulation. Both retinotopic organisation and topographic distribution will be used to determine the cortical origins of the recorded response. To ensure the results do not arise as a consequence of luminance artefacts in the stimulus, two control experiments will be performed. Firstly, the results will be compared with the evoked magnetic response to achromatic gratings. Similarities between the response evoked from the two different stimuli would indicate the chromatic waveform being contaminated by luminance artefacts. Secondly, a small field size will be used to estimate the effect, if any, of display equipment non-linearities and retinal inhomogeneities. Finally, co-registration between MEG and MRI data will be used to establish the cortical origins of the recorded response.

5.2 Method

5.2.1 Stimuli

Sinusoidal stimuli were generated using a Cambridge Research Systems VSG2/2 grating generator as described in section 2.9. Red and green gratings were generated and modulated independently to provide physical isoluminance. The gratings were then combined 180 degrees out of phase to produce physically isoluminant red/green gratings. This is shown in Figure 5.1. The isoluminant point is typically determined by heterochromatic flicker photometry. However, the contrast sensitivity to chromatic gratings is not independent of spatial or temporal frequency and therefore such a method cannot reliably identify the isoluminant point when the experimental stimulus is set at lower spatial and temporal frequencies. An additional complicating factor is that there appears to be a degree of variation in the spectral characteristics of colour opponent cells, resulting in a lack of an absolute null point at which all red/green opponent cells cease to respond (Zrenner, 1983b; Logothetis et al., 1990). Scalp recorded evoked magnetic responses require in the order of one million synapses to respond before a response can be measured (Hämäläinen et al., 1993). Hence the above considerations have little effect on the gross recorded response and the isoluminant point was estimated to be at physical isoluminance. Similarly, small departures from the isoluminant point due to chromatic aberrations and non-linearities

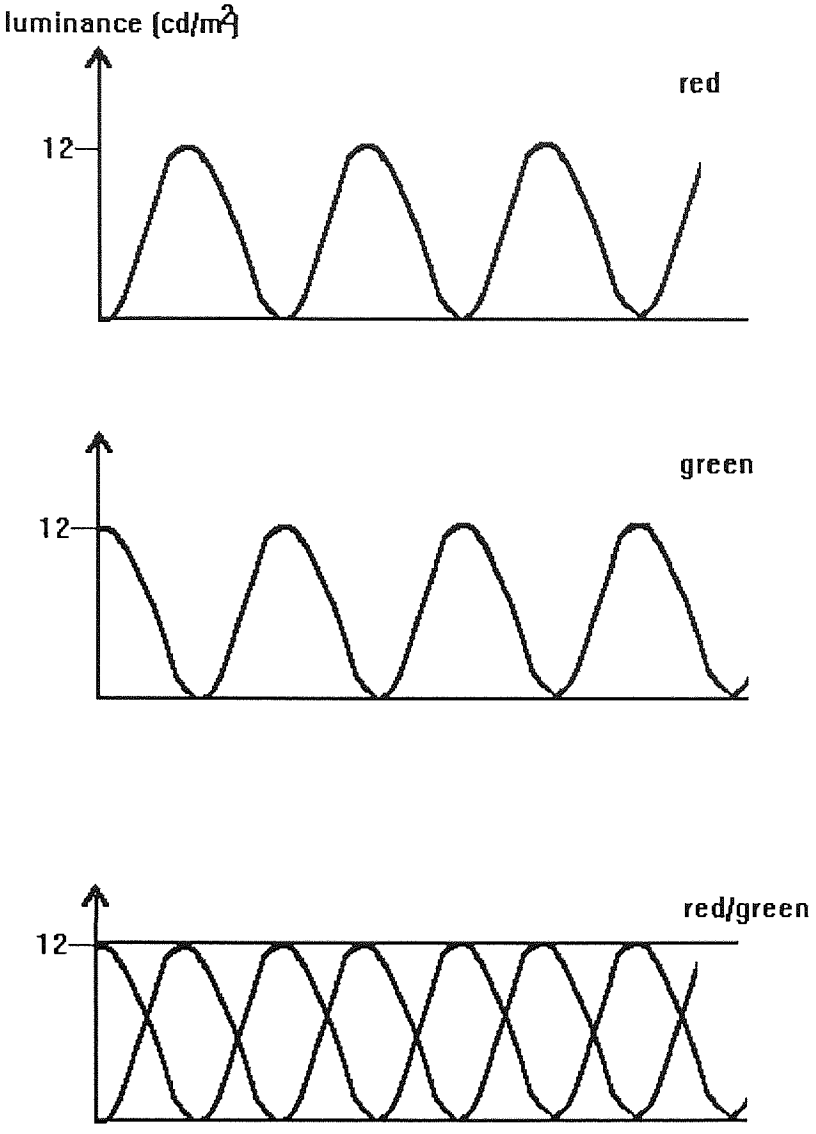

Figure 5.1. Generation of physically isoluminant gratings

in the display equipment were assumed to have minimal effect on the recorded results. This approach is supported by the minor departure of subjective isoluminance from the physical isoluminant point shown by studies which have used subjective measures of isoluminance (Mullen and Boulton, 1992) and by the lack of change in VEPs when the stimulus deviates slightly from subjective isoluminance (Crognale et al., 1992, 1993; Rabin et al., 1994).

However, even if it is assumed that the stimulus display is at subjective isoluminance, chromatic aberration can have the effect of introducing significant luminance modulation in the stimulus (Bradley et al., 1992). Hence two control conditions were recorded to ensure the results to chromatic stimulation were not due to luminance artefacts. The first of these recorded the response evoked by 20% and 80%

achromatic gratings. The second recorded the response evoked from a reduced field size of 2 x 2 degrees to minimise artefacts induced by retinal inhomogeneities and display equipment non-linearities. These control conditions therefore enabled the contribution of luminance artefacts to the response to be estimated.

The mean luminance of the display was 12cd/m^2 for both stimulus conditions. The spatial frequency was 1 cycle/degree and the gratings were presented horizontally using a square temporal envelope of 1s. During an interstimulus interval of 500ms the gratings were replaced with a homogeneous background of the same mean hue and luminance. Pattern onset stimulation was selected as this mode of presentation activates the sustained cells of the colour-opponent system and has been shown to produce results that are able to differentiate between different colour contrasts more effectively than pattern reversal stimulation (Murray et al., 1987). The phase of the gratings was randomised for each stimulus presentation as this can increase the amplitude of the response (Murray et al., 1987). All stimuli were viewed binocularly through a system of front silvered mirrors at a distance of 3 metres and fixation was maintained by use of a fixation mark.

To establish the retinotopic properties of the evoked response and therefore its likely cortical origin, the stimuli were designed with reference to the cruciform model of striate cortex (Jeffreys and Axford, 1972a,b), shown in Figure 5.2. This predicts the orientation of dipole generators in striate cortex responding to stimulation of different regions of the visual field.

The cruciform model therefore makes specific predictions regarding the orientation of dipole generators within area V1 activated by stimulation of various regions of the visual field. Stimulation with a half visual field would produce cancellation of the vertical dipoles and a resultant dipole contralateral to the visual field stimulated, pointing laterally towards the contralateral hemisphere. Stimulation of the right upper quadrant would produce a resultant dipole pointing down and to the left and stimulation of the right lower quadrant would produce a dipole pointing up and to the left. Confining the visual stimuli to quadrants of the visual field therefore enables the cruciform model to be used to assess the likelihood of a response originating in striate cortex, or area V1.

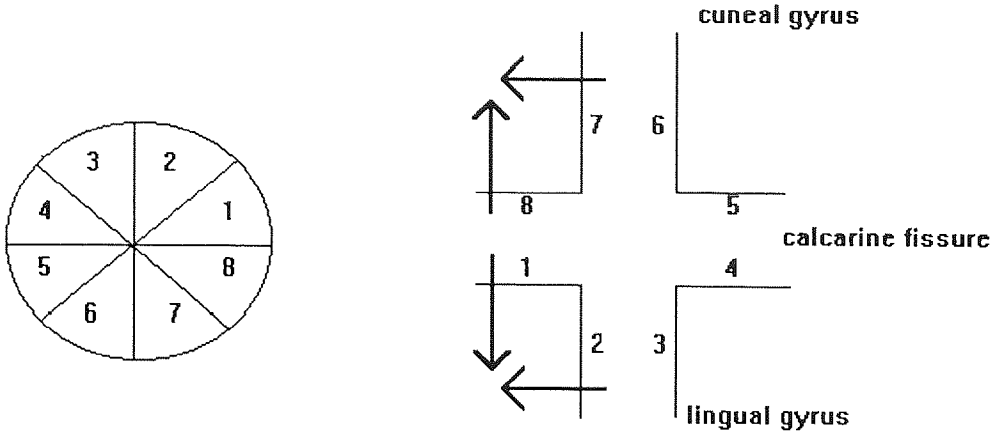

Figure 5.2 The cruciform model of striate cortex showing the projection of different regions of the visual field. The arrows indicate the direction of dipole generators activated by pattern onset stimulation of the right visual field.

The stimuli were therefore presented in each quadrant of the visual field separately. Analysis of the results utilised a single equivalent dipole model so activation of both hemispheres or spatially separate dipoles above and below the calcarine fissure would reduce the validity of the results. To restrict input to a discrete region of area V1 and to avoid activation of multiple regions of cortex due to dual representation of the horizontal and vertical meridians the stimuli were displaced 0.5 degrees from the principal meridians.

The field size selected for the experiment was 4 x 6 degrees. This was judged the optimum size for minimising luminance artefacts due to retinal inhomogeneities while ensuring the stimulated area of visual field extended sufficiently along the horizontal meridian so that its representation projected onto the medial surface of the calcarine fissure. MEG is sensitive only to the tangential components of the magnetic field so that confining the stimulus to the central few degrees, while minimising the likelihood of luminance artefacts, would render MEG relatively insensitive to the signal due to the representation of this region on the occipital pole with its resulting radial orientation. To ensure this field size did not result in the recorded response being contaminated by luminance artefacts two control experiments were performed. The first recorded the evoked magnetic response to gratings of 20% and 80% achromatic contrast. The second recorded the evoked magnetic response to isoluminant chromatic gratings in a

2 x 2 degree field. If luminance artefacts in the large field case are minimal it would be expected that the small field case would produce similar but lower field strength signals.

5.2.2 Procedure

The visual evoked magnetic response was recorded using the Aston 19-channel SQUID magnetometer as described in section 2.9. The subjects were seated inside an electromagnetically shielded room and viewed the stimuli binocularly by use of a system of front-silvered mirrors. This enabled the dewar to be positioned above the occipital cortex, directly above the back of the head. The dewar was centred above EEG 10-20 electrode position Oz with the position of each gradiometer determined more precisely using a Polhemus three-dimensional digitising system. The subjects maintained position by use of a bite bar. The door to the shielded room was closed and the bias voltage of each of the gradiometers adjusted so that the gradiometer output lay within the dynamic range of the SQUID amplifier. The evoked response from each quadrant of the visual field was then recorded, with the order of each quadrant being randomised. The averaging epoch was 512ms and 100 epochs were recorded and averaged together. On completion of the recording the position of the bite bar, and therefore the subject, with respect to the dewar was digitised thus enabling accurate co-registration of signal and MRI information. Data was analysed using topographic contour mapping and source localisations performed using a single equivalent current dipole model. The time of source analysis was determined by maxima in the magnetic global field power. This is defined as the sum of squares of the gradiometer output at each time instant. The equivalent current dipole position, orientation and strength was examined with reference to the cruciform model. For those subjects for whom MRI data was available (FF, IH and KS), Monte-Carlo error analysis was performed thus yielding a confidence region which was co-registered with the MRI. This enabled identification of the cortical volume generating the recorded evoked signal.

5.2.3 Subjects

Three females (FF, VT and CS) and two males (IH and KS) volunteered for the experiment. Their ages ranged from 28 to 39 and all had normal visual fields and colour vision and a normal or corrected-to-normal Snellen acuity of 6/6.

5.3. Results

5.3.1. Isoluminant chromatic gratings

The visual evoked magnetic response to isoluminant chromatic gratings for each of the quadrants of the visual field is shown in Figures 5.3-5.13 for each of the subjects investigated. In these and all subsequent figures, an upward trace deflection corresponds to red on the field map which represents outgoing magnetic field. A downward trace deflection, blue on the field map, represents ingoing magnetic field. The map is viewed from the back of the head and the position of the recording channels for each of the subjects is shown in Figure 5.22. The time of the map is indicated for each quadrant and corresponds to the peak in the power spectrum, which occurs at the time of the major component peak. The equivalent current dipole calculated at the time of the map is shown in white. For those subjects for which Monte-Carlo analysis is performed, (IH, FF and KS) the equivalent current dipole statistics are shown in Table 5.1. For the remainder of the subjects, the equivalent current dipole was calculated and is shown on the field maps. The colour scale on the map indicates the maximum magnetic field recorded in units of femtoTesla. Global field power is shown for a 500ms epoch and the latency of major peaks in the field power are indicated. The evoked magnetic responses for each of the subjects will now be described in more detail.

1. Subject VT: Figures 5.3-5.4

The responses evoked from each quadrant of the visual field were dominated by a major component peaking at 97-100ms. The field strength of this component was high, ranging from 325-715fT, with the lower quadrants being of higher field strength. One quadrant, the right upper, displayed a second component of lower field strength peaking at 156ms. The equivalent current dipole solutions were situated on the midline with an orientation that changed consistently with visual field stimulated. The orientations are as predicted by the cruciform model.

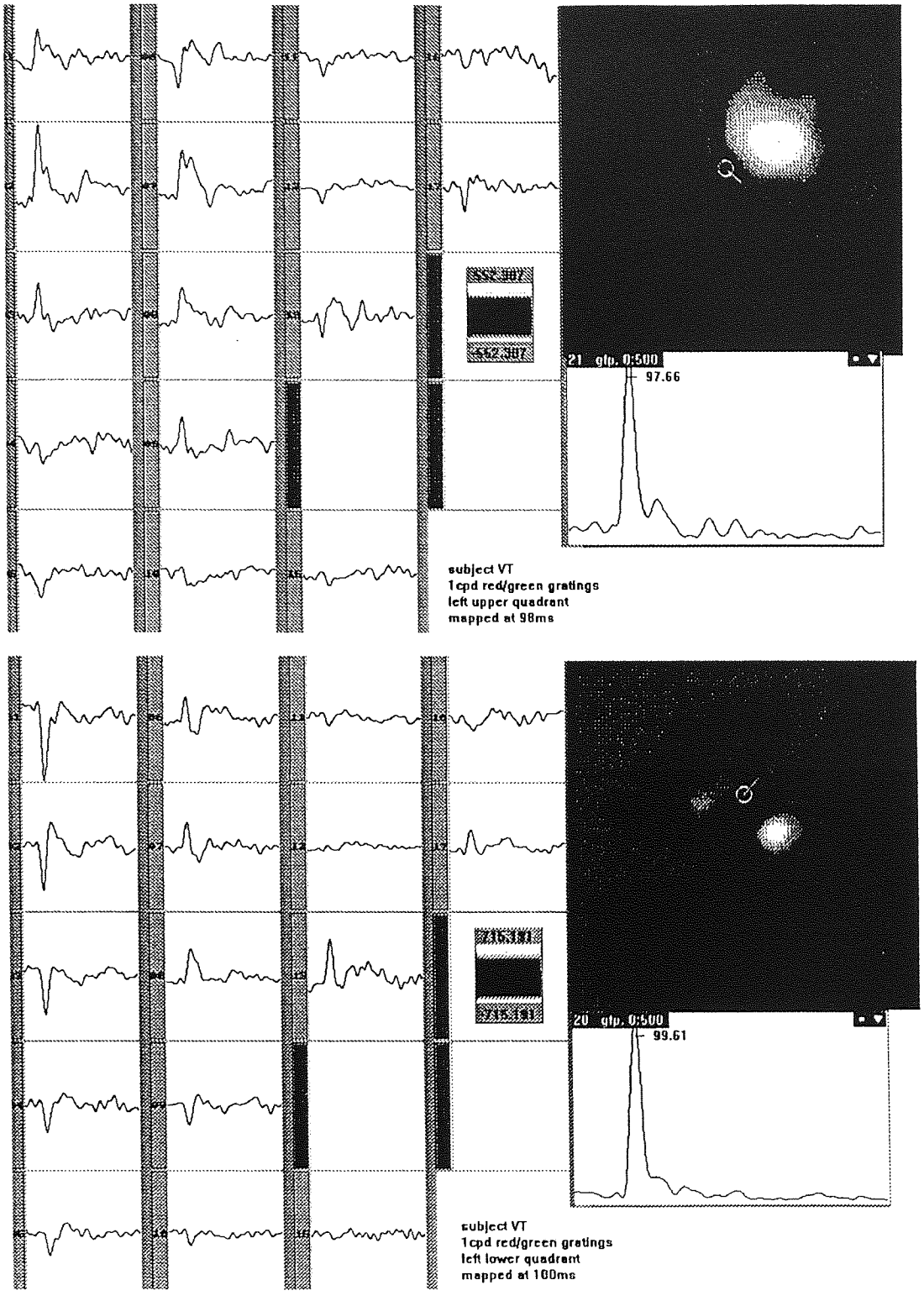

Figure 5.3 Waveforms and field maps to left upper and lower quadrant chromatic stimulation for subject VT

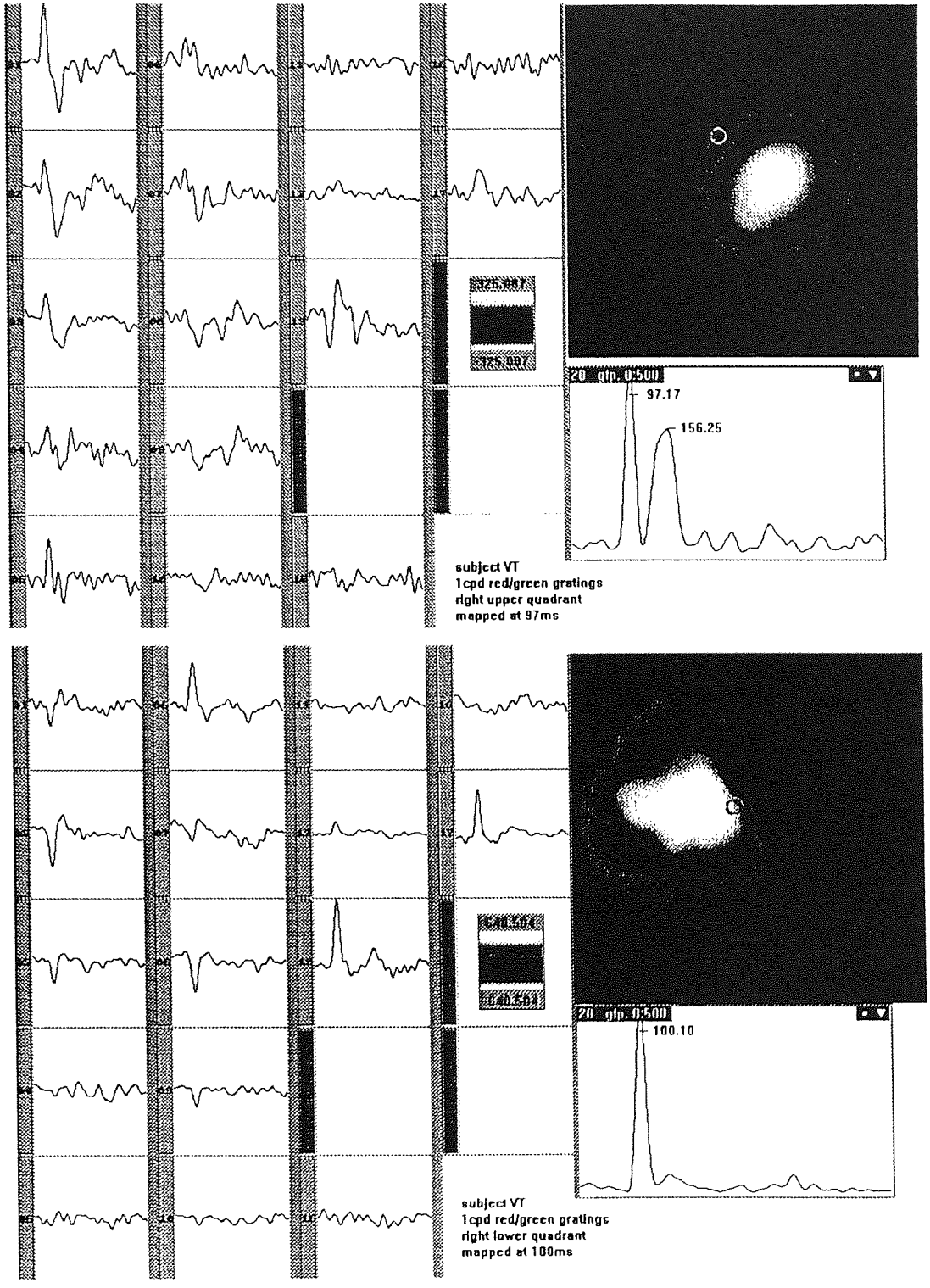

Figure 5.4 Waveforms and field maps to right upper and lower quadrant chromatic stimulation for subject VT

2. Subject CS: Figures 5.5-5.6

The responses evoked from each quadrant of the visual field were dominated by a major component, peaking at 105-108ms. Again, the field strength was high, ranging from 316-713fT with higher field strength signals evoked by lower quadrant stimulation. A single quadrant, the left upper, displayed a second component which peaked at 186ms. Three of the four quadrants evoked dipole generators whose orientation was as predicted by the cruciform model. The fourth quadrant, the left upper, evoked a dipole pointing downwards; rotated 45 degrees clockwise to that predicted.

3. Subject FF: Figures 5.7-5.8

The responses evoked from each quadrant of the visual field were dominated by a major component, peaking at 89-94ms. The field strength was high, ranging from 312-528fT, the lower quadrants evoking higher field strength signals. Two of the quadrants, the left upper and lower, showed evidence of secondary components. The left upper quadrant response showed a second component at 146ms and the left lower quadrant response showed two additional components at 123ms and 220ms. Nevertheless, at the time of the major component peak for both left upper and lower quadrant stimulation, examination of Table 5.1 shows the data to be explained by a single current dipole. Stimulation with all but one of the quadrants evoked dipoles as predicted by the cruciform model of striate cortex. The exception was the left lower quadrant which evoked an equivalent current dipole pointed upwards and as such was rotated 45 degrees anticlockwise. This can be explained by examination of the calcarine fissure on the subject's MRI, shown in Figure 5.9.

Figure 5.9 demonstrates the asymmetrical nature of the calcarine fissure. The left lower quadrant projects to the upper surface of the right hemisphere calcarine fissure which in subject FF is angled upwards. The dipole generator, being oriented perpendicular to the cortical sheet would then be pointing medially and not upwards. With the vector addition of the lateral dipole, the resultant dipole generator would be oriented upwards, as observed.

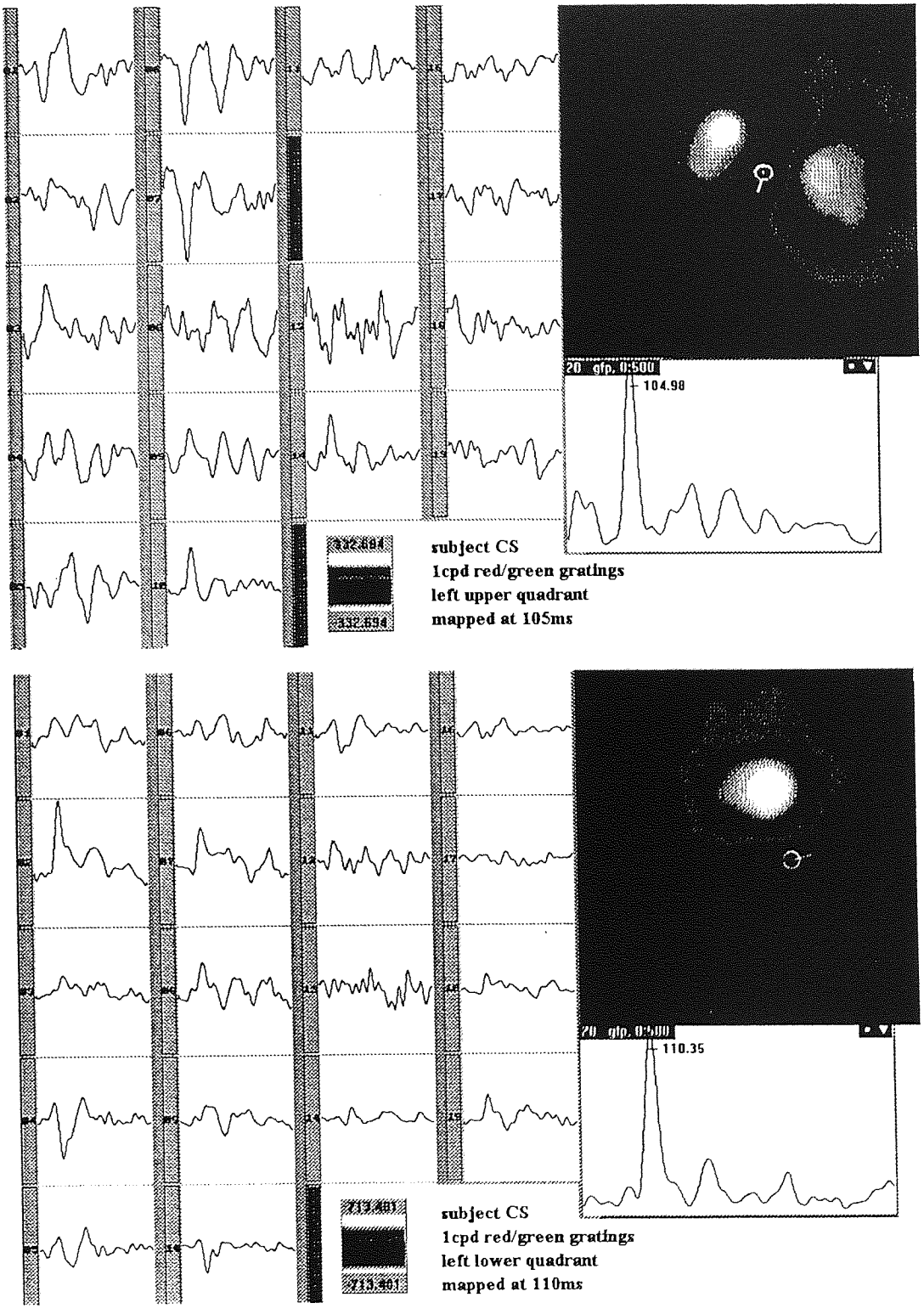

Figure 5.5 Waveforms and field maps to left upper and lower quadrant stimulation for subject CS

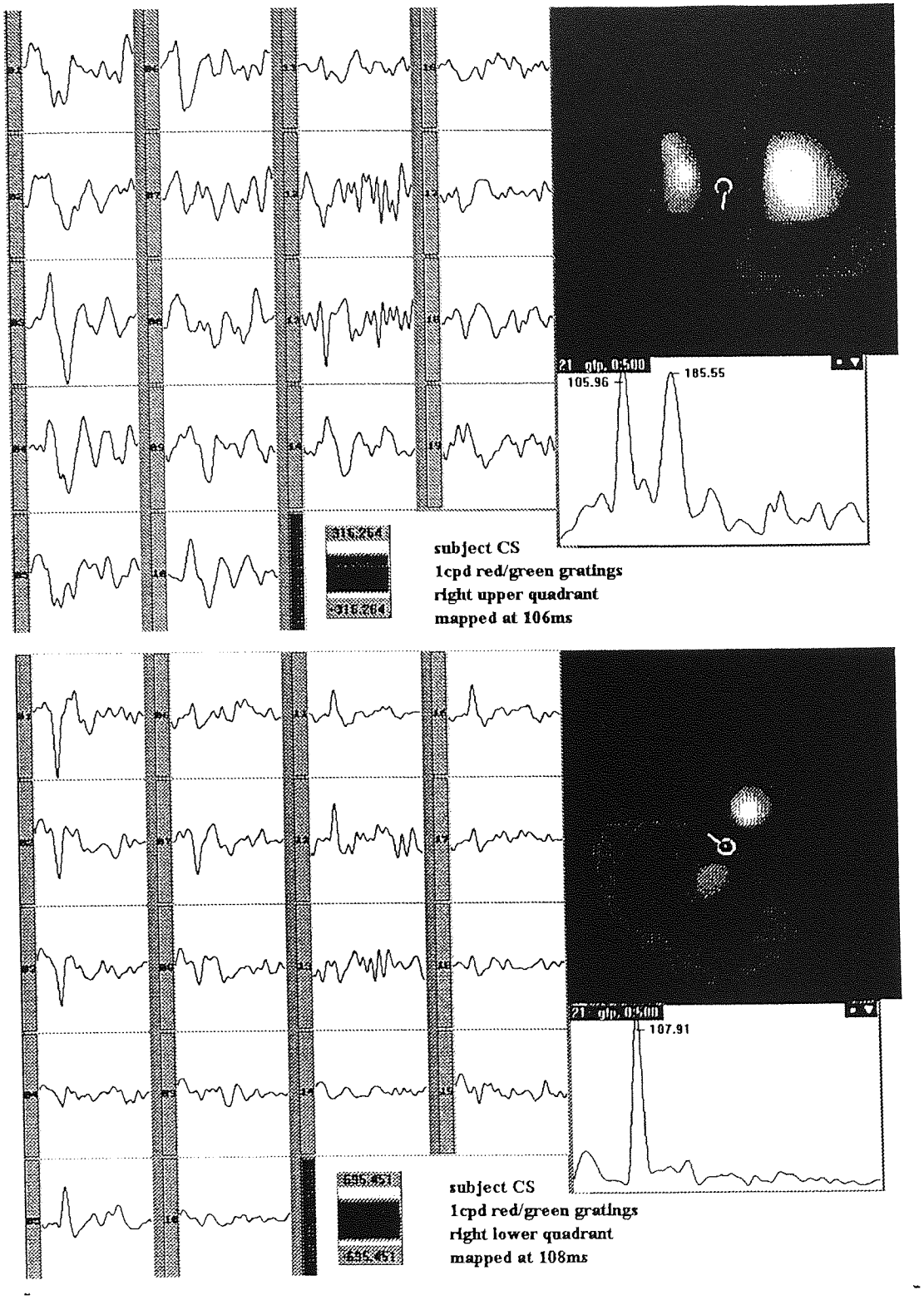

Figure 5.6 Waveforms and field maps to right upper and lower quadrant chromatic stimulation for subject CS

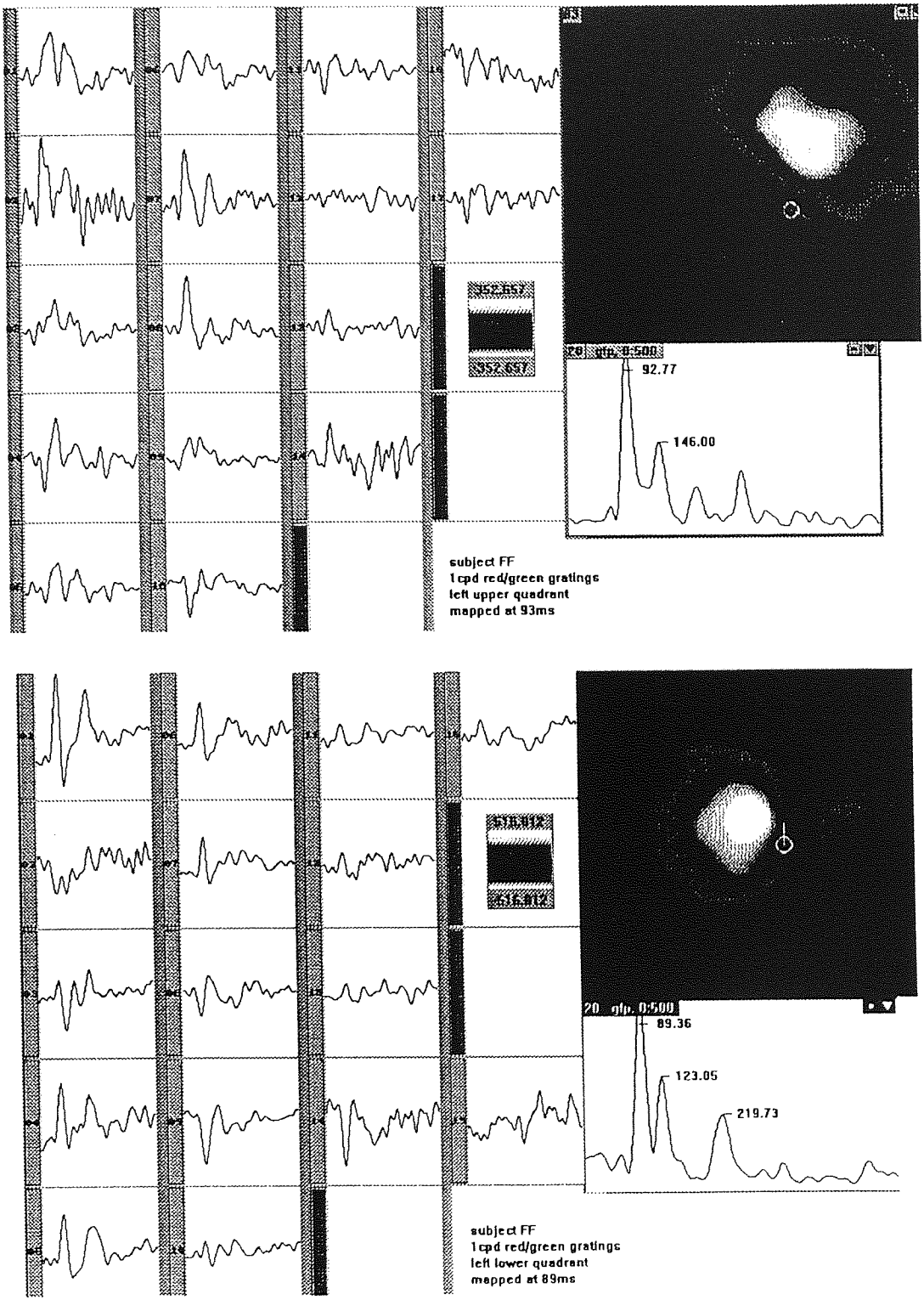

Figure 5.7 Waveforms and field maps to left upper and lower quadrant chromatic stimulation for subject FF

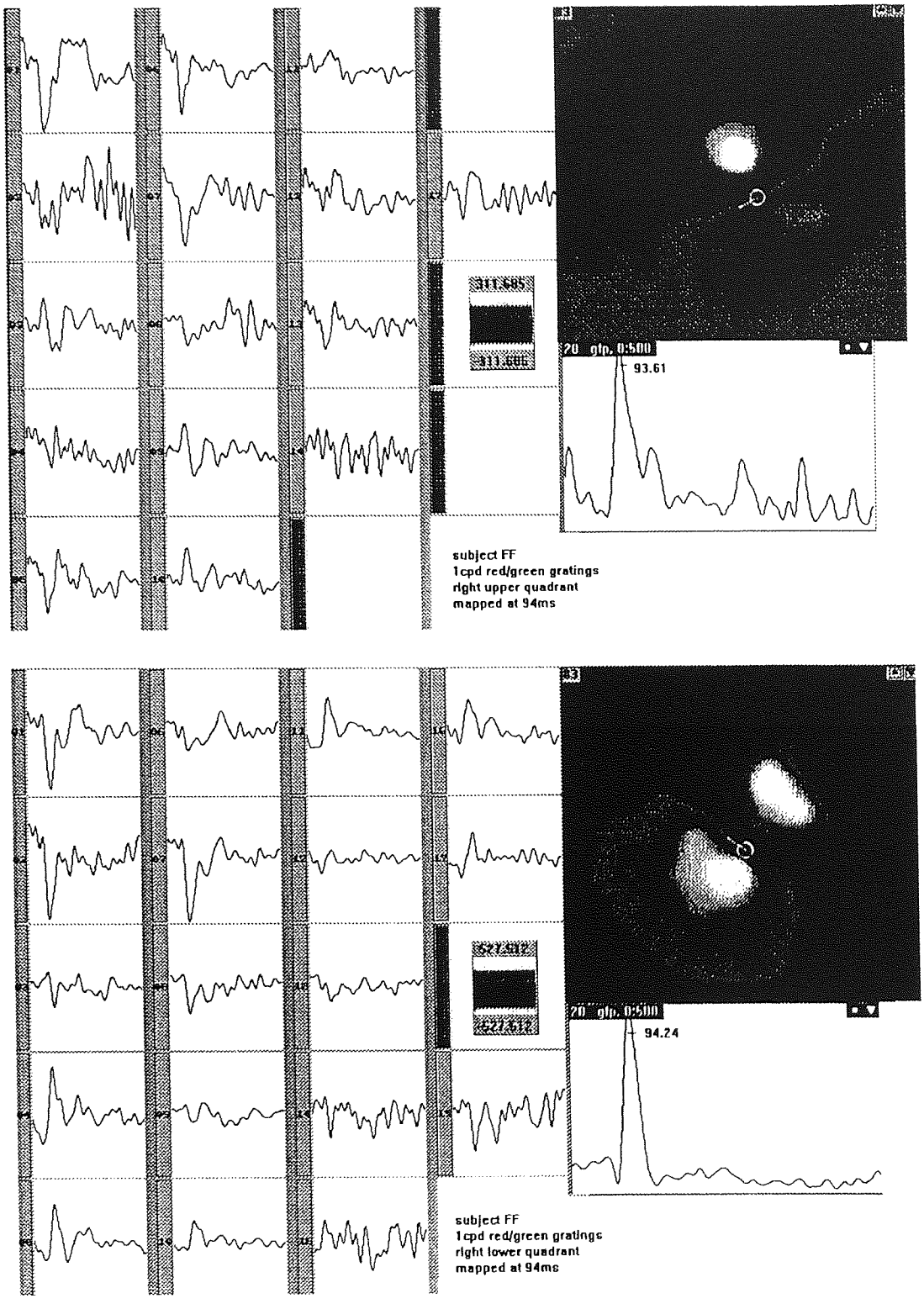

Figure 5.8 Waveforms and field maps to right upper and lower quadrant chromatic stimulation for subject FF

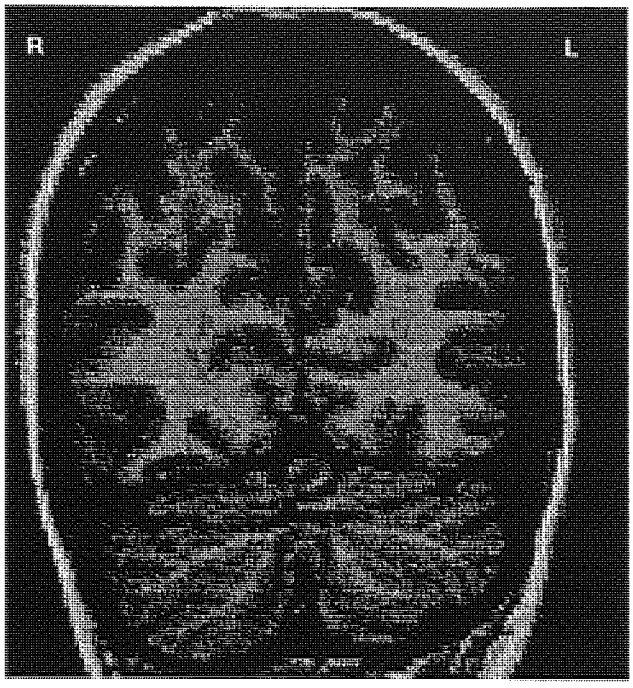

Figure 5.9 Vertical MRI section of subject FF. The calcarine fissure is highlighted in red.

4. Subject KS: Figures 5.10-5.11

The responses evoked from the lower quadrants of the visual field were dominated by a major component which peaked at 101-104ms. The field strength of this component was high, ranging from 312-475fT. The left lower quadrant also evoked a second component of lower field strength at 134ms. The two upper quadrants were of low field strength, 90-175fT, and were dominated by a later component which peaked at 159ms. An earlier component at 101-106ms was visible but of low field strength, in the case of the right upper quadrant, of the same field strength as the background noise. Nevertheless, the early components were topographically mapped and the dipole solutions were found to have an orientation as predicted by the cruciform model. However, only the lower quadrant solutions reached significance, evidenced by Table 5.1, so only these were subjected to further analysis.

5. Subject IH: Figures 5.20-5.23

The evoked responses for subject IH tended to be of low field strength, ranging from 159-480fT. Only the right upper and lower quadrants evoked a single early component which peaked at 105-106ms. The left upper quadrant was dominated by a

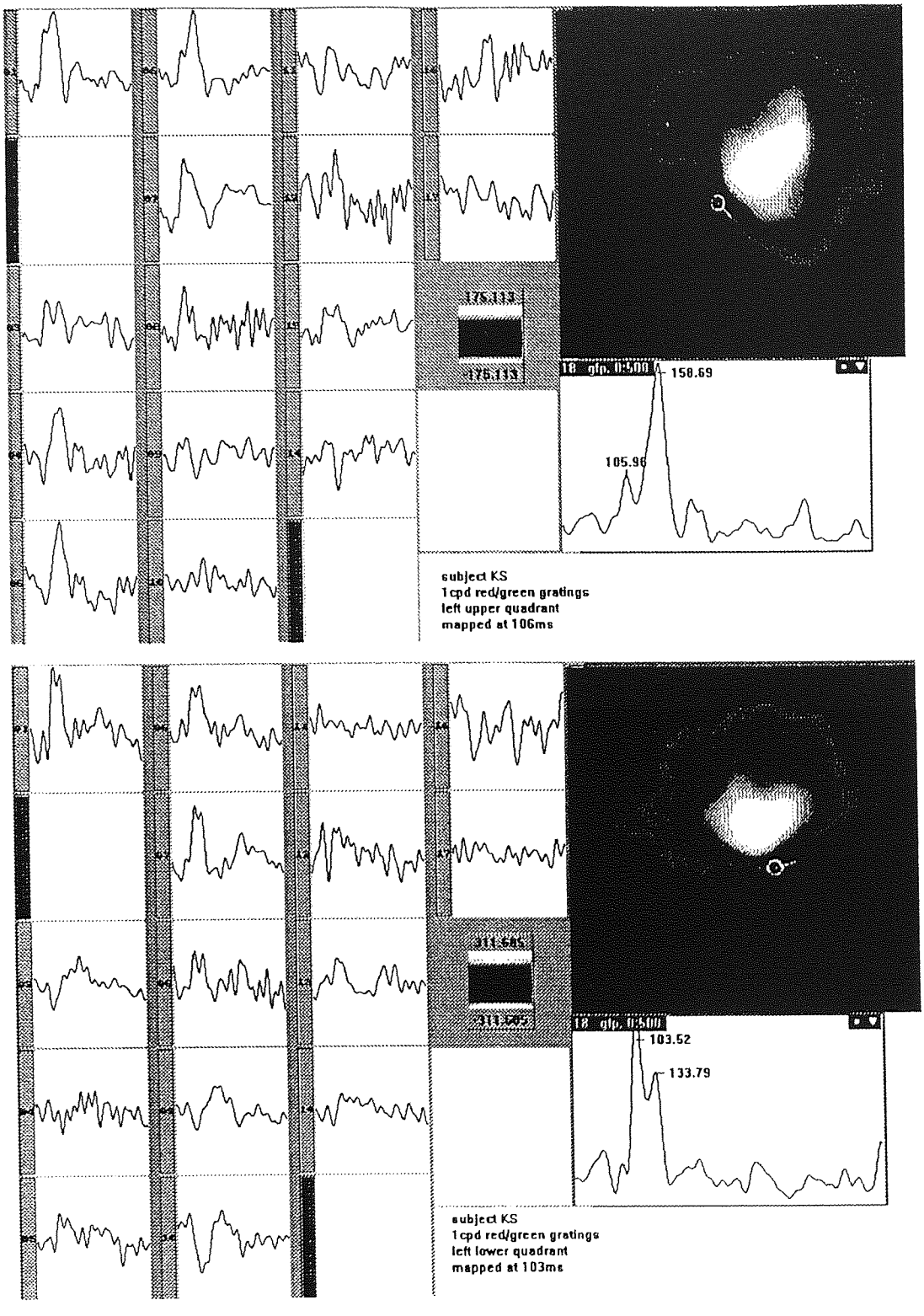

Figure 5.10 Waveforms and field maps to left upper and lower quadrant chromatic stimulation for subject KS

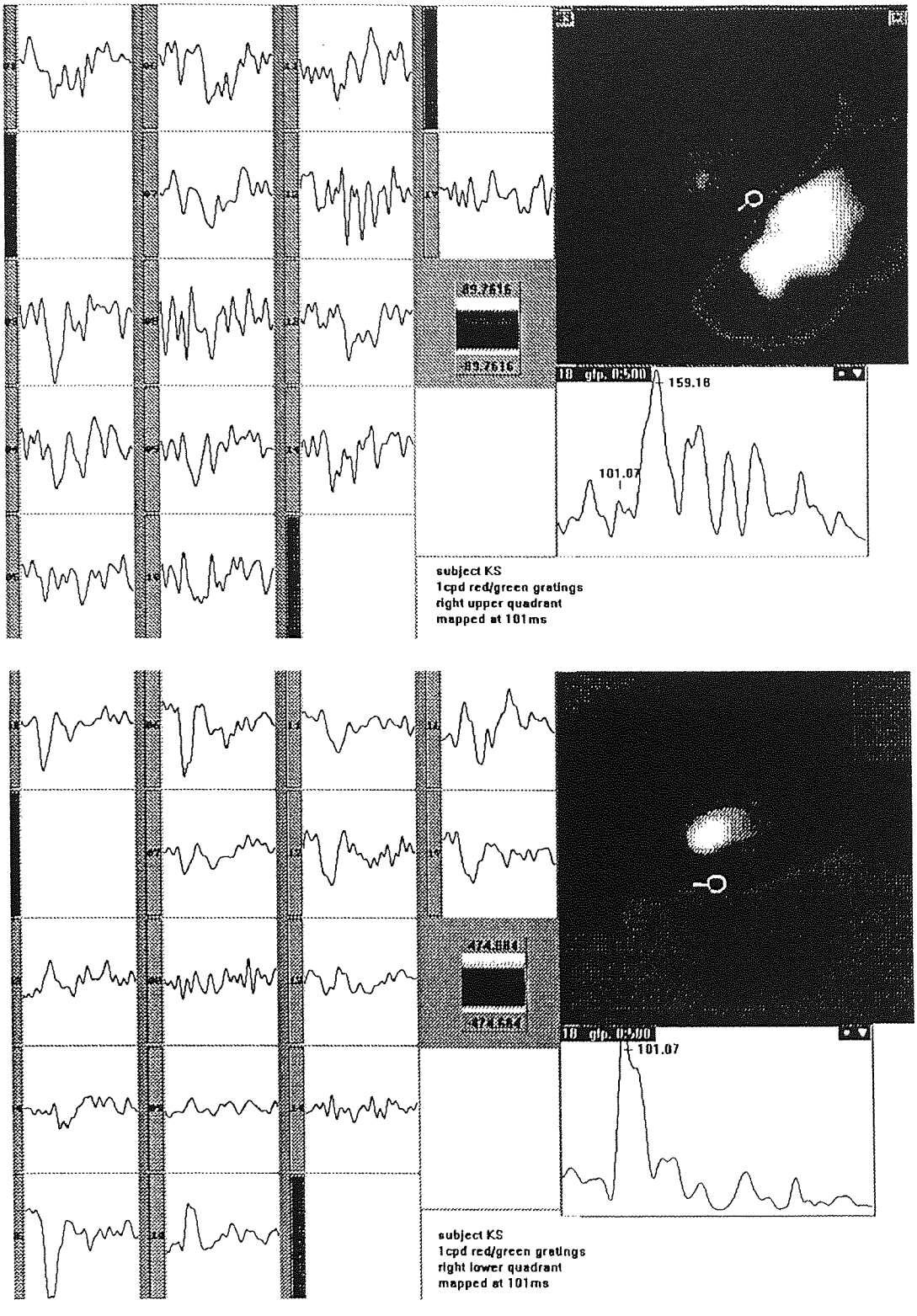

Figure 5.11 Waveforms and field maps to right upper and lower quadrant chromatic stimulation for subject KS

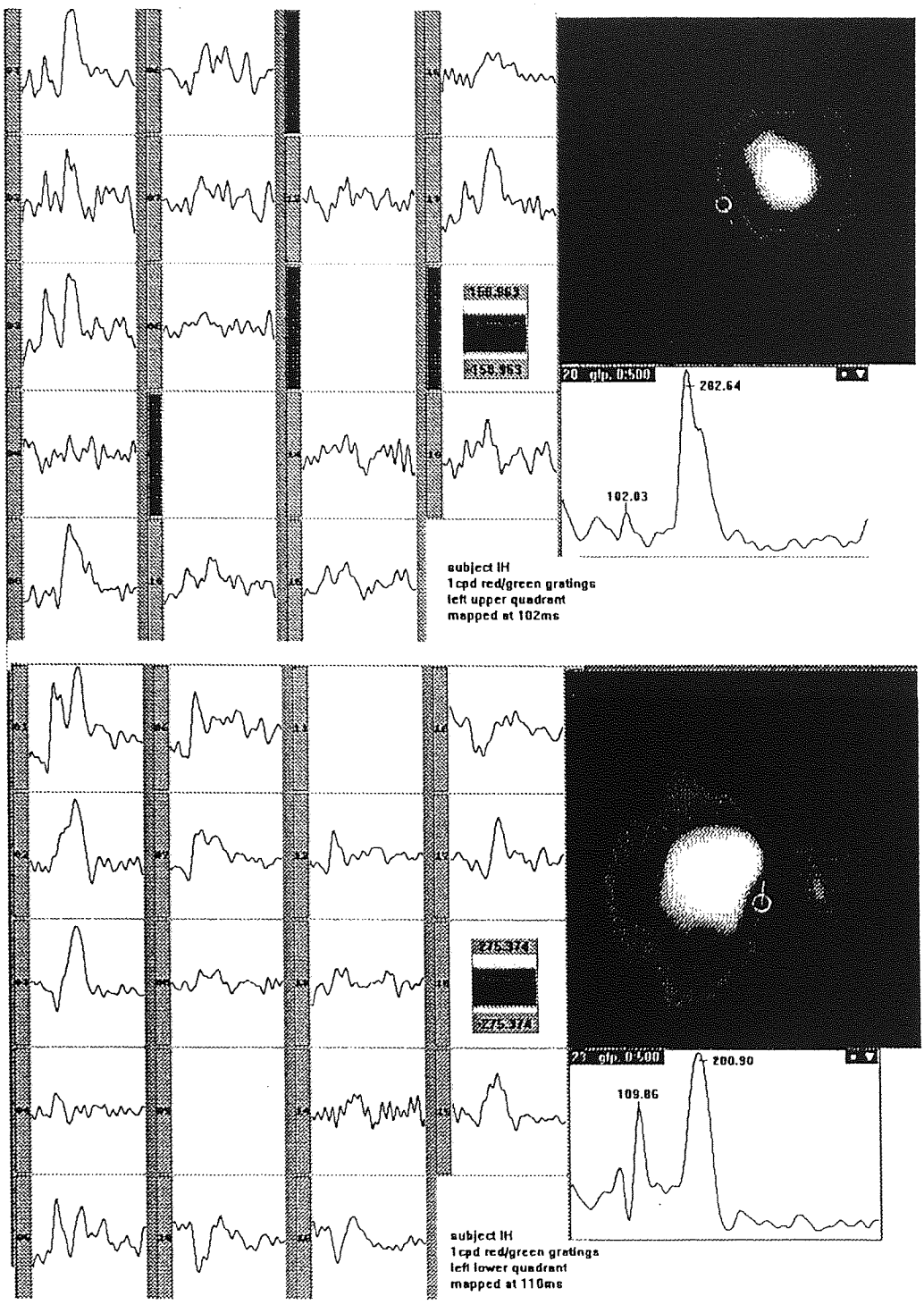

Figure 5.12 Waveforms and field maps to left upper and lower quadrant chromatic stimulation for subject IH

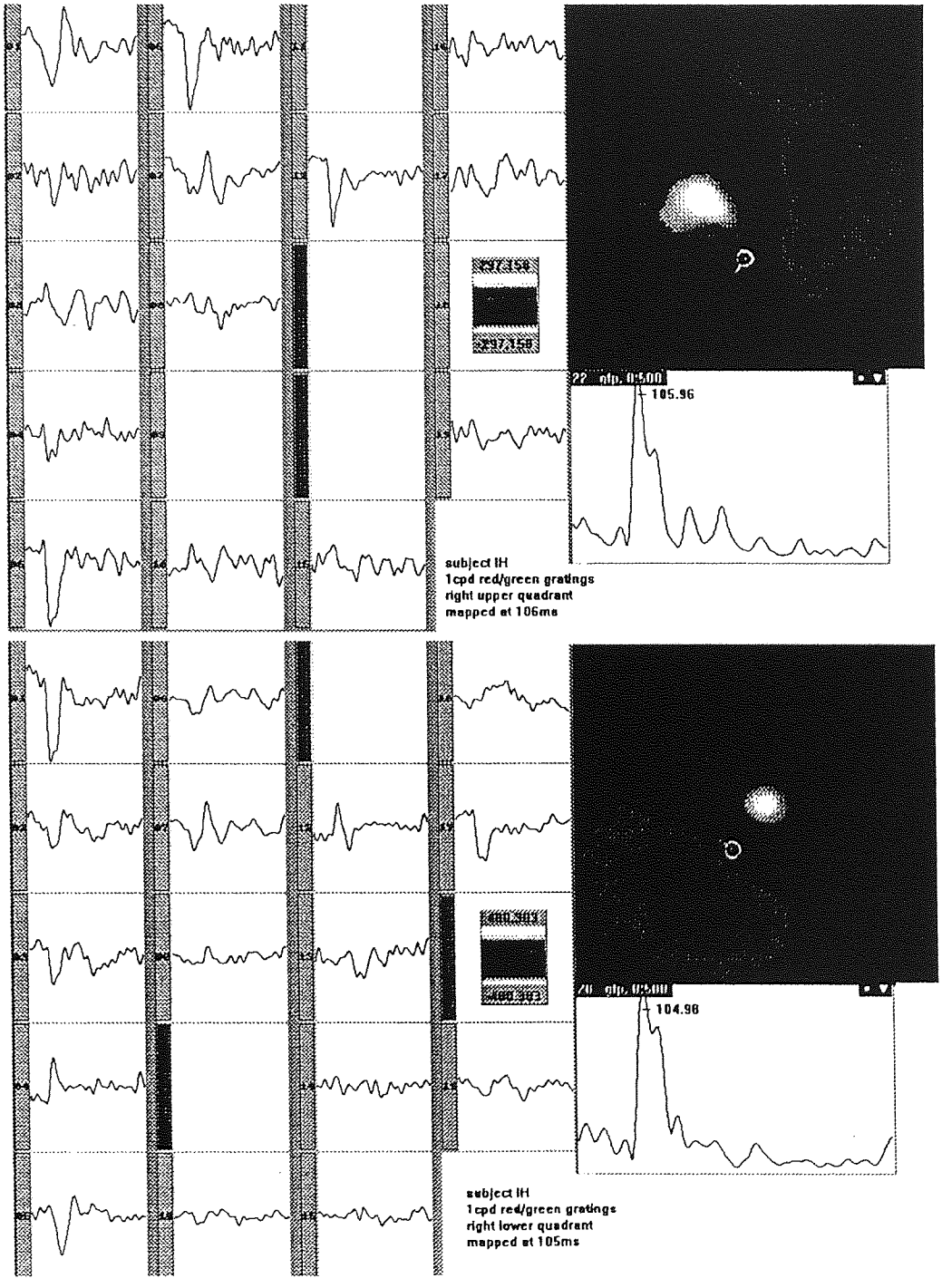

Figure 5.13 Waveforms and field maps to right upper and lower quadrant chromatic stimulation for subject IH

subject	quadrant	latency (ms)	correlation co-efficient	χ^2	gamma-Q	no. channels
	LU	93	.96	14	.387	18
FF	LL	88	.99	20	.040	16
	RU	91	.98	9.8	.548	16
	RL	94	.99	18	.079	17
	LU	102	.87	27	.002	15
KS	LL	104	.98	2.9	.983	15
	RU	101	.87	7.7	.565	14
	RL	101	.98	11	.327	15
	LU	102	.95	5.9	.823	16
IH	LL	110	.98	11	.410	16
	RU	106	.96	7.7	.061	15
	RL	105	.99	3.9	.973	15

Table 5.1 Statistics of the equivalent current dipole for subjects IH, FF and KS. Dipoles with correlation < .95 are rejected as non-significant.

late component at 203ms. An earlier component at 102ms was apparent in the waveforms but occurred only at the level of the background noise. The left lower quadrant comprised two major components, the first at 110ms and the second, of slightly higher field strength, at 210ms. The early components were topographically mapped and the equivalent current dipoles were found to be oriented as predicted by the cruciform model of striate cortex.

Examination of equivalent current dipole solutions reveals that for every quadrant of the visual field for each subject the dipole is located on or near the midline pointing towards the contralateral hemisphere with its orientation changing consistently with visual field stimulated. The dipole orientations are as predicted by the anatomy of the calcarine fissure. The dipole statistics shown in Table 5.1 indicate that, with the exception of the response to upper field stimulation for subject KS, all solutions reach significance. The majority of the data is well described by an equivalent current dipole, evidenced by the high gammaQ values and the low χ^2 values for the dipole solutions.

The 95% confidence regions yielded by Monte-Carlo analysis of the data is superimposed on the subjects' MRI data in Figures 5.14-5.16. The higher field strength of the lower visual field stimuli result in improved signal to noise ratios and the dipole solutions have higher gammaQ values and smaller confidence regions. For subject FF, shown in Figure 5.14, the confidence regions are small and it can be seen that the lower visual field projects to the upper surface of the calcarine fissure while the upper visual fields project to the lower surface of the calcarine fissure. All confidence regions lie close to the midline. The activated volume of cortex is therefore consistent with a V1 origin.

For subject IH the confidence regions, shown in Figure 5.15, are larger and the calcarine fissure is less clearly defined. However, with the exception of the right lower quadrant, which is displaced from the midline slightly to the left, all confidence regions lie close to the midline. Both upper and lower quadrants lie on the ascending branch of the calcarine fissure hence the results are consistent with a V1 origin.

For subject KS only the lower visual field quadrants provided significant dipole fits as defined in section 2.11 and therefore only the lower quadrants were used to generate Monte-Carlo confidence regions shown in Figure 5.16. These are positioned some 2cm away from the midline in the contralateral hemisphere on the level of the calcarine fissure. The right lower quadrant response region is located more inferiorly than the left lower quadrant response region. This can be explained by examination of the vertical MRI slice in Figure 5.17 which has the lateral arms of the calcarine fissure marked in blue. The two arms are asymmetric with the left hemisphere arm extending more inferiorly than the right hemisphere arm. Thus the volume of cortex generating the evoked response lies at the end of the lateral arm of the calcarine fissure. The visual area within which this region is contained within is thus ambiguous, being on the level of the calcarine fissure but somewhat more lateral than has been observed in subjects FF and IH. However, the orientation of the dipoles would suggest that the response is dominated by the activity of cells within V1.

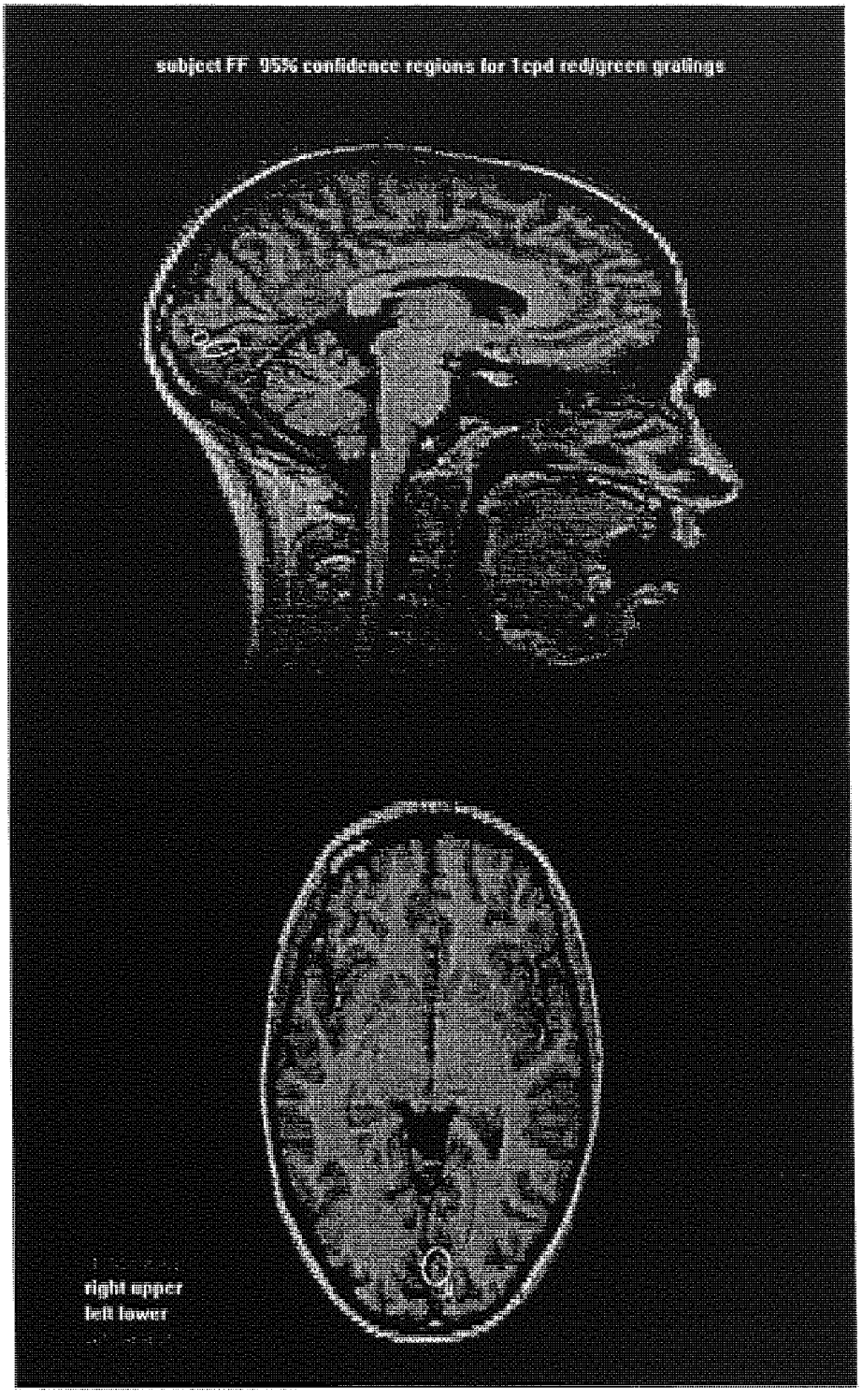

Figure 5.14 95% confidence regions of dipole locations following chromatic stimulation of all four quadrants of the visual field for subject FF

Figure 5.15 95% confidence regions of dipole locations following chromatic stimulation of all four quadrants of the visual field for subject IH

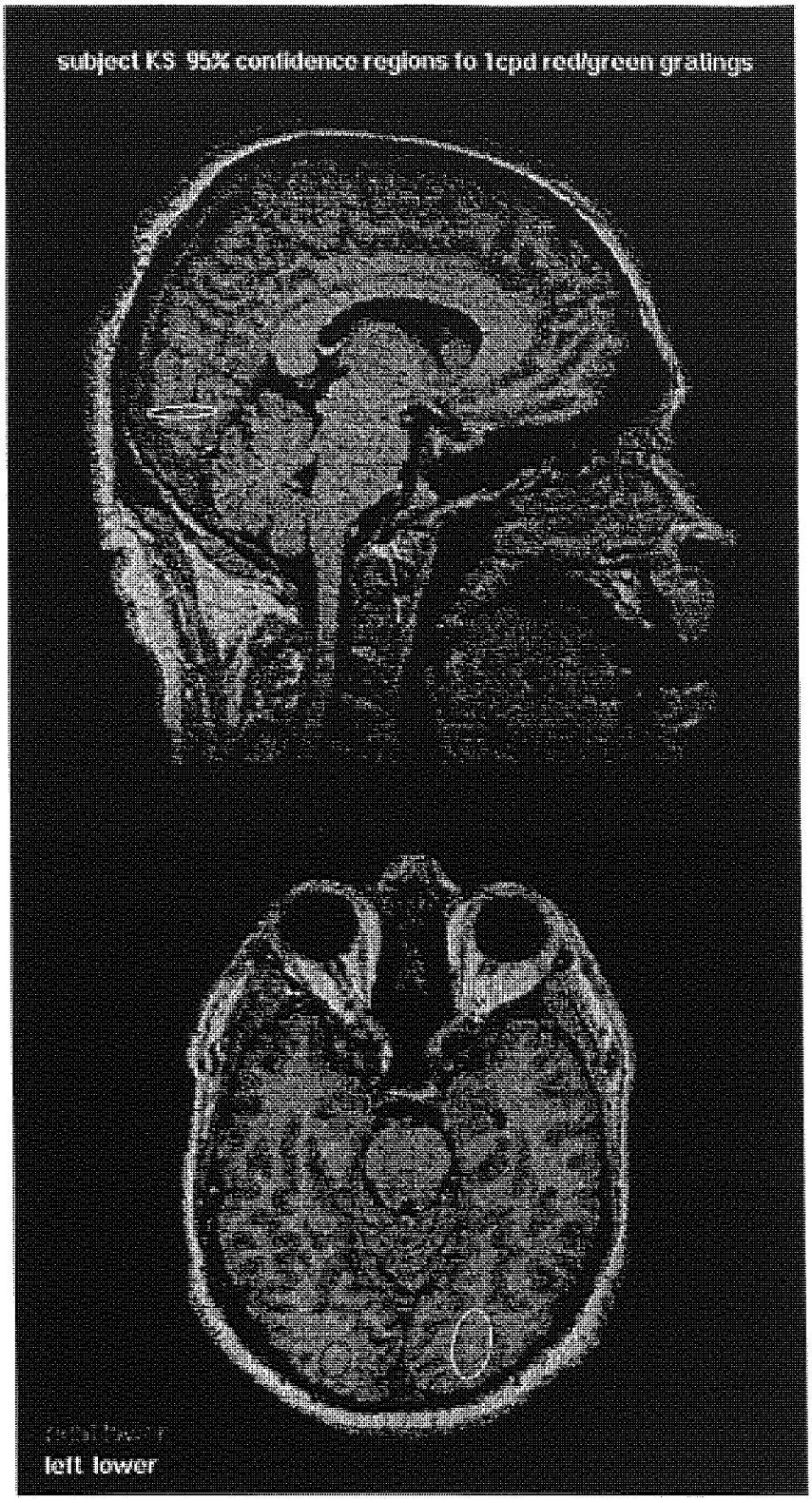

Figure 5.16 95% confidence regions of dipole locations following chromatic stimulation of left and right lower quadrants for subject KS

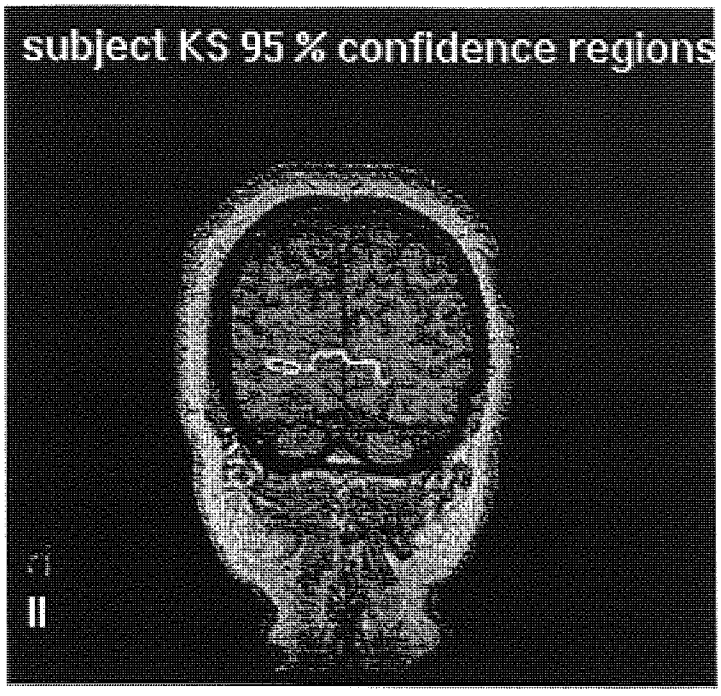

Figure 5.17 Location of the 95% confidence regions with respect to the calcarine fissure for subject KS

5.3.2 Control Experiment 1: achromatic gratings

The evoked response to achromatic stimulation was considerably more variable and of lower amplitude than that evoked by isoluminant chromatic stimulation. The response was no longer dominated by a single major component with between two and four components present. This is shown by the waveforms and global field power in the response to right upper and lower quadrant stimulation in Figure 5.18. As in the response to chromatic stimulation there was a bias towards the lower hemifield but analysis of the results reveals a lack of clear retinotopic organisation. This pattern was observed for both 20% and 80% achromatic contrast hence only the response to 80% contrast are shown. The initial peak of the response occurred at a latency of around 66ms and subsequent peaks occurred at 92 and 117ms although only the first of these was well described by a single equivalent current dipole. There was much variability in the latency of the response both between subjects and between different quadrants of the visual field. The equivalent current dipoles generated at the time of the peaks do

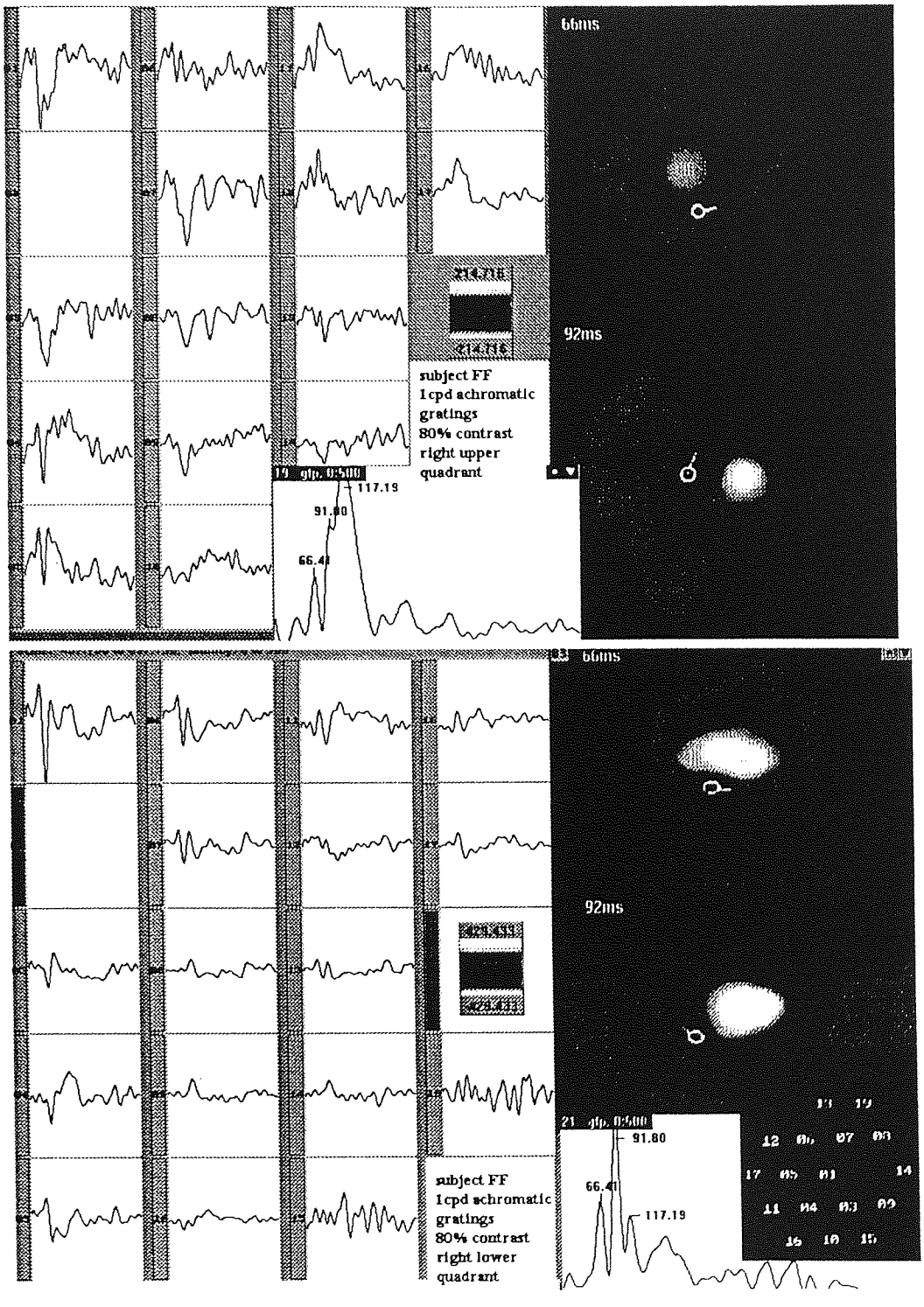

Figure 5.18 Waveforms and field maps to stimulation with 80% achromatic contrast in the right upper and lower quadrants for subject FF

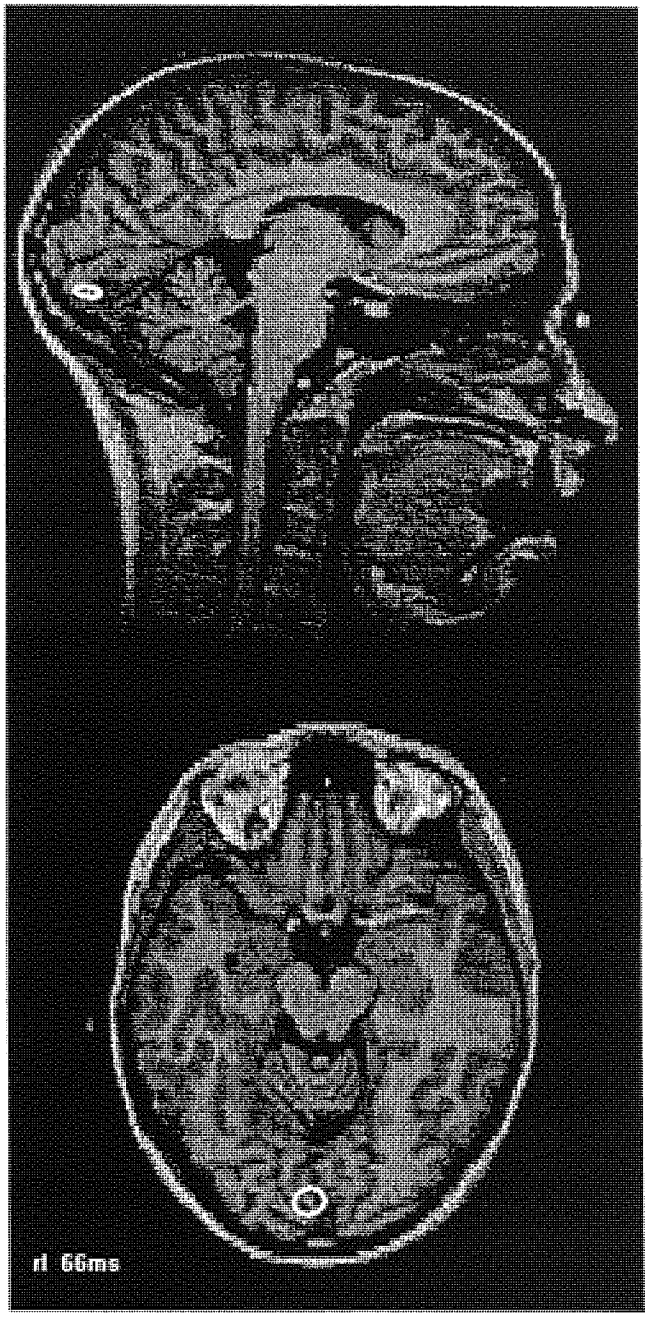

Figure 5.19 95% confidence region of dipole location following stimulation with 80% achromatic contrast in the right lower quadrant for subject FF

not show the consistent shift in orientation with stimulation of different regions of the visual field as observed in the chromatic response, as seen in the field maps at 66ms and 92ms in Figure 5.18. Co-registration of MEG and MRI data is shown in Figure 5.19 for the first peak in the field power following right lower quadrant stimulation.

5.3.3 Control Experiment 2: 2 x 2 degree field

The visual evoked magnetic response to isoluminant chromatic gratings in a 2 x 2 degree field for each of the quadrants of the visual field is shown in Figure 5.20-5.21 for subject FF. The field strength was low, ranging from 133-365fT, with the lower quadrants evoking higher magnetic field strengths. With the exception of the left lower quadrant, the responses are dominated by a single component, peaking at 96-111ms. The left lower quadrant comprises an additional component peaking at 145ms. The evoked responses show similar morphology to the large field case, with the dipole solutions positioned on the midline and their orientations changing consistently with visual field stimulated. The dipole orientations are consistent with the cruciform model of striate cortex.

5.4 Discussion

The evoked magnetic response to isoluminant chromatic gratings was recorded and its topography and cortical location investigated. The evoked response was dominated by a single major component peaking at 89-110ms. No latency differences were noted between upper and lower visual fields. The latency of this component peak was highly consistent both between different quadrants of the visual field and between subjects. The response was of high field strength, 528fT in comparison with the equivalent luminance response of 429fT for subject FF.

A second component was present in a small number of quadrants. This was more variable, peaking between 136-209ms, and tended to be of lower field strength. In two subjects, IH and KS, this second component occasionally dominated the response but this occurred only in those quadrants evoking low field strength signals. A comparison of the field maps of the primary and secondary response reveals both dipole solutions to have similar positions but their orientation is rotated by 180 degrees. This suggests that the second component may reflect a repolarisation process in the region of cortex

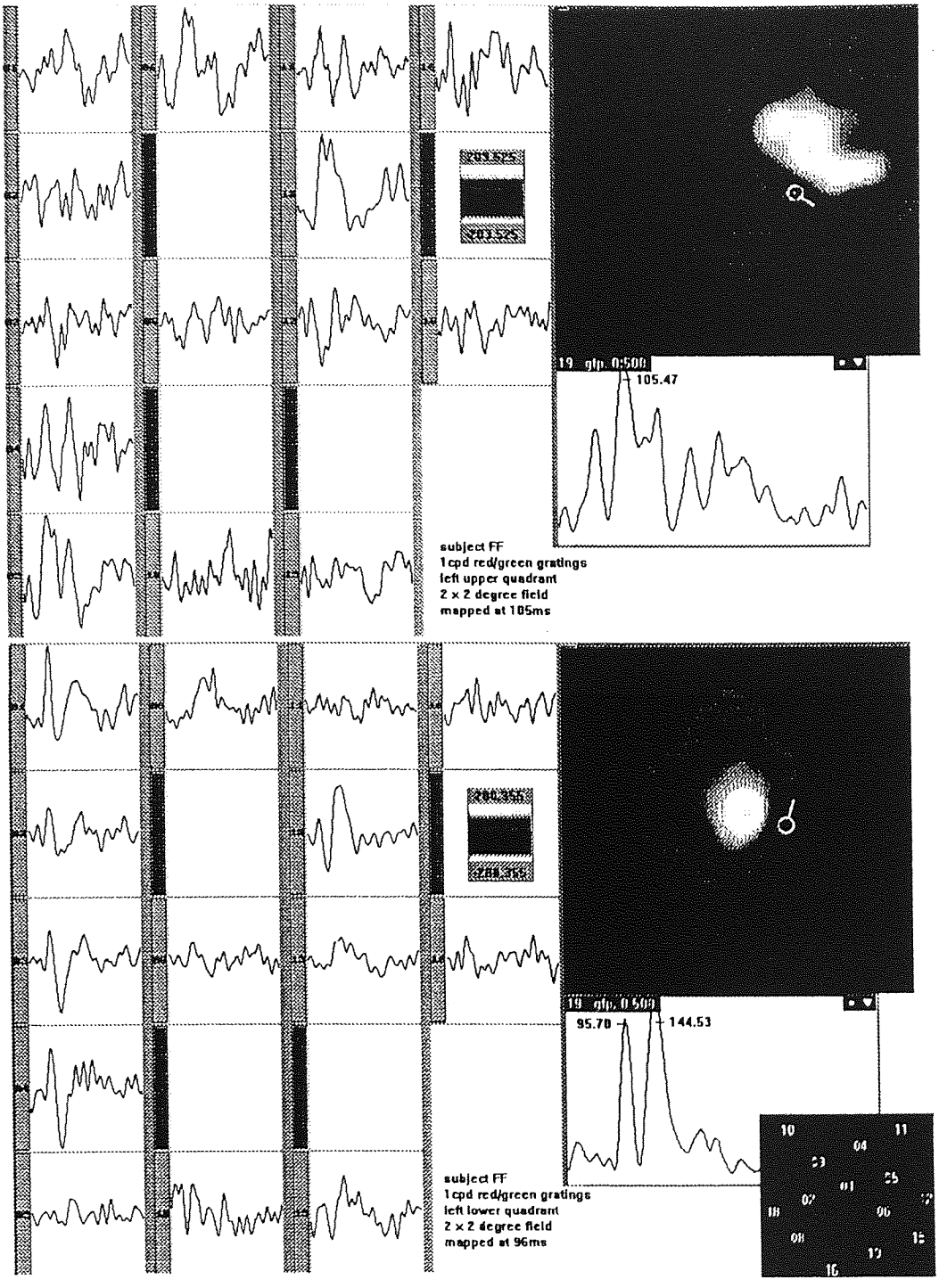

Figure 5.20 Waveforms and field maps to left upper and lower quadrant chromatic stimulation in a 2 x 2 degree field for subject FF

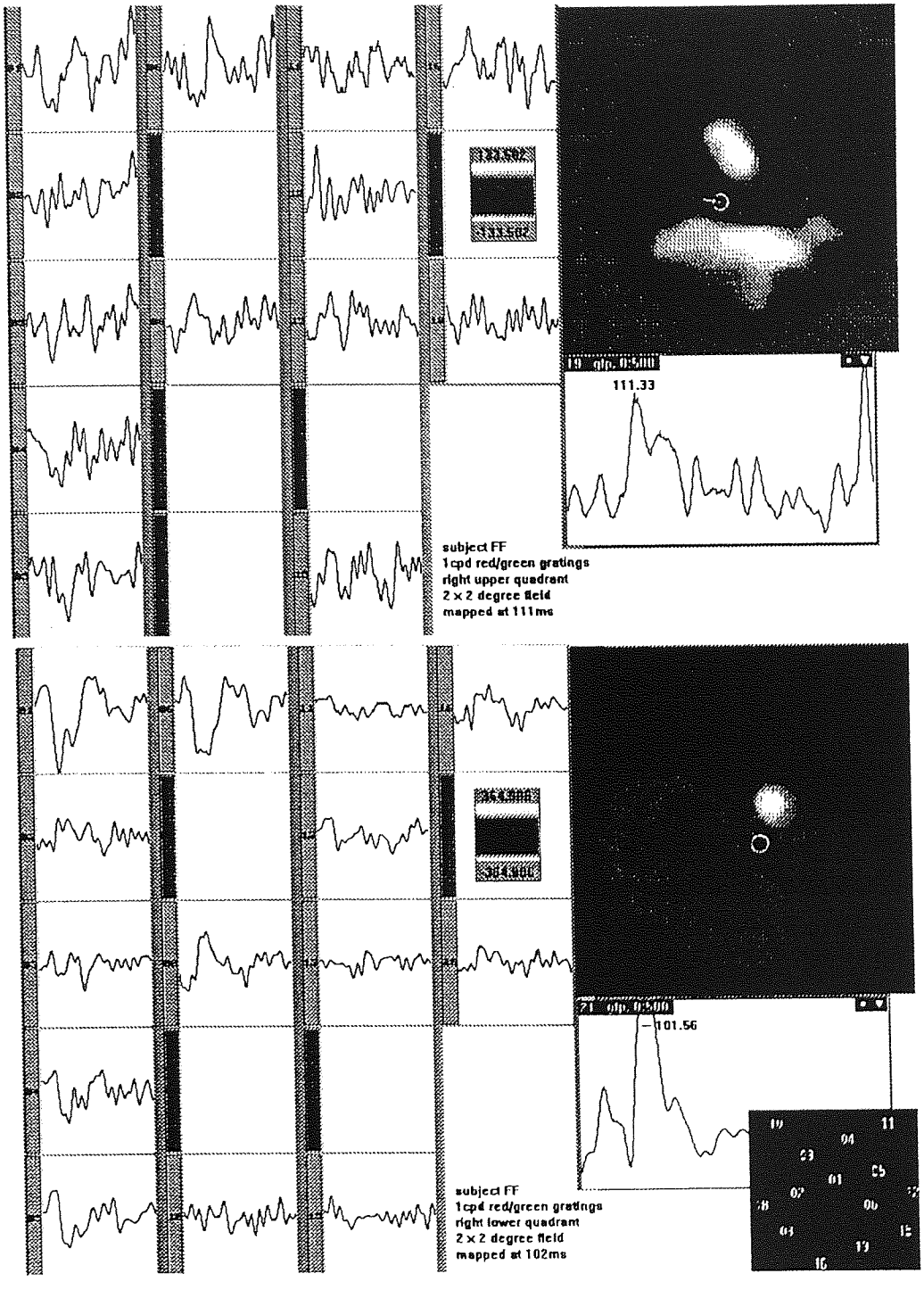

Figure 5.21 Waveforms and field maps to right upper and lower quadrant chromatic stimulation in a 2 x 2 degree field for subject FF

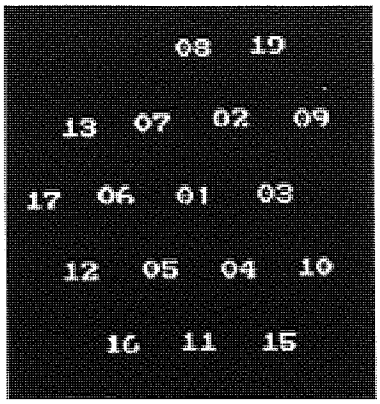

subject VT

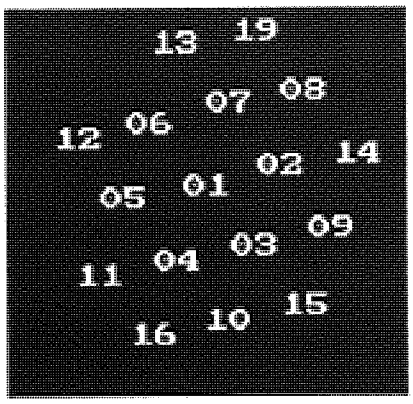

subject FF

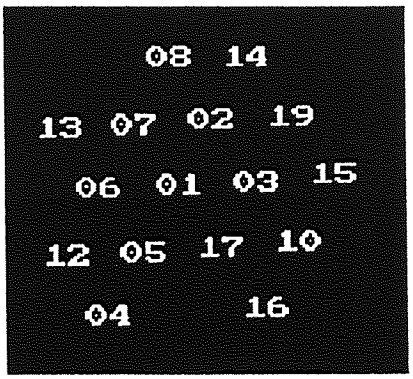

subject IH

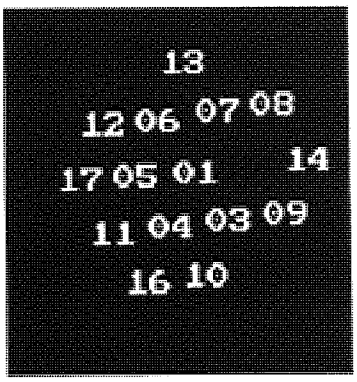

subject KS

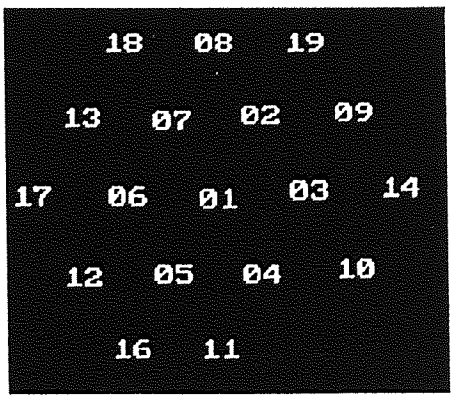

subject CS

Figure 5.22 Recording positions for each of the subjects in the chromatic gratings experiment

generating the initial response.

There was a bias towards the lower quadrants, which evoked stronger field strength signals in every subject. This field strength difference could be marked; comparison of the right upper and lower quadrant for subject FF in Figure 5.8 reveals the field strength to rise from 312fT to 528fT when lower rather than upper quadrant stimulation was used. This effect can be explained by consideration of the anatomy of striate cortex. The upper visual field projects to the lower surface of the calcarine fissure while the lower field projects to the upper surface, shown in Figure 3.9. This is demonstrated by the location of the confidence regions on the MRI of subject FF in Figure 5.14. The upper quadrants clearly project to the inferior surface of the calcarine fissure while the lower quadrants project to the upper surface. This results in the representation of the lower visual field being closer to the gradiometer input coils. As the magnetic field falls off with the cube of distance (see equation 2.5) this reduction in measured field strength between upper and lower quadrants is as expected. Similar reports of amplitude reductions for upper compared to lower field stimulation have been made for electrical evoked potentials (Nesfield, 1992).

The topography of the response is highly consistent between subjects and the data is well modelled by an equivalent current dipole, indicated by the high correlations and gammaQ values shown in Table 5.1. For a number of dipole solutions, particularly for subject FF, the χ^2 values are higher than would be expected if the model provides a good fit to the data. However, the Monte-Carlo confidence regions shown in Figure 5.14 are small which supports the data being well described by a current dipole. The dipole solutions are located on or near the midline pointing laterally towards the contralateral hemisphere with an orientation that changes consistently with the quadrant of visual field stimulated. This orientation shift is exactly as predicted by the cruciform model of striate cortex. The only exceptions to this are from stimulation of the left upper quadrant of subject CS which evokes a dipole pointing vertically down; rotated some 45 degrees with respect to that predicted by the cruciform model and the left lower quadrant for subject FF. These slight anomalies are likely to be due to variations in the anatomy of the striate cortex (Stensaas et al., 1974, Wong-Riley et al., 1993). Indeed, for subject FF the MRI is available and the orientation shift can be explained by the angle of the calcarine fissure.

The pattern of results obtained is as described by the 90ms component of Darcey et al. (1980) and is highly suggestive of activation of area V1. MRI data was available for three of the five subjects (FF, IH and KS). The dipole solutions were subject to

Monte-Carlo analyses yielding confidence regions within which the dipole generators were assumed to lie. The confidence regions for subject FF are small hence co-registration of this information with the MRI allows firm conclusions to be drawn regarding the origin of the evoked response. Upper quadrants of the visual field project to the lower surface of the calcarine fissure contralateral to the visual field stimulated while lower quadrants project contralaterally to the upper surface of the calcarine fissure. This is consistent with the known retinopy of striate cortex and as such the data strongly suggests activation of units within area V1.

For subject IH the confidence regions are larger and it is not possible to conclude with such certainty the exact location of the active cortical regions. Both upper and lower quadrants project to a superior branch of the calcarine fissure. The main fissure runs extremely inferiorly and neither upper or lower quadrants project to this branch. The confidence regions of the lower field quadrants are suitably small to confine the active regions to the upper surface of the contralateral calcarine fissure, although the right lower quadrant projection is displaced slightly from the midline. Upper quadrants have larger confidence regions centred over the midline, slightly displaced towards the contralateral hemisphere. The lateral displacement of the right lower quadrant projection raises the possibility of a contribution to the response from units in area V2. However, if this were so, it would be expected that there would be a greater separation between upper and lower visual field representations. Furthermore, the dipole statistics in Table 5.1 show a gammaQ of .973 and a χ^2 of 3.9 and as such are highly suggestive of the activity at the time of the power peak arising from a single equivalent current dipole. Hence, although the right lower quadrant representation is slightly more lateral than expected, these results are consistent with a V1 origin for the evoked magnetic response.

This same lateral displacement is seen for the confidence regions for subject KS in Figure 5.16. Both left and right lower quadrant representations are displaced some 2cm into the contralateral hemisphere. However, both project onto the level of the calcarine fissure as seen on the saggital MRI slice; the dipole generator in the left hemisphere being located more inferiorly than the corresponding dipole generator in the right hemisphere. The dipole statistics shown in Table 5.1 indicate the data is well described by a single equivalent current dipole model at the time of the power peak. If extrastriate cortex contributed significantly to the evoked response it would be expected that the lower quadrant dipole generators would be located above the level of the calcarine fissure. Instead, the active area of cortex is located the lateral end of the arms of the calcarine fissure. This is apparent in Figure 5.17 in which the extent of the

calcarine fissure is highlighted. Indeed, this accounts for the more inferior position of the dipole location for right lower stimulation. The calcarine fissure is asymmetrical in subject KS, extending more inferiorly in the left hemisphere resulting in the representation of the right lower visual field being located more inferiorly in the left hemisphere. This location at the ends of the calcarine fissure is surprising as this region usually contains a representation of the peripheral visual field although the stimulus extended only 6.5 degrees along the horizontal meridian. However, if this lateral position extends in to visual area V2, the mirror image organisation of this area with respect to V1 would result in the dipole location also being in that region usually representing the peripheral regions of the visual field and a V2 origin is therefore no more likely than a V1 origin.

Hence although the results for subject KS show some ambiguity, those of subject FF and IH indicate the visual evoked magnetic response to isoluminant chromatic gratings arises from a single dipole generator located in V1 of human visual cortex. However, to determine that this region is responding to the chromatic nature of the stimuli, the results must be compared with those obtained from an achromatic, luminance modulated stimulus and a small field chromatic stimulus.

Examination of the response to achromatic stimulation, shown in Figure 5.18, reveals three points of note. Firstly, the response is of lower field strength than that evoked by chromatic stimulation, 429fT compared with 528fT for the chromatic response. Secondly, the achromatic response is more complex, comprising three distinct components rather than the single component observed following isoluminant chromatic stimulation. Thirdly, the initial component peak following achromatic stimulation occurs earlier than that of the single component peak following chromatic stimulation. From this it can be concluded that the signals recorded following chromatic stimulation are as a result of its chromatic content and are not due to luminance artefacts in the stimulus. If this were so, the chromatic response would be of lower field strength than its achromatic counterpart as a result of the lower luminance contrast modulation in the stimulus and the morphology would be expected to be similar or more complex than that following achromatic stimulation. Instead, the response to chromatic stimulation is larger and simpler, which suggests that we are observing cortical activation solely due to a chromatic detecting mechanism. The higher amplitude signal recorded in response to chromatic stimulation was described for electrical evoked potentials by Crognale et al. (1993). They found that luminance only stimulation evoked small, variable responses while chromatic stimulation evoked high amplitude signals. Similarly, intracortical electrical recordings in macaque (Givre

et al., 1995) show that chromatic stimulation evokes a response which is of higher amplitude and occurs later than that evoked by achromatic stimulation.

Finally, it is noted that the initial activity of the achromatic response occurs at a latency much earlier than that of the chromatic response. The first achromatic component peaks at 66ms compared with the chromatic response single component peak at 94ms. This latency difference is consistent, although more marked than that reported by other studies (Murray et al., 1987; Jeffreys, 1989; Krasukopf et al., 1989). As both chromatic and luminance information travel within the parvocellular pathway and should therefore arrive at striate cortex at the same time, this large latency difference must be attributed to activation by the magnocellualr pathway. The magnocellular pathway is sensitive to low spatial frequency luminance stimuli and not to chromatic modulation. The response to achromatic and not, therefore, chromatic stimulation should show evidence of magnocellular activation. Studies in area V1 of macaque have shown that the activation of magnocellular and parvocellular recipient layers is not simultaneous, with 4Cα becoming active some 20ms prior to 4Cβ (Nowak et al., 1995; Givre et al., 1995). Hence in human, a difference in peak latency of 28ms is consistent with differential magnocellular and parvocellular activation.

The evoked magnetic response to a small field chromatic stimulus displays similar topography and dipole characteristics to that evoked by the larger field size. This indicates that luminance artefacts due to display equipment non-linearities and retinal inhomogeneities do not confound the results of the experiment. Any such luminance artefacts in the larger field stimulus would have the effect of introducing additional components into the response and this is not observed. There is a reduction in field strength with the smaller field stimulus with a corresponding poorer signal to noise ratio but this is consistent with the decreased volume of cortex activated. There is an increase in latency of the component peak of between 7 and 17ms for the response evoked by the smaller field size response, consistent with the findings of Plant et al. (1983). Hence the differences in the responses evoked by small and large field stimulation can be attributed solely to differences in the field size and not to the introduction of luminance artefacts in the large field case. The results indicate that the evoked magnetic response to chromatic stimulation is dominated by cells within area V1 of visual cortex.

CHAPTER 6

SPATIAL FREQUENCY CHARACTERISTICS OF THE CHROMATIC EVOKED MAGNETIC RESPONSE

6.1 Introduction

The previous chapter describes the evoked response recorded to isoluminant chromatic gratings. This chapter will examine the effect on the response of changing the spatial frequency of the stimulus.

An investigation of the spatial frequency response properties of cells in macaque striate cortex has been described by Thorell et al. (1984). The majority of cells were found to respond both to chromatic and luminance stimuli but behaved in a manner dependent on the stimulus type, their response peaking at lower spatial frequencies for chromatic stimulation than for luminance stimulation. They distinguished complex cells which showed a bandpass spatial tuning function to isoluminant chromatic stimuli and simple cells which showed a lowpass function. However, Thorell did not specify which cortical layers her cell population was taken from. It is now known that chromatic-selective cells are concentrated in the blob regions of layers 2 and 3 of V1 hence their work may not characterise the spatial frequency tuning properties of chromatic cells in V1.

The contrast sensitivity function of the human chromatic system was determined by Mullen (1985). By eliminating chromatic aberrations from the stimulus she was able to show that the chromatic system has a lowpass spatial frequency function with a resolution of 11-12 cycles/degree. This was true for both the L/M and the S/(L+M) systems. In contrast, red/black and green/black monochromatic gratings revealed the luminance system to have a bandpass spatial frequency response, peaking at 0.8-4 cycles/degree with a resolution of 32-33 cycles/degree. More recent work has suggested that the resolution of the chromatic system may be higher than found was originally thought, up to 21 cycles/degree in the fovea (Anderson et al., 1991). However, while human psychophysical data can determine the output characteristics of the chromatic system as a whole, it cannot reveal the response properties of cells at a particular stage of cortical processing. As Chapter 5 demonstrated the striate origin of the chromatic evoked magnetic response, it is of value to use these responses to

investigate the spatial frequency tuning properties of chromatic sensitive cells in area V1.

The chromatic electrical evoked potential has been described by Murray et al. (1987) who noted the change in amplitude with differing spatial frequencies. The majority of the study utilised a single electrode so that no information on the topography or origin of the response could be ascertained. Also, the lowest spatial frequency used in the study was 1 cycle/degree, hence the full spatial frequency tuning properties of the response could not be determined. The response to gratings of 1 cycle/degree was of low amplitude with the maximal amplitude signal obtained following stimulation with gratings of 3-5 cycles/degree. However, no attempt was made to assess the effect of decreasing the number of cycles displayed; an effect which may account for the low spatial frequency attenuation found. Furthermore, the changes described were marked in only one of the three subjects reported, and one of the subjects showed no consistent response.

A more robust electrical evoked response to chromatic modulation was reported by Rabin et al. (1994) who described the amplitude and latency dependence of the evoked potential on spatial frequency, and to a lesser extent, temporal frequency. The spatial frequency amplitude response function was found to be bandpass, peaking at 1-2 cycles/degree with a high frequency cut-off of 5-10 cycles/degree. The latency of the response peak showed a curvilinear relationship with spatial frequency, increasing above and below 1-2 cycles/degree. However, this study was also limited to a single recording electrode and therefore cannot distinguish between changes in amplitude and changes in topography.

A more thorough investigation of both the response topography and the spatial tuning properties of chromatic sensitive cells in V1 was therefore considered appropriate. This chapter aims to determine the spatial frequency tuning function of chromatic sensitive cells in area V1 of human visual cortex by examining the magnitude of the evoked magnetic response to isoluminant chromatic gratings of various spatial frequencies. The results will be compared with single cell recordings in macaque striate cortex and with the known human psychophysical properties of the chromatic system. Co-registration of MEG and MRI data will be examined to determine any change in the cortical region activated by differing spatial frequencies.

6.2 Method

6.2.1 Stimuli

Isoluminant red/green gratings were generated as in section 5.2.1 and presented in the right lower quadrant of the visual field. This quadrant has been shown to evoke a high field strength response (see Chapter 5). The field size was 4 x 6 degrees and the stimulus was displaced 0.5 degrees from the principal meridians to restrict cortical input to a discrete region of area V1. The spatial frequency of the gratings was varied between 0.25 and 8 cycles/degree. However, with the lowest spatial frequency used, 0.25 cycles/degree, only one cycle of sinusoid could be displayed which could result in an artefactual reduction in magnetic field power. To asses the effect of the number of cycles displayed, a control experiment was performed in which the field size was doubled and the response to the lower spatial frequencies re-recorded. In this way an estimate of the effect of low cycle number was obtained.

6.2.2 Procedure

The visual evoked magnetic response was recorded using the Aston 19-channel SQUID magnetometer system as described in section 2.9 using a procedure as section 5.2.2. The evoked response from gratings of different spatial frequencies was recorded and the data analysed using the magnetic global field power. The peak of the field power was identified and its latency and magnetic field power determined. This measure is appropriate as for each subject, recordings were made with the same dewar position and hence the field power is directly comparable across spatial frequencies within the same subject. Comparison between subjects was enabled by normalising the field power to the percentage of maximum response. Analysis was based on the magnetic field power in preference to the equivalent current dipole moment to avoid obtaining spuriously large values of dipole moment resulting from low strength signals being attributed to dipoles positioned deep within the cortex. Hence latency and magnetic field power were analysed for each of the subjects and plotted as a function of spatial frequency.

6.2.3 Subjects

Four females (KL, LB, JD and FF) and two males (IH and KS) volunteered for the experiment. Their ages ranged from 28 to 39 years and all had normal visual fields and colour vision and a normal or corrected-to-normal Snellen acuity of 6/6.

6.3 Results

The global field power of the evoked magnetic response to isoluminant chromatic gratings for a number of spatial frequencies is shown in Figures 6.1-6.6 for each of the subjects. The time and magnetic field power of the peak corresponding to the V1 chromatic evoked response, as described in Chapter 5, is shown for each spatial frequency. The time window is 500ms and the scale is shown individually for each subject. When the component reached the level of the background noise and could not be clearly identified, the magnetic field power of the component was taken to be zero.

In general the response was dominated by a single major component at all spatial frequencies although for some subjects, particularly KS and JD, a number of spatial frequencies showed evidence of additional activity. However, the major component was readily identifiable in all subjects for all spatial frequencies up to 3-6 cycles/degree and analysis was performed on the latency and magnetic field power of this component.

6.3.1. The effect of spatial frequency on latency

For each subject response latency increased with increasing stimulus spatial frequency, varying from 87-98ms for the 0.25 cycles/degree gratings to 134-142ms for the 4 cycles/degree gratings. Individual data is shown in Figure 6.7. Although there were a few anomalies, the graphs of Figure 6.7 show a clear increase in the peak latency of the response with increasing spatial frequency.

6.3.2 The effect of spatial frequency on magnetic field power

There was a clear dependence of magnetic field power on spatial frequency with each subject displaying a bandpass function which peaked at 1-2 cycles/degree, shown in Figure 6.8. The attenuation of magnetic field power was more marked for high spatial frequencies and the field power of the recorded response fell to the level of the noise at 4-8 cycles/degree.

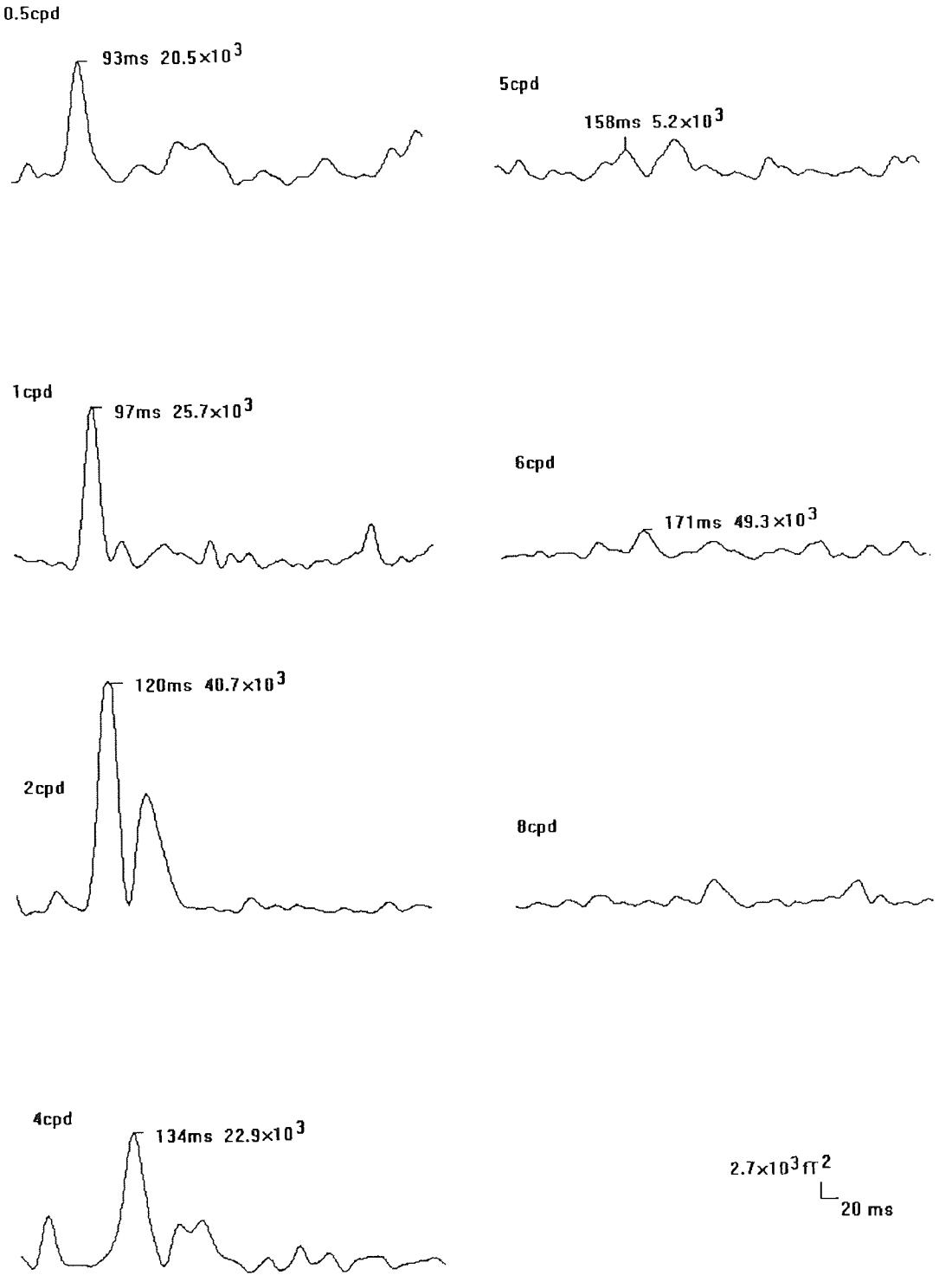

Figure 6.1 Latency and magnetic field power for the peak of the evoked response to isoluminant red/green gratings of various spatial frequencies for subject KL.

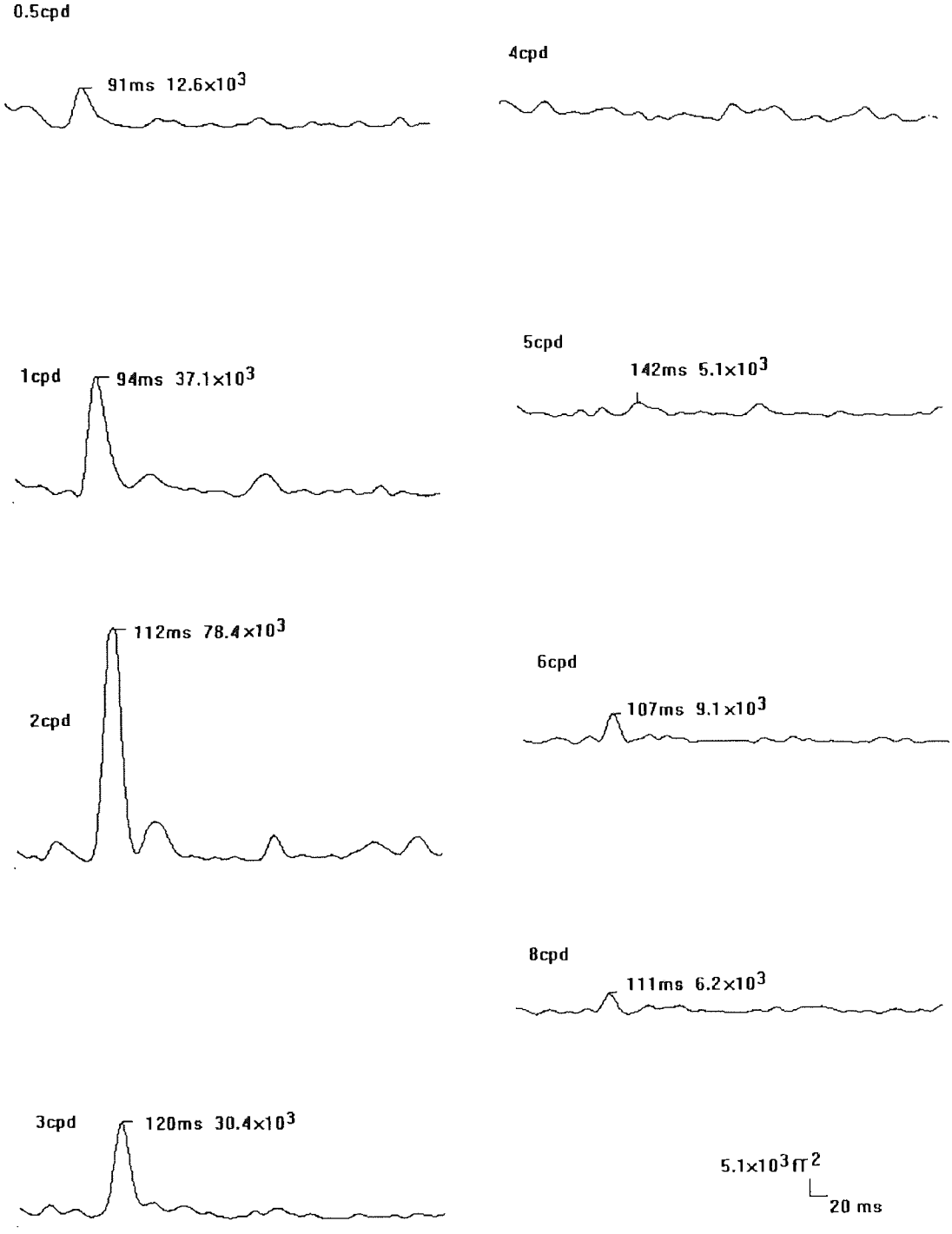

Figure 6.2 Latency and magnetic field power for the peak of the evoked response to isoluminant red/green gratings of various spatial frequencies for subject LB.

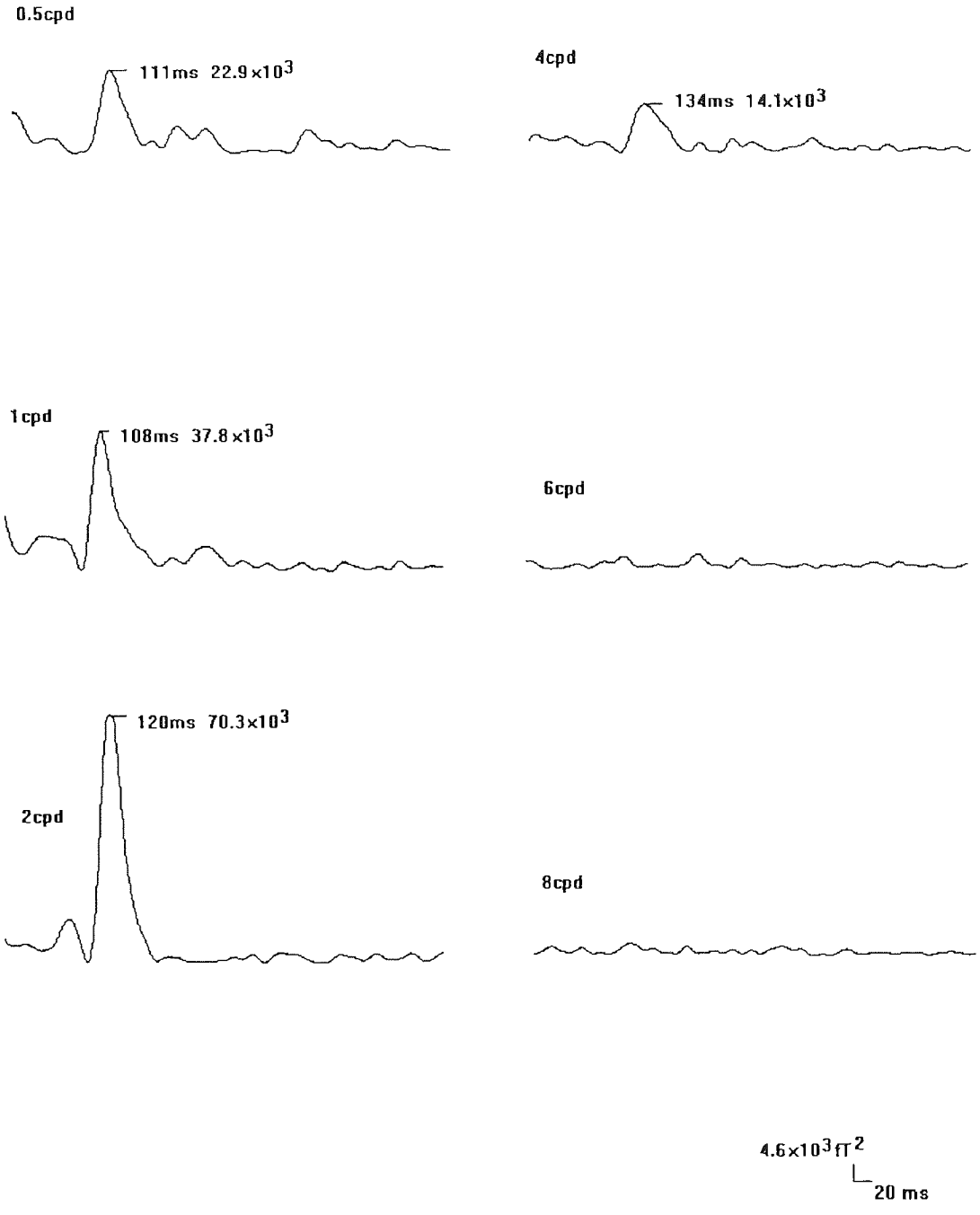

Figure 6.3 Latency and magnetic field power for the peak of the evoked response to isoluminant red/green gratings of various spatial frequencies for subject IH.

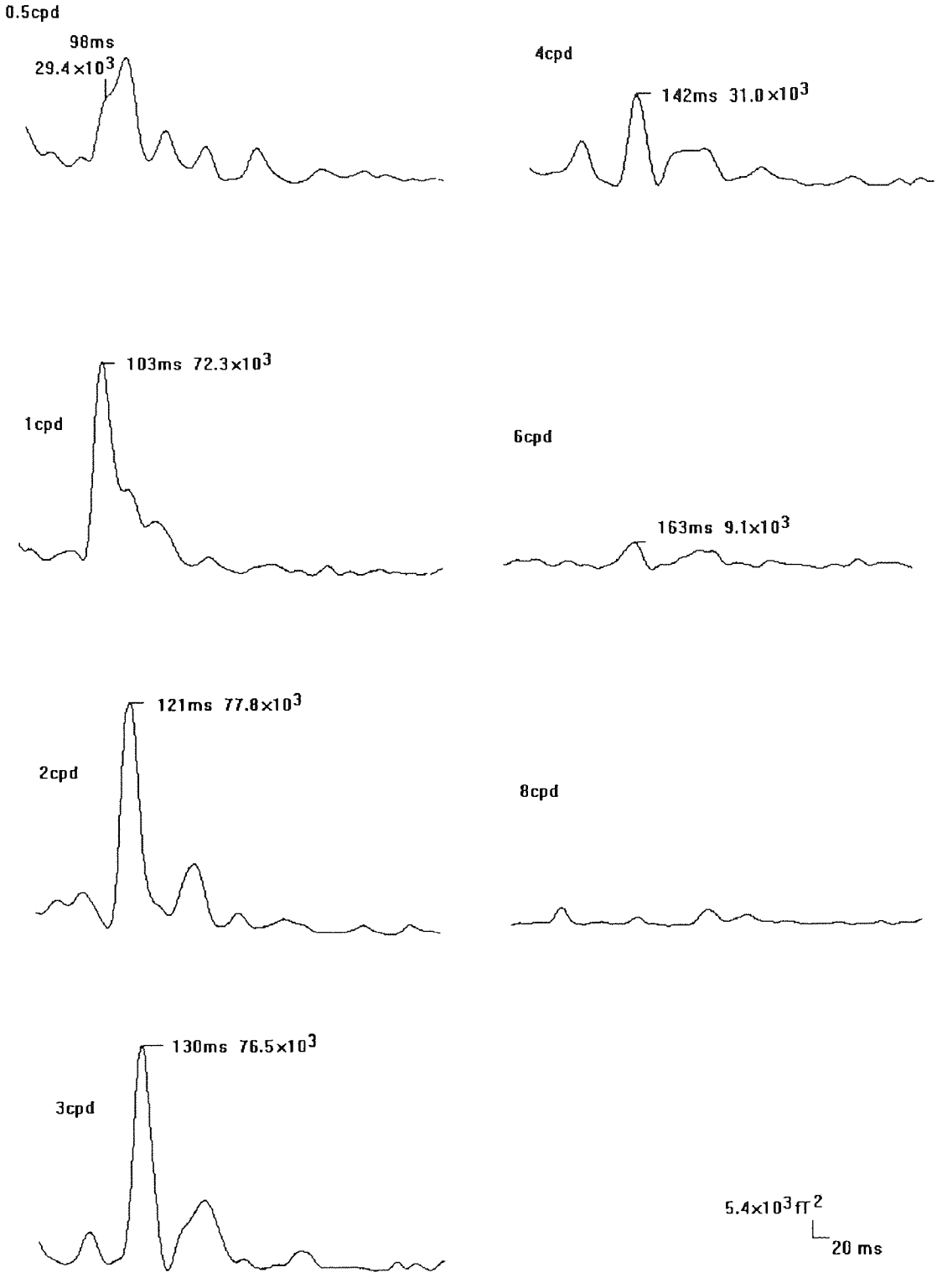

Figure 6.4 Latency and magnetic field power for the peak of the evoked response to isoluminant red/green gratings of various spatial frequencies for subject KS.

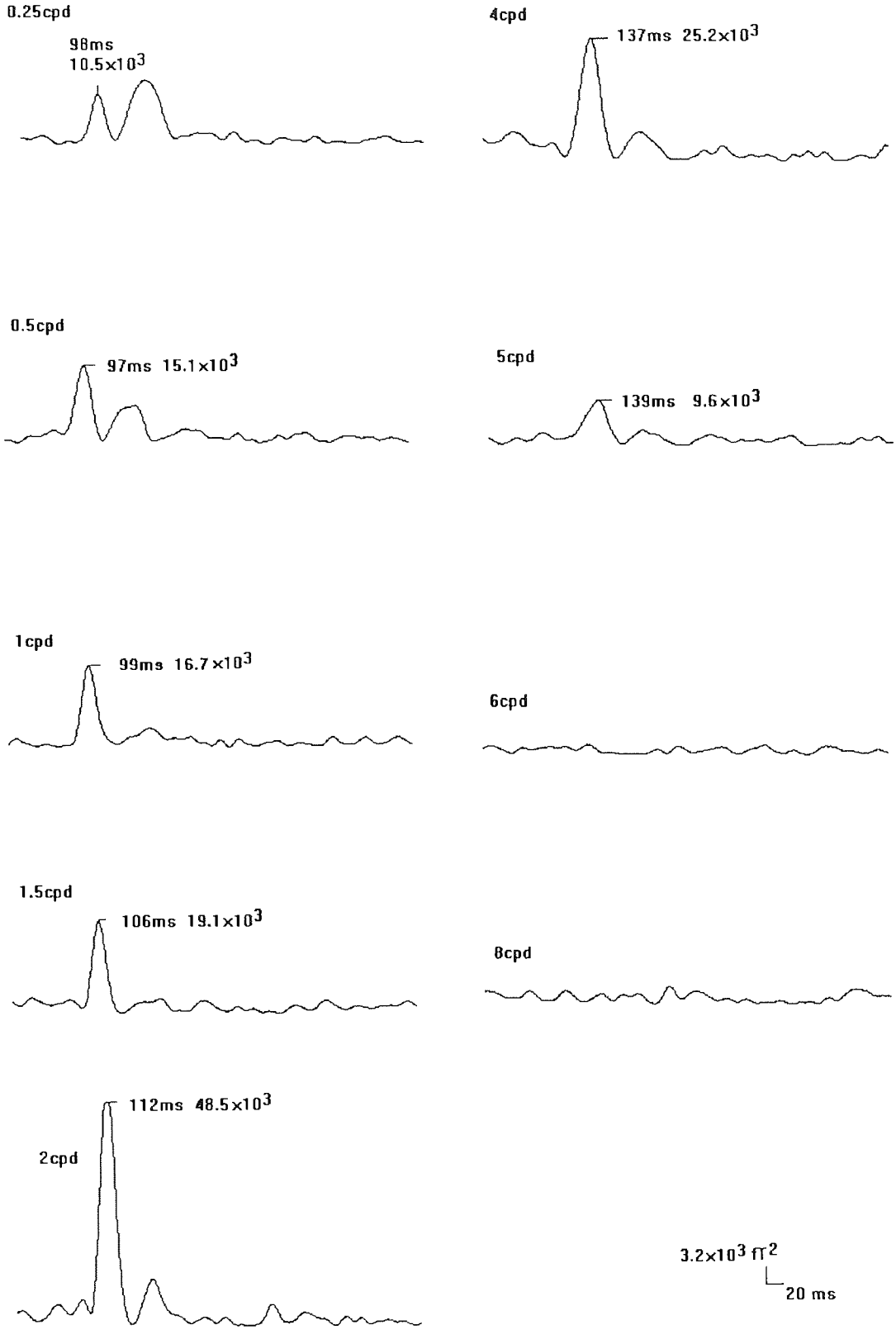

Figure 6.5 Latency and magnetic field power for the peak of the evoked response to isoluminant red/green gratings of various spatial frequencies for subject JD.

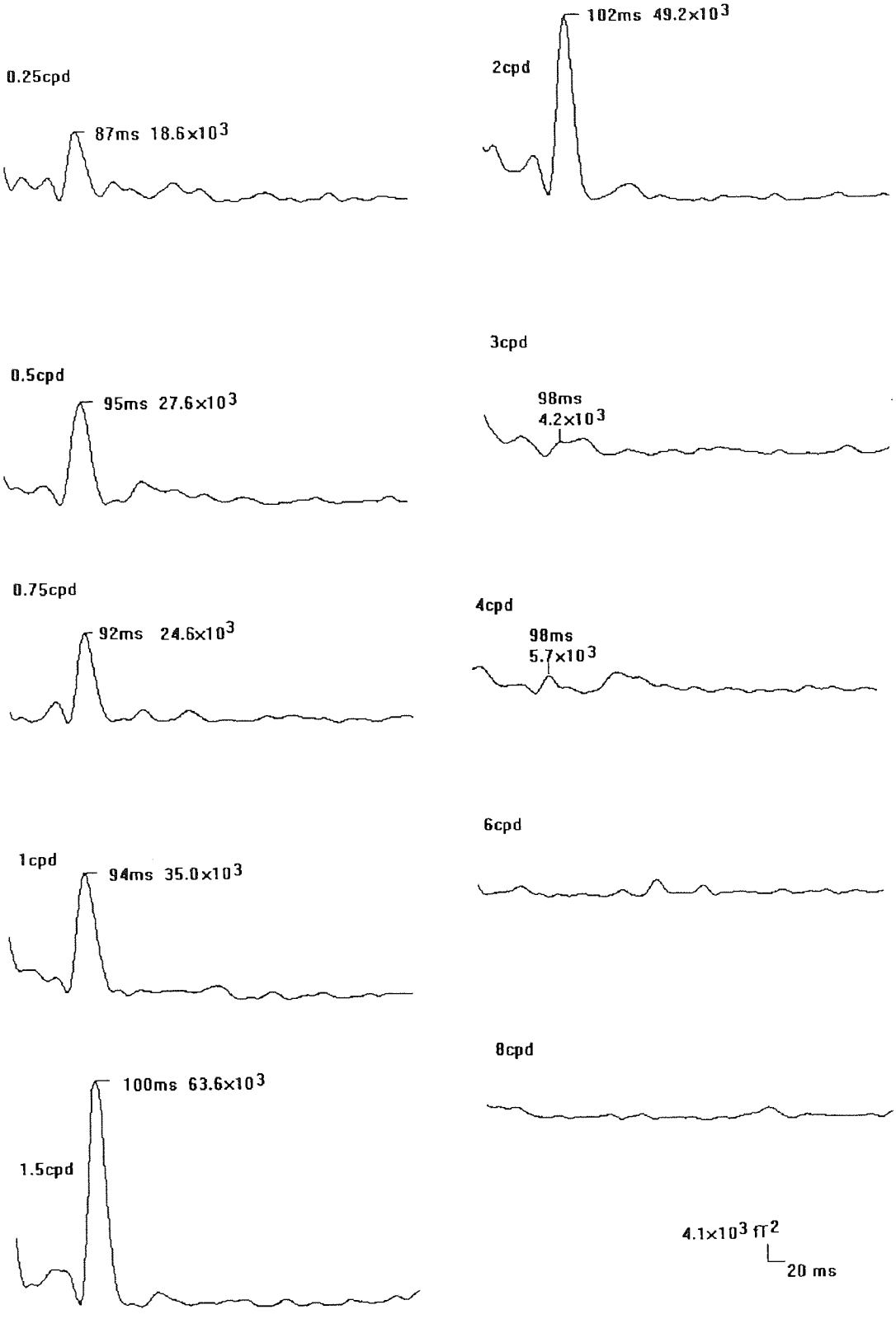

Figure 6.6 Latency and magnetic field power for the evoked response peak to isoluminant red/green gratings of various spatial frequencies for subject FF. 4, 6 and 8 cycles/degree recorded during a different session to the remaining traces

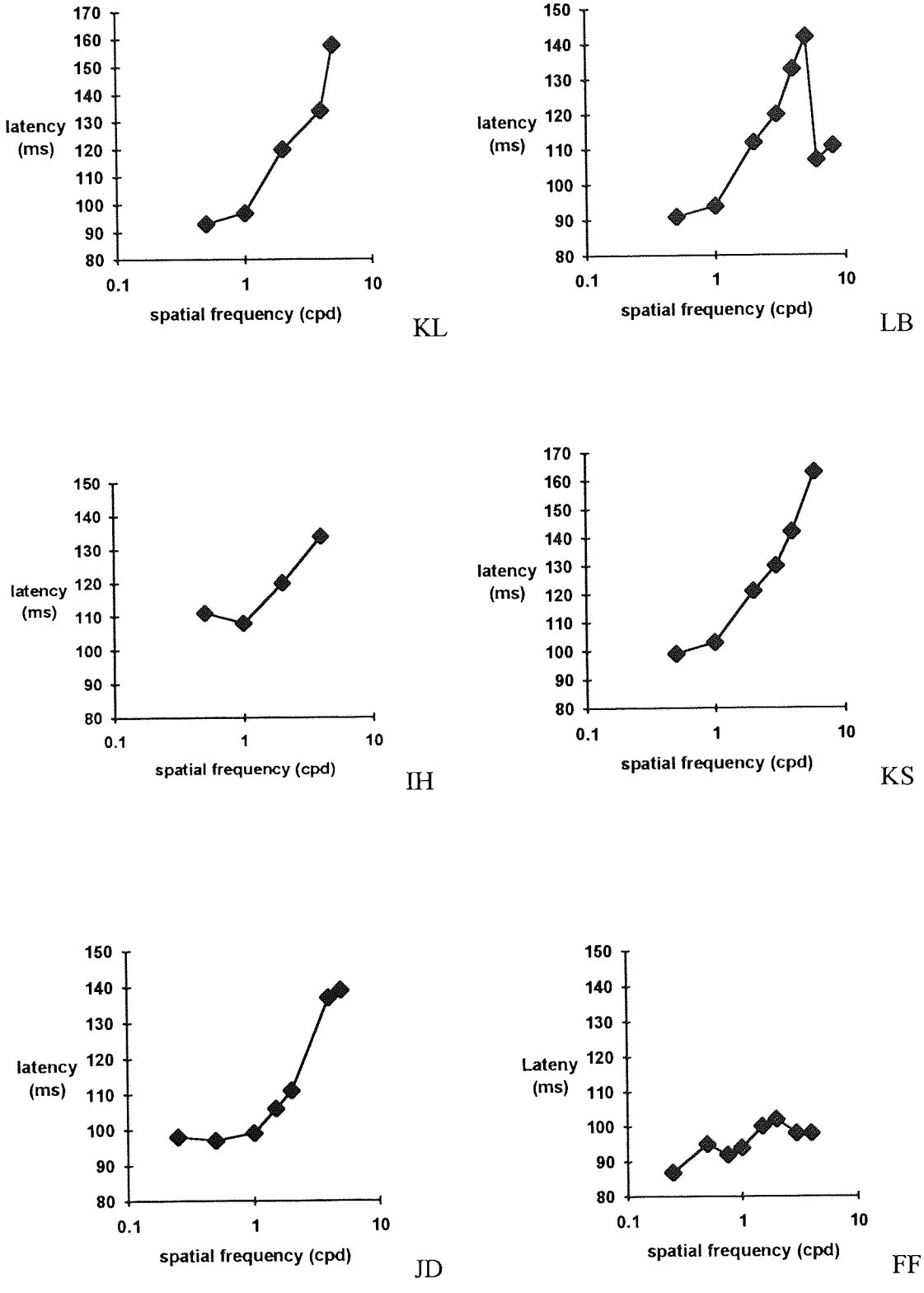

Figure 6.7 Latency as a function of spatial frequency for all subjects

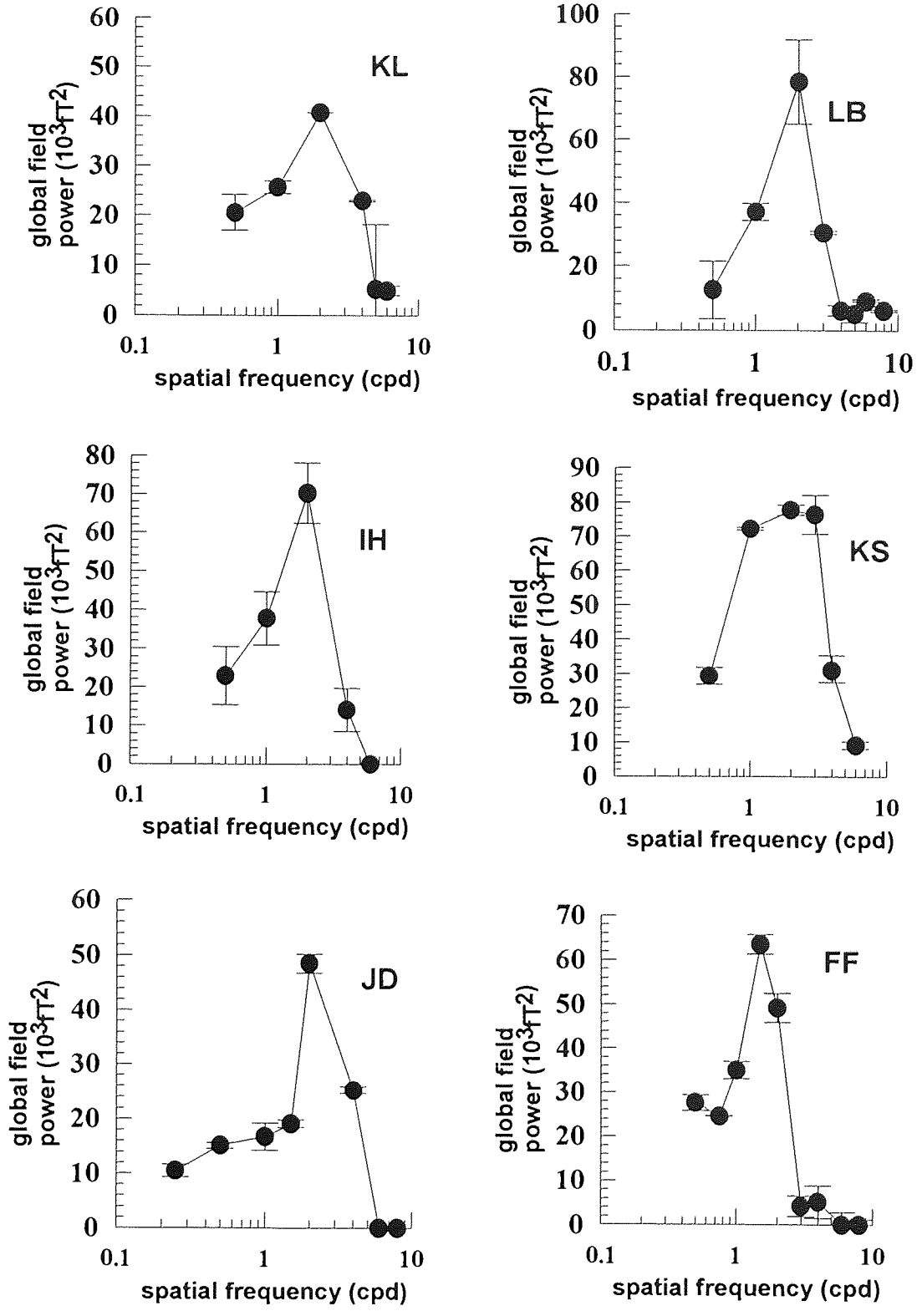

Figure 6.8 The effect of spatial frequency on magnetic field power for all subjects

6.3.3 Control experiment: the effect of cycle number on the evoked response

The results indicate an attenuation in field power of the evoked magnetic response at low spatial frequencies. Although not in agreement with the comprehensive investigation of Mullen (1985), earlier psychophysical research (Granger and Heurtley, 1973) found a similar drop in sensitivity at low spatial frequencies. Mullen (1985) suggests that this apparent drop in sensitivity was due to the low number of cycles displayed at low spatial frequencies and adjusted her field size to control for this. To examine the effect of cycle number on the magnitude of the evoked magnetic response, the experiment was repeated for spatial frequencies between 0.25 and 3 cycles/degree for subject FF using an 8 x 12 degree field. The results are shown in Figure 6.9.

Comparison with the global field power following 4 x 6 degree stimulation indicates an increase in the magnetic field power of the response consistent with the increased area of visual field stimulated. However, the response now saturates at a lower spatial frequency than the 4 x 6 degree field case, as can be seen in Figure 6.10 which shows the effect of spatial frequency on magnetic field power.

A direct comparison of the two field sizes used can be made by normalising the global field power and plotting both sets of data together, as shown in Figure 6.11. The graph in Figure 6.11 suggests that the reduced number of cycles displayed at low spatial frequencies contributes towards the attenuation of the response at spatial frequencies below 1 cycle/degree. The effect of number of cycles contained in the stimulus is shown in Figure 6.12.

Figure 6.12 shows that at low cycle numbers the two data sets are similar but for higher numbers of cycles the two curves diverge, with the smaller field size falling off more rapidly. This indicates that at low spatial frequencies the magnetic field power is limited by the number of cycles in the display and when higher numbers of cycles are displayed the magnetic field power is limited by the spatial frequency of the gratings.

6.3.4 Cortical localisation of the response

To determine the cortical volume generating the evoked magnetic response an equivalent current dipole inversion algorithm was applied and Monte-Carlo error analysis performed to obtain confidence regions over a range of spatial frequencies. The results are shown in Figure 6.13 for subjects FF and IH. The confidence regions are larger for those spatial frequencies evoking lower field power responses but there is no consistent change in cortical location with changing spatial frequency. For

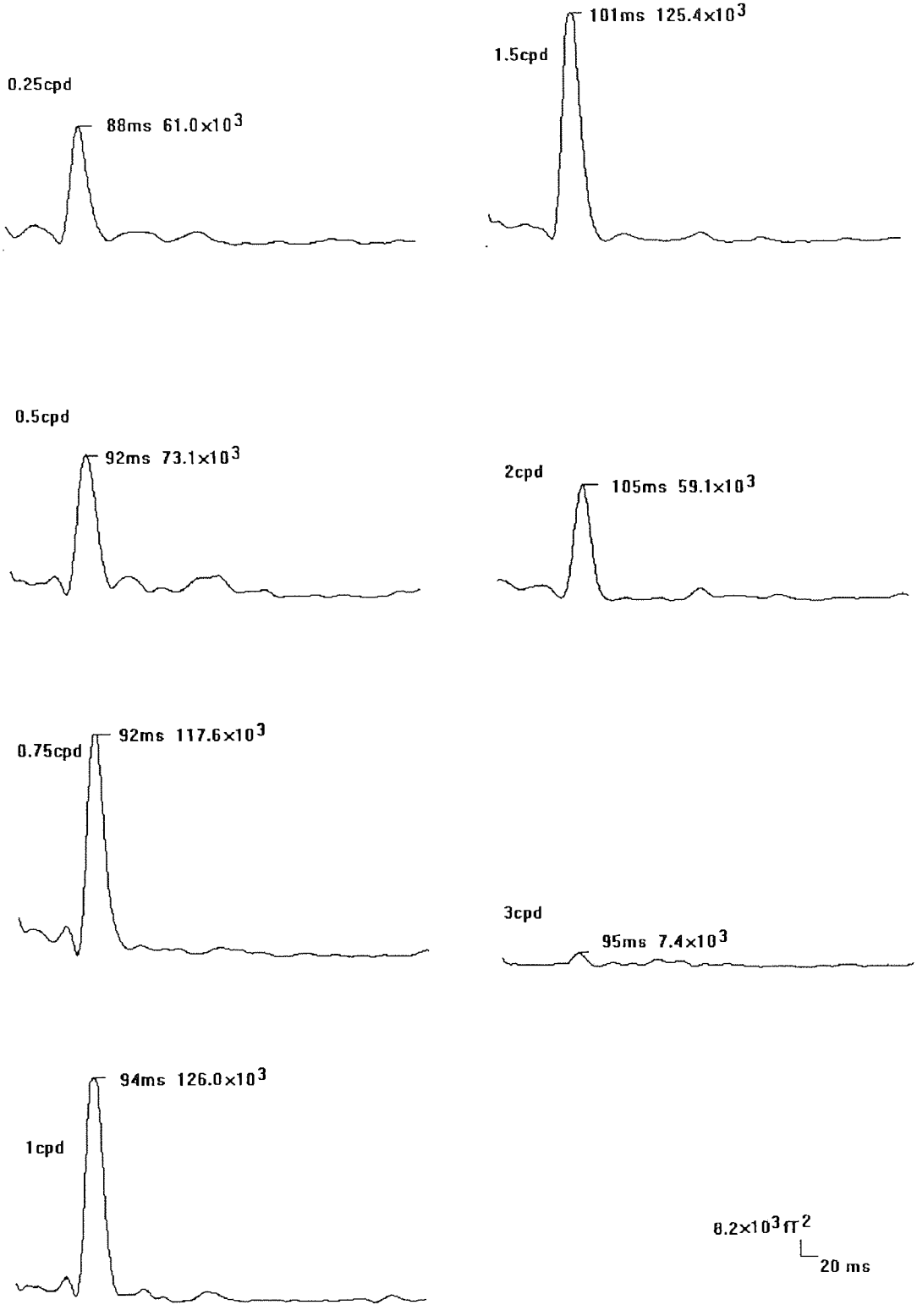

Figure 6.9 Latency and magnetic field power for the peak of the evoked response to isoluminant red/green gratings of various spatial frequencies in an 8 x 12 degree field for subject FF

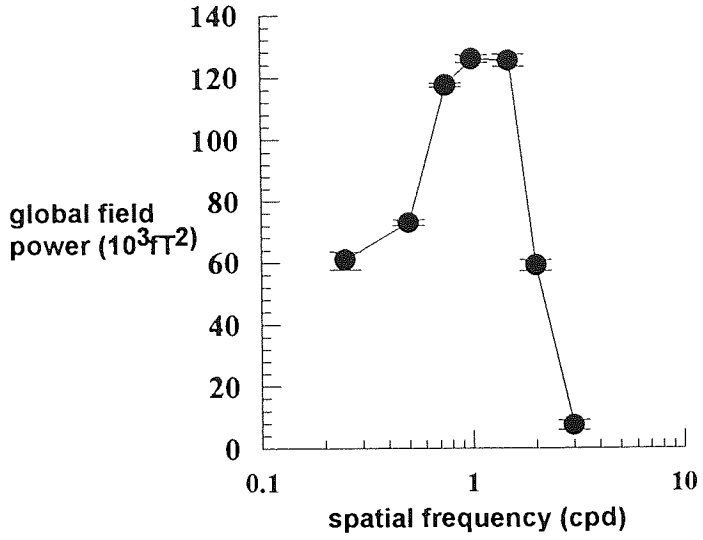

Figure 6.10 The effect of spatial frequency on magnetic field power in an 8 x 12 degree field for subject FF

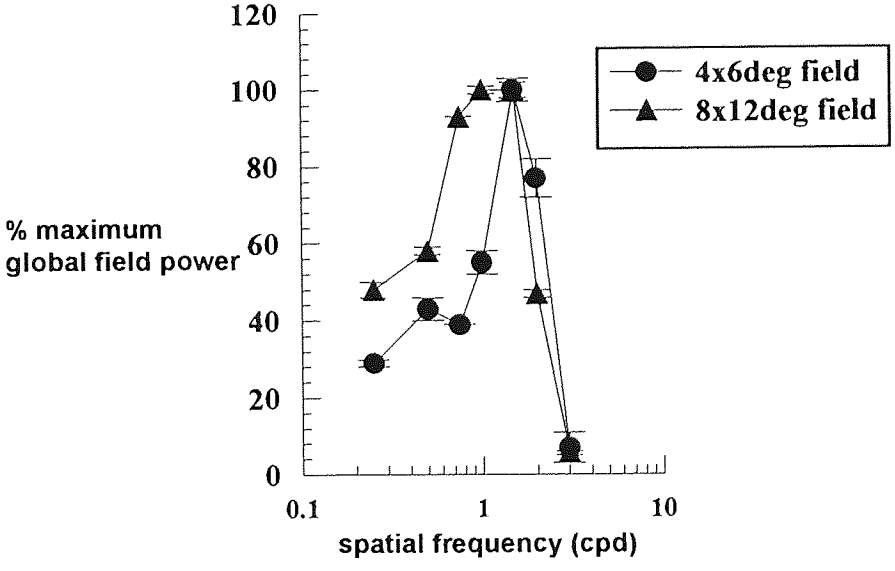

Figure 6.11 Normalised magnetic field power for 4 x 6 and 8 x 12 degree field sizes for subject FF

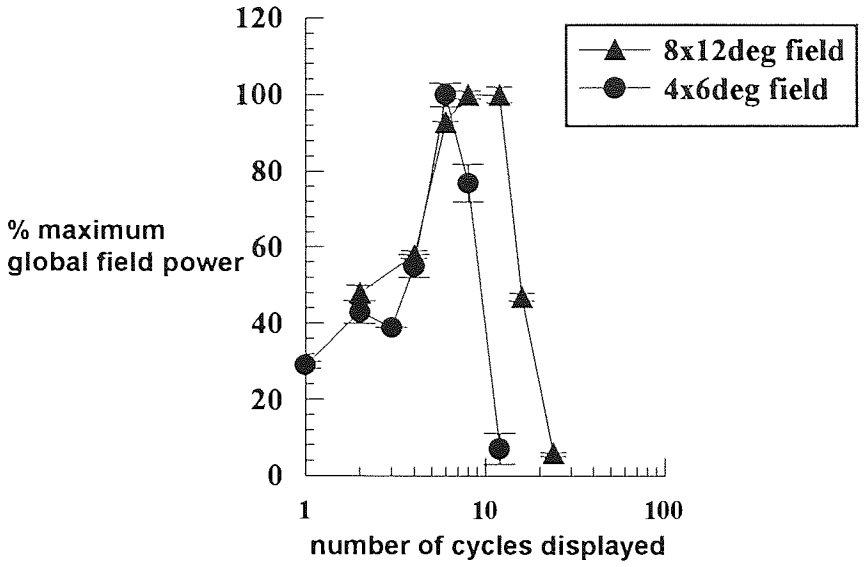

Figure 6.12 Normalised global field power as a function of cycles in the display for subject FF

subject FF all confidence regions are clustered together along the calcarine fissure.

6.4 Discussion

An analysis of the effect of spatial frequency on the latency and magnetic field power of the evoked magnetic response was undertaken. Equivalent current dipole solutions were obtained and Monte-Carlo simulations established the cortical regions generating the evoked response for a range of spatial frequencies.

The results demonstrate a clear trend of increasing latency with increasing spatial frequency. As such this is consistent with the results of Plant et al. (1983) who demonstrated that above 2 cycles/degree there was an increase in latency with increasing spatial frequency of achromatic gratings. The latency changes presented here closely resemble those reported for chromatic evoked potentials by Rabin et al. (1994) who also observed this curvilinear latency function, with latency increasing above and below 1-2 cycles/degree. However, in a similar study of the chromatic evoked potential, Murray et al. (1987) did not note any increase in latency with increasing spatial frequency.

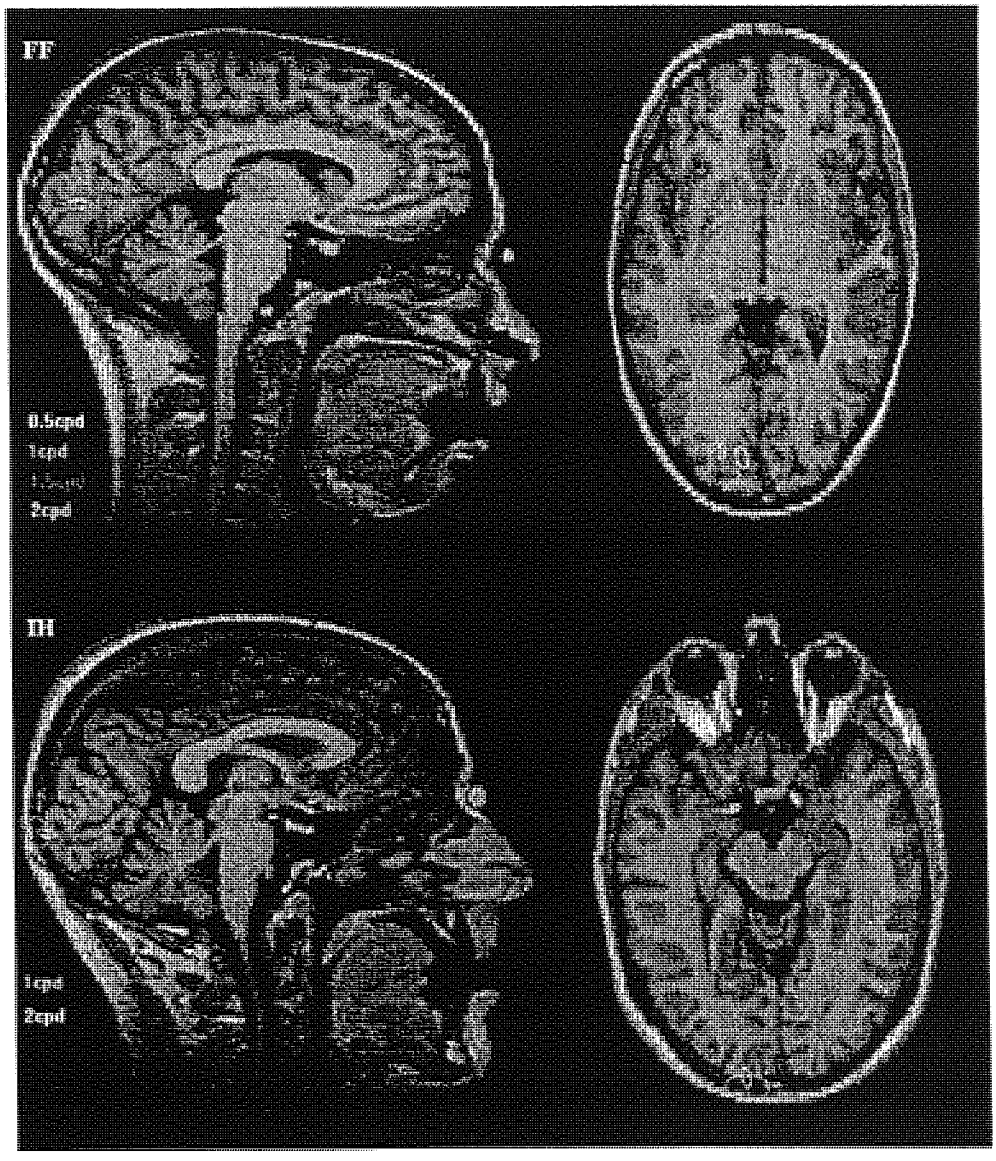

Figure 6.13 Confidence regions for the dipole locations evoked by a range of spatial frequencies for subjects FF and IH

Above 1 cycle/degree there was a monotonic increase in latency with increasing spatial frequency. Below 1 cycle/degree, three subjects exhibited a curvilinear relationship with an increase in spatial frequency producing no change or a decrease in latency. For subject LB, Figures 6.2 and 6.8 show that although the response falls to noise levels at 4 and 5 cycles/degree, there is a small increase in magnetic field power at 6 and 8 cycles/degree with the response becoming more apparent. This is accompanied by a decrease in latency, as shown in Figure 6.7. This re-emergence of the signal out of the background noise may indicate the effect of chromatic aberrations producing luminance artefacts in the higher spatial frequency gratings. For subject FF the increase in latency with spatial frequency saturates at 2 cycles/degree, with the response to 3 cycles/degree and 4 cycles/degree being of slightly shorter latency. This occurred both for the small and large visual field conditions. Chromatic aberrations are less likely to cause problems with luminance artefacts at spatial frequencies below 4 cycles/degree (Bradley et al., 1992) and if this was the cause of the latency shift it would be expected that with increased spatial frequencies, and therefore more chance of introducing luminance artefacts, the latency shift and field power would increase. Although there is a slight field power increase at 4 cycles/degree, this is comparable with experimental error and the response falls to noise levels at 6-8 cycles/degree. Hence the results are not satisfactorily explained by a luminance intrusion in the response to high spatial frequencies and the decrease in latency may be due to an increase in synchrony caused by the lower number of responding neurones.

Previous explanations for the increase in latency of the response to achromatic stimulation, discussed in section 4.8.3, are based on the decrease in contrast sensitivity at high spatial frequencies hence the latency increase may be due to a decrease in supra-threshold contrast. The chromatic contrast sensitivity function is lowpass and sensitivity starts to decrease at 0.8 cycles/degree (Mullen, 1985). The increase in latency observed may therefore reflect the decrease in sensitivity to the stimuli above 1 cycle/degree.

The spatial frequency tuning function of each subject showed bandpass characteristics with the response peaking at 1-2 cycles/degree and falling to the level of the noise at 4-8 cycles/degree. As such this is similar to the spatial frequency tuning function recorded by Rabin et al. (1994) which also comprised a peak at 1-2 cycles/degree although with a slightly higher cut-off frequency of 5-10 cycles/degree. A bandpass function was also found in electrical evoked response recordings by Murray et al. (1987) although the function peaked at the higher spatial frequencies of 3-5 cycles/degree. Thorell et al. (1984) summed the response to chromatic stimulation of

108 cells in macaque striate cortex and found a lowpass spatial frequency function peaking at 1-2 cycles/degree, similar to that described psychophysically in humans by Granger and Heurtley (1973), showing a degree of low frequency attenuation. This was thought to reflect the activity of simple cells at low spatial frequencies and complex cells at higher spatial frequencies. When the activity of simple cells was examined separately, there was little low frequency attenuation and the results resemble those of Mullen (1985) who in her psychophysical investigation of the human chromatic system found that using field sizes of 2-23 degrees resulted in no low frequency decrease in chromatic sensitivity. She suggested that previous psychophysical reports of such a decrease (Granger and Heurtley, 1973; Kelly, 1983) may be due to insufficient numbers of cycles displayed. Indeed, Howell and Hess (1978) showed that the psychophysical contrast sensitivity is not independent of field size and cycle number until four or more stationary cycles are displayed.

A control experiment was therefore performed to investigate the effect of field size and therefore cycle number on the evoked response. When the field size was doubled from 4 x 6 degree to 8 x 12 degrees the response doubled in magnetic field power. This is consistent with the increased volume of cortex stimulated. However, Figure 6.21 offers a normalised comparison of the response under the two conditions. The magnetic field power bandwidth widens for the larger field condition as the response saturates earlier, suggesting the limited number of cycles displayed for the low spatial frequency gratings contributes towards the observed low frequency attenuation. This is further demonstrated in Figure 6.22 which plots the normalised magnetic field power against the number of cycles displayed in the stimulus. At the low cycle number end of the graph, both field sizes give similar results while above 8 cycles, the curves diverge.

This indicates that when a low number of cycles are present in the stimulus, the magnetic field power of the response is limited by the number of cycles displayed. However, when more than 8 cycles of the stimulus are displayed, the signal field power is limited by the spatial frequency of the stimulus. This saturation at 8 cycles contrasts with the psychophysical observation that contrast sensitivity saturates when 4 cycles are displayed (Howell and Hess, 1978) and with the results of Plant et al. (1983) who noted that amplitude saturation occurs when 50 cycles are displayed. The high cycle number of Plant et al. (1983) may represent a confounding effect of spatial frequency and field size.

The discrepancy between the results of psychophysical observations and evoked magnetic response data presented here can be explained by considering the neuronal

activity necessary for detection by each technique. To perceive a stimulus, relatively few neurones must signal the presence of the stimulus (Newsome et al., 1989). To record a clear evoked magnetic response the number of simultaneously active neurones must be in the order of one million so that the signal is sufficiently large to be distinguishable from the background noise (Hämäläinen et al., 1993). However, as described in section 4.8.1, Kulikowski (1977a) demonstrated the electrical P150 component was highly correlated with the detectability of the stimulus. The evoked responses were averaged separately on the basis of whether the subject detected the stimulus pattern and it was found that while those stimuli that were detected gave clear responses, those stimuli which were not detected gave no distinguishable response. This may reflect a difference in the characteristics of the achromatic response recorded by Kulikowski and the chromatic response described here. Also, the amount of neuronal activity required to record an electrical and magnetic evoked response may differ due to the relatively small magnetic field power of the magnetic evoked response in comparison to the ambient magnetic field.

Hence although a reduction in field power at low spatial frequencies was caused by the low number of cycles in the stimulus, due to physical restraints imposed by the recording equipment it was not possible to establish if the response would approach a lowpass function if sufficient cycle numbers were displayed. It remains possible that the chromatic contrast sensitivity function is formed by an envelope of channels tuned to different spatial frequencies with more neurones tuned to 1-2 cycles/degree than to lower and higher spatial frequencies.

The second point on which the results presented here differ with previous psychophysical and elecrophysiological reports of the spatial frequency tuning function of the chromatic system is the resolution of the system. Mullen (1985) and Thorell et al. (1984) reported a resolution of 11-12 cycles/degree. More recent psychophysical investigation suggests that this may be as high as 21 cycles/degree, although resolution falls off rapidly with retinal eccentricity (Anderson et al., 1991). The evoked magnetic response falls to the level of the noise at between 4 and 8 cycles/degree with the majority of subjects having a response at noise levels at 6 cycles/degree. This is comparable with the results of Murray et al. (1987) who reported the chromatic electrical evoked response being of low amplitude at 8 cycles/degree and Rabin et al. (1994) who reported a cut-off frequency of 5-10 cycles/degree. These slightly higher values may arise due to these studies utilising full field stimulation rather than the relatively small field quadrants used here. The increased volume of cortex activated by a large full field stimulus would result in a greater field strength and therefore the

evoked response being recordable closer to threshold. The difference between the evoked magnetic response data and the psychophysical and single cell electrophysiology can be explained by the argument presented above in that many neurones must simultaneously respond before an evoked response can be recorded. As the sensitivity of the chromatic system decreases, less cells will respond and while there may be sufficient numbers to allow detection of a stimulus and to be recorded directly from single cells, their numbers may not be sufficient to produce a clear evoked magnetic response. MEG may therefore provide a more accurate measure of the relative numbers of units tuned to a particular spatial frequency than detection thresholds used in psychophysical studies.

Finally, confidence regions for the equivalent current dipole cortical locations were examined over a range of spatial frequencies. The volume of the confidence regions increases in a manner consistent with the lower signal to noise ratio obtained from higher spatial frequencies. Nevertheless it is apparent that there is no change in cortical location as the spatial frequency of the stimulus increases. The data does not, therefore, support the work of Aine et al. (1990) who found a change in the location and orientation of the equivalent current dipole with changing spatial frequency of achromatic gratings. However, the data reported here is consistent with the anatomical arrangement of striate cortex. Within a cortical module spatial frequency is encoded radially, with optimal spatial frequency increasing with radial distance from the blob centres (Tootell et al., 1988e; Edwards et al., 1995). Hence with many cortical modules active, there should be no net change in cortex activated with changing spatial frequency. The changes noted by Aine et al. (1990) may therefore be due to poor dipole fits due partly to the use of a full field stimulus and only a two dipole model. A full field stimulus will activate four spatially separate regions of cortex, even if it assumed that only area V1 is active at the time of analysis. The use of a two dipole model will inevitably lead to errors in the dipole solutions obtained.

Hence the results presented in this chapter show that the spatial frequency tuning curve of the chromatic evoked response is bandpass, peaking at 1-2 cycles/degree and falling to the level of the noise at approximately 6 cycles/degree. The reduction in magnetic field power observed for low spatial frequencies was found to be influenced by the low number of cycles present in the stimulus display. The cortical location of the dipole generator of the evoked magnetic response was found to invariant with spatial frequency. The results are in agreement with the known spatial frequency properties of area V1 and add further support to the V1 origin of the chromatic evoked magnetic response.

CHAPTER 7

TEMPORAL FREQUENCY CHARACTERISTICS OF THE CHROMATIC EVOKED MAGNETIC RESPONSE: *the contribution of colour to motion perception*

7.1 Introduction

The contribution of colour to the perception of motion is an issue which attracts considerable debate. Various hierarchical processing models of the visual system indicate a clear dichotomy of colour and motion processing (Livingstone and Hubel (1988a; Van Essen, 1985). In these models luminance provides the only input to motion analysis and is carried by the magnocellular system and proceeds from layer 4C α to layer 4B in striate cortex, then to the thick stripes of V2 before arriving at the motion area MT (V5). Colour information, however, is carried in the parvocellular system and travels via layer 4Cβ to layers 2 and 3 of striate cortex, then to the thin stripes of V2 before arriving at the colour centre V4.

This separation of information is consistent with reports of decreased sensitivity of the motion system at isoluminance. Ramachandran and Gregory (1978) reported that when subjects viewed the apparent motion of a red/green checkerboard pattern, the impression of motion disappeared when the checks were made isoluminant. They concluded that colour and motion were analysed separately by the visual system and that colour provides, at best, only a weak cue to motion perception. This was followed by a number of reports of perceptual motion-related phenomena that were reduced or abolished at isoluminance.

Many authors reported drifting chromatic gratings as appearing to move more slowly than luminance gratings of the same spatial and temporal frequencies (Cavanagh et al., 1984; Derrington and Henning, 1993; Henning and Derrington, 1994; Mullen and Boulton, 1992). Ramachandran (1987) described how the motion of one feature could be "captured" by another so that the two appear to move together. The effect was more marked when the two features were isoluminant such that when a luminance difference was introduced the motion capture was reduced. Luminance motion signals were thought to capture stationary chromatic borders but moving chromatic borders were thought to be incapable of generating motion capture. It was concluded that

colour provides weak if any input to the perception of motion and that colour is merely "painted in" to a scene.

While the direction of motion of an achromatic gratings can be discerned at its detected threshold (Anderson and Burr, 1985), the threshold for detecting an isoluminant chromatic grating is lower than that for identifying the direction of its motion (Lindsay and Teller, 1990; Anderson and Burr, 1991). In this way Lindsay and Teller (1990) examined the detection, orientation and discrimination threshold ratios of chromatic and luminance modulated gratings. They showed that there are large, task-specific losses in the ability to discriminate motion at isoluminance and concluded that the residual capacity for motion discrimination at isoluminance may be due to artefactual intrusion of luminance information.

This conclusion is questioned by the results of Logothetis et al. (1990) who examined the performance on psychophysical tasks together with single cell recordings in the LGN of rhesus monkey. They found that texture perception and motion and depth perception were all compromised but not abolished at isoluminance. Both magnocellular and parvocellular cells were effected but the activity of neither system was abolished. Their findings suggest that the impairment of vision at isoluminance cannot be attributed solely to the inactivation of the magnocellular pathway. This was supported by a number of lesion studies which selectively destroyed the magnocellular or parvocellular layers in the LGN of rhesus monkey (Schiller, 1991) and macaque (Merigan et al., 1991). While high temporal frequency motion information was conveyed by the magnocellular pathway, lower temporal frequencies were found to be carried by both magnocellular and parvocellular pathways.

However, it was generally assumed that it was the magnocellular pathway that provided the major input to motion perception. Contrary to this, Anderson et al. (1995) showed using psychophysical techniques that in the human peripheral retina, the parvocellular pathway is capable of the detection and discrimination of motion and limits motion acuity at all temporal frequencies. They argued that if this was true of the peripheral retina under conditions favouring magnocellular cells, it is likely the parvocellular system plays an important role in motion perception at all retinal eccentricities

However, these studies examined the ability of different pathways to convey achromatic motion information. While it is now apparent the parvocellular pathway is capable of carrying such luminance based motion, is it also capable of using chromatic

information in the perception of motion? Cavanagh and Favreau (1985) demonstrated using the motion after effects that chromatic motion can be transferred to luminance stimuli and vice versa. They concluded that colour provides an input to motion perception that is unlikely to arise from luminance artefacts or residual activity in the magnocellular pathway. The effect was shown to decrease with increasing spatial and temporal frequencies in a manner typical of the chromatic parvocellular system and not the luminance magnocellular system (Cavanagh and Anstis, 1991). This was supported by Kremers et al. (1992) who measured both the sensitivity of macaque retinal ganglion cells and the human psychophysical sensitivity function to chromatic and luminance stimulation. The results indicated that magnocellular cells have a bandpass temporal response to chromatic, luminance and combined chromatic and luminance stimulation. Parvocellular cells, however, were found to have a lowpass temporal frequency response to chromatic stimulation and a reduced sensitivity to luminance stimulation. To stimuli with both chromatic and luminance modulation it was thought that the chromatic channel underlies detection below 3Hz and the achromatic channel above 3Hz. The results suggest the sensitivity function is an envelope of chromatic and achromatic mechanisms supported by magnocellular and parvocellular systems.

There are several lines of support for the existence of multiple motion systems. Stone and Thompson (1992) showed that the perceived speed of slowly moving luminance-defined targets is contrast-dependent while that of fast moving targets is not. This was thought to arise from the rapid contrast saturation of magnocellular cells underlying the detection of fast-moving targets. Similarly, Hawken et al. (1994) showed that for temporal frequencies greater than 4Hz, motion processing of both isoluminant and luminance stimuli is contrast independent and that isoluminant stimuli do not appear to be slowed down. They concluded that a single motion pathway is required to encode motion at intermediate to high temporal frequencies but that two pathways are required to account for motion sensitivity at low temporal frequencies. This was supported by later work (Gegenfurtner and Hawken, 1995) which demonstrated that the chromatic motion discrimination threshold is dependent both on temporal frequency and retinal eccentricity. Motion discrimination of low temporal frequency isoluminant gratings was thought to be undertaken by a mechanism specialised for foveal vision. However, while retaining the concept of a high and low temporal frequency motion systems, Gorea et al. (1993a,b) suggest the low temporal frequency mechanism is capable of utilising both chromatic and luminance information at an early stage of processing while the high temporal frequency system comprises separate pathways for colour and luminance information.

Evidence for two chromatic-sensitive motions systems was also found by Derrington and Henning (1993) who noted a difference in threshold for the detection and direction discrimination for chromatic but not for luminance modulated stimuli in the parafovea. For foveally-viewed gratings, detection and discrimination thresholds were approximately equal for both chromatic and luminance gratings. Their results were attributed to a low level or first-order motion system which is not as sensitive to isoluminant chromatic input as to luminance input. The high sensitivity to chromatic gratings was thought to be due to a high level foveal system which is sensitive to both chromatic and luminance information. This dual pathway for chromatic information was supported by Cropper and Derrington (1994) who demonstrated that a fast, first-order motion mechanism was used to analyse luminance and high contrast chromatic gratings while for low contrast chromatic gratings, detection thresholds were suggestive of a slow, second-order mechanism. A low and high level distinction was suggested by Culham and Cavanagh (1994) to explain the results of their motion capture experiment. Motion capture was found to occur at isoluminance and when the direction of motion was ambiguous, observers perceived motion in the direction to which they attended. They suggested motion capture arises from a low level contribution of colour-opponent mechanisms and from higher attentional processes utilising both chromatic and luminance information.

Hence recent psychophysical investigations point to the existence of more than one motion system, although the form this division takes is debatable. The evidence is suggestive of mechanisms for high and low temporal frequencies although it is unclear whether colour and luminance information are combined or if they are analysed separately. The mechanism governing the detection of low temporal frequency chromatic gratings does not underlie the discrimination of its motion, evidenced by the different detection/discrimination ratios described above. However, it is possible that for low temporal frequencies, there is one motion mechanism which is more sensitive to luminance modulations but can also discriminate chromatic motion with increased contrast. The mechanism underlying the detection but not the discrimination of motion of lower contrast isoluminant chromatic targets may be a non-motion-specific mechanism which responds to the presence of a grating but does not signal its motion.

By examining the magnitude of the response evoked by isoluminant gratings which vary in temporal frequency, it may be possible to discern the presence of distinct motion detecting mechanisms. To investigate this issue the evoked magnetic response was recorded to isoluminant chromatic gratings at temporal frequencies of 0-40Hz. The response to stationary gratings has been shown to originate in area V1 (Chapter

5). The latency and global field power of the evoked response will be examined for evidence of single or multiple mechanisms responding to chromatic stimuli over a wide range of temporal frequencies at the level of V1.

7.2 Method

7.2.1 Stimuli

Isoluminant red/green gratings were generated as in section 5.2.1 and presented in the right lower quadrant of the visual field. This quadrant has been shown to evoke a high field strength response (see Chapter 5). The field size was 4 x 6 degrees and the stimulus was displaced 0.5 degrees from the principal meridians to restrict the primary cortical input to a distinct region within V1. The spatial frequency of the gratings was 2 cycles/degree as this provides the maximum field strength response (see Chapter 6). The temporal drift frequency of the grating was varied between 0Hz and 40Hz. For the 0Hz condition, the phase of the gratings was varied between each stimulus presentation. For the achromatic control condition the gratings were of 20% contrast and were matched for mean luminance (cd/m^2) and spatial frequency (2 cycles/degree).

7.2.2 Procedure

The visual evoked magnetic response was recorded using the Aston 19-channel SQUID magnetometer system as described in section 2.9 using a procedure as section 5.2.2. The evoked response from gratings of different temporal frequencies was recorded and the data analysed using magnetic global field power. This measure is appropriate as for each subject, recordings were made with the same dewar position and hence the field power is directly comparable across temporal frequencies within the same subject. Comparison between subjects was enabled by normalising the field power to the percentage of maximum response. Hence latency and magnetic field power were analysed for each of the subjects and plotted as a function of temporal frequency.

7.2.3 Subjects

Three females (KL, LB and JD) and two males (IH and KS) volunteered for the experiment. Their ages ranged from 28 to 39 and all had normal visual fields and colour vision and a normal or corrected-to-normal Snellen acuity of 6/6.

7.3 Results

The global field power of the evoked magnetic response to 2 cycles/degree gratings drifting between 0Hz and 40Hz is shown for each of the 5 subjects in Figures 7.1-7.5. The latency and magnetic field power of the peak corresponding to the V1 chromatic evoked response as described in Chapter 5 is shown for each temporal frequency. The time window is 500ms and the scale is shown individually for each subject. When the component reached the level of the background noise and could not be clearly identified, the magnetic field power of the component was taken to be zero.

The response is dominated by a major component peaking at between 101-126ms. The field power shows bimodal dependence on temporal frequency, tending to be maximal for stationary gratings, dropping with increased temporal frequency before rising again to maximal or near maximal values at 4Hz. The field power then decreases with increasing temporal frequency, reaching a value comparable with the noise level at 40Hz. A second, low field strength component at 156-174ms is seen for some temporal frequencies in four of the subjects but this is less consistent.

The temporal frequency tuning functions are shown in Figure 7.6 for each of the subjects. For subject LB, the field power does not rise to maximum values at 4Hz but nevertheless, a notch is apparent in the field power plot. For subject KL the field power does not show a maximum for stationary gratings but increases with increasing temporal frequency, reaching a maximum at 4Hz before falling slightly and remaining constant until 32Hz when the field power drops abruptly, approaching the noise level at 40Hz. To aid comparison between subjects the normalised field power as a function of temporal frequency is shown for all subjects in Figure 7.7.

The latency of the evoked response peak is highly consistent between subjects and is shown as a function of temporal frequency in Figure 7.8. The latency rises gradually with increasing temporal frequency, reaching a peak at 8-16Hz before dropping again to relatively low latencies, lower than are observed for the stationary gratings. This drop in latency, associated with a low field strength, is suggestive of the response being dominated by a different mechanism than for the lower temporal frequency responses. There are two major possibilities for this alternative mechanism. Firstly that the high drift rate changes the isoluminant ratio so that chromatic aberrations introduce luminance artefacts into the display (Bradley et al., 1992). The recorded response could then arise from luminance sensitive mechanisms. Alternatively, a sub-population of chromatic sensitive cells may be responding. Such a shorter response

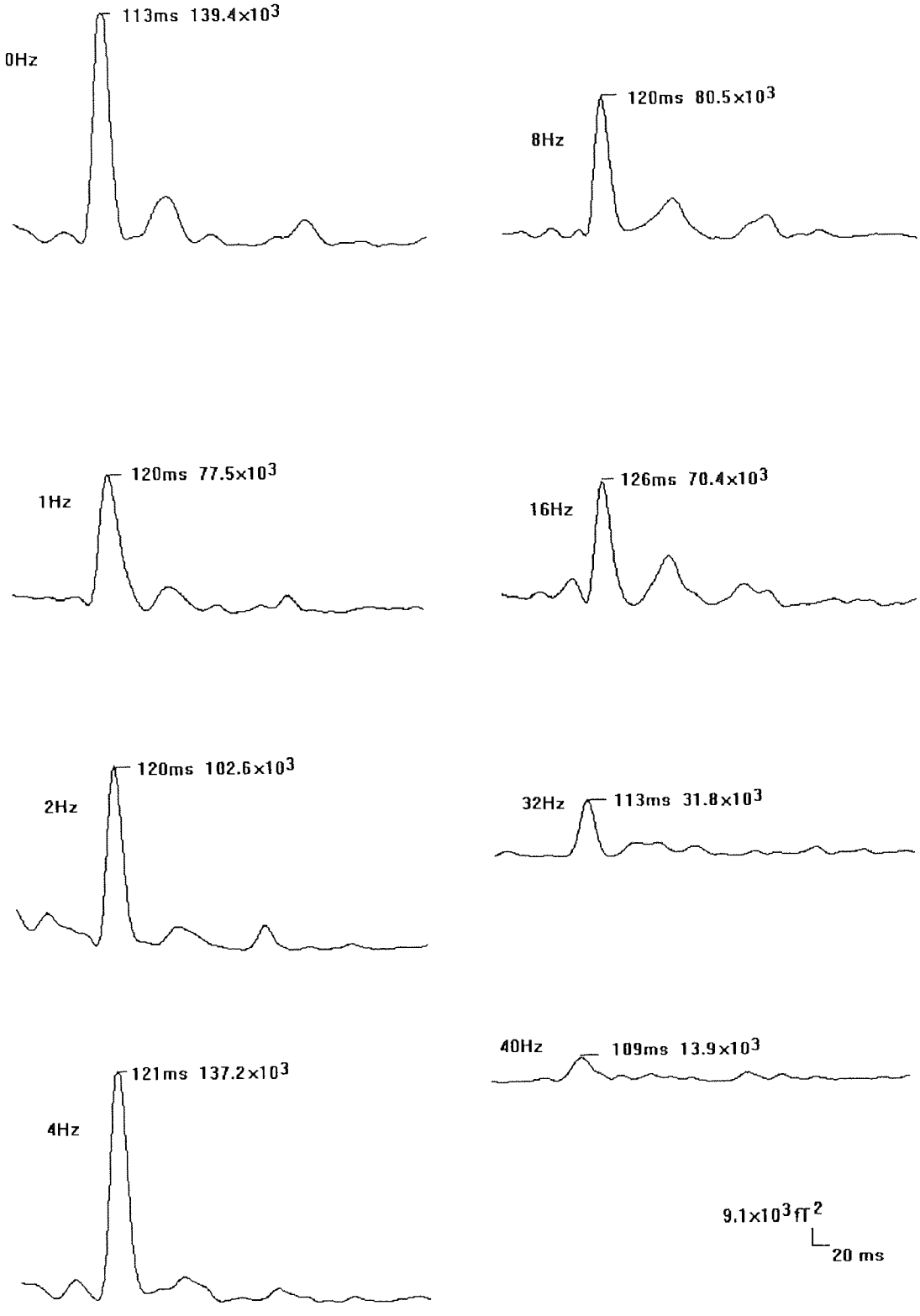

Figure 7.1 Latency and magnetic field power for the peak of the evoked response to isoluminant red/green gratings of various temporal frequencies for subject KS

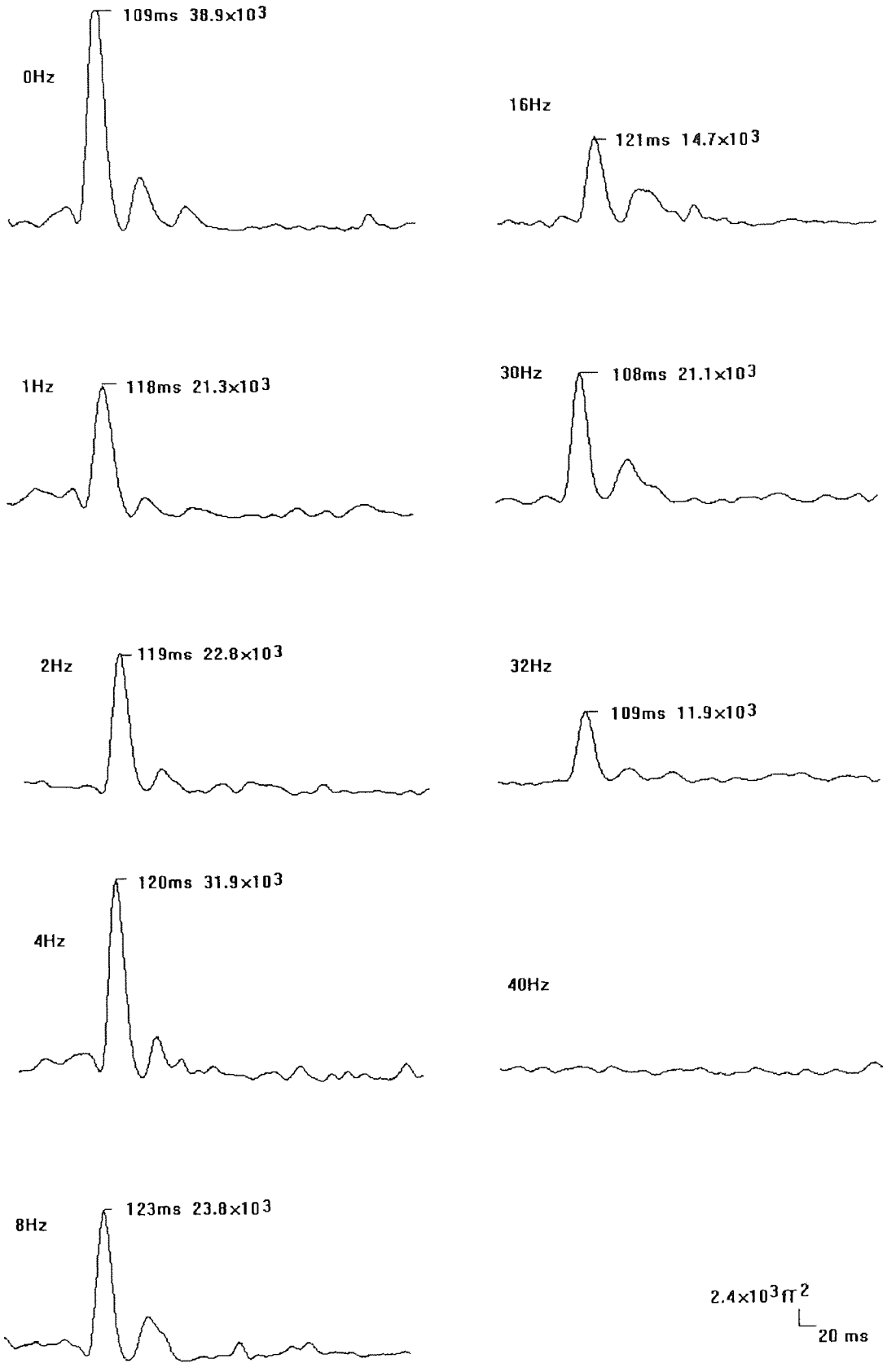

Figure 7.2 Latency and magnetic field power for the peak of the evoked response to isoluminant red/green gratings of various temporal frequencies for subject JD

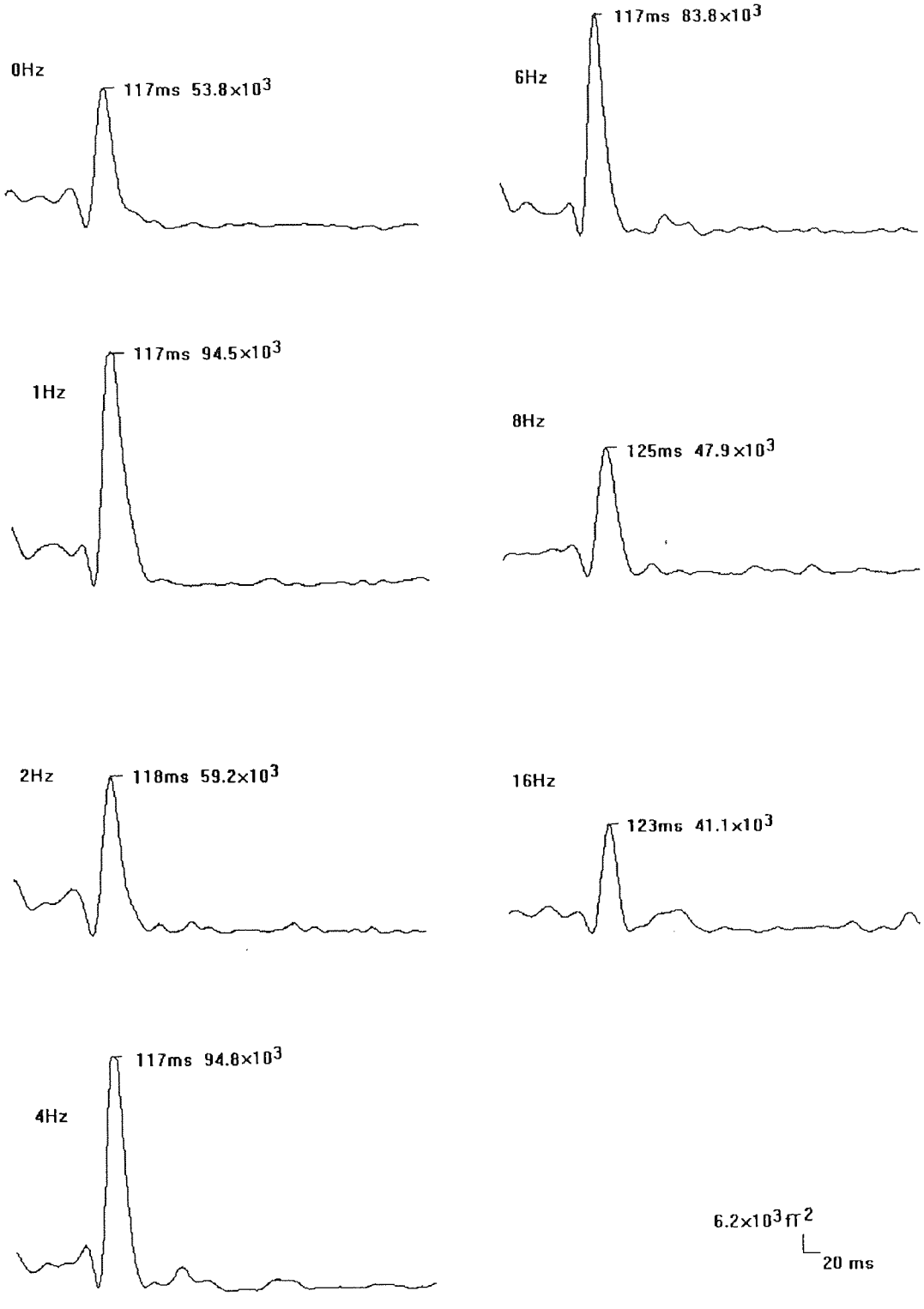

Figure 7.3 Latency and magnetic field power for the peak of the evoked response to isoluminant red/green gratings of various temporal frequencies for subject IH

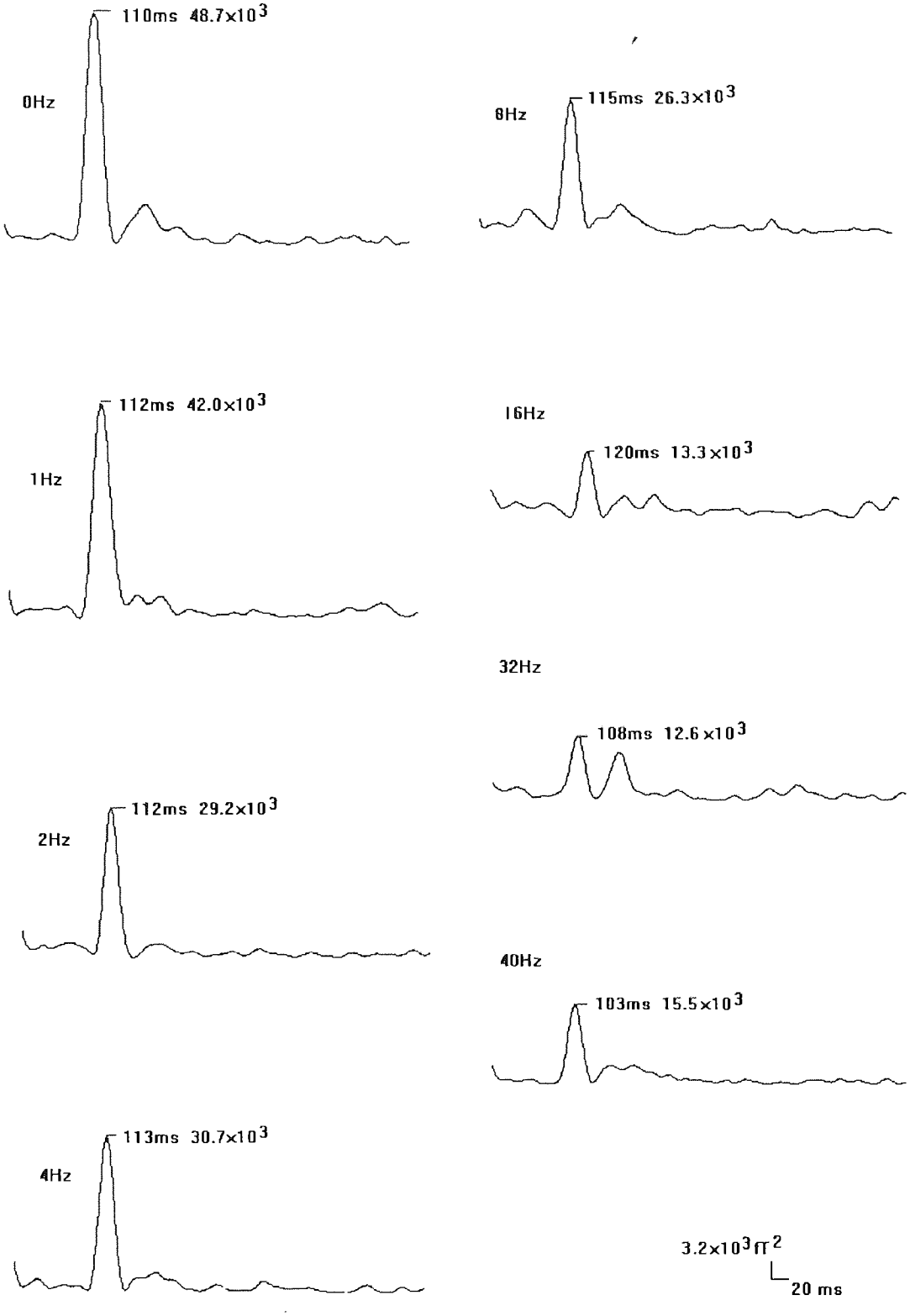

Figure 7.4 Latency and magnetic field power for the peak of the evoked response to isoluminant red/green gratings of various temporal frequencies for subject LB

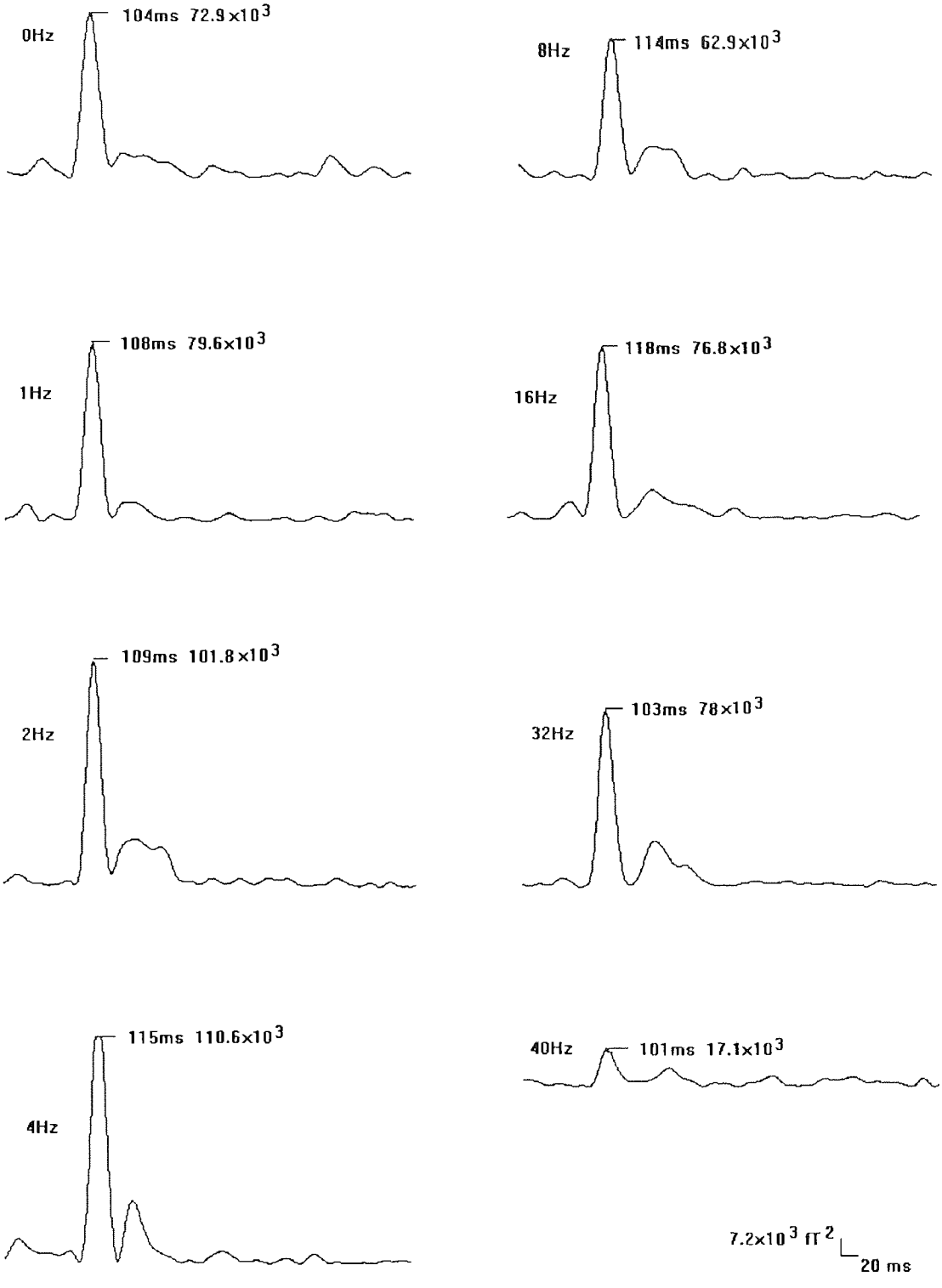

Figure 7.5 Latency and magnetic field power for the peak of the evoked response to isoluminant red/green gratings of various temporal frequencies for subject KL

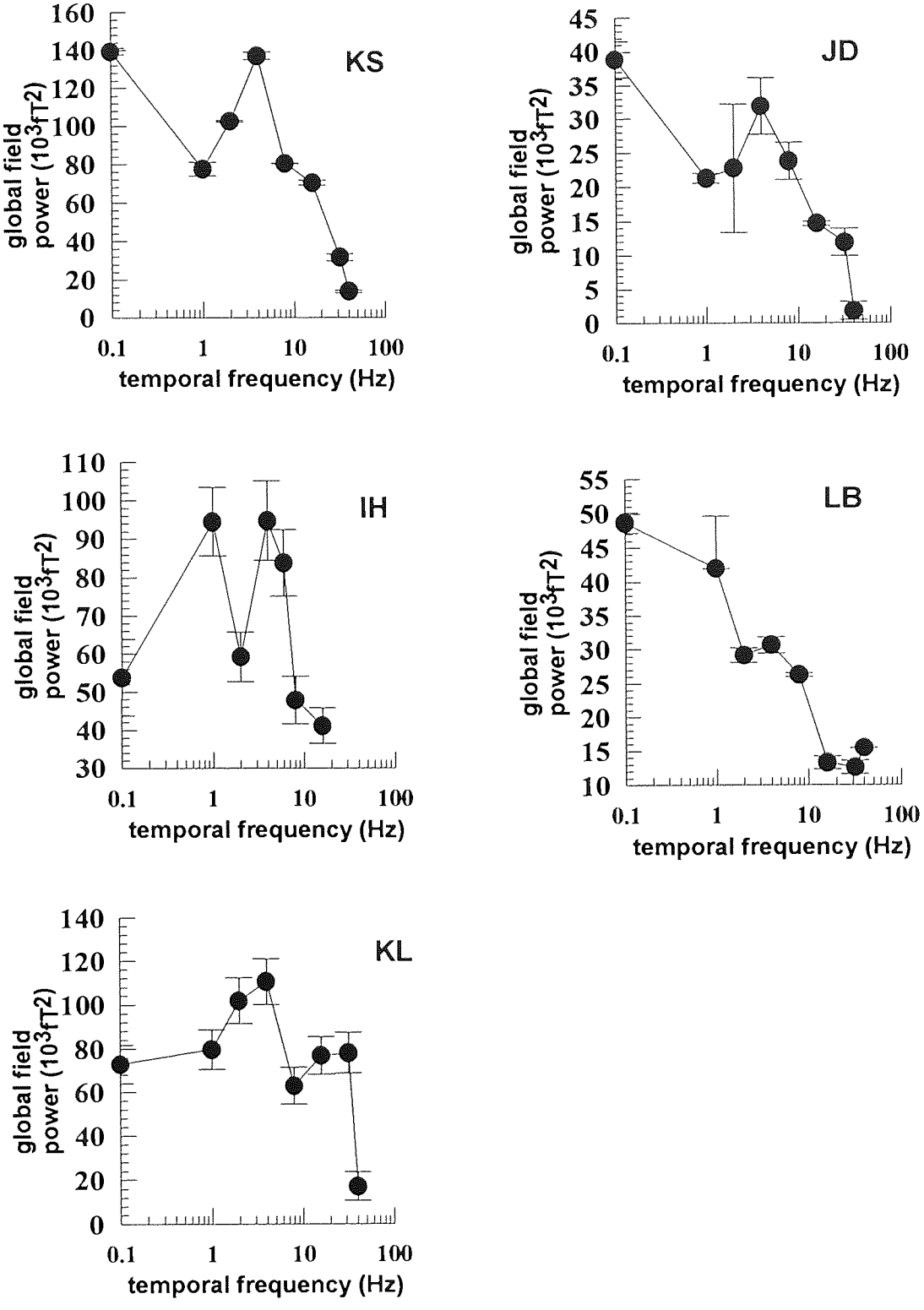

Figure 7.6 Magnetic field power of the peak response as a function of temporal frequency for all subjects

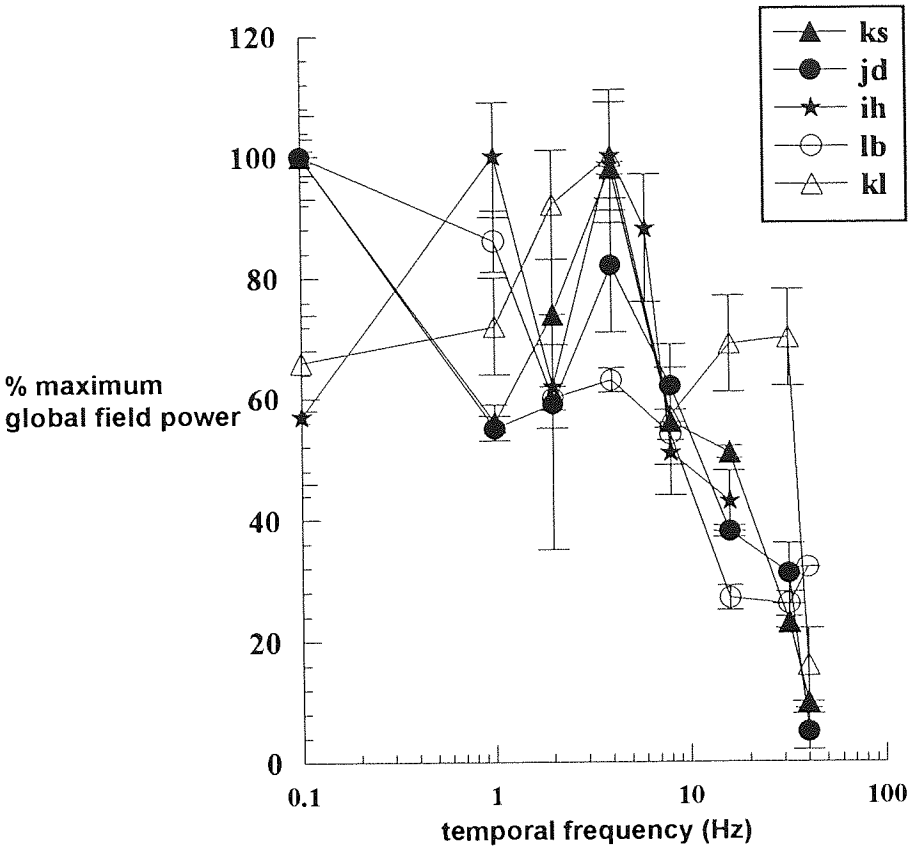

Figure 7.7 Normalised magnetic field power as a function of temporal frequency for all subjects

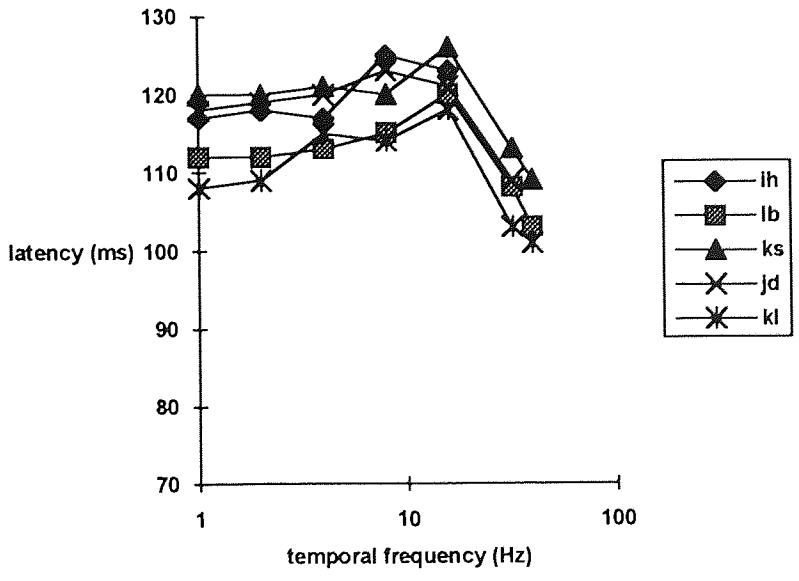

Figure 7.8 Latency as a function of temporal frequency for all subjects

latency would be appropriate for cells sensitive to high temporal frequencies.

To determine which of these possible explanations is more likely to be correct, a control experiment was performed in which the temporal frequency tuning properties of the achromatic response was recorded for subject JD. The contrast of the gratings was 20% as this value will exceed the contrast of possible luminance artefacts introduced by chromatic aberrations (Bradley et al., 1992). The global field power is shown as a function of temporal frequency together with the chromatic evoked response in Figure 7.9. The field power of the luminance response is low and the response itself is barely distinguishable from the noise and cannot be identified at temporal frequencies above 16Hz. Although the recordings were made on different days so that due to slight dewar positioning differences the amplitudes of the two response sets are not strictly comparable, it is evident that the chromatic evoked response at high temporal frequencies does not arise as a function of luminance artefacts.

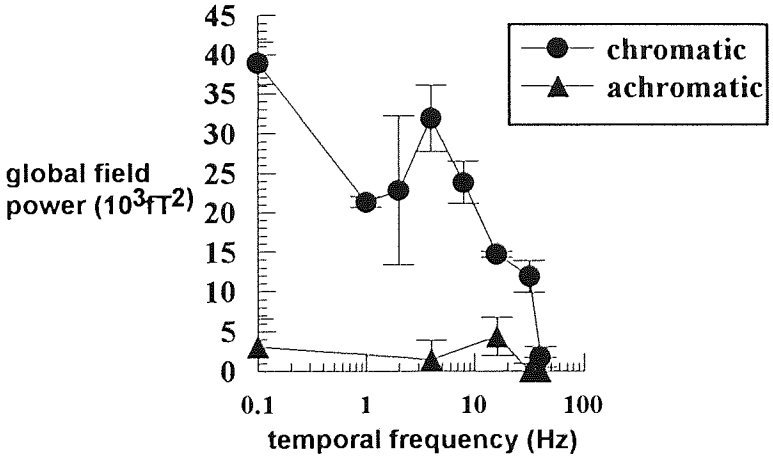

Figure 7.9 Magnetic field power of the evoked response to chromatic and achromatic gratings

To confirm that the response to all temporal frequencies is likely to arise from the same cortical region, Monte-Carlo error analysis was performed for the data recorded from subject IH. The 95% confidence regions obtained are shown in Figure 7.10. All confidence regions overlap and lie along an ascending branch of the calcarine fissure, as seen in Chapter 5. Hence the same cortical region responds to all chromatic temporal frequencies.

Figure 7.10 95% confidence regions for dipole locations following chromatic stimulation at a range of temporal frequencies for subject IH

7.4 Discussion

The evoked magnetic response was recorded to 2 cycles/degree isoluminant chromatic gratings drifting at between 0Hz and 40Hz. The response was dominated by a major component whose field power and latency varied with the drift temporal frequency of the stimulus. In three of the five subjects, the field power was bimodal, reaching near-maximal values at 0-1Hz and again at 4Hz. In a fourth subject an increase in field power for the 4Hz condition was apparent in the data but this increase was not marked. A fifth subject showed maximal responses only at a drift rate of 4Hz.

Such an increase in amplitude of the VEP has also been noted by Rabin et al. (1994) for pattern reversal stimulation, particularly for modulation of the S cone, at a counterphase frequency of 4Hz. However, no discussion of the significance of the amplitude increase was offered.

This consistent peak at 4Hz is surprising as psychophysical techniques do not indicate an increase in sensitivity to chromatic gratings at this temporal frequency. The chromatic evoked magnetic response has been shown to arise from area V1 (see Chapter 5). It is possible that this increase in magnetic field power indicates the activation of more than one cell population; the increased number of cells responding at 4Hz resulting in the observed increase in recorded field power. This is supportive of more than one mechanism responding to moving chromatic targets, either in the form of multiple temporal frequency channels with overlapping sensitivity regions as is found with achromatic motion sensitivity (Anderson and Burr, 1985; Hess and Snowden, 1992), analogous to spatial frequency channels (Campbell and Robson, 1968), or two separate mechanisms responding optimally to stationary and 4Hz temporal frequency stimulation.

Other than the peak in field power at 4Hz the results are consistent with psychophysical observations of the chromatic temporal tuning function. There is a decreased sensitivity with increasing temporal frequency and the response falls to the level of the noise around 40Hz. Although many psychophysical studies do not investigate frequencies as high as 40Hz, extrapolating their published threshold plots gives a cut-off frequency consistent with the 32-40Hz indicated by this study (Gegenfurtner and Hawken, 1995; Mullen and Boulton, 1992; Kelly, 1983). When a difference occurs, the cut-off frequency for the evoked magnetic response data is higher than that obtained psychophysically. This may be due to tracking eye movements reducing the effective temporal frequency of the chromatic gratings for the

long stimulus duration of this study.

The decrease in latency of the peak response above 8-16Hz is suggestive of a different mechanism sensitive to high temporal frequencies. There are two possible explanations for this drop in latency. Firstly, the response arises from luminance artefacts due to display or retinal inhomogeneities. Secondly that a separate chromatic-sensitive cell population or mechanism gives rise to the recorded response. A control experiment recorded the response to achromatic, luminance modulated gratings of 20% contrast over a range of temporal frequencies. The low field strength obtained indicates that the cell population giving rise to the chromatic evoked magnetic response is relatively insensitive to luminance modulations and the response is therefore likely to arise from chromatic sensitive mechanisms over the entire range of temporal frequencies investigated. That lower latencies were obtained for high temporal frequency gratings suggests that the cells generating the response are coding the motion of the gratings rather than signalling their presence. A mechanism that merely detected the presence of gratings would not be expected to show a change in latency with changing temporal frequency. The direction of latency change is as expected as a more rapid response would be beneficial for cells encoding high temporal frequency information. The lower field power of the response indicates that it is a relatively small population of cells that respond to high temporal frequencies. To confirm that the cells responding are located in the same cortical region as the cells sensitive to lower temporal frequencies, Monte-Carlo error analysis of the data from subject IH were performed. The confidence regions obtained, shown in Figure 7.12, confirm that cortical location that does not change with increasing temporal frequency. The results are therefore not contaminated by activity arising from additional cortical regions and demonstrate that cells within visual area V1 code for chromatic motion over a wide range of temporal frequencies.

CHAPTER 8

THE LUMINANCE EVOKED MAGNETIC RESPONSE: SPATIAL FREQUENCY CHARACTERISTICS

8.1 Introduction

Within the human visual system it has been proposed that parvocellular units are capable of encoding both chromatic and luminance information; the double duty hypothesis (Ingling and Martinez-Uriegas, 1985; Ingling, 1991). This is supported by single cell recordings in area V1 of macaque (Thorell et al., 1984) that demonstrate that the majority of cortical cells are capable of responding to both chromatic and luminance stimulation. Similarly, studies which selectively lesion magnocellular and parvocellular pathway cells in macaque (Merigan et al., 1991) and rhesus monkey (Schiller, 1991) demonstrate that parvocellular cells respond both to chromatic and to luminance stimulation. Indeed, Thorell et al. (1984) reported that 53% of cells tested responded equally well to chromatic and luminance stimulation. Single opponent cells were shown to have lowpass characteristics for chromatic stimulation and bandpass characteristics for luminance stimulation. Double-opponent cells demonstrated bandpass behaviour towards both stimulus types. A summed population of 108 cortical cells showed lowpass chromatic response characteristics and bandpass luminance characteristics. This is in agreement with psychophysical studies. Mullen (1985) undertook a comprehensive investigation of the spatial frequency tuning properties of the chromatic and luminance systems. The contrast sensitivity function to chromatic modulation was found to be lowpass, as discussed in Chapter 6. In contrast, the contrast sensitivity function to luminance modulation (green/black and yellow/black) was bandpass, peaking at 0.8-4 cycles/degree with a cut-off frequency of 32-33 cycles/degree.

Previous evoked potential studies have demonstrated a response arising from chromatic sensitive mechanisms (Murray et al., 1987; Jeffreys, 1989; Crognale et al., 1992, 1993; Rabin et al., 1994). This chromatic response is negative, and as such is of opposite polarity to the positive luminance generated response, and is of longer latency than the equivalent luminance evoked response. These differences are not in accord with single cell studies which find that the same cells respond to luminance and chromatic stimulation. There are two explanations for these response differences.

Firstly that different cell populations underlie the surface recorded response. Secondly, the way in which the same group of cells respond is different following chromatic and luminance stimulation, perhaps responding more sustainedly following chromatic stimulation so that a different phase of the response dominates the negative surface recorded response.

To investigate the differences between responses evoked by chromatic and luminance stimulation this chapter aims to record the evoked magnetic response to luminance modulated patterns. Stimulation with achromatic, yellow/black and red/black gratings will be compared with the results obtained following isoluminant red/green stimulation. The spatial frequency characteristics of the response will be determined and the results compared with both single cell recordings within macaque visual area V1 and with the psychophysical properties of the human visual system. The inverse solution of the response will be obtained and the dipole cortical locations will be compared with those obtained following isoluminant chromatic stimulation described in Chapter 6. In this way the cortical activation patterns following chromatic and luminance stimulation will be compared and the cell-type underlying the evoked response will be examined.

8.2 Method

8.2.1 Stimuli

Four stimuli were used during the course of the experiment. Red/green grating were generated as in section 5.2.1 to produce isoluminant chromatic modulation. These same gratings were combined in phase to produce luminance modulated yellow/black gratings. To compare the spatial frequency tuning of isochromatic gratings, red/black rather than green/black as used by Mullen (1985) was selected as cells within macaque area V1 have been shown to give a larger response following stimulation with red light rather than green (Givre et al., 1995). The red/black gratings were generated by use of the same gratings as in section 5.2.1 but with the green phosphor turned off. The mean luminance of the red phosphor was adjusted to match that of the red/green and yellow/black conditions. Finally, achromatic gratings of 80% contrast were generated to examine the effect of luminance modulation without a net chromatic component. All gratings had a mean luminance of 12cd/m^2 and were presented in the right lower quadrant of the visual field. This quadrant has been shown to evoke a high field strength response (see Chapter 5). The field size was 4 x 6 degrees and the stimulus was displaced 0.5 degrees from the principal meridians to restrict cortical input to a

small region of area V1. The spatial frequency of the gratings was varied between 0.25 and 8 cycles/degree.

8.2.2 Procedure

The visual evoked magnetic response was recorded using the Aston 19-channel SQUID magnetometer system as described in section 2.9 using a procedure as section 5.2.2. Data was analysed using the magnetic global field power which is appropriate as for each subject, recordings were made with the same dewar position and the field power is therefore directly comparable across spatial frequencies within the same subject. Comparison between subjects was enabled by normalising the field power to the percentage of maximum response. Hence latency and magnetic field power were analysed for each of the subjects and plotted as a function of spatial frequency.

8.2.3 Subjects

Two females (FF and JD) and two males (IH and KS) volunteered for the experiment. Their ages ranged from 28 to 39 and all had normal visual fields and colour vision and a normal or corrected-to-normal Snellen acuity of 6/6.

8.3 Results

8.3.1 The response of subject FF to four stimulus conditions

The evoked magnetic response to luminance stimulation was more complex than the isoluminant chromatic response described in Chapters 5-7, The response comprised a major component and up to two additional components which were strongly influenced by the spatial frequency of the stimulus. The response to red/black stimulation is shown in Figure 8.1 for 0.5 cycles/degree (upper panel) and 4 cycles/degree (lower panel). The time window is 500ms and the global field power is shown for both spatial frequencies. The magnetic field was mapped at the peak of the response, 92ms for both spatial frequencies and the equivalent current dipole is marked in white. The orientation of the dipole is as predicted by the cruciform model of striate cortex (see Figure 5.2), pointing up and to the left following stimulation of the right lower quadrant.

The global field power of the evoked magnetic response to red/black, yellow black and achromatic stimulation over a range of spatial frequencies is shown in Figure 8.2 for subject FF. For comparison, the response recorded during the same session for

isoluminant chromatic stimulation is shown for 2 and 4 cycles/degree. A more comprehensive range of spatial frequencies for isoluminance chromatic stimulation is shown in Figure 6.6. The trace duration is 500ms and the time of the major peak is shown for each spatial frequency.

The response to red/black, yellow/black and achromatic stimulation showed very similar morphology, with the latency of the peaks of all three conditions lying within 12ms at each spatial frequency. The spatial frequency tuning of the major response for each of the three luminance modulation conditions was similar. This is shown in Figure 8.3. The response was bandpass, peaking at 4 cycles/degree with a cut-off frequency of 12 cycles/degree. The spatial frequency tuning of the red/green response is shown for spatial frequencies of 2 cycles/degree and 4 cycles/degree. The chromatic response peaked at 2 cycles/degree and approached the level of the noise at 4 cycles/degree, consistent with the findings of Chapter 6 which showed the response to be bandpass with a peak at 1-2 cycles/degree.

The latency of the major luminance component varied between 86ms and 114ms with spatial frequencies above 4 cycles/degree evoking later responses. The field power of the response was less similar between different luminance conditions with the red/black gratings evoking the highest field power response and the achromatic gratings the lowest. The response morphology was more complex than that observed following isoluminant chromatic stimulation with up to three components being observed at all spatial frequencies. For the red/black gratings the spatial frequency was reduced to 0.25 cycles/degree when the early component dominated the response. When present this early component varied between 62ms and 79ms. An additional later component was observed for the higher spatial frequencies and the latency of this component varied between 123 and 172ms.

The effect of spatial frequency on the latency of the major response component is shown for each of the four stimulus conditions in Figure 8.4. The three luminance conditions show similar results with latency increasing slightly with spatial frequency. The latency of the achromatic response shows more variability although the increase in latency with spatial frequency is still apparent. The effect of spatial frequency on the latency of the isoluminant red/green response is much more marked. Although only two spatial frequencies are shown there is a large increase in latency and both latencies are greater than those of the luminance conditions.

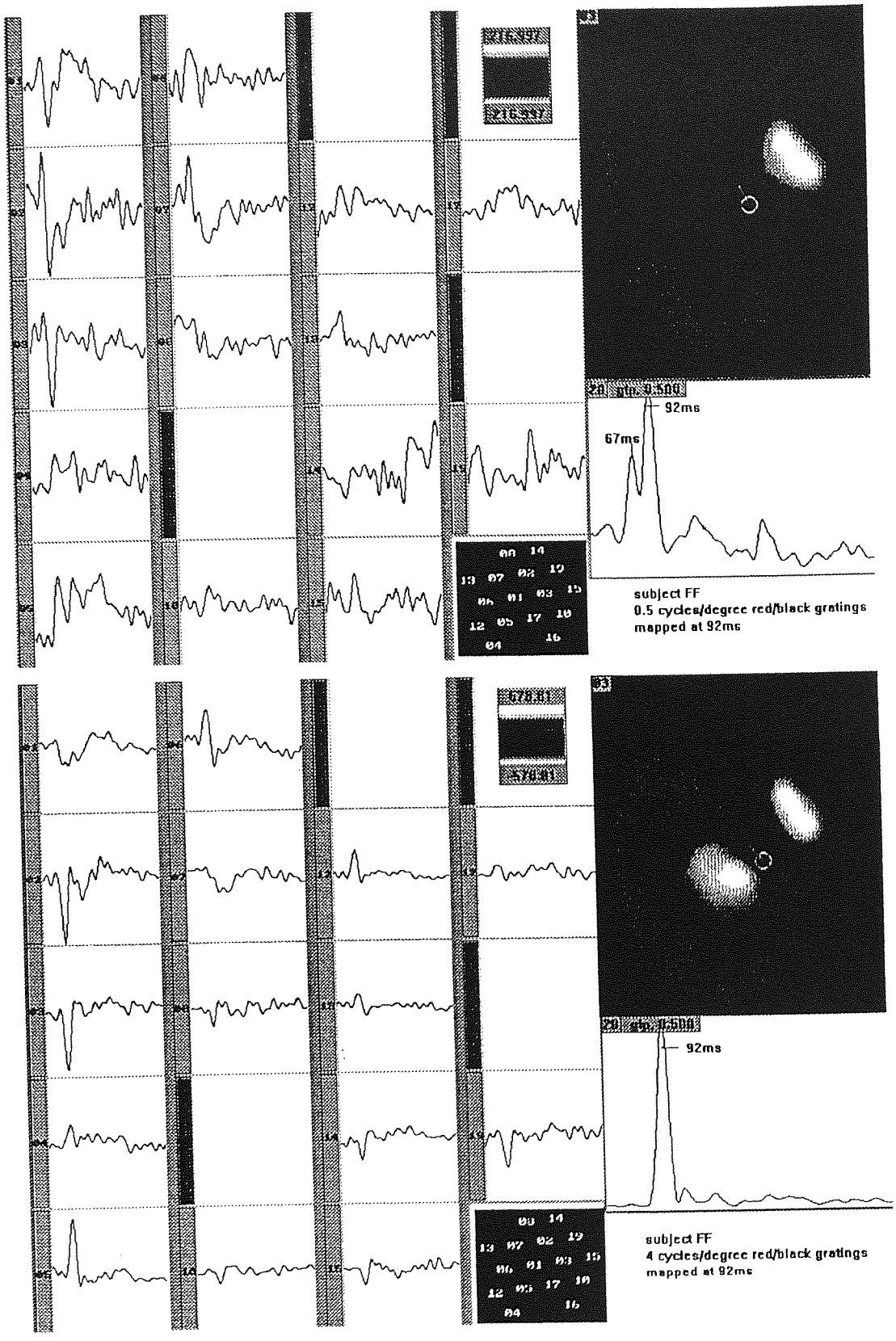

Figure 8.1 The evoked magnetic response and field map to red/black gratings of 0.5 cycles/degree (upper panel) and 4 cycles/degree (lower panel) for subject FF

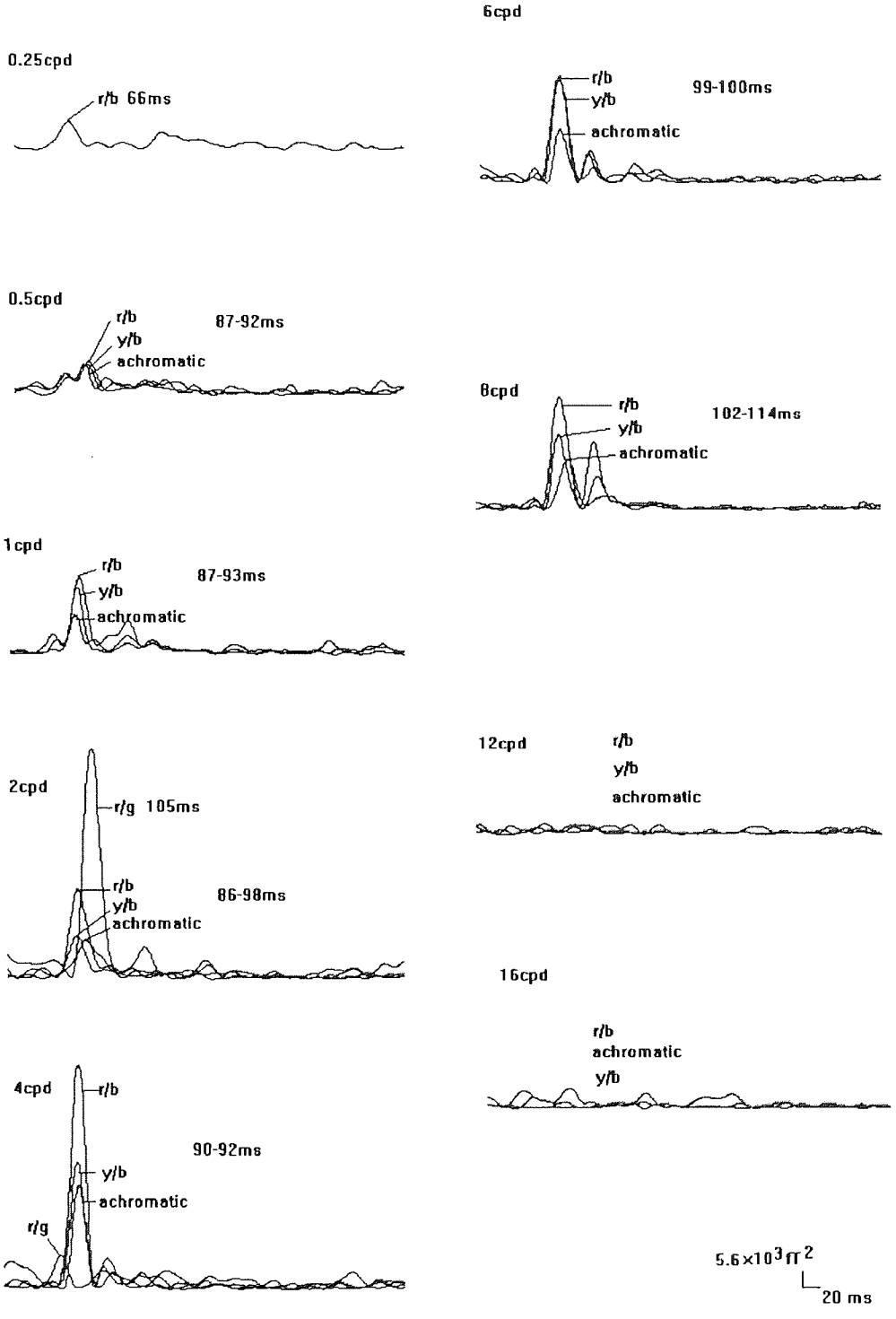

Figure 8.2 Global field power and latencies of the peak response to red/black (r/b), yellow/black (y/b), achromatic and red/green (r/g) gratings between 0.25 and 16 cycles/degree for subject FF.

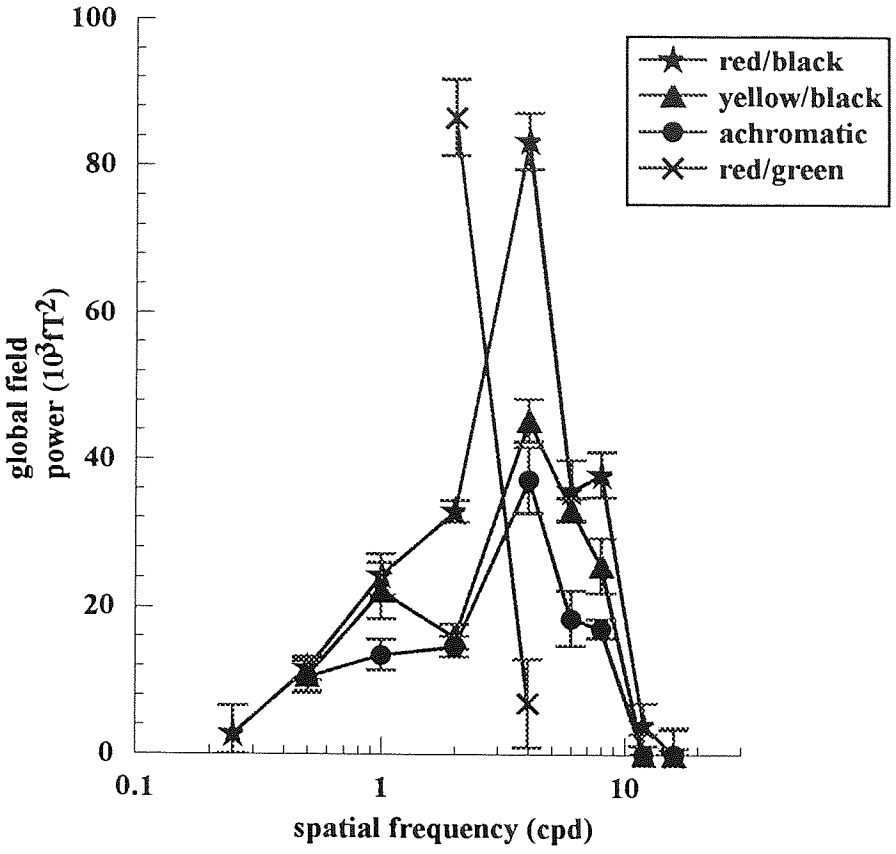

Figure 8.3 The effect of spatial frequency on field power of the major component for each of the four stimulus conditions for subject FF

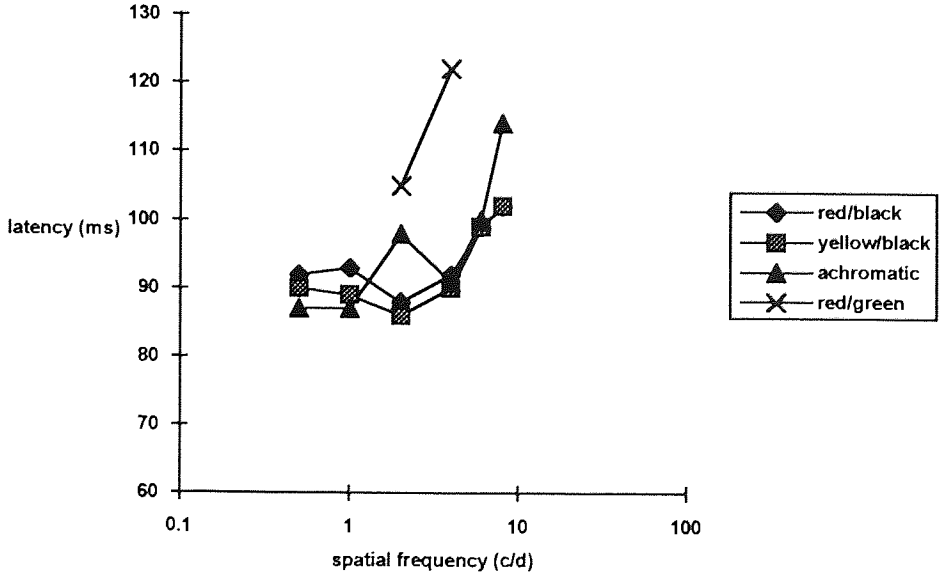

Figure 8.4 The effect of spatial frequency on latency of the major component for each of the four stimulus conditions for subject FF

The effect of spatial frequency on the field power and the latency of the early and late components of the response is shown in Figures 8.5 and 8.6. The early components are apparent only at and below spatial frequencies of 1 cycle/degree. In contrast, the later component, while apparent for a wider range of spatial frequencies, peaks at 2 cycles/degree for the achromatic response and at 6 cycles/degree and 8 cycles/degree for the red/black and yellow/black response respectively.

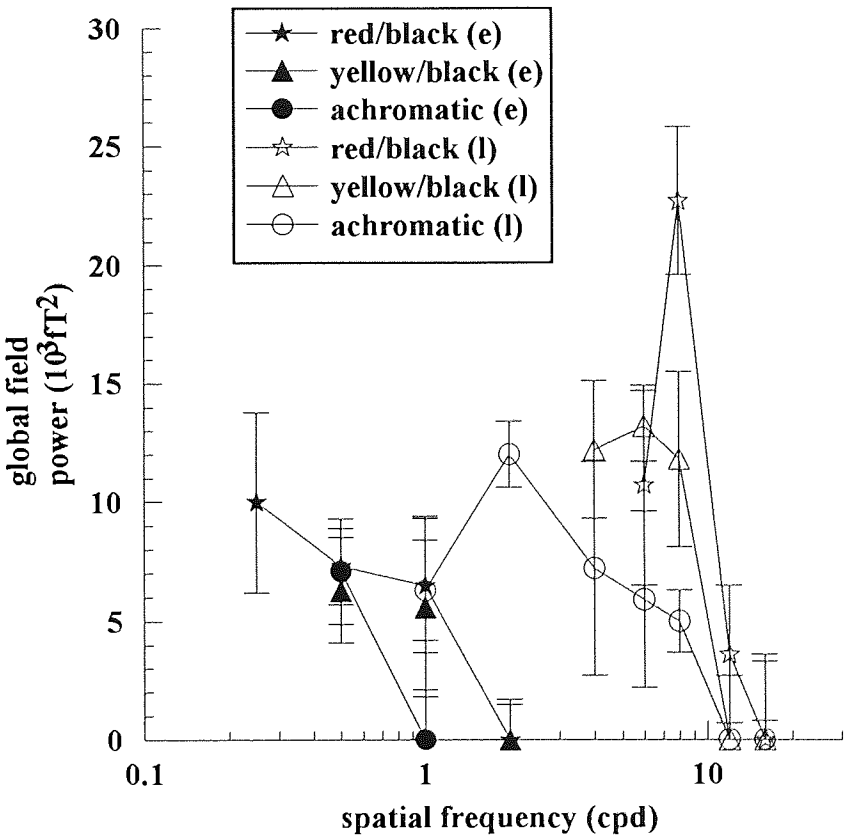

Figure 8.5 The effect of spatial frequency on the field power of the early (e) and late (l) components of the luminance evoked response

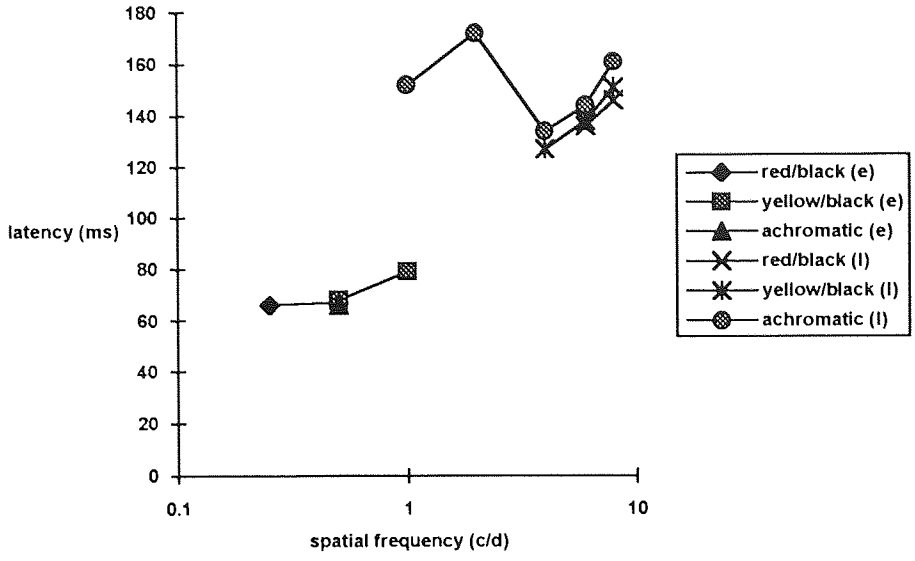

Figure 8.6 The effect of spatial frequency on the latency of the early (e) and late (l) components of the luminance evoked response

8.3.2 The major response to red/black gratings for subjects JD, IH and KS

For the remaining three subjects, the spatial frequency tuning properties of the luminance evoked response was investigated using red/black gratings which was representative of the luminance response and evoked the highest magnetic field strength signals. The global field power changes with spatial frequency are shown for the three subjects in Figures 8.7-8.9. As with subject FF, the response was more complex than the isoluminant chromatic response and comprised up to three distinct components. The field power of the major component was low and both latency and field power were more variable than the isoluminant response.

The spatial tuning characteristics of the major response component is shown in Figure 8.10 for each of the three subjects. The evoked response shows bandpass characteristics for each of the subjects, peaking at 4-6 cycles/degree with the response approaching the level of the noise at 16 cycles/degree. The effect of spatial frequency on the latency of the major component is shown in Figure 8.11. For all three of the subjects latency shows a curvilinear dependence on spatial frequency, above 4 cycles/degree showing a monotonic increase in latency with spatial frequency.

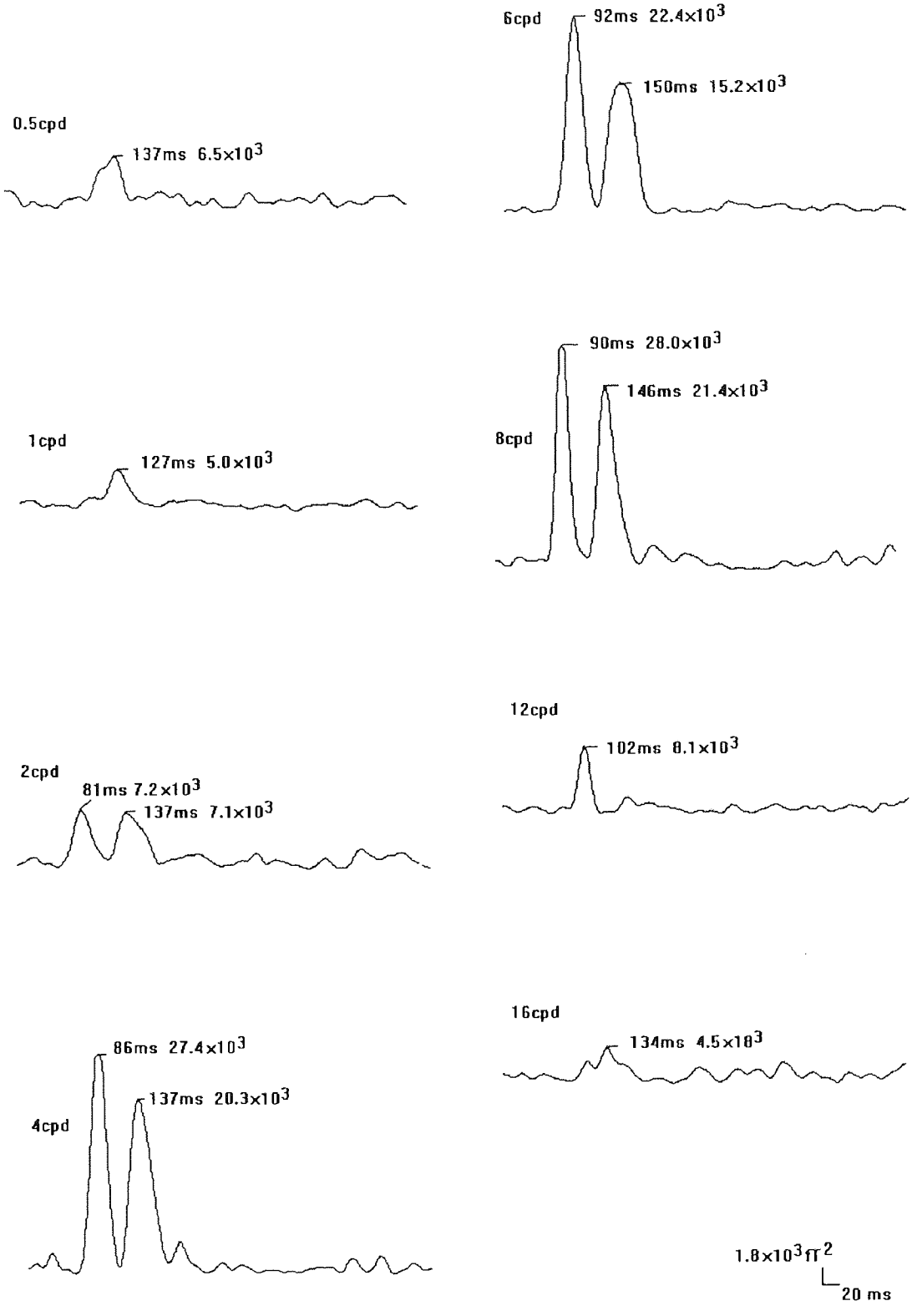

Figure 8.7 Global field power of the red/black response as a function of spatial frequency for subject JD

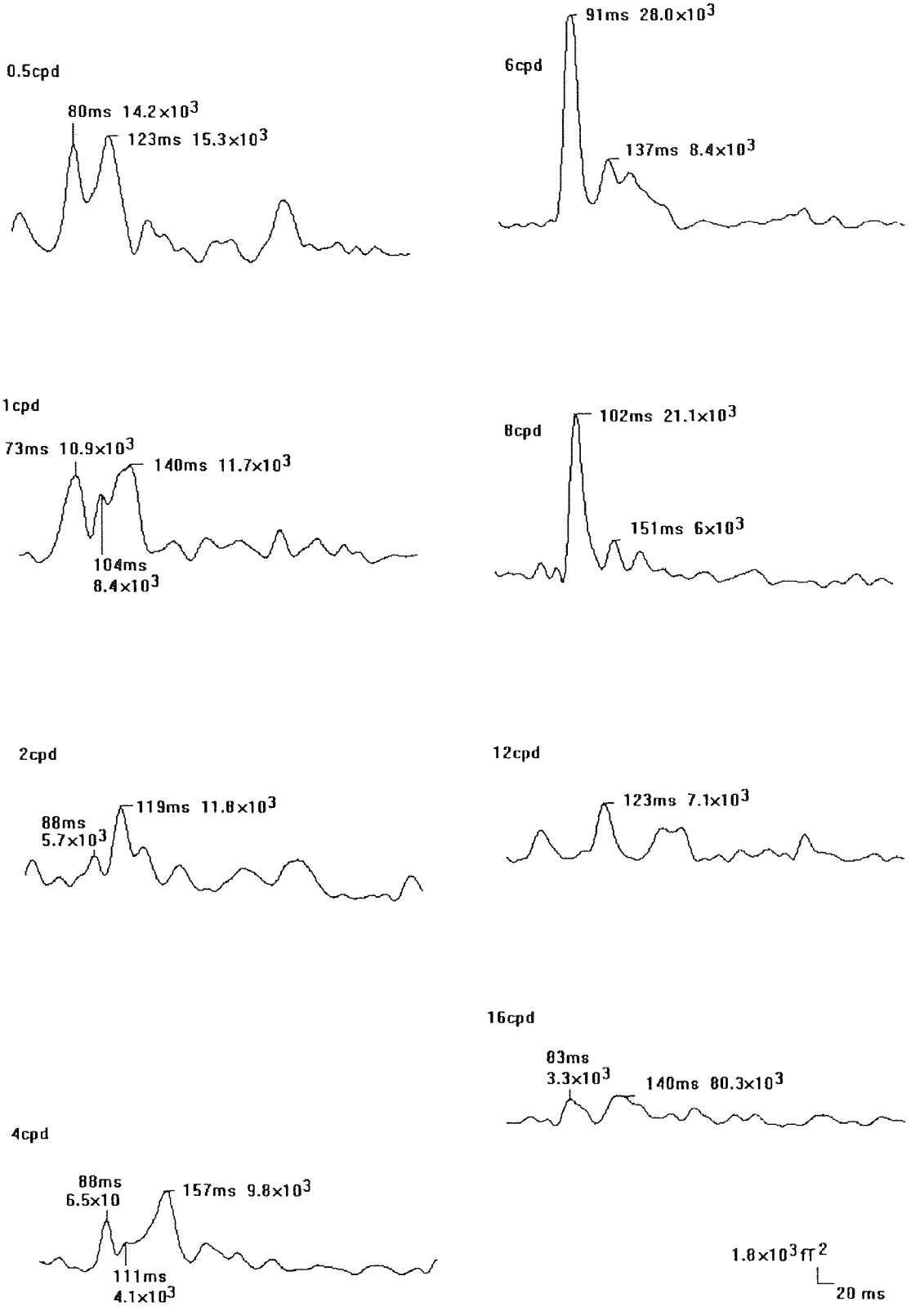

Figure 8.8 Field power of the red/black response as a function of spatial frequency for subject IH

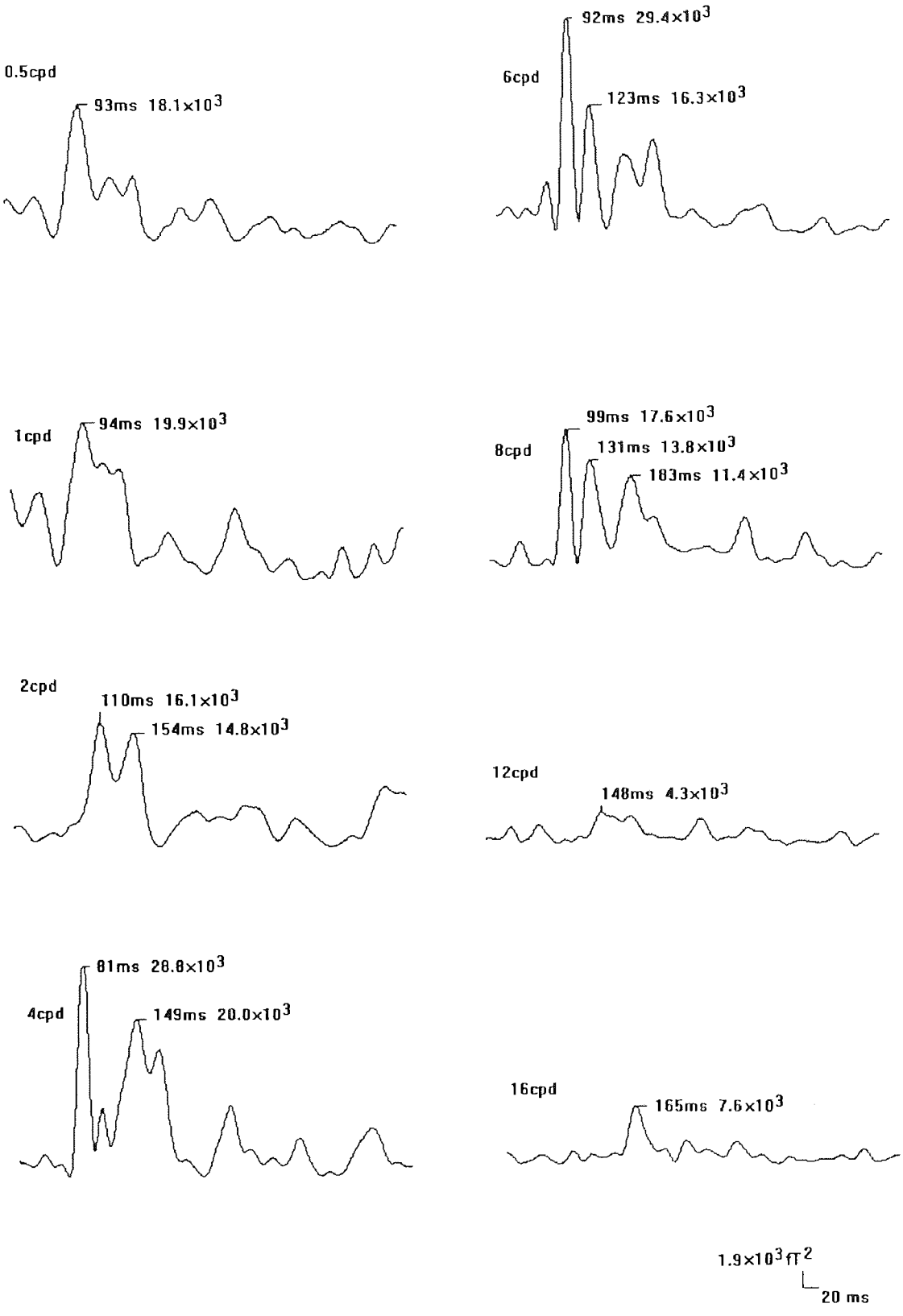

Figure 8.9 Field power of the red/black response as a function of spatial frequency for subject KS

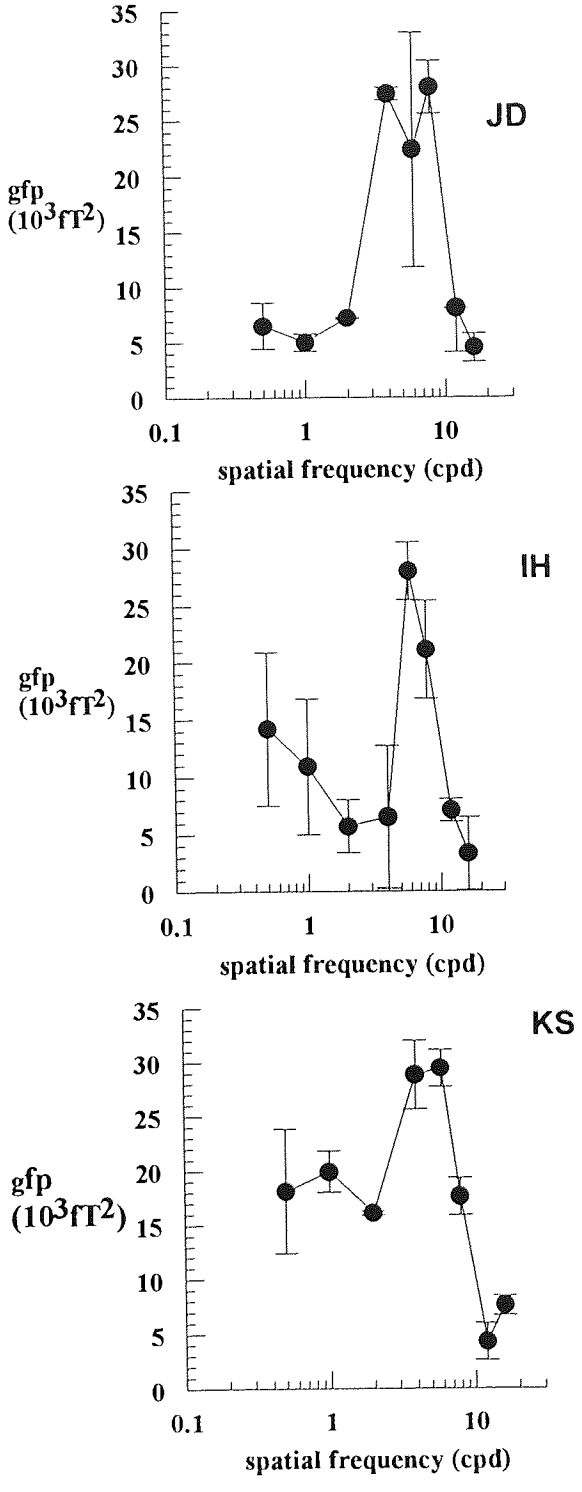

Figure 8.10 The effect of spatial frequency on global field power of the red/black response for three subjects

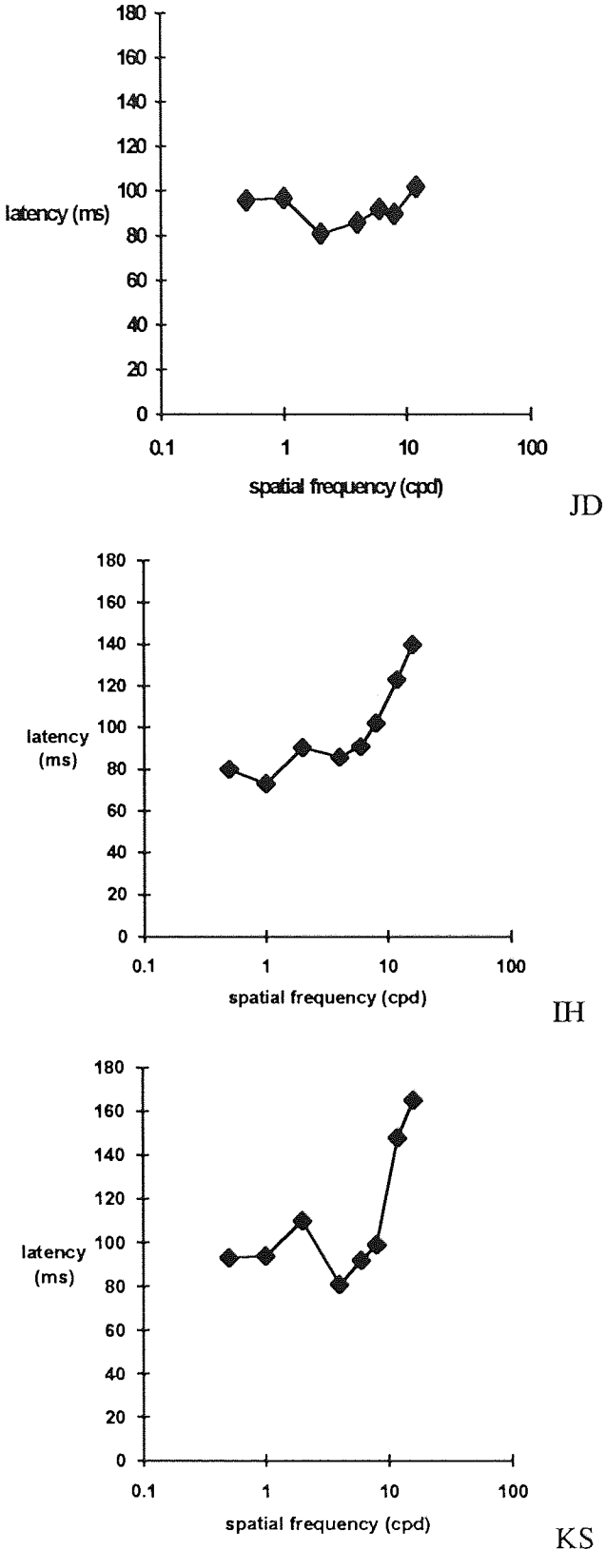

Figure 8.11 The effect of spatial frequency on the latency of the major component of the red/black response for three subjects

8.3.3 Cortical localisation of the response components

Monte-Carlo error analyses of the equivalent current dipole solutions were obtained and co-registered with MRI information to determine the cortical activation pattern following presentation of the different stimulus conditions. For subject FF the time of the peak response for each condition was selected (2 cycles/degree for isoluminant red/green and 4 cycles/degree for the three luminance conditions) and Monte-Carlo analysis performed. The resulting confidence ellipsoids, shown in Figure 8.12, are clustered together in close proximity to the calcarine fissure.

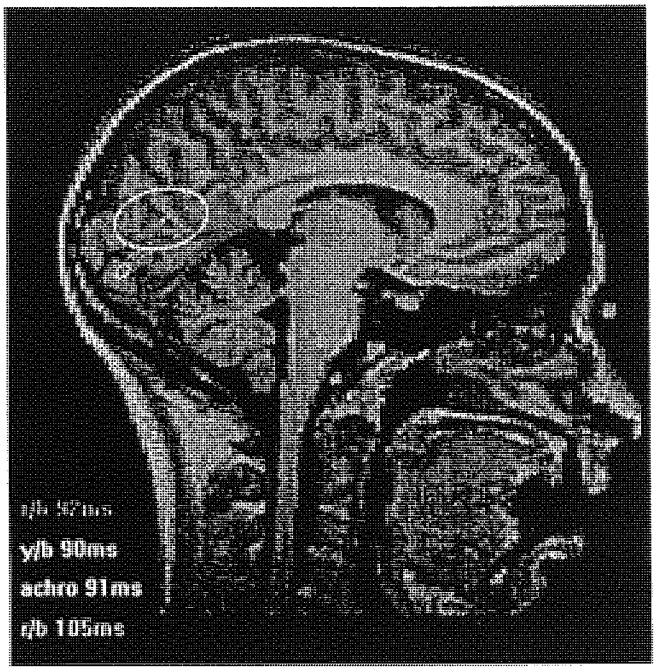

Figure 8.12 95% confidence regions for the peak response for all four stimulus conditions for subject FF

However, the luminance response was composed of up to three distinct components. To investigate the cortical localisations of these components an equivalent current dipole model was applied to the peaks in the power plots for each subject. As a single dipole model was used the analysis was performed at those time points for which the response was dominated by a single component. The appropriate spatial frequencies were 0.25, 1, 2, 4, 6 and 8 cycles/degree for subject FF, 0.5, 1, 6 and 8 cycles/degree for subject IH, 2, 4, 6 and 8 cycles/degree for subject KS and 2, 4, 6 and 8 cycles/degree for subject JD.

The 95% confidence regions obtained by Monte-Carlo simulation are shown in Figures 8.13-8.16 for all the subjects. For subject FF, the early component produced good localisations for 0.25 cycles/degree and 1 cycle/degree and these are shown in the upper panel of Figure 8.13. The major component, however, provided good localisations for a wide range of spatial frequencies, shown in the lower panel of Figure 8.13. Monte-Carlo analysis was performed for the major and the late components of the remainder of the subjects. In Figures 8.14-8.16 the major component is shown in yellow and the late component in red for four different spatial frequencies. The results provide evidence for the existence of multiple generators underlying the luminance evoked response. The confidence regions for subject IH show clear spatial separation of the two generators for each spatial frequency. Subject JD shows the generators of the two response components originating in the same cortical location. For subject KS the confidence regions indicate the generators may be spatially separate. Furthermore, at 8 cycles/degree there is evidence of three response generators originating in different cortical locations.

8.4 Discussion

The evoked magnetic response to luminance modulated sinusoidal gratings was recorded from four subjects at spatial frequencies between 0.25 cycles/degree and 16 cycles/degree. As a comparison, isoluminant red/green gratings were also recorded at 2 and 4 cycles/degree. An analysis of the effect of spatial frequency on magnetic field power and latency was undertaken and a comparison of the cortical activation patterns following isoluminant chromatic and luminance stimulation was made.

The morphology and the latency of the major response to all three luminance conditions was very similar. This is suggestive of the same mechanism generating the

Figure 8.13 95% Monte-Carlo confidence regions for the early and major components at various spatial frequencies for subject FF

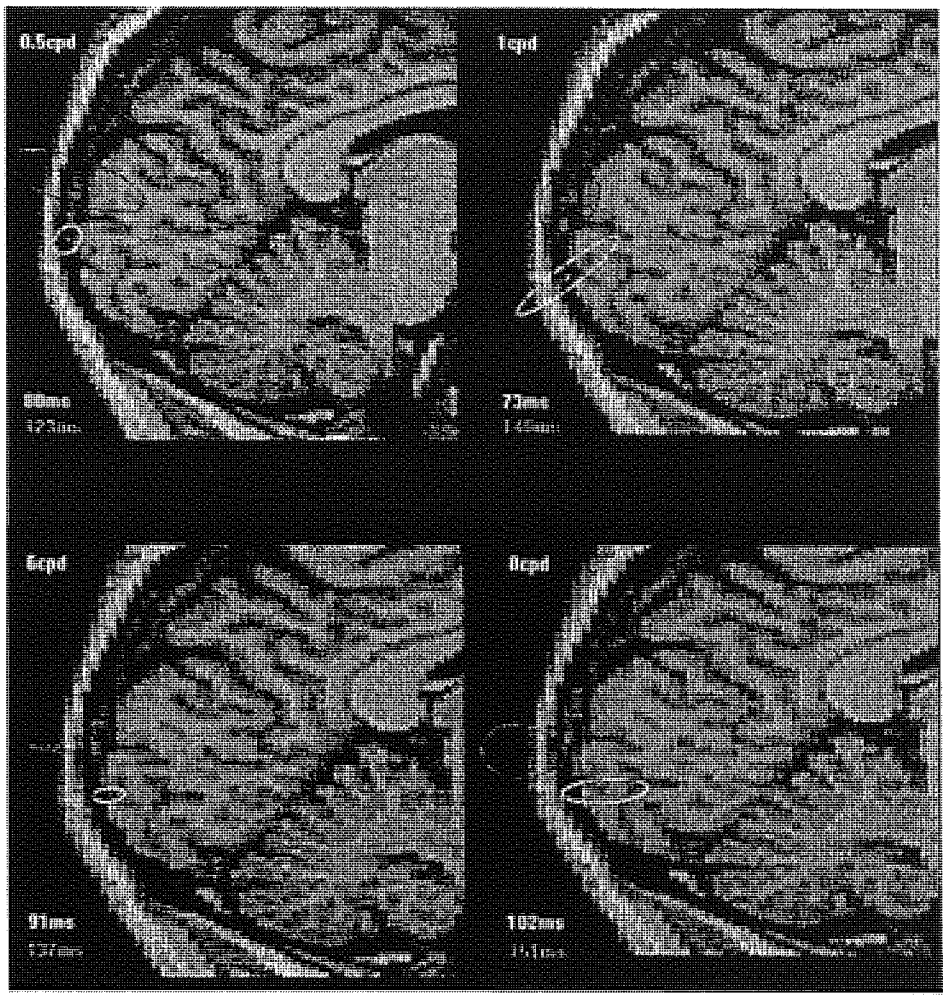

Figure 8.14 95% Monte-Carlo confidence regions for the major and late components at various spatial frequencies for subject IH

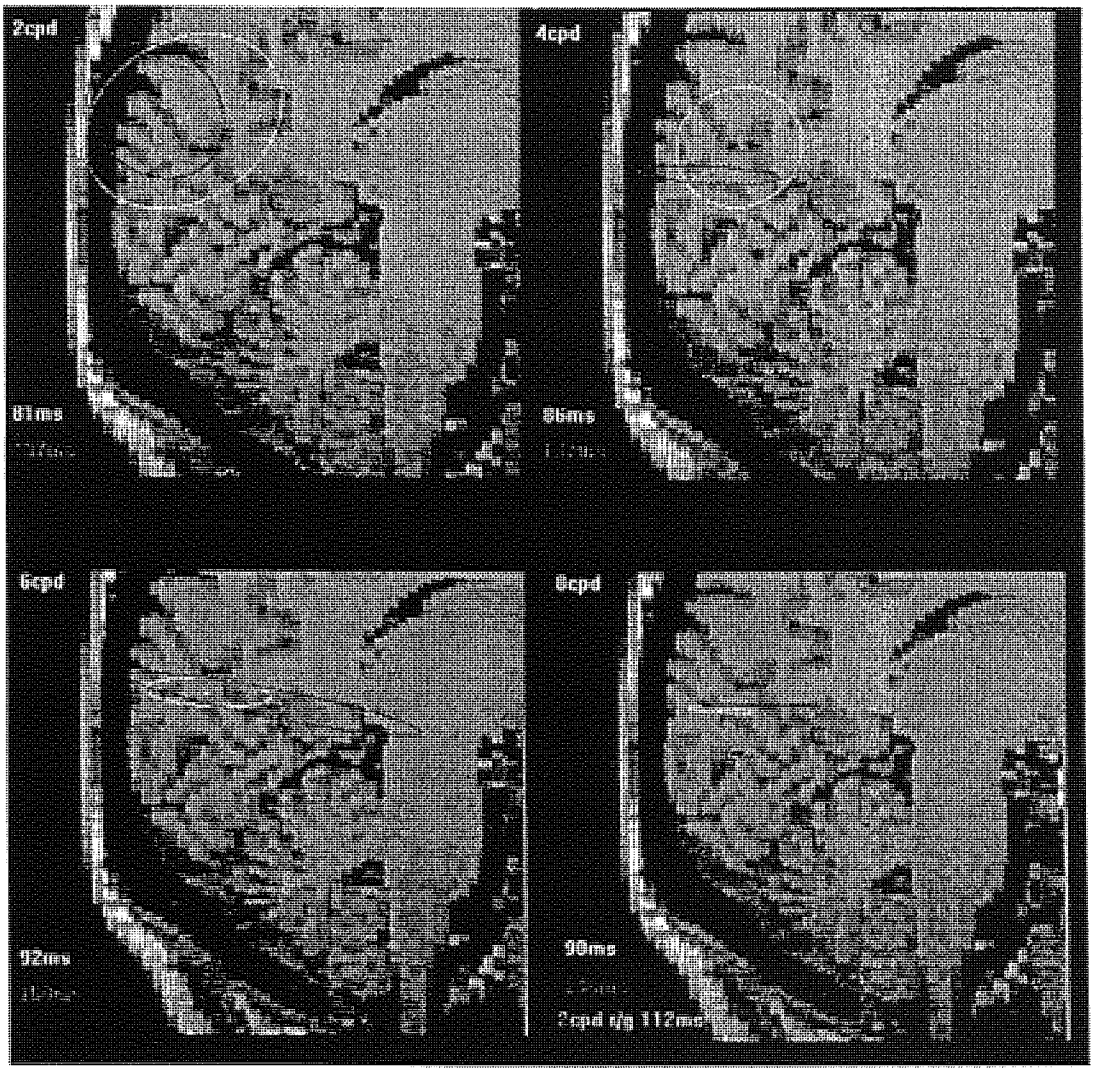

Figure 8.15 95% Monte-Carlo confidence regions for the major and late components at various spatial frequencies for subject JD

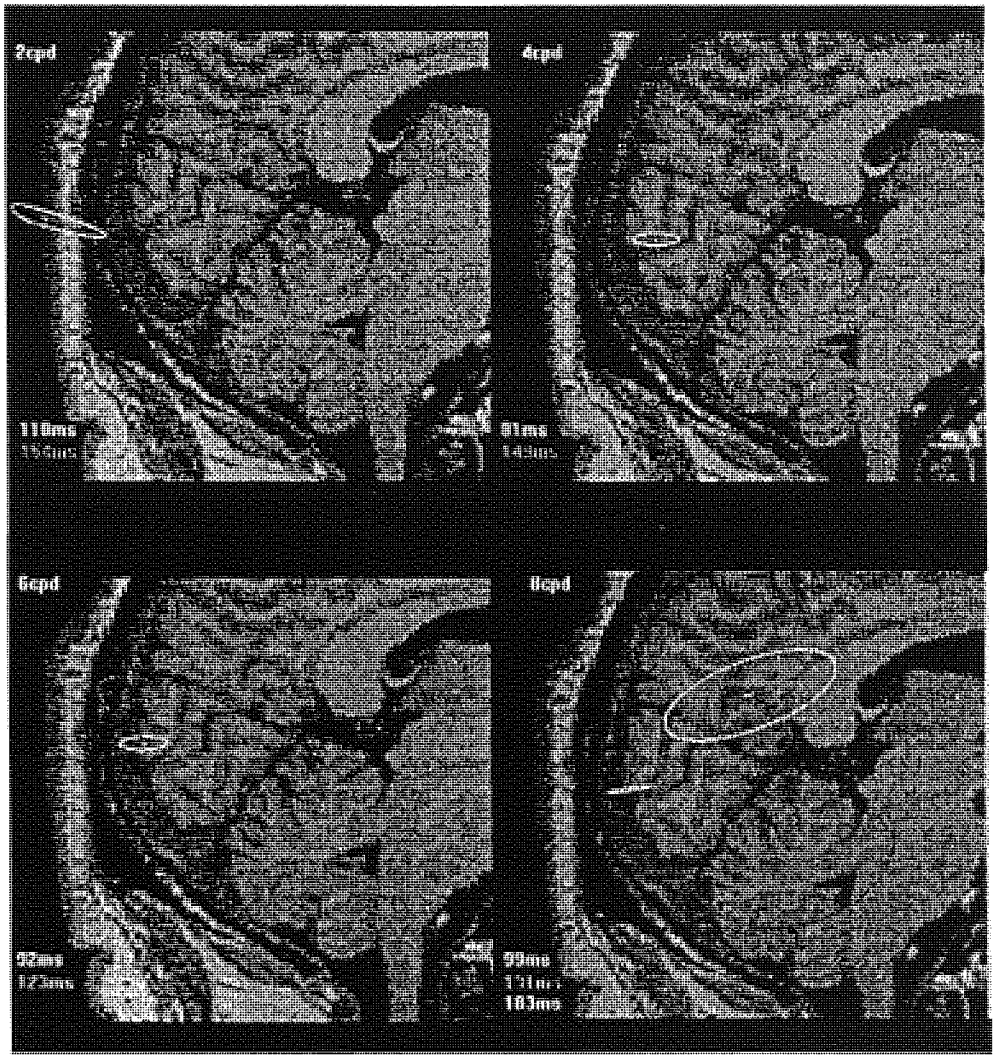

Figure 8.16 95% Monte-Carlo confidence regions for the major and late components at various spatial frequencies for subject KS

evoked response to all three luminance stimulus types. Support for this is obtained by examination of Figure 8.12 which shows the 95% confidence regions for the equivalent current dipole location following stimulation with each of the luminance conditions at the optimal spatial frequency of 4 cycles/degree for subject FF. The dipole location of the red/green response at the peak response of 2 cycles/degree is also shown. Although there are slight changes of position, all confidence regions are clustered together along the calcarine fissure and as such are suggestive of a V1 origin. This is supported by the orientation of the equivalent current dipole of the major component of both red/black and isoluminant red/green gratings being as predicted by the cruciform model of V1. The confidence regions generated from achromatic stimulation was larger than the other conditions. This may be due to the lower field strength of the response producing poorer dipole solutions and thus more uncertainty in the location of the dipole generator.

As would be predicted by the receptive field properties of the cortical cells, the results are consistent with the same cell population responding to all three luminance conditions. While the different morphology and latency of the isoluminant red/green response cannot support the same cell population giving rise to all components of the chromatic and luminance responses, the similar equivalent current dipole orientation of the isoluminant response and the major component of the luminance response suggest that at least this major component is generated by cells of the same area. Indeed, co-registration of the dipole confidence regions with MRI information are suggestive of the same visual area, V1, underlying the peak of the surface recorded activity following both luminance and isoluminant stimulation.

Although the response morphologies are very similar for the three luminance conditions, the field power of the red/black response is generally higher than the yellow/black and the achromatic response. This is indicative of a significant contribution from L^+/M^- single opponent cells to the recorded response. These cells would respond to the presence of red light but not to the addition of spatially co-extensive green light as is present in yellow/black and in achromatic gratings. Indeed, Tootell et al. (1988c) found the majority of cells within layers 2 and 3 of macaque area V1 to be single opponent cells.

Despite this relative increase in magnetic field strength for the red/black condition, the luminance modulated response is of lower field strength than the chromatic response of equivalent spatial frequency. For subject FF the response to isoluminant red/green gratings was recorded in the same experimental session as the luminance modulated

response. The highest field strength was evoked by a 2 cycles/degree red/green grating although the maximal field strength evoked by red/black gratings was only slightly lower. However, the spatial frequency tuning function shown in Figure 6.8 reveals the red/green response to peak at 1.5 cycles/degree. Hence the peak red/green response recorded during the luminance experimental session would be considerably higher than the peak red/black response. Indeed, although recorded during different experimental sessions so not strictly comparable, examination of field strength for red/black stimulation in Figures 8.7-8.9 and for red/green stimulation in Figures 6.1-6.5 reveals the isoluminant chromatic response to be consistently larger in all subjects. Again, this is suggestive of a significant contribution from single opponent cells to the recorded response. These cells would respond both to red/black gratings and to red/green gratings. As the red/green gratings would stimulate both L^+/M^- and M^+/L^- cells it would be expected that this stimulus type would produce the largest response. This is consistent with previous reports of a robust visual evoked potential to isoluminant chromatic stimulation which is of higher amplitude than that evoked by luminance stimulation (Crognale et al., 1993; Rabin et al., 1994).

The spatial frequency tuning of the luminance response for all three conditions is shown in Figure 8.3 for subject FF and for red/black modulation for the remaining three subjects in Figure 8.10. For all subjects the luminance response is bandpass, peaking at 4-8 cycles/degree and approaching the level of the noise at 12-16 cycles/degree. This is consistent with previous reports of the optimal spatial frequency of the response to achromatic gratings being between 4 cycles/degree (Jones and Keck, 1978) and 8 cycles/degree (Plant et al., 1983). The results are also comparable both with single cell recordings from macaque striate cortex (Thorell et al., 1984) and with psychophysical results (Mullen, 1985), shown in Figure 3.4, which demonstrate that the luminance response is bandpass, peaking at 0.8-4 cycles/degree with a cut-off frequency of 32-33 cycles/degree. Furthermore, Thorell et al. (1984) showed single opponent cells to have bandpass characteristics to luminance stimuli and lowpass characteristics to isoluminant chromatic stimuli. This is consistent with the major response peak of the chromatic and the luminance evoked magnetic response being generated by the same cell population; single cells within area V1.

The peak frequency found in this study is a little higher than these previous reports, peaking at 4-8 cycles/degree, although as discussed in Chapter 6 the shift to higher spatial frequencies may be partly an effect of the lower number of cycles displayed for low spatial frequencies. In addition, as Thorell et al. (1984) did not specify the cortical

layers from which their recordings were made, it is possible that the surface recorded response is dominated by parvocellular cells within layers 2 and 3 of V1 which may be tuned to higher spatial frequencies than magnocellular cells. Furthermore, the spatial frequency tuning functions described here are based on the field power of the major component. As discussed below, the earlier component is more apparent at low spatial frequencies and this low frequency activation may shift the psychophysical and single cell spatial frequency tuning curves to lower spatial frequencies.

The cut-off frequency found in this study, 12-16 cycles/degree, is lower than that found psychophysically and from single cell studies. However, even at 16 cycles/degree the majority of subjects had a clearly identifiable response and it is possible that a response, even if reduced to the level of the noise, could be recorded to spatial frequencies higher than 16 cycles/degree. In addition, as discussed in Chapter 6, the lower cut-off frequency observed here may be due to the requirement of a large number of neurones to respond in order for the surface recorded signal to be observable above background noise. Nevertheless, the spatial frequency tuning function is consistent with psychophysical and single cell studies and is clearly different from the lowpass isoluminant chromatic function, indicated in Figure 8.3 and shown in more detail in Figure 6.8.

A further difference between the luminance modulated and isoluminant chromatic response is the relative complexity of the signal. With few exceptions, the chromatic response shows a single, major component. The luminance response, however, comprises up to three distinct components. Figures 8.3 and 8.5 show the spatial frequency tuning of the major (Figure 8.3) and early and late (Figure 8.5) components of the evoked magnetic response for subject FF. The major component was present for all spatial frequencies while the early component was apparent only at low spatial frequencies and the late component, which was more persistent for the achromatic condition, mainly at moderate to high spatial frequencies. The early and late components were more variable and showed a greater difference between the three luminance conditions than did the major component. Indeed, the late achromatic response peaked at 2 cycles/degree while the remaining luminance conditions peaked at 6-8 cycles/degree. This may be due to the relatively low field strength making identification of the power peaks more difficult for these components. However, this late achromatic component spatial frequency tuning peak at 2 cycles/degree is consistent with the spatial frequency tuning of the N2-P2 component of the achromatic evoked potential to grating onset described by Plant et al. (1983) and shown in Figure 4.7. The differences in the early and late components of the evoked magnetic response

to different luminance conditions may therefore indicate the recruitment of different cell populations.

The latencies of these components were stable between luminance conditions, as shown in Figure 8.4 for the major component and Figure 8.6 for the late component. Again, this is suggestive of the same cell population generating all three responses. The latency of the major component showed a curvilinear relationship with spatial frequency, increasing above and below 2 cycles/degree. The achromatic condition showed more variability although the increase in latency with spatial frequency remained clear. The remaining three subjects confirm this trend, shown in Figure 8.11. By comparison, the latency of the red/green response for subject FF was longer and increased steeply between 2 and 4 cycles/degree. However, examination of Figure 6.7 indicates the red/green response to show a similar dependence on spatial frequency although latencies are longer and are shifted towards lower spatial frequencies.

Any trend of latency with changes in spatial frequency for the early component (62-79ms) was more difficult to identify as the component was apparent only at low spatial frequencies. This early component may parallel the C0 component described by Lesèvre and Joseph (1979) for achromatic checkerboard onset. Its presence may reflect early activation of the cortex by rapidly conducting magnocellular pathway afferents. This explanation would be consistent with the lack of such an early response in the isoluminant chromatic response. Furthermore, Nowak et al (1995) showed that the initial activation of layer 4Cα of macaque area V1 by the magnocellular pathway occurred some 20ms earlier than the initial parvocellular activation. Although MEG has spatial resolution comparable with PET and fMRI (Hämäläinen et al., 1993), this is not sufficient to distinguish between magnocellular and parvocellular layers within V1. However, the early component of the 0.25 cycles/degree and 1 cycle/degree red/black response for subject FF, shown in Figure 8.14, demonstrate a V1 origin. As the major component, occurring some 20-30ms later also localises to V1, the results support a sequence of activation of first the magnocellular layers and then the parvocellular layers of V1.

The late component was not of sufficient magnitude to afford localisation analysis for subject FF. However, subjects IH, JD and KS demonstrate high field strength later components and such analysis is shown in Figures 8.14-8.16. These figures reveal a large degree of inter-subject variability. The 95% confidence regions for subject IH, shown in Figure 8.14, show consistent spatial separation of the two components for all of the spatial frequencies. The major component is located along the ascending arm of

the calcarine fissure and as such is consistent with a V1 origin. The location of this component is very similar to that of the isoluminant chromatic response. The late component, however, consistently localises to the fissure above that of the major component. There is also a lateral shift but this is not marked for all spatial frequencies. The results are therefore consistent with a V1 origin for the major component and a V2 origin for the later component. The later component peaks at 123-151ms and as such occurs 43-67ms later than the V1 response. This is a longer delay than would be expected for the initial activation of V2. Nowak et al. (1995) showed that in macaque, V2 is activated, at least within the magnocellular layers, nearly simultaneously with V1. However, the activity may represent a later response within area V2.

The remainder of the subjects do not show such a clear spatial separation of the major and late components. The confidence region for both the major and late components for subject JD, shown in Figure 8.15, localise to above the calcarine fissure, on the cuneal gyrus and its superior fissure. Although the confidence regions are relatively large for 2 cycles/degree and 4 cycles/degree, the higher field strength signals of 6 cycles/degree and 8 cycles/degree produce uncertainty primarily in the depth of the dipole, which is as expected if there is activation along the length of the fissure. Hence both the major and the late components are consistent with a V2 origin. For comparison, the lower left panel also shows the confidence region for the response to 2 cycles/degree red/green gratings. This lies on the upper surface of the calcarine fissure and is therefore consistent with a V1 origin. Hence for subject JD, there is a clear difference in the activation sequence between stimulation with chromatic and luminance patterns.

For subject KS, shown in Figure 8.16, the major component lies along the upper surface of the calcarine fissure and as such is consistent with a V1 origin. The later component at 123-154ms, although generally positioned superiorly with respect to the major component, produces large confidence regions and thus no conclusions can be drawn about the active area of cortex this component represents. It is possible that the component arises from distributed activity in many cortical regions. A single dipole model would therefore be inappropriate and would result in the large confidence regions observed. An interesting point to note in the response to 8 cycles/degree is that a third component occurs at a latency of 183ms. This third component lies in approximately the same region as the late component observed for the other three spatial frequencies and the middle component, at 131ms, is shifted inferiorly. As the confidence region is large, no firm conclusions can be drawn regarding the cortical

origin of the component. However, if the response is confined to a small region of cortex and not the cerebellum, the remaining area enclosed by the confidence ellipse is the fusiform gyrus. This region has been described as the V4, the colour centre of the cortex (Zeki, 1983a,b,c; Zeki et al., 1991; Zeki, 1993) and may well be activated by a stimulus that contains both chromatic and luminance components. However, this component is not apparent at any of the other spatial frequencies and the localisation obtained from this experiment is not sufficiently good to conclude with certainty that a V4 response has been identified.

CHAPTER 9

HIGHER CORTICAL PROCESSING OF CHROMATIC INFORMATION

9.1 Introduction

The concept of segregation of visual information on a functional basis has gained increasing popularity over the last 15-20 years with hierarchical processing models (for example, Livingstone and Hubel, 1988a; Van Essen, 1985) considering the processing of colour is seen as a distinct mechanism, projecting via layer 4Cβ to the blobs of layers 2 and 3 of striate cortex, then to the thin stripes of area V2 before arriving at V4, the colour centre.

More recently, the functional distinction between blobs and interblobs has blurred and there is evidence of magnocellular input to the blobs (Livingstone and Hubel, 1984; Edwards et al., 1995). As magnocellular pathway cells do not carry chromatic information (Merigan et al., 1991; Schiller, 1991), the function of blobs as regions of colour processing has been called into question. Indeed, there have been suggestions that blobs are specialised for the analysis of low spatial frequency information rather than colour information (Tootell et al., 1988c,e; Edwards et al., 1995).

Nevertheless, the concept of a cortical centre specialised for the analysis of colour has been retained. The first such evidence of a colour centre came from clinical cases of achromatopsia; the selective loss of the ability to perceive colours (Verrey, 1888; Damasio et al., 1980). Such cases typically have lesions of the lingual and fusiform gyri, although there have been cases reported with lesions solely of the fusiform gyrus resulting in achromatopsia.

Electrophysiological evidence of the existence of functionally separate areas within visual cortex was provided by single cell studies in rhesus monkey (Zeki, 1978b). Areas containing a high proportion of directionally sensitive cells were thought to be indicative of a motion analysis area, which was termed MT or V5. An additional area was found to contain a high proportion of colour sensitive cells and it was suggested that this was the location of a colour area, which was termed V4 (Zeki, 1983a,b,c). The response of cells within V4 appeared to reflect the perception of colour rather

than the wavelength composition of the stimulus and it was suggested that the area may be involved in colour constancy (Zeki, 1980). However, in monkey, lesions to V4 also result in deficits in form perception and object recognition (Heywood and Cowey, 1987). Hence although the evidence suggests that V4 plays a major part in colour perception, this may not be its only function.

Recently, there have been several attempts to locate V4 in humans. Using PET, a comparison was made of rCBF when subjects viewed a chromatic and achromatic mondrian (Zeki et al., 1991). In addition to the activation of areas V1 and V2, which occurred for all stimulus types, the chromatic stimulus resulted in activation of the fusiform and lingual gyri. It was reported that this demonstrated the location of the human colour centre, V4. However, the differences in metabolic activity found using PET are very small so that averages across subjects are made. Due to the differences in cortical anatomy between subjects (Ono et al., 1990) this is not an optimal procedure. In addition, PET has poor spatial resolution and temporal resolution of the order of minutes (Hämäläinen et al., 1993; Harding, 1993). Hence it is inappropriate as a tool with which to investigate the temporal activation sequence of different areas of visual cortex.

While fMRI offers excellent spatial resolution, its value as a functional imaging tool is again limited by its poor temporal resolution. However, with the development of echo planar techniques the problem of temporal resolution has been partially addressed. Nevertheless, while scan times of seconds offers an improvement over more traditional fMRI methods this is still insufficient to follow cortical activation patterns. In addition, echo planar techniques improve temporal resolution at the expense of spatial resolution; in order to reduce scanning time the volume of cortex scanned is reduced and the investigation is often confined to a small region of cortex.

Such an approach was used by Sakai et al., (1995) in their fMRI investigation of the fusiform gyrus. They examined changes in BOLD when subjects looked at coloured circles and grey circles and they reported greater correlation of activity with the stimulus when the subjects looked at coloured circles. They claimed the results demonstrate the location of the human colour centre within the fusiform gyrus. However, the colour stimulus used in the experiment was not isoluminant but contained both colour and luminance modulation. This fact alone may have caused a higher correlation of cortical activity with the stimulus. Furthermore, scanning was confined to the fusiform gyrus. The evoked magnetic response data presented in Chapters 5-8 show a stronger response in area V1 following chromatic rather than

achromatic stimulation yet this does not imply that V1 contains the human colour centre. Sakai et al., (1995) cannot therefore demonstrate the location of the colour centre without comparing the results with other cortical areas.

It appears, therefore, that only MEG offers sufficient spatial and temporal resolution to distinguish between the activation of different cortical regions. Previous chapters have recorded the chromatic evoked magnetic response and have shown that the major response component arises in V1. In Chapter 8 the response to luminance and chromatic modulation was examined and it was demonstrated that in some subjects, distinct peaks in the magnetic field power arose from different cortical regions. In one subject Monte-Carlo error analysis suggested that one such peak may have been generated in the fusiform gyrus, which has been described as area V4. This chapter describes preliminary recordings of the evoked magnetic response generated by higher cortical processing of chromatic information and in particular, attempts to localise the human colour centre, V4. The temporal characteristics of the response will be examined to investigate the sequence and duration of activity within human extrastriate visual cortex.

9.2 Method

9.2.1 Stimuli

Isoluminant red/green gratings were generated as in section 5.2.1 and presented in a field size of 4 x 6 degrees. The spatial frequency of the gratings was 2 cycles/degree as this provides the maximum field strength response (see Chapter 6). Chapter 5 demonstrated the response to isoluminant chromatic gratings comprised a dipole located on or near the midline with orientation as predicted by the cruciform model of the calcarine fissure. To record the V1 response, left lower quadrant stimulation was used, displaced 0.5 degrees from the principal meridians as in Chapters 5-8. However, the pronounced activation of V1 is sufficiently high to obscure the activity arising from areas such as V4 which may be located some distance away from the gradiometers. In order to decrease the resulting dipole originating in V1, full field stimulation was also used. With stimulation of all four quadrants of the visual field, the dipoles generated will act to cancel and thus reduce the recorded magnetic field from this area. This is shown in Figure 9.1.

As the dipoles are not all of equal moments and slight anomalies of orientation have

been observed, it is unlikely that a full field stimulus will result in complete cancellation of the V1 source. However, the use of such a stimulus should lead to a decrease in the resultant field strength and activity arising from higher cortical processing may be more apparent.

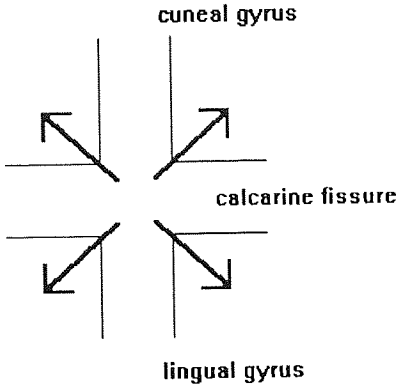

Figure 9.1 Predicted dipole activation within area V1 following full field stimulation.

9.2.2 Procedure

The visual evoked magnetic response was recorded using the Aston 19-channel SQUID magnetometer system as described in section 2.9. Both clinical and PET studies have suggested the location of area V4 as the fusiform and lingual gyri. The recording position was therefore moved laterally and inferiorly with respect to the usual Oz recording position and was centred approximately 3cm below O2 with the position of each gradiometer determined more precisely using a Polhemus digitising system. The evoked response to gratings presented in the left lower quadrant and in a full field was then recorded. The averaging epoch was 512ms and 200 epochs were recorded and averaged together. For subject VT the primary V1 response was also recorded for 100 epochs with the dewar centred over Oz.

9.2.3 Subjects

Two females (JD and VT) volunteered for the experiment. Their ages ranged from 27 to 32 years and all had normal visual fields and colour vision and a normal or corrected-to-normal Snellen acuity of 6/6.

9.3 Results

Figures 9.2-9.3 show the waveforms, global field power and field maps evoked by isoluminant chromatic stimulation recorded from two subjects using left lower quadrant and full field stimulation. The primary component from area V1 dominated the response for both subjects. For subject JD, due to the inferior recording position, the response was of low field strength. For subject VT the inferior recording position resulted in a response to left lower quadrant stimulation that was of high field strength but whose dipole fit did not reach statistical significance. The measurement was therefore repeated with the dewar positioned above Oz to enable a signal to be recorded that was suitable for cortical localisation.

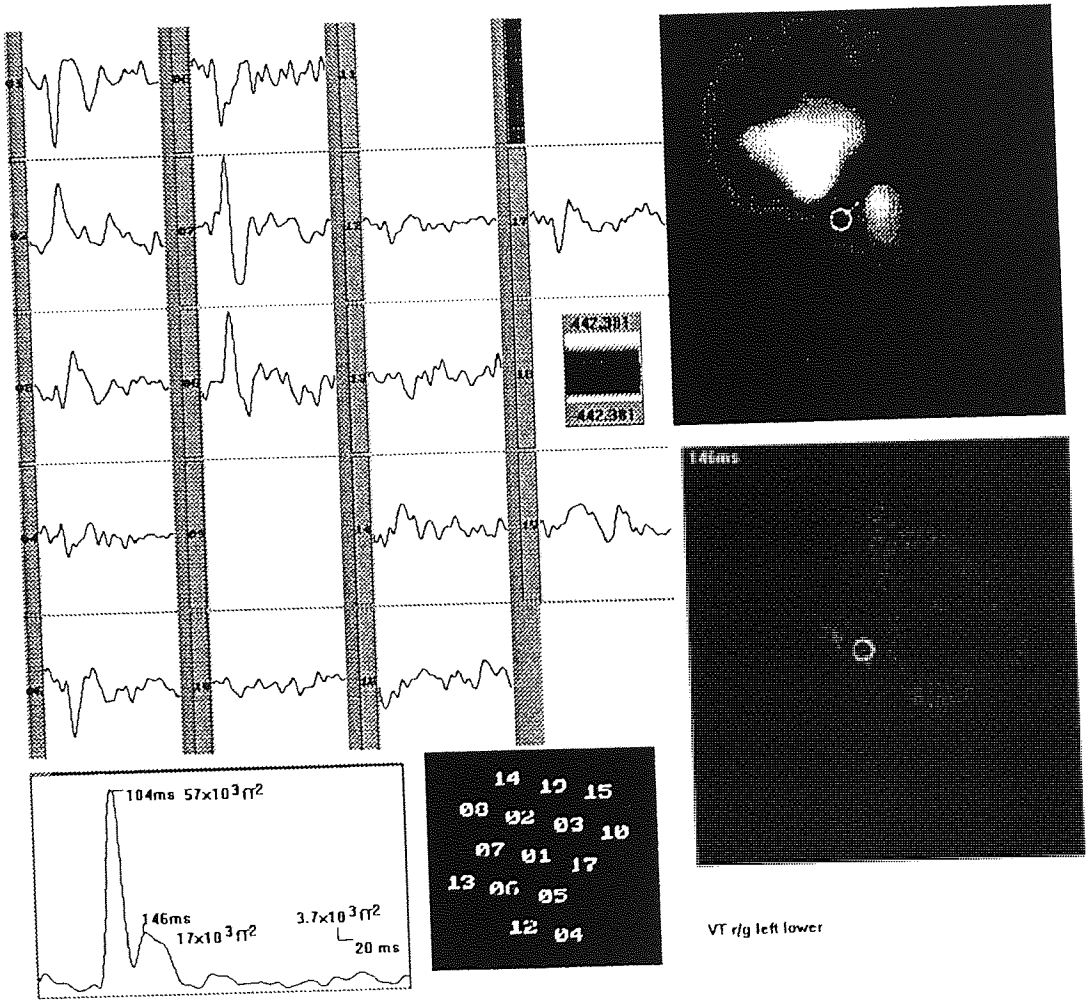

Figure 9.2 Waveforms and field map of the response of subject VT to chromatic gratings in the left lower quadrant

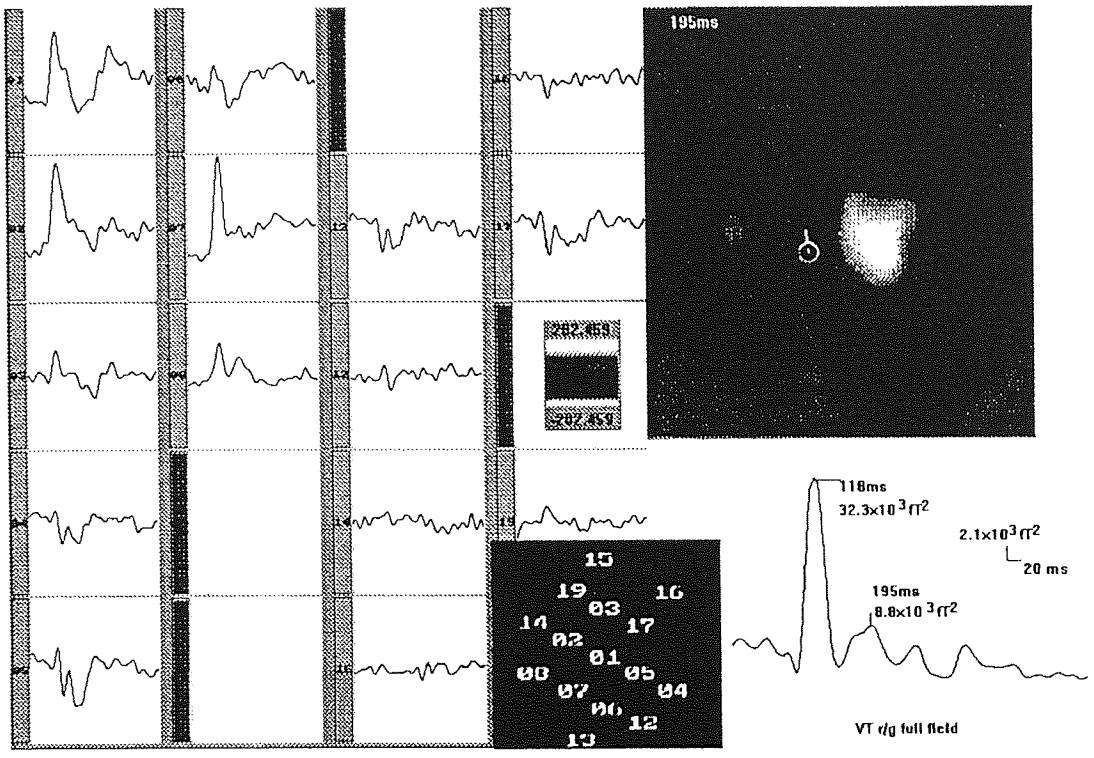

Figure 9.3 Waveforms and field map of the response of subject VT to chromatic gratings with full field stimulation

For the both subjects, the major response to left lower quadrant stimulation peaked at 104-113ms and the equivalent current dipole pointed up and to the right, as predicted by the cruciform model of striate cortex. For subject VT an additional component occurred at 146ms with an orientation that was rotated 90 degrees with respect to that of the major response. This later component was of lower field power than the major component and was not apparent following full field stimulation. For both subjects, full field stimulation resulted in a decrease of the major component. Although this component dominated the full field response its magnetic field strength fell from $57x10^3fT^2$ for the left lower quadrant condition to $32.3x10^3fT^2$ for the full field condition for subject VT and from $7.6x10^3fT^2$ to $4.5x10^3fT^2$ for subject JD. A later component was noted for the full field condition which peaked at 183-195ms. This component was of lower field strength, $17.3x10^3fT^2$ for subject VT and $4.1x10^3fT^2$ for subject JD.

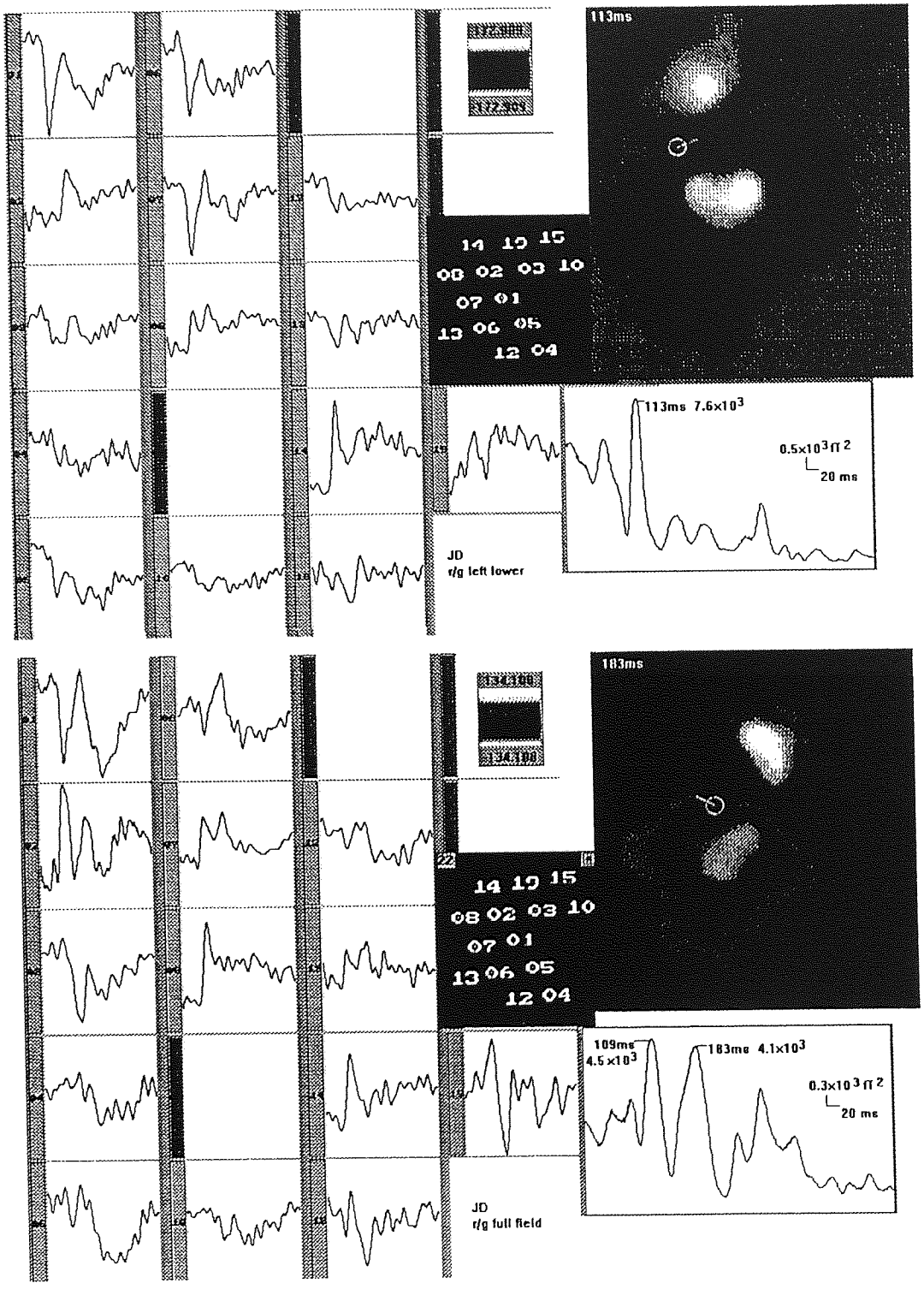

Figure 9.4 Waveforms and field map of the response of subject JD to chromatic gratings for left lower quadrant (upper panel) and full field (lower panel) stimulation

An equivalent current dipole model was applied to each of the power peaks in the response of the two subjects; this was appropriate as the peaks were distinct and it was therefore assumed the response was dominated by a single mechanism at the time of the peak. This was supported by the correlation coefficients, and gammaQ values obtained. These statistics and the value of the dipole moment, Q, are shown in Table 9.1.

subject	stimulation	latency(ms)	probable location	correlation co-efficient	gammaQ	χ^2	Q (nAm)
VT	left lower	104	V1	0.98	0.001	30	8.8
	left lower	146	V2	0.96	0.046	17	5.3
	full field	195	V4	0.97	0.076	17	8.6
JD	left lower	113	V1	0.99	0.512	8.2	5.0
	full field	183	V4	0.96	0.563	7.7	3.5

Table 9.1 Parameters of the single equivalent current dipole fits for subjects VT and JD. Number of active channels was 15 for VT and 14 for JD.

Monte-Carlo analysis of the data was performed which yielded 95% confidence regions for the dipole locations. Co-registration of this data with MRI information is shown in Figures 9.5-9.6. The confidence regions for the power peaks in the response were found to be small and spatially distinct. Figure 9.5 shows the location of the volume of cortex generating the three power peaks for subject VT. These correspond with the calcarine fissure, the fissure superior to the cuneal gyrus and the fusiform gyrus. All three regions lie on the midline

The confidence regions generated by the two power peaks for JD shown in Figure 9.6 are also small and spatially distinct. The regions activated are the calcarine fissure for the first component and the lingual and fusiform gyri for the second. The later component is more lateral with respect to the earlier, lying within the right hemisphere while the earlier component is situated on the midline.

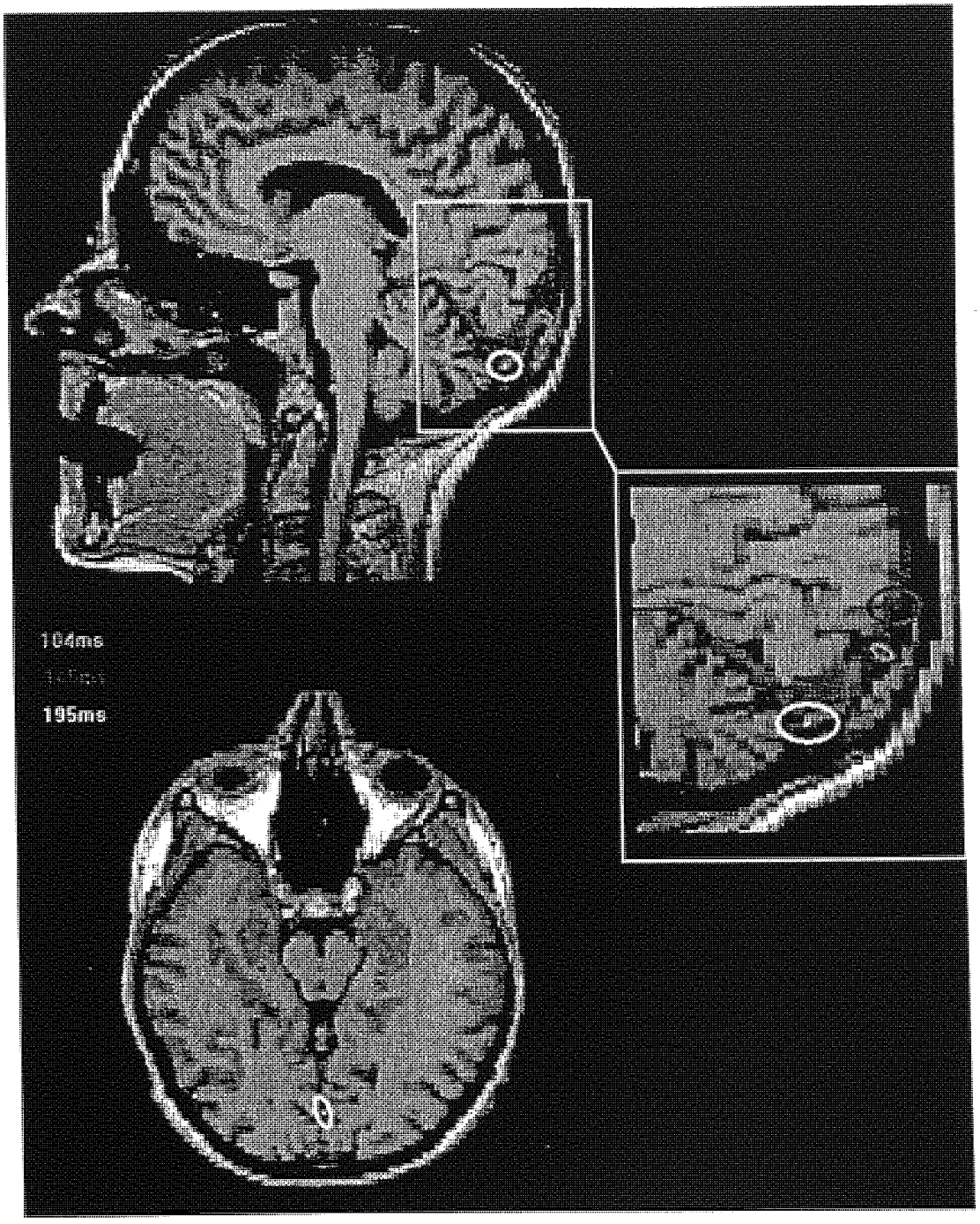

Figure 9.5 Confidence regions of the dipole locations following chromatic stimulation for subject VT

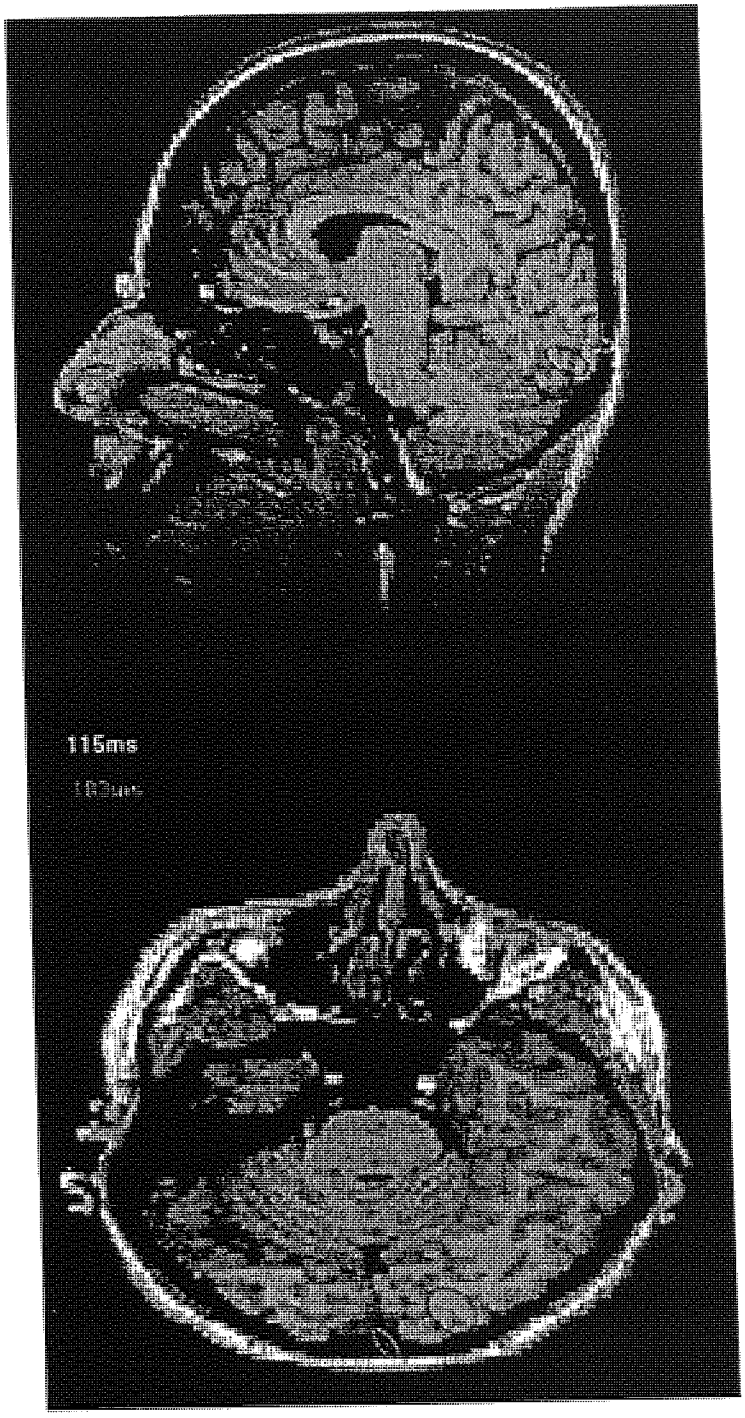

Figure 9.6 Confidence regions of the dipole locations following chromatic stimulation for subject JD

9.4 Discussion

The evoked magnetic response was recorded to isoluminant chromatic gratings in order to investigate higher cortical processing mechanisms in human visual cortex. The waveforms and magnetic field power for the two subjects to left lower quadrant stimulation, shown in Figures 9.2 and 9.4, indicate that the response is dominated by a major component. This component, which peaks at 104-113ms, is well modelled by a single dipole for subject JD, evidenced by the high correlation and gamma Q and low χ^2 values in Table 9.1. For subject VT the χ^2 values are higher than would be expected for a good fit of the model to the data. However, the correlation co-efficients and gammaQ values are significant and the Monte-Carlo confidence regions generated are small. Hence it can be concluded that the model provides an a sufficiently good fit to the data for subject VT.

The dipole moments of 8.8nAm for subject VT and 5.0nAm for subject JD are the strongest components found throughout the recording epoch. Co-registration of the dipole solution with MRI information reveals the active volume for both subjects to lie along the calcarine fissure, consistent with a V1 origin.

Examination of the field power of subject VT in Figure 9.2 reveals a second component at 146ms. Although of lower field power and dipole moment, this component is also well modelled by a single current dipole, indicated by the dipole statistics in Table 9.1. The Monte-Carlo confidence region is small, again indicating a good fit by a single dipole model, and is situated on the superior cuneal fissure. As such this is consistent with a V2 origin.

Investigation of the late component at 183-195ms was complicated by the high field power V1 component which dominated the response and obscured the late component. Presentation of the stimulus in a full field resulted in a decrease in field strength of the V1 response and the late component became more apparent. Although this approach results in the V1 response being unsuitable for modelling with a single current dipole, this is not true of V4. In macaque (Zeki, 1993) and probably human (Clarke and Miklossy, 1990; Zeki, 1991) V4, situated on the lingual and/or the fusiform gyri, contains a representation of both upper and lower visual fields. Hence the use of a full field stimulus should not result in the cancellation of dipole moments as will result for V1. If this were not so and there exists a dorsal V4, the spatial separation of dorsal and ventral V4 should not result in any cancellation of the response.

The equivalent current dipoles are 8.6nAm for subject VT and 3.5nAm for subject JD and as such are of lower strength than the V1 component. Co-registration of the Monte-Carlo confidence regions with MRI data reveal the active cortex to lie on the posterior fusiform gyrus for subject VT and on both the lingual and fusiform gyri for subject JD. This is consistent with reports of the location of a colour centre gained from single cell studies in monkey (Zeki, 1980; 1993), PET studies (Zeki, 1991), post-mortem evidence (Clarke and Miklossy, 1990) and from fMRI studies (Sakai et al., 1995).

There have been previous intra-cortical recordings made within macaque V1 and V4, although in response to flashes of white light rather than to spatially modulated isoluminant patterns (Givre et al., 1994). They show that while V1 contributes mainly to the surface recorded N40, and P55-80ms activity, V4 contributes mainly to the N95, P120 and late negative responses. As the flash response has different morphology to the pattern response (see Chapter 4) the latencies are not directly comparable. However, the latency of the V4 response of 183-195ms recorded here is not unrealistic. The time between the peak responses recorded from V1 and V4 is 91ms for subject VT and 70ms for subject JD. This is longer than expected for initial activation times as Givre et al., (1994) found that there was a 25ms delay between commencement of activity in V1 and V4. The response recorded from V4 is therefore unlikely to correspond to the initial activation of this area. This is consistent with the reports of Givre et al., (1994) whose results show that the strongest response recorded directly from V4 was not the initial P80 but the later N95 and P120. Similarly, the latency between the peak response from V1 and that from V2 for subject VT is 42ms. This is longer than would be expected from the response of single cells within macaque areas V1 and V2. Nowak et al. (1995) demonstrated that in macaque, processing commences nearly simultaneously within V1 and V2. Hence the V2 response is also unlikely to represent the initial activation of this area. The temporal characteristics of the evoked response therefore indicate that activation occurs over a prolonged period within extrastriate cortical areas.

Chapter 8 notes possible activation of the fusiform gyrus at 131ms following stimulation with red/black gratings. This is considerably earlier than the latencies recorded here to red/green gratings and may either represent processing differences due to the different stimuli used, or a different phase in the activity of this region of cortex. Indeed, Givre et al., (1994) note considerable variability in the later responses recorded directly from cells within macaque V4. The variation in latencies between

subjects may therefore represent variability in the response of V4 itself. This is clearly a subject which requires further investigation. The visual evoked magnetic response, particularly for the later components, may reflect secondary activation of higher cortical areas. These reverberatory responses may arise from feedbackward connections from higher areas, or subsequent feedforward connections from V1 and V2.

Given the short latencies between initial activations of areas V1, V2 and V4 suggested from macaque data, the prolonged nature of the dominant V1 response may obscure the activity arising from these higher areas. The use of a single dipole model precludes the identification of simultaneously active areas but is applicable to those time periods which are dominated by the activity of a single area, as evidenced by the dipole statistics in Table 9.1. Hence by limiting analysis to distinct peaks in the evoked magnetic response power, activation of areas V1, V2 and V4 have been identified.

CHAPTER 10

CONCLUSIONS

The results of this thesis show that MEG is a valuable tool for examining the properties of different areas and populations of neurones within the human visual cortex. Specifically, the results indicate that it is possible to activate preferentially different populations of neurones within area V1 and different visual areas (V2 and V4) by using appropriately designed stimuli.

The evoked magnetic response recorded to isoluminant red/green gratings was described in Chapter 5. The response was dominated by a major component which did not arise from possible luminance artefacts in the stimulus. At the time of maximum magnetic field power the response was well described by an equivalent current dipole which was positioned on or close to the midline. The orientation of the dipole changed consistently with the visual field stimulated in a manner consistent with anatomical models of the calcarine fissure. Co-registration with MEG and MRI data revealed the upper visual field to be represented on the lower surface of the calcarine fissure and the lower visual field on the upper surface of the calcarine fissure. This demonstrates the origin of the chromatic evoked magnetic response as striate cortex, visual area V1.

Having isolated a neuronal population within a specific area of cortex, if a sufficiently high signal-to-noise ratio is obtained it is possible to characterise the spatio-temporal characteristics of that cell population. Chapter 6 examined the spatial frequency tuning properties of chromatic sensitive cells within area V1. The spatial frequency tuning curve of the chromatic evoked response was found to be bandpass, peaking at 1-2 cycles/degree and falling to the level of the noise at approximately 6 cycles/degree. The high spatial frequency cut-off point, while consistent with that found by previous evoked response studies, was lower than that found by single cell electrophysiology and by psychophysical measures. This was thought to be due to the larger number of responding neurones required to record an evoked magnetic response. While the organism as a whole can perceive a stimulus when a very small number of neurones respond to that stimulus (Newsome et al., 1989), MEG requires in the order of fifty thousand neurones to be simultaneously active before a clear evoked response is recorded (Pizella and Romani, 1990). Hence MEG may provide a more accurate measure of the magnitude of cells tuned to a particular spatial frequency than the

detection thresholds traditionally used in psychophysics.

The decreased sensitivity to low spatial frequency patterns was found to be influenced by the small number of cycles displayed at the lower spatial frequencies tested. Due to physical restraints imposed by the recording equipment it was not possible to establish if the response would approach a lowpass function if sufficient cycle numbers were displayed. It remains possible that the chromatic contrast sensitivity function is formed by an envelope of channels tuned to different spatial frequencies with more neurones tuned to 1-2 cycles/degree than to lower and higher spatial frequencies. The cortical location of the dipole generator of the evoked magnetic response was found to be invariant with spatial frequency in agreement with the known spatial frequency properties of area V1.

Chapter 7 examined the effect of temporal frequency on the magnetic field power and latency of the chromatic evoked magnetic response. There were two peaks in the temporal frequency tuning function with maximal field power obtained at 0-1Hz and at 4Hz. Such bimodal sensitivity is not apparent in psychophysical investigations (Gegenfurtner and Hawken, 1995; Mullen and Boulton, 1992; Kelly, 1983) and may be indicative of two chromatic mechanisms with overlapping temporal frequency sensitivities.

The latency of the evoked magnetic response increased to a maximum at 8-16Hz before dropping again to values which were lower than those observed following the presentation of stationary gratings. This suggests the cells generating the evoked response encode the motion of the stimulus rather than simply detecting its presence. The response to achromatic gratings at a range of temporal frequencies was of low field strength and thus luminance artefacts did not underlie the response to chromatic gratings at any temporal frequency. This drop in latency following high temporal frequency chromatic stimulation therefore suggests the activation of a sub-population of cells tuned for high temporal frequencies.

Monte-Carlo analysis demonstrated that there was no change in cortical origin of the response for different temporal frequencies, providing evidence to suggest that cells in V1 encode the motion of chromatic targets over a wide range of temporal frequencies.

Having established the spatio-temporal tuning properties of chromatic sensitive cells in V1, Chapter 8 examined the spatial frequency tuning characteristics of the cells generating the luminance evoked magnetic response. The evoked response was shown

to be more complex than the isoluminant chromatic response, comprising up to three distinct components. The spatial frequency tuning function, based on the magnetic field power of the major component, showed bandpass characteristics, peaking at 4-6 cycles/degree with a cut-off frequency of 12-16 cycles/degree. This is consistent with single cell recordings in macaque (Thorell et al., 1984) and with human psychophysical data (Mullen, 1985) although with a more marked low frequency fall off. This may be due to the effect of low cycle numbers displayed in the stimulus and also that the early component which dominated at low spatial frequencies was not included in the spatial frequency tuning curve. The lower high frequency cut-off may be due to, as discussed above, the requirement that a large number of neurones respond for the evoked response to be detected above background noise.

The spatial frequency tuning characteristics of the responses to chromatic and luminance data suggest that single-opponent cells within area V1 underlie both the isoluminant chromatic response and the major peak of the luminance response. While it is known that double-opponent cells exist at the level of the cortex (Livingstone and Hubel, 1984), the results suggest that the majority of cells within area V1 are single-opponent. Although the data indicates that the same population of cells responds to chromatic and luminance stimuli, the luminance response was more complex than the isoluminant chromatic response. This is suggestive of the activation of an additional cell population. The early component observed following luminance stimulation may reflect activation of magnocellular layers within area V1 while the later component may arise from the activity of higher processing mechanisms. The results provide evidence to suggest that differences in processing of chromatic and luminance information occur as early as area V1 of human visual cortex.

Monte-Carlo analysis of the power peaks revealed a degree of inter-subject variability. Confidence regions tended to be large, supportive of widespread cortical activation. The data showed evidence of a progression of cortical activation from V1 to V2. For one subject, Monte-Carlo analysis also revealed possible activation of the fusiform gyrus.

To further examine the sequence of cortical activation patterns as information is analysed within progressively higher centres, Chapter 9 aimed to identify area V4, which has been described as the colour centre of human visual cortex. The statistical parameters of the dipoles obtained indicated that at the times of the power peaks, the response could be modelled by a current dipole. Three such peaks were observed in the response of subject VT and two in the response of subject JD. Co-registration of

Monte-Carlo analysis and MRI data revealed the dipole generators to lie within areas consistent with V1, V2 and V4 for subject VT and areas V1 and V4 for subject JD. The locations of these extrastriate areas match those indicated in PET and fMRI studies. MEG therefore provides validation for these techniques which offer only indirect evidence of cortical activity.

The data indicates that it is possible to follow sequences of cortical activation using MEG. The latencies observed for activation within extrastriate visual cortex imply that the activity dominating the evoked response does not arise from the initial activation of these cortical areas. The data thus provides evidence to suggest that activation of extrastriate cortex occurs over a prolonged time interval. Currently, the localisation algorithm is limited to time periods in which the recorded activity is dominated by a discrete cortical region. Hence although MEG offers the temporal resolution to follow the initial activation of V1, V2 and higher cortical areas, a single equivalent dipole algorithm is not sufficient to achieve this.

Considering the complexity of the human visual cortex it is perhaps suprising that a single equivalent current dipole can be used to model the data. However, such models have been successfully utilised in many studies and the dipole statistics in Tables 5.1 and 9.1 indicate that such a model provides a good description of the data presented in this thesis. Hence it can be concluded that if the stimuli are designed to restrict the activation of cortex to a discrete region a current dipole can be used to model the response at times in which the response is dominated by a single component. This is particularly true when the active regions of cortex is close to the sensing coils; as cortical dipolar-like activity falls off with the square of the distance then the activity from cortical generators some distance away from the sensors will contribute less to the recorded response.

The results presented in this thesis point to the value of MEG as a method of validating other functional imaging techniques and also to enlarge upon the results of psychophysics and single cell studies. The spatial tuning properties of cells within area V1 were found to be similar but not identical to human psychophysical data. The differences for low spatial frequencies may to some extent be due to limitations in the size of the display equipment. However, for higher spatial frequencies, the differences can be accounted for by the requirement that a large number of neurones be simultaneously active before a clear evoked magnetic response is recorded. This contrasts both with psychophysical measures and with single cell electrophysiology. Single cells studies examine the response of a small sample of cells and it is difficult to

determine if this sample is representative of the whole neuronal population. Similarly, a psychophysical decision can be based upon the activity of very few neurones (Newsome et al., 1989) so when the detection of a stimulus is above threshold, there is no way of knowing if very few or very many neurones are responding to that stimulus. Furthermore, psychophysical measures reflects the output of the whole visual process and cannot distinguish between the response of cells at different stages of visual processing.

In contrast, once a neuronal population has been identified, by examining the magnitude of the response over a range of spatio-temporal frequencies MEG can provide an estimate of the relative number of cells tuned to a particular spatial and temporal frequency. The use of masking techniques may reveal the number of spatial and temporal frequency channels present and also the relative number of cells within that channel. This can be achieved for cells at any level of the visual processing mechanism. Co-registration of MEG and MRI information enables the location of the responding cells to be determined so that a description of the spatio-temporal properties of cells within different areas of visual cortex can be obtained.

REFERENCES

Aguilar, M. & Stiles, W.S. (1954) Saturation of the rod mechanism of the retina at high levels of stimulation. *Optica Acta* 1; 1: 59-65.

Ahlfors, S.P., Ilmoniemi, R.J. & Hämäläinen, M.S. (1992) Estimates of visually evoked cortical currents. *Electroenceph. Clin. Neurophysiol.* 82: 225-236.

Aine, C.J., Bodis-Wollner, I. & George, J.S. (1990) Generators of visually evoked neuromagnetic responses. Spatial-frequency segregation and evidence for multiple sources. In S. Sato (ed) *Advances in Neurology 54: Magnetoencephalography.* pp 141-155. Raven Press, New York.

Aine, C.J., Supek, S., Ranken, D., George, J.S. & Flynn, E.R. (1993) MEG studies of human vision: identification of areas V1 and V2. In Deecke, L., Baumgartner, C., Stroink, G. and Williamson S.J. (eds) *Recent Advances in Biomagnetism: Proc. 9th International Conference on Biomagnetism* pp10-11.

Allison, J.D., Casagrande, V.A. & Bonds, A.B. (1995) The influence of input from the lower cortical layers on the orientation tuning of upper layer V1 cells in primate. *Vis. Neurosci.* 12: 309-320.

Allison, T., Matsumya, Y., Goff, G.D. & Goff, W.R. The scalp topography of human visual evoked potentials. *Electroenceph. Clin. Neurophysiol.* 42:185-197.

Allman, J., Miezin, F. & McGuinness, E.L. (1985a) Direction and velocity specific responses from beyond the classical receptive field in the middle temporal visual area (MT). *Perception* 14: 105-126.

Allman, J., Miezin, F. & McGuinness, E.L. (1985b) Stimulus specific responses from beyond the classical receptive field: Neurophysiological mechanisms for local-global comparisons in visual neurones. *Ann. Rev. Neurosci.* 357: 277-403.

Anderson, S.J. & Burr, D.C. (1985) Spatial and temporal selectivity of the human motion detecting system. *Vision Res.* 5:1147-1154.

Anderson, S.J., Mullen, K.T. & Hess, R.F. (1991) Human peripheral spatial resolution for achromatic and chromatic stimuli: limits imposed by optical and retinal factors. *J. Physiol.* 442: 47-64.

Anderson, S.J., Drasdo, N. & Thompson, C. M. (1995) Parvocellular neurons limit motion acuity in human peripheral vision. *Proc. R. Soc. Lond. B* 261: 129-138.

Anderson, S.J., Holliday, I.E., Singh, K.D. & Harding G.F.A. (1995) Localisation and functional analysis of human cortical area MT (V5) using magneto-encephalography. *Manuscript in preparation for Proc. R. Soc. Lond. B.*

Anhelt, P.K., Kolb, H. & Pflung, R. (1987) Identification of a subtype of cone photoreceptor, likely to be blue sensitive, in the human retina. *J. Comp. Neurol.* 255:18-34.

Armstrong, R.A., Slaven, A. & Harding, G.F.A. (1991) The influence of age on the flash visual evoked magnetic response (VEMR) *Ophthalmol. Physiol. Opt.* 11: 71-75.

Azzopardi, P. & Cowey, A. (1993) Preferential representation of the fovea in the primary visual cortex. *Nature* 361: 719-721.

Bach, M. & Ullrich, D. (1994) Motion adaptation governs the shape of motion evoked cortical potentials. *Vision Res.* 34: 1541-1547.

Bardeen, J., Cooper, L.N. & Schrieffer, J.R. (1957) Theory of superconductivity. *Phys. Rev.* 108: 1175-1204.

Barkley, G.L., Tepley, N., Moran, J.E. & Welch, K.M.A. (1995) DC-MEG studies of migraine patients and controls. In Deecke, L., Baumgartner, C., Stroink, G. and Williamson S.J. (eds) *Biomagnetism: fundamental research and clinical applications.* Amsterdam: IOS Press. pp 70-74.

Barnes, G.R. (1995) The development of calibration and adaptive filtering procedures for neuromagnetic studies of human visual function. PhD Thesis. Aston University.

Barth, D.S. (1991) Emprical comparison of the MEG and EEG: Animal models of the direct cortical response and epileptiform activity in neocortex. *Brain Topography* 4(2): 85-93.

Baule, G. & McFee, R. (1963) Detection of the magnetic field of the heart. *Am. Heart J.* 66: 95-96.

Benedek, G., Janaky, M., Adamkovich, N, Rubicsek, G & Sary, G. (1993) Scotopic pattern-reversal visual evoked potentials. *Clin. Vision Sci.* 8: 47-54.

Benevento, L.A. & Fallon, J.H. (1975) The ascending connections of the superior colliculus in the rhesus monkey (*Macacca mulatta*). *J. Comp. Neurol.* 160: 339-362.

Blakemore. C., Nachmias, J. & Sutton, P. (1970) The perceived spatial frequency shift: evidence for frequency-selective neurones in the human brain. *J. Physiol.* 210: 727-750.

Blakemore, C., Muncey, J.P.J. & Ridley, R.M. (1973) Stimulus specificity in the human visual system. *Vision Res.* 13: 1915-1931.

Blumhardt, L.D. (1987) The abnormal pattern visual evoked response in neurology. In A.M. Halliday, S.R. Butler & R. Paul (eds) *A Textbook of Clinical Neurophysiology*. Wiley. pp 307-342.

Blumhardt, L.D., Barrett, G. & Halliday, A.M. (1977) The asymmetrical visual evoked potential to pattern reversal in one half field and its significance for the analysis of visual field defects. Br. J. Ophthalmol. 61: 456-461.

Blumhardt, L.D. & Halliday, A.M. (1979) Hemisphere contributions to the composition of the pattern-evoked potential waveform. *Exp. Brain Res*, 36: 53-69.

Bodis-Wollner, I., Ghilardi, M.F.& Mylin, L.H. (1986) The importance of stimulus selection in VEP Practice: The clinical relevance of visual physiology. In R.Q. Craco & I. Bodis-Wollner (eds) *Evoked Potentials*. New York: AR Liss pp 15-27.

Bogousslavasky, J., Miklossy, J., Deruaz, J., Assal, G. & Regli, F. (1987) Lingual and fusiform gyri in visual processing: A clinicopathologic study of altitudinal hemianopia. *J. Neurol. Neurosurg. Psychiat.* 50: 607-614.

Bowmaker, J.K., Darnall, H.J.A. & Mollon, J.D. (1980) Microspectophotometric demonstration of four classes of photoreceptor in an old world primate *Macaca fasicularis. J. Physiol.* 298: 131-143.

Bradley, A., Zhang, X., Thibos, L. (1992) Failures of isoluminance caused by ocular chromatic aberrations. *Applied Optics* ; 31(19): 3657-3667.

Brenner, D., Williamson, S.J. & Kaufman, L. (1975) Visually evoked magnetic fields of the human brain. *Science* 190: 480-482.

Bullier, J. & Henry, G.H. (1979a) Ordinal position of neurons in cat striate cortex. *J. Neurophysiol.* 42: 1251-1263.

Bullier, J. & Henry, G.H. (1979b) Neural path taken by afferent streams in striate cortex of the cat. *J. Neurophysiol.* 42: 1264-1270.

Bullier & Henry (1979c) Laminar distribution of first-order neurons and afferent terminals in cat striate cortex. *J. Neurophysiol.* 42: 1271-1281.

Burkhalter, A. & Van Essen, E.D. (1986) Processing of color, form and disparity in visual areas VP and V2 of ventral extrastriate cortex in the macaque monkey. *J. Neurosci.* 6: 2327-2351.

Butler, S.R., Georgiou, G.A., Glass, A., Hancox, R.J., Hopper, J.M. & Smith, K.R.H. (1987) Cortical generators of the CI component of the pattern-onset visual evoked potential. *Electroenceph. Clin. Neurophysiol.* 68:256-267.

Campbell, F.W. & Robson, J.G. (1968) Application of Fourier analysis to the visibility of gratings. *J. Physiol.* 197: 551-566.

Carelli, P. & Pizzella, V. (1992) Biomagnetism: an application of superconductivity. *Supercond. Sci. Technol.* 5: 407-420.

Casagrande, V.A. & DeBruyn, E.J. (1982) The Galago visual system: aspects of normal organization and developmental plasticity. In P.C. Haines (ed) *The Lesser Bushbaby (Galago) An Animal Model: Selected Topics.* Boca Raton. CRC Press. pp 138-168.

Casagrande, V.A. & Norton, T.T. (1990) Lateral genicualte nucleus: A review of its physiology and function. In A.G. Leventhal (ed) *The Neural Basis of Visual Function.* Hampshire: Macmillan. pp 41-84.

Cavanagh, P. (1984) The contribution of color to motion. In Valberg A., Lee B. B. (eds) *From pigments to perception.* New York: Plenum Press. pp 151-164.

Cavanagh, P., Favreau, O.E. (1985) Color and luminance share a common motion pathway. *Vision Res.* 25: 1595-1601.

Cavanagh, P., Anstis, S. (1991) The contribution of color to motion in normal and color-deficient observers. *Vision Res.* 31: 2109-2148.

Ciganek, M.L. (1961) The EEG response (evoked potential) to light stimulus in man. *Electroenceph. Clin. Neurophysiol.* 13: 165-172.

Clark, V. P., Courchesne, E. & Grafe, M. (1992) In vivo myeloarchitectonic analysis of human striate and extrastriate cortex using magnetic resonance imaging. *Cerebral Cortex* 2: 417-424.

Clarke, S. & Miklossy, J. (1990) Occipital cortex in man: organisation of callosal connections, related myelo- and cytoarchitecture and putative boundaries of functional visual areas. *J. Comp. Neurol.* 298: 188-214.

Cleland, BG., Dubin M.W. & Levick, W.R. (1971) Sustained and transient neurones in the cat's retina and lateral geniculate nucleus. *J. Physiol.* 217: 473-496.

Cobb, W.A. & Dawson, G.D. (1960) The latency and form in man of the occipital potentials evoked by bright flashes. *J. Physiol.* 152: 108-121.

Cohen, D. (1968) Magnetoencephalography: Evidence of magnetic fields produced by alpha rhythm currents. *Science* 161: 784-786.

Cohen, D. (1972) Magnetoencephalography: Detection of the brains electrical activity with a superconducting magnetometer. *Science* 175: 646-666.

Cohen, D., Edelsack, E. & Zimmerman, J.E. (1970) Magnetocardiograms taken inside a shielded room with a point-contact magnetometer. *Appl. Phys. Lett.* 16: 278-280.

Cohen, D., Cuffin, B.N., Yunokuchi, K., Maniewski, R., Purcell, C., Cosgrove, G.R., Ives, J., Kennedy, J.G. & Schomer, D.L. (1991) MEG versus EEG localization test using implanted sources in the human brain. *Ann. Neurol.* 28: 811-817.

Connolly, M. & Van Essen, D. (1984) The representation of the visual field in parvocellular and magnocellular layers of the lateral geniculate nucleus in the macaque monkey. *J. Comp. Neurol.* 226: 554-564.

Corletto, F., Gentilomo, A., Rodadini, A, Rossi, G.F. & Zattoni, J. (1967) Visual evoked potentials as recorded from the scalp and from the visual cortex before and after surgical removal of the occipital pole in man. *Electroenceph. Clin. Neurophysiol.* 22: 378-380.

Cowey, A. & Stoerig, P. (1989) Projection patterns of surviving neurons in the dorsal lateral geniculate-nucleus following discrete lesions of striate cortex - Implications for residual vision. *Exp. Brain Res.* 75: 631-638.

Cragg, B.G. & Ainsworth, A. (1969) The topography of the afferent projections in the circumstriate visual cortex of the monkey studied by the nauta method. *Vision Res.* 9: 733-747.

Crognale, M.A., Rabin, J R., Adams, A.J. & Switkes, E. (1992) VEP correlates of spatio-chromatic processing. *Invest. Ophthalmol. Vis. Sci. Suppl.* 33: 701.

Crognale, M., Switkes, E., Rabin, J., Scheck, M., Haegerstrom-Portnoy, G. & Adams, A. (1993) Application of the spatiochromatic visual evoked potential to detection of congenital and acquired color-vision deficiencies. *J. Opt. Soc. Am. A* ; 18 (8): 1818-1825.

Cropper, S.J. & Derrington, A.M. (1994) Motion of chromatic stimuli: first-order or second-order ? *Vision Res.* 34: 49-55.

Crowley, C.W. & Budiman, J. (1989) Reducible integral equation for a dipole in a quasispherical conductor. In M. Hoke, S., Erné, Y. Okada, G. Romani (eds) *Biomagnetism: Clinical Aspects.* Amsterdam: Elsevier. pp 699-703.

Cuffin, B.N. & Cohen, D. (1977) Magnetic fields of a dipole in special volume conductor shapes. *IEEE Trans. Biomed. Eng.* BME-24: 372-381.

Culham, J.C. & Cavanagh, P. (1994) Motion capture of luminance stimuli by equiluminous color gratings and by attentive tracking. *Vision Res.* 34: 2701-2706.

Curcio, C.A., Sloan, K.R., Packer, O., Hendrickson, A.E. & Kalina, R.E. (1987) Distribution of cones in human and monkey retina: Individual variability and radial asymmetry. *Science* 236: 579-582.

Dacey, D.M. & Peterson, M.R. (1992) Dendritic feld size and morphology of midget and parasol ganglion cells of the human retina. *Proc. Natn. Acad. Sci.* 89: 9666-9670.

Dagnelie, G. (1986) Pattern and motion processing in primate visual cortex. PhD Thesis. University of Amsterdam.

Damasio, A., Yamada, T., Damasio, H., Corbett, J. & McKee, J. (1980) Central achromatopsia: behavioural, anatomic and physiologic aspects. Neurology 30: 1064-1071.

Daniel, P.M. & Witterage, D. (1961) The representation of the visual field in the cerebral cortex of monkeys. *J. Physiol.* 159: 203-221.

Darcey, T.M., Ary, J.P. & Fender, D.H. (1980) Spatio-temporally visually evoked scalp potentials in response to partial-field patterned stimulation. *Electroenceph. Clin. Neurophysiol.* 50: 348-355.

DeMonasterio, F.M. (1978) Properties of concentrically organised X and Y ganglion cells of macaque retina. *J. Neurophysiol.* 41: 1394-1417.

DeMonasterio, F.M. & Gouras, P. (1975) Functional properties of ganglion cells of the rhesus monkey retina. *J. Physiol.* 251: 167-195.

Derrington, A.M., Krauskopf, J. & Lennie, P. (1984) Chromatic mechanisms in lateral geniculate nucleus of macaque. *J. Physiol.* 357: 219-240.

Derrington, A.M. & Lennie, P. (1984) Spatial and temporal contrast sensitivities of neurones in the lateral geniculate nucleus of macaque. *J. Physiol.* 357: 219-240.

Derrington, A.M. & Henning, G.B. (1993) Detecting and discriminating the direction of motion of luminance and colour gratings. *Vision Res.* 33: 799-811.

Desimone, R., Schein, S.J., Moran, J. & Ungerleider, J. (1985) Contour, color and shape analysis beyond the striate cortex. *Vision Res.* 25: 441-452.

Desimone, R. & Schein, S.J. (1987) Visual properties of neurones in area V4 of the macaque: sensitivity to stimulus form. *J. Neurophysiol.* 57: 835-868.

DeValois, R.L., Morgan, H. & Snodderly, D.M. (1974) Psychophysical studies of monkey vision III. Spatial luminance contrast sensitivity tests of macaque and human observers. *Vision Res.* 14: 75-81.

DeValois, K.K., DeValois, R.L. & Yund, E.W. (1979) Responses of striate cortex cells to gratings and checkerboard patterns *J. Physiol.* 291: 483-505.

DeValois, R.L., Yund, E.W. & Hepler, N. (1982) The orientation and direction selectivity of cells in macaque visual cortex. *Vision Res.* 22: 531-544.

DeValois, R.L., Albrecht, D.G. & Thorell, L.G. (1982) Spatial frequency selectivity of cells in macaque visual cortex. *Vision Res.* 22: 545-559.

DeValois, R.L. & Jacobs, G.H. (1984) Neural mechanisms of colour vision. In I. Darian-Smith (ed) *Handbook of physiology*: 1, 3 pp 425-456. Bethseda, American Physiological Society.

DeValois, R.L., Thorell, L.G. & Albrecht, D.G. (1985) Periodicity of striate cortex cell receptive fields. *J. Opt. Soc. Am. A.* 2: 1115-1123.

DeValois, R.L. & DeValois, K.K. (1990) *Spatial Vision.* New York: Oxford Univeristy Press.

De Yoe, E.A. & Van Essen, D.C. (1985) Segregation of efferent connections and receptive field properties in visual area V2 of the macaque. *Nature* 317: 58-61.

De Yoe, E.A. & Van Essen, D.C. (1988) Concurrent processing streams in the monkey visual cortex. *Trends in Neurosciences* 11; 5: 219-226.

Dobelle, W.H., Turkel, J., Henderson, D.C. & Evans, J.R. (1979) Mapping the representation of the visual field by electrical stimulation of human cortex. *Am. J. Ophthalmol.* 88: 727-735.

Dobkins, K.R. & Albright, T.D. (1993) What happens if it changes color when it moves?: Psychophysical experiments on the nature of chromatic input to motion detectors. *Vision Res.* 33: 1019-1036.

Drasdo, N. (1991) Neural substrates and threshold gradients in peripheral vision. In Kulikowski, J.J., Walsh, V. and Murray, I.J. (eds) *The limits of vision*. Hampshire: Macmillan.

Dubner, R. & Zeki, S.M. (1971) Response properties and receptive fields of cells in an anatomically defined region of the superior temporal sulcus in the monkey. 35: 528-532.

Ducati, A., Fava, E & Motti E.D.F. (1988) Neuronal generators of the visual evoked potentials: Intracerebral recording in awake humans. *Electroenceph. Clin. Neurophysiol.* 71: 89-99.

Ducla-Soares, E. (1989) Volume current effects on MEG and modelling. In S.J. Williamson, M. Hoke, G. Stroink & M. Kotani (eds) *Advances in Biomagnetism.* New York: Plenum Press. pp 533-538.

Dunajski, Z. & Peters, M. (1995) Development of the fetal magnetocardiograms from the 13th week of gestation onwards. In Deecke, L., Baumgartner, C., Stroink, G. and Williamson S.J. (eds) *Biomagnetism: fundamental research and clinical applications.* Amsterdam: IOS Press. pp 704-708.

Edwards, D.P., Purpura, K.P. & Kaplan, E. (1995) Contrast sensitivity and spatial frequency response of primate cortical neurons in and around the cytochrome oxidase blobs. *Vision Res.* 35: 1501-1523.

Enroth-Cugell, C. & Robson, J.G. (1966) The contrast sensitivity of retinal ganglion cells of the cat. *J. Physiol.* 187: 517-552.

Erné, S.N. & Romani, G.L. (1985) Performances of higher order planar gradiometers for biomagnetic source localization. In H.D. Hahlbohm & H. Lubbig (eds) *SQUID 85: Superconducting quantum interference devices and their applications.* Berlin: Walter de Gruyter. pp 951-961.

Estévez, O. & Spekreijse, H. (1974) Relationship between pattern appearance-disappearance and pattern reversal responses. *Exp. Brain Res.* 19: 233-238.

Fagaly, R.L. (1990) Neuromagnetic instrumentation. In S. Sato (ed) *Advances in Neurology 54: Magnetoencephalography.* Raven Press, New York. pp 11-32.

Felleman, D.J. & Van Essen, D.C. (1987) Receptive field properties of neurones in area V3 of macaque monkey exrastriate cortex. *J. Neurophysiol.* 57: 889-920.

Ferrera, V.P., Nealey, T.A. & Maunsell, J.H.R. (1992) Mixed parvocellular and magnocellualr geniculate signals in area V4. *Nature.* 358: 756-758.

Flanagan, J.G. & Harding, G.F.A. (1986) Source derivation of the visual evoked potential. *Doc. Ophthalmol.* 62: 97-105.

Foster, K.H., Gaska, J.P., Nagler, M. & Pollen, D.A. (1985) Spatial and temporal frequency selectivity of neurones in cortical areas of V1 and V2 of the macaque monkey. *J. Physiol.* 365: 331-363.

Gallen, C.C., Bucholz, R., Sobel, D.F., Swartz, B.J., Hirschkoff, E.C., Barkley, G. & Malik, G. (1995) Magnetoencephalography with advanced 3D MR imaging in pre-surgical planning and interoperative monitoring. In Deecke, L., Baumgartner, C., Stroink, G. and Williamson S.J. (eds) *Biomagnetism: fundamental research and clinical applications.* Amsterdam: IOS Press. pp 43-49.

Gastaut, H. & Regis, H. (1965) Visual evoked potentials recorded transcranially in man. In L.D. Proctor, W.R. Adey (eds) *The Analysis of Central Nervous System and Cardio-Vascular system Data Using Computer Methods.* Washington: NASA.

Gattas, R., Sousa, A.P.B. & Gross, C.G. (1988) Visuotopic organization and extent of V3 and V4 of the macaque. *J. Neurosci. 8*: 1831-1845.

Gegenfurtner, K.R. & Hawken, M.J. (1995) Temporal and chromatic properties of motion mechanisms. *Vision Res.* 35: 1547-1563.

Gilbert, C.D. (1977) Laminar differences in receptive field properties of cells in cat visual cortex. *J. Physiol.* 268: 391.

Gilbert, C.D. & Wiesel, T.N. (1979) Morphology and intercortical projections of functionally characterize neurones in the cat visual cortex. *Nature* 280: 120-125.

Givre, S.J., Schroeder, CE., Arezzo, J.C. (1994) Contribution of extrastriate area V4 to the surface recorded flash VEP in the awake macaque. *Vision Res.* 34: 415-438.

Givre, S.J., Arezzo, J.C. & Schroeder, C.E. (1995) Effects of wavelength on the timing and laminar distribution of illuminance-evoked activity in macaque V1. *Vis. Neurosci.* 12: 229-239.

Gorea, A., Papathomas, T.V. & Kovacs, I. (1993a) Motion perception with spatiotemporally matched chromatic and achromatic information reveals a "slow" and a "fast" motion system. *Vision Res.* 33: 2515-2534.

Gorea, A., Papathomas, T.V. & Kovacs, I. (1993b) Two motion systems with common and separate pathways for color and luminance. *Proc. Natl. Acad. Sci. USA.* 90: 11197-11201.

Gouras, P. (1968) Identification of cone mechanisms in monkey ganglion cells. *J. Physiol.* 199: 533-547.

Gouras, P. (1984) Color vision. *Progress in retinal research.* 3: 227-261.

Gouras, P. (1990) Cortical mechanisms of colour vision. P. Gouras (ed). *The Perception of Colour.* Hampshire: Macmillan pp 179-197.

Gouras, P. & Kruger, (1979) Responses of cells in foveal cortex of the monkey to pure color contrast. *J. Neurophysiol.* 42; 3: 830-860.

Gouras, P. & Zrenner, E. (1981) Colour coding in primate retina. *Vision Res.* 21:1591-1598.

Granger, E.M. & Heurtley, J.C. (1973) Visual chromaticity transfer function. *J. Opt. Soc. Am.* 63:1173-1174.

Grynszpan, F & Geslowitz, D.B. (1973) Model studies of the magnetocardiogram. *Biophys J.* 13: 911-925.

Gur, M. & Akri, V. (1992) Isoluminant stimuli may not expose the full contribution of colour to visual functioning: spatial contrast sensitivity measurements indicate interactions between colour and luminance processing. *Vision. Res.* 2: 1253-1262.

Haimovic, I.C. & Pedley, T.A. (1982) Hemifield pattern reversal visual evoked potentials II. Lesions of the chiasm and posterior visual pathways. *Electroenceph. Clin. Neurophysiol.* 54: 121-131.

Halliday, A.M., Barrat, G. Halliday, E. & Michael, W.F. (1977) The topography of the pattern-evoked potential. In J. Desmedt (ed) *Visual evoked potentials in man: new developments*. Oxford: Clarendon Press. pp 121-133.

Hämäläinen, M., Hari, R., Ilmoniemi, R., Knuutila, J. & Lounasmaa, O. (1993) Magnetoencephalography- theory, instrumentation and applications to noninvasive studies of the working human brain. *Rev. Mod. Phys.* 65: 413-496.

Hammond, P. & MacKay, D.M. (1975) Differential responses of cat visual cortical cells to textured stimuli. *Exp. Brain Res.* 306: 275-296.

Harding, G.F.A. (1974) The use of visual evoked responses to flash stimulation in assessment of visual defect. *Electroenceph. Clin. Neurophysiol.* 36: 551.

Harding, G.F.A. (1991) Origin of visual evoked cortical potentials components. In J.R. Heckenlively and G.B. arden (eds) *Principles and Practice of Clinical Electrophysiology of Vision*. St. Louis: Mosby. pp 132-144.

Harding, G.F.A. (1993) How surgeons could navigate the brain. *New Scientist.* 11th Dec. pp 28-31.

Harding, G.F.A., Smith, G.S., Smith, P.A. (1980) The effect of various stimulus parameters on the lateralisation of the visual evoked potential. In Barker C (ed) *Evoked Potentials*. Lancaster: MTP Press. pp 213-218.

Harding, G.F.A. & Rubenstein, M.P. (1981) Early components of the visual evoked potential in man - are they of subcortical origin ? *Doc. Ophthalmol.* 27: 49-65.

Harding, G.F.A. & Dhanesha, U. (1986) The visual evoked subcortical potential to pattern reversal stimulation. *Clin. Vis. Sci.* 1: 179-184.

Harding, G.F.A., Janday, B. & Armstrong, R. (1992) The topographic distribution of the magnetic P100M to full and half field stimulation. *Doc. Ophalmol.* 80: 63-73.

Harding, G.F.A., Odom, J.V., Spileers, W & Spekreijse, H. (On behalf of the International Society for Clinical Electrophysiology of Vision) (1995) Standards for clinical VEP measurements. *Arch. Neurol.* (Submitted)

Hari, R., Aittoniemi, K., Järvinen, M.-L., Katila, T & Varpula, T. (1980) Auditory evoked transient and sustained magnetic fields of the human brain: Localization of neuronal generators. *Exp. Brain Res.* 40: 237-240.

Hari, R. & Ilmoniemi, R.J. (1986) Cerebral magnetic fields. *CRC Crit. Rev. Biomed. Eng.* 14: 93-126.

Harting, J.K., Casagrande, V.A. & Weber, J.T. (1978) The projection of the primate superior colliculus upon the dorsal lateral genicualte nucleus: Autoradiographic demonstration of interlaminal distribution of tectogeniculate axons. *Brain Res.* 93-99.

Hawken, M.J., Gegenfurtner, K.R. & Tang, C. (1994) Contrast dependence of color and luminance motion mechanisms in human vision. *Nature* 367: 268-270.

Hendrickson, A.E., Hunt, S.P. & Wu, J.Y. (1981) Immunocytochemical localiztion of glutamic acid and decarboxylase in monkey striate cortex. *Nature* 292: 605.

Hendry, S.H.C. & Yoshioko, T. (1994) A neurochemically distinct third channel in the macaque dorsal lateral geniculate nucleus. *Science* 264: 575-577.

Henning, G.B. & Derrington, A.M. (1994) Speed, spatial-frequency, and temporal-frequency comparisons in luminance and colour gratings. *Vision Res.* 34: 2093-2101.

Hess, R.F. & Snowden, R.J. (1992) Temporal properties of human visual filters-numbers, shapes and spatial covariation. *Vision Res.* 32: 47-59.

Heywood, C.A. & Cowey, A. (1987) On the role of cortical area V4 in the discrimination of hue and pattern in macaque monkeys. *J. Neurosci.* 7: 2601.

Hicks, T.P., Lee, B.B. & Vidyasagar, T.R. (1983) The response of cells in macaque lateral geniculate nucleus to sinusoidal gratings. *J. Physiol.* 337: 183-200.

Hobley, A. (1988) The investigation of the primary response of the flah visual evoked response. PhD Thesis, Aston University.

Holmes, G. (1918) Disturbances of vision by cerebral lesions. *Brit. J. Ophthalmol.* 2: 353-384.

Horton, J.C. (1984) Cytochrome oxidase patches: a new cytoarchtectonic feature of monkey visual cortex. *Phil. Trans. R. Soc. Lond. B* 304: 199.

Horton, J.C. (1992) The central visual pathway. In W.M. Hart (ed) *Adler's Physiology of the Eye*. St Louis: Mosby pp 728-777.

Horton, J.C. & Hubel, D. H. (1981) Regular patchy distribution of cytochrome oxidase staining in primary visual cortex of macaque monkey. *Nature* 292: 762.

Horton, J.C. & Hoyt, W.F. (1991) The representation of the visual field in the human striate cortex. *Arch Opthalmol.* 109: 816-824.

Howell, E.R. & Hess, R.F. (1978) The functional area for summation to threshold for sinusoidal gratings. *Vision Res.* 18: 369-374.

Hubel, D.H. (1988) *Eye, Brain and Vision.* NewYork: Scientific American Library.

Hubel, D.H. & Livingstone, M.S. (1985) Complex-unoriented cells in a subregion of primate area 18. *Nature* 315: 325-327.

Hubel, D.H. & Livingstone, M.S. (1987) Segregation of form, color and stereopsis in primate area 18. *J. Neuroscience.*; 7: 3378-3415.

Hubel, D.H. & Wiesel, T.N. (1959) Receptive fields of single neurones in the cat's striate cortex. *J. Physiol.* 148; 574-591.

Hubel, D.H. & Wiesel, T.N. (1962) Receptive fields, binocular interactions and functional architecture in the cat's visual cortex. *J. Physiol.* 160: 106-154.

Hubel, D.H. & Wiesel, T.N. (1965) Receptive fields and functional architecture in two non-striate visual areas (18 and 19) of the cat. *J. Neurophysiol.* 28: 229-289.

Hubel, D.H. & Wiesel, T.N. (1972) Laminar and columnar distribution of geniculocortical fibres in macaque monkey. *J. Comp. Neurol.* 146: 421-450.

Hubel, D.H. & Wiesel, T.N. (1974) Sequence regularity and geometry of orientation columns in the monkey striate cortex. *J. Comp. Neurol.* 158: 267-294.

Hubel, D.H., Wiesel, T.N. & Stryker, M.P. (1978) Anatomical demonstration of orientation columns in macaque monkey. *J. Comp. Neurol.* 177: 361.

Ingling, C.R. (1991) Psychophysical correlates of parvo channel function. In Valberg A., Lee B. B. (eds) *From pigments to perception.* New York: Plenum Press: 413-424.

Ingling, C.R. & Martinez-Uriegas, E. (1985) The spatiotemporal properties of the r-g X cell channel. *Vis Res.* 25: 33-38.

Ioannides, A.A., Boton, J.P.R., Hasson, R. & Clarke, C.J.S. (1989) Localised and distributed source solutions for the biomagnetic inverse problem II. In S.J. Williamson, M. Hoke, G. Stroink & M. Kotani (eds) *Advances in Biomagnetism.* Plenum Press, New York.

Jakobsson, P. & Johansson, B. (1992) The effect of spatial frequency and contrast on the latency in the visual evoked potential. *Doc. Opthalmol.* 79: 187-194.

Jeffreys, D.A. (1977) The physiological significance of pattern visual evoked potentials. In J. Desmedt (ed) *Visual evoked potentials in man: new developments.* Oxford: Clarendon Press. pp134-167.

Jeffreys, D.A. (1989) Evoked potentials studies of contour processing in human visual cortex. In Kulikowski, J.J., Dickinson, C.M. and Murray, I.J. (eds) *Seeing colour and contour*. Oxford: Pergammon Press. pp 529-545.

Jeffreys, D.A. & Axford, J.G. (1972a) Source locations of pattern specific components of human visual evoked potentials I: Components of striate cortical origin. *Exp. Brain Res.* 16: 1-21.

Jeffreys, D.A. & Axford, J.G. (1972b) Source locations of pattern specific components of human visual evoked potentials II: Components of extrastriate cortical origin. *Exp. Brain Res.* 16: 22-24.

Jones, R. & Keck, M.J. (1978) Visual evoked reponse as a function of gratings spatial frequency. *Invest. Opthalmol. Visual Sci.* 17: 652-659.

Josephson, B. (1962) Possible new effects in superconducting tunneling. *Phys. Letters* 1: 251-253.

Kaplan, E. & Shapley, R.M. (1986) The primate retina contains two types of retinal ganglion cells with high and low contrast sensitivity. *Proc. Natn. Acad. Sci. USA*. 83: 2755-2757.

Kaplan, E., Lee, B.B. & Shapley, R.M. (1990) New views of primate retinal function. In Osborne, N. and Cohaden, J. (eds) *Progress in retinal research Vol. 9*. New York: Pergammon Press.

Kaufman, L. & Williamson, S.J. (1980) The evoked magnetic field of the human brain. *Ann. N.Y. Acad. Sci.* 340: 45-65.

Kelly, D.H. (1983) Spatiotemporal variation of chromatic and achromatic contrast thresholds *Journal of the optical society of America* 73: 742-750.

Koch, C. (1987) The action of the corticofugal pathway on sensory thalamic nuclei: A hypothesis. *J. Neurosci.* 23: 399-406.

Kolb, H. (1970) Organisation of the outer plexiform layer of the primate retina: Electron microscopy of Golgi-impregnated cells. *Philos. Trans R. Soc. Lond. (Biol.)* 258: 261-283.

Kolb, H. (1979) The inner plexiform layer in the retina of the cat: Electron microscopic observations. *J. Neurocytol.* 8: 295-329.

Kolb, H. (1991) The neural organsiation of the human retina. In Hickenlively, J.R. and Arden G.B. (eds) *Principles and practice of clinical electrophysiology of vision.* St. Louis: Mosby.

Kolb, H. & DeKorver, L. (1988) Synaptic input to midget ganglion cells of the human retina. *Invest. Ophthalmol. Vis. Sci.* 29: 326.

Kolb, H., Ahnelt P, Fisher S.K., Linberg K.A. & Keri C. (1989) Chromatic connectivity of the three horizontal cell types in the human retina. *Invest. Ophthalmol. Vis. Sci.* 30: 348.

Krauskopf, J., Klemic, G., Lounasmaa, O.U., Travis, D., Kaufman, L. & Williamson, S.J. (1989) Neuromagnetic measurements of visual responses to chromaticity and luminance. In: S.J. Williamson, M. Hoke, G. Stroink & M. Kotani (eds) *Advances in Biomagnetism.* Plenum Press, New York. pp 209-212.

Kraut, M.A., Arezzo, J.C. & Vaughan, H.G. (1985) Intracortical generators of the flash VEP in monkeys. *Electroenceph. Clin. Neurophysiol.* 62: 300-312.

Kremers, J, Lee, B.B. &Kaiser, P.K. (1992) Sensitivity of macaque retinal ganglion cells and human observers to combined luminance and chromatic temporal modulation. *J. Opt. Soc. Am. A.* 9: 1477-1485.

Kriss, A. & Halliday, A.M. (1980) A comparison of occipital potentials evoked by pattern onset, offset and reversal by movement. In C. Barber (ed) *Evoked Potentials.* Lancaster: MTP. pp205-212.

Kuba, M. & Zuzana, K. (1992) Visual evoked potentials specific for motion onset. *Doc. Ophthalmol.* 80: 83-89.

Kulikowski, J.J. (1977a) Visual evoked potentials as a measure of visibility. In J. Desmedt (ed) *Visual evoked potentials in man: new developments.* Oxford: Clarendon Press. pp 168-183.

Kulikowski, J.J. (1977b) Separation of occipital potentials related to the detection of pattern and movement. In J. Desmedt (ed) *Visual evoked potentials in man: new developments*. Oxford: Clarendon Press. pp 184-196.

Kulikowski, J.J. & Walsh, V. (1990) On the limits of colour detection and discrimination. In J.J. Kulikowski, V. Walsh and I.J. Murray (eds) *The limits of vision*. Macmillan.

Kulikowski, J.J., McKeefry, D., Walsh, V. & Carden, D. (1993) Visual evoked potentials and their neuronal correlates. In *Proc. Society for the Promotion of Visual Sciences 2*: 5.

Kurita-Tashima, S., Tobimatsu, S, Nakayama-Hiromatsu, M. & Kato, M. (1991) Effect of check size on the pattern reversal visual evoked potential. *Electroenceph. Clin. Neurophysiol.* 80: 161-166.

LaBerge, D. & Buchsbaum, M.S. (1990) Positron emission tomographic measures of pulvinar activity during an attention task. *J. Neurosci.* 10: 613-619.

Lee, B.B., Virsu V. & Creutzfeldt, O.D. (1983) Linear signal transmission from prepotentials to cells in the macaque lateral geniculate nucleus. *Exp. Brain Res.* 52:50-56.

Lehmann, D., Torcey, T.M. & Skrandies, W. (1982) Intracerebral and scalp fields evoked by hemiretinal checkerboard reversal and modelling of their dipole generators. In J. Courjon, F. Mauguiere and M. Revol (eds) *Clinical Applications of Evoked Potentials in Neurology*. New York: Raven Press. pp 41-48.

LeMay, M. & Kido, D.K. (1978) Asymmetries of the cerebral hemispheres on computed tomograms. *J. Comp. Ass. Tomog.* 2: 471-476.

Lennie, P. & D'Zmura, M. (1988) Mechanisms of color vision. *CRC Critical Reviews in Neurobiology* 3: 333-400.

Lesèvre, N. & Joseph, J.P. (1979) Modifications of the pattern evoked potential (PEP) in relation to the stimulated part of teh visual field (clues for the most probable origin of each component). *Electroenceph. Clin. Neurophysiol.* 47: 183-203.

Leventhal, A.G., Rodieck, R.W. & Dreher, B. (1981) Retinal ganglion cells classes in the old world nonkey: Morphology and central projections. *Science*. 213: 1139-1142.

Linberg, K.A., Fisher, S.K. & Kolb, H. Are there three types of horizontal cell in the human retina? *Invest. Ophthalmol. Vis. Sci.* 28: 262.

Lindsay, P.M. & Norman, D.A. (1972) *Human information processing.* New York: Academic Press.

Lindsey, D. & Teller, D. (1990) Motion at isoluminance: discrimination / detection ratios for moving isoluminant gratings. *Vision Res.* 30: 1751-1761.

Livingstone, M.S. & Hubel, D.H. (1982) Thalamic inputs to cytochrome oxidase-rich regions in monkey visual cortex. *Proc. Natl. Acad. Sci.* 79: 6098.

Livingstone, M.S. & Hubel, D.H. (1984) Anatomy and physiology of a colour system in the primate visual cortex. *J. Neurosci.* 4: 309-356.

Livingstone, M. & Hubel, D.H. (1987) Psychophysical evidence for separate channels for the perception of form, color, movement and depth. *J. Neurosci.* 7: 3416-3468.

Livingstone, M.S. & Hubel, D.H. (1988a) Segregation of form, color, movement and depth: anatomy, physiology and perception. *Science* 240: 740-750.

Livingstone, M.S. & Hubel, D.H. (1988b) Segregation of form, color, movement, and depth: anatomy, physiology and perception. *J. Nuerosci.* 8;11: 4334-4339.

Logothetis, N.K., Schiller, P.H., Charles, E.R. & Hurlbert A.C. (1990) Perceptual deficits and the activity of the color-opponent and broad band pathways at isoluminance. *Science* 247:214-217.

Lopes da Silva, F.H., Wieringa, H.J. & Peters M.J. (1991) Source localisation of EEG versus MEG: Empirical comparison using visually evoked responses and theoretical considerations. *Brain Topography* 4:133-142.

Lorrain, P., Corson, D.P. & Lorrain, F. (1988) *Electromagnetic fields and waves.* New York: Freeman.

Lund, J.S., Lund, R.D., Hendrickson, A.E., Bunt, A.H. & Fuchs, A.F. (1975) The origin of afferent pathways from the primary cortex, area 17, of the macaque monkey as shown by retrograde transport of horseradish peroxidase. *J. Comp. Neurol.* 164: 287-304.

Maier, J., Dagniele, G., Spekreijse, H. & Van Dijk, B.W. (1987) Principal components analysis for source localization of VEPs in man. *Vision Res.* 37: 165-177.

Manahilov, V., Riemslag, F.C.C. & Spekreijse, H. (1992) The laplacian analysis of the pattern onset response in man. *Electroenceph. Clin. Neurophysiol.* 82: 220-224.

Mariani, A.P. (1984a) Bipolar cells in monkey retina selective for cones likely to be S sensitive. *Nature*. 308: 184-186.

Mariani, A.P. (1984b) The neuronal organization of the outer plexiform layer of the primate retian. *Int. Rev. Cytol. 86: 285-320.*

Mariani, A.P., Kolb, H. & Nelson, R. (1984) Dopamine-containing amacrine cells of rhesus monkey retina parallel rods in spatial distribution. *Brain Res.* 322: 1-7.

Matlashov, A.N., Zhuravlev, Yu.E. & Lipovich, A.Ya. (1989) Electric noise supression in multichannel neuromagnetic system. In: S.J. Williamson, M. Hoke, G. Stroink & M. Kotani (eds) *Advances in Biomagnetism.* New York: Plenum Press.

Matlashov, A.N., Slobodchikov, V., Bakharev, A, Zhuravlev, Y & Bodarenko, N. (1993) Biomagnetic multichannel system built with 19 cryogenic probes. In Deecke, L., Baumgartner, C., Stroink, G. and Williamson S.J. (eds) *Recent Advances in Biomagnetism: Proc. 9th International Conference on Biomagnetism* pp 284-285.

Maunsell, J.H.R. & Newsome, W.T. (1987) Visual processing in monkey extrastriate cortex. *Ann Rev. Neurosci.* 10: 363-401.

Medvick, P., Lewis, P.S., Aine, C.J. & Flynn, E.R. (1990) Monte Carlo analysis of localization errors in magnetoencephalography. In S.J. Williamson, M. Hoke M. Kotani & G. Stroink (eds) *Advances in Biomagnetism.* New York: Plenum Press: 543-546.

Meredith, J.T. & Celesia, G.G. (1982) Pattern reversal visual evoked potentials and retinal eccentricity. *Electroenceph. Clin. Neurophysiol.* 53: 243-253.

Merigan, W. (1991) P & M pathway specialisation in the macaque. In Valberg A., Lee B. B. (eds) *From pigments to perception.* New York: Plenum Press: pp 117-125.

Merigan, W.H., Byrne, C.E. & Maunsell, J.H.R. (1991) Does primate moton perception depend on the magnocellular pathway ? *J. Neurosci.* 11: 3422-3429.

Michael, C.R. (1987) Double opponent color cells in layer 4C project to the blobs and interblobs in monkey striate cortex. *Invest. Ophthalmol. Vis. Sci.* suppl 196.

Michael, W.F. & Halliday, A.M. (1971) Differences between the occipital distribution of the upper and lower field pattern-evoked responses in man. *Brain Res.* 32: 311-329.

Mishkin, M. (1982) A memory system in the monkey. *Phil. Trans. R. Soc. Lond. B.* 298: 85-95.

Mishkin, M., Ungerleider, L.G. & Macko, K.A. (1983) Object vision and spatial vision: Two cortical pathways. *Trends in Neurosci.* 6: 414-417.

Modena, I., Ricci, G.B., Barbanera, s., Leoni, R., Romani, G.L. & Carelli, P. (1982) Biomagnetic measurements of spontaneous brain activity in epileptic patients. *Electroenceph. Clin. Neurophysiol.* 54: 622-628.

Movshon, J.A., Adelson, E.H., Gizzi, M.A. & newsome, W.T. (1986) The analysis of moving visual patterns. In C. Chagas, R. Gattas and C. Gross (eds) *Pattern Recognition Mechanisms.* pp 117-151. N.Y. Springer-Verlag.

Mullen, K.T. (1985) The contrast sensitivity of human colour vision to red-green and blue-yellow chromatic gratings. J. *Physiol.* 359: 381-400.

Mullen, K.T. & Boulton, J.C. (1992) Absence of smooth motion perception in color vision. *Vision Res.* 32 (3): 483-488.

Mullen, K.T. & Kingdom, A.A. (1991) Colour contrast in form perception. In Gouras, P. (ed) *The Perception of Colour.* Macmillan

Murphy, G.M. (1985) Volumetric asymmetry in the human striate cortex. *Exp. Neurol.* 88: 288-302.

Murray I.J., Parry N.R.A., Carden D. & Kulikowski J.J. (1987) Human visual evoked potentials to chromatic and achromatic gratings. *Clinical Vision Science*; 1 (3): 231-244.

Myers, R.E. (1962) Commisural connections between occipital lobes of the monkey. *J. Comp. Neurol.* 118: 1-16.

Nagy A.L. & Doyal J.A. (1993) Red-green color discrimination as a function of stimulus field size in peripheral vision. *J. Opt. Soc. Am. A*; 10: 1147-1156.

Naka K.I. & Rushton W.A. (1966) S-potentials from colour units in the retina of fish (*Cyprinidae*). *J. Physiol.* 185: 587-599.

Nelson R. & Kolb H. (1983) Synaptic patterns and response properties of bipolar and ganglion cells in the cat retina. *Vision Res.* 23: 1183-1195.

Nesfield, C.J. (1992) *The effect of stimulus location on the major components of the visual evoked response*. PhD Thesis, Aston University.

Newsome, W.T., Gizzy, M.S. & Movshon, J.A. (1983) Spatial and temporal properties of neurones in macaque MT. *Invest Ophthalmol. Vis. Sci.* 24: 106.

Newsome, W.T., Wurtz, R.H. Dursteler, M.R. & Mikami, A. (1985a) Deficits in visual motion perception following ibotenic acid lesions of the middle temporal visual area of macaque monkey. *J. Neurosci.* 5: 825-840.

Newsome, W.T., Britten, K.H. & Movshon, J.A. (1989) Neuronal correlates of a perceptual decision. *Nature* 341: 52-54.

Nowak, L.G., Munk, M.H.J. & Bullier, J. (1995) Visual latencies in areas V1 and V2 of the macaque monkey. *Vis. Neurosci.* 12: 371-384.

Ogren, M.P. & Hendrickson, A.E. (1977) The distribution of pulvinar terminals in visual areas 17 and 18 of the monkey. *Brain Res.* 137: 343-350

Okada, Y. (1983a) Neurogenesis of evoked magnetic fields. In S.J. Williamson, G.L. Romani, L. Kaufman & I. Modena (eds) *Biomagnetism: An Interdisciplinary Approach.* pp399-408. NATO ASI series. New York: Plenum Press.

Opfer, J.E., Yeo, Y.K., Pierce, J.M. & Rorden, L.H. (1974) A superconducting second-derivative gradiometer. *IEEE Trans Mag.* MAG-9: 536-539.

Ossenblok, P. (1992) *The sources of the pattern VEP in man.* PhD Thesis.

Ossenblok, P. & Spekreijse, H. (1991) The extrastriate generators of the EP to checkerboard onset: A source localization approach. *Electroenceph. Clin. Neurophysiol.* 80: 181-193.

Pantev, C., Hoke, M., Lehnertz. K., Lütkenhöner, B., Angianakis, G. & Wittkowski, W. (1988) Tonotopic organisation of the human auditory cortex revealed by transient auditory evoked magnetic fields. *Electroenceph. Clin. Neurophysiol.* 69: 160-170.

Parker, D.M. & Salzen, E.A. (1977) The spatial sensitivity of early and late waves within the human visual evoked response. *Perception* 6: 85-95.

Parker, D.M. & Salzen, E.A. (1977) Latency changes in the visual evoked response to sinusoidal gratings. *Vision Res.* 17: 1201-1204.

Perry, V.H. & Cowey, A. (1984) Retinal ganglion cells that project to the superior colliculus and pretectum in the macaque monkey. *Neuroscience* 12: 1125-1137.

Perry, V.H., Oehler, R. & Cowey, A. (1984) Retinal ganglion cells that project to the dorsal lateral geniculate nucleus in the macaque monkey. *Neuroscience.*; 12 (4): 1101-1123.

Perry, V.H. & Cowey, A. (1985) The ganglion cell and cone distributions in the monkey retina: Implications for central magnification factors. *Vision Res.* 25: 1795-1810.

Perry, V.H. & Siveira, L.C.L. (1988) Functional lamination in the ganglion cell layer of the macaque's retina. *Neurosci.* 25: 217-224.

Peterson, S.E., Robinson, D.L. & Keys, W. (1985) Pulvinar nuclei of the behaving rhesus monkey: visual responses and their modulations. *J. Neurophysiol.* 54: 867-886.

Peterson. S.E., Robinson, D.L. & Morris, J. D. (1987) The contribution of the pulvinar to visual spatial attention. *Neuropsychologica* 25: 97-105.

Piechl, L. & Wässle, H. (1979) Size, scatter and coverage of ganglion cell receptive field centres in the cat retina. *J. Physiol.* 291: 117-141.

Pizella, V. & Romani, G.L. (1990) Principles of magnetoencephalography. In S. Sato (ed) *Advances in Neurology 54: Magnetoencephalography*. New York: Raven Press. pp 1-10.

Plant, G.T., Zimmern, R.L. & Durden, K. (1983) Transient visually evoked potentials to the pattern reversal and onset of sinusoidal gratings. *Electroenceph Clin. Neurophysiol.* 56: 147-158.

Polyak, S.L. (1941) *The Retina.* Chicago: University of Chicago Press.

Press, W.H., Teukolskly, S.A., Vettering, W.T. & Flannery, B.P. (1992) *Numerical Recipes in C.* Cambridge: Cambridge University Press.

Purpura, K., Kaplan, E. & Shapley, R.M. (1988) Background light and the contrst gain of primate P and M retinal ganglion cells. *Proc. Natn. Acad. Sci. USA.* 85: 4534-4537.

Rabin, J,. Switkes, E., Crognale, M., Scheck, M.E. & Adams, A.J. (1994) Visual evoked potentials in three-dimensional color space: correlates of spatio-chromatic processing. *Vision Res.* 34: 2657-2671.

Rafal, R.D. & Posner, M.I. (1987) Deficits in human spatial attention following thalamic lesions. *Proc. Natl. Acad. Sci. USA* 84: 7349-7353.

Ramachandran, V.S. (1987) Interaction between colour and motion in human vision. *Nature* 328: 645-647.

Ramachandran, V.S. & Gregory, R.L. (1978) Does colour provide an input to human motion perception? *Nature* 275: 55-56.

Regan, D. (1973) Evoked potentials specific to spatial patterns of luminance and colour. *Vision Res.* 13: 2381-2402.

Regan, D. (1989) *Human brain electrophysiology. Evoked potentials and evoked magnetic fields in science and medicine.* New York: Elsevier.

Regan, D. & Richards, W. (1971) Independence of evoked potentials and apparent size. *Vision Res.* 11: 679-684.

Regan, D. & Spekreijse, H. (1974) Evoked potential indications of colour blindness. *Vision Res.* 14:89-95.

Richer, F., Martinez, M., Cohen, H. & Saint-Hilaire, J.-M. (1991) Visual motion perception from stimulation of the human medial parieto-occipital cortex. *Exp. Brain Res.* 87: 649-652.

Robinson, D.L., McClurkin, J.W., Kertzman, C. & Peterson, S.E. (1991) Visual responses of pulvinar and collicular neurons during eye movements of awake, trained macaques. *J. Neurophysiol.* 66: 485-496.

Robinson, D.L. (1993) Functional contributions of the primate pulvinar. In T.P. Hicks, S. Molotchnikoff & T. Onon (eds) *Progress in Brain Research Vol. 95: The Visually Responsive Neuron. From Basic Neurophysiology to Behaviour.* Amsterdam: Elsevier. pp 371-380.

Robson, J.A. (1983) The morphology of corticofugal axons to the dorsal lateral genicualte nucleus in the cat. *J. Comp. Neurol.* 216: 89-103.

Rodieck, R.W. (1965) Quantitative analysis of cat retinal ganglion cell response to visual stimuli. *Vision Res.* 5: 583-601.

Rodieck, R.W. (1988) The primate retina. *Comparative Primate Biology* 4: *Neurosciences.* 203-278.

Rodieck, R.W. (1991) Which cells code for colour. In A. Valberg and B.B. Lee *From pigments to perception.* New York: Plenum Press. pp 83-93.

Rodieck, R.W. & Stone, J. (1965) Analysis of receptive fields of cat retinal ganglion cells. *Vision Res.* 5: 583-601.

Romani, G., Williamson, S. & Kaufman, L. (1982) Biomagnetic instrumentation. *Rev. Sci. Instrum.* 53, 12: 1815-1845.

Romani, G. & Pizella, V. (1990) Localization of brain activity with magnetoencephalography. In S. Sato (ed) *Advances in Neurology 54: Magnetoencephalography.* New York: Raven Press. pp 67-77.

Sakai, K, Watabe, E., Onodera, Y., Uchida, I, Kato, H., Yamamoto, E, Koizumi, H. & Miyashita, Y. (1995) Functional mapping of the human color centre with echo–planar magnetic resonance imaging. *Proc. R. Soc. Lond. B.* 261: 89–98.

Salin, P.A., Girard, P. & Bullier, J. (1993) Visuotopic organization of corticocortical connections in the visual system. In T.P. Hicks, S. Molotchnikoff & T. Onon (eds) *Progress in Brain Research Vol. 95: The Visually Responsive Neuron. From Basic Neurophysiology to Behaviour.* Amsterdam: Elsevier pp169-178.

Sarvas, J. (1987) Basic mathematical and electromagnetic concepts of the biomagnetic inverse problem. *Phys. Med. Biol.* 32: 11-22.

Schein, S.J., Marrocco, R.T. & DeMonasterio, F.M. (1982) Is there a high concentration of color-selective cells in area V4 of monkey visual cortex ? *J. Neurophysiol.* 47: 193-213.

Scherg, M. (1984) Spatio-temporal modelling of early auditory evoked potentials. *Rev. Laryngol.* 105: 163-170.

Scherg, M. & Berg, P. (1991) Use of prior knowledge in brain electromagnetic source analysis. *Brain Topog.* 4: 143-150.

Schiller, P.H. (1991) The color opponent and the broad band channels of visual system. In Valberg A., Lee B.B. (eds) *From pigments to perception.* New York: Plenum Press. pp 127-133.

Schiller, P.H., Finlay, B.L. & Volman, S.F. (1976) Quantitative studies of single cell properties in monkey striate cortex. I. Spatiotemporal organization of receptive fields. *J. Neurophysiol.* 39: 1288-1291.

Schiller, P.H. & Malpeli, J. (1978) Functional specificity of lateral genicualte nucleus laminae of the rhesus monkey. *J. Neurophysiol.* 41: 788-797.

Schiller, P.H., Sandell, J.H. & Maunsell, J.H.R. (1986) Functionsof the ON and OFF channels of the visual system. *Nature*; 322:824-825.

Shapley, R. & Perry, V.H. (1986) Cat and monkey retinal ganglion cells and their visual functional roles. *Trends in Neuroscience*; 9: 229-235.

Sherman, S.M. & Koch, C. (1986) The control of retinogeniculate transission in the mammalian lateral geniculate nucleus. *Exp. Brain Res.* 63:1-20.

Shipp, S. & Zeki, S. (1985) Segregation of pathways leading from area V2 to areas V4 and V5 of macaque monkey visual cortex. *Nature* 315: 322-325.

Spekreijse, H. (1991) Localization of the electromagnetic sources of the pattern onset response in man. In A. Valberg and B.B. Lee *From pigments to perception.* New York: Plenum Press. pp 211-223.

Spekreijse, H., Estévez, O. & van der Tweel, L.H. (1973) Luminance responses to pattern reversal. *Doc. Opthalmol. Proc. Ser.* 10: 205-211.

Spekreijse, H. Van Der Tweel, L.H. & Zuidema, T. (1973) Contrast evoked responses in man. *Vision Res.* 13: 1577-1601.

Spekreijse, H., Estévez, O. & Reits, D. (1977) Visual evoked potentials and the physiological analysis of visual processes in man. In J.E. Desmedt (ed) *Visual Evoked Potentials: New Developments.* Oxford: Clarendon Press.

Stefan, H, Schneider, S., Abraham-Fuchs, K., Baver, J, Feistel, H., Pawlik, G., Neubauer, U., Röhrlein, G. & Huk, W.J. (1990) Magnetic source localization in focal epilepsy. Multichannel meg correlated with MR brain imaging. *Brain* 113: 1347-1359.

Stensaas, S.S,. Donald, M.A., Eddington, R. & Dobelle, W.H. (1974) The topography and variability of the primary visual cortex in man. *Journal of Neurosurgery* 40:747-755.

Stoerig, P. & Cowey, A. (1993) Blinsight: neurons and behaviour. In T.P. Hicks, S. Molotchnikoff & T. Onon (eds) *Progress in Brain Research Vol. 95: The visually responsive neuron. From Basic Neurophysiology to Behaviour.* Amsterdam: Elsevier. pp 445-459.

Swadlow, H.A. (1983) Efferent systems of primary visual cortex: A review of structure and function. *Brain Res. Rev.* 6: 1-24.

Switkes, E., Tootell, R.B.H., Silverman, M.S. & DeValois, R.L. (1986) Picture processing techniquesapplied to autoradiographic studies of visual cortex. *J. Neurosci. Methods.* 15: 269-280.

Swinney, K.R. & Wikswo, J.P. (1980) A calculation of the magnetic field of a nerve action potential. *Biophys. J.* 32: 719-732.

Tanaka, K., Hikosaka, H., Saito, H., Yukie, Y., Fukada, Y. & Iwai, E. (1986) Analysis of local and wide-field movements in the superior temporal visual area of the macaque monkey. *J. Neurosci.* 6: 134-144.

Thorell, L.G., DeValois, R.L. & Albrecht, D.G. (1984) Spatial mapping of monkey V1 cells with pure color and luminance stimuli. *Vision Res.* 24: 751-769.

Tigges, J. & Tigges, M. (1985) Subcortical sources of direct projections to visual cortex. In A. Peters and E.G. Jones (eds) *Cerebral Cortex.* New York: Plenum Press. pp 351-378.

Tolhurst, D.J. & Ling, L. (1988) Magnification factors and the organization of the human striate cortex. *Hum. Neurobiol.* 6: 247-254.

Tootell, R.B.H., Silverman, M.S. & DeValois, R.L. (1981) Spatial frequency columns in primary visual cortex. *Science* 214: 813-815.

Tootell, R.B.H., Silverman, R.S., DeValois, R. L. & Jacobs, G.H. (1983) Functional organization of the second cortical visual area of primates. *Science* 220: 737-739.

Tootell, R.B.H., Hamilton, S.L. & Silverman, M.S. (1985) Topography of cytochrome oxidase activity of the owl monkey cortex. *J. Neurosci.* 8: 1594-1609.

Tootell, R.B.H., Silverman, R.S., Hamilton, S.L., DeValois, R. L., Switkes, E. & DeValois, R.L. (1988a) Functional anatomy of macaque striate cortex. I. Ocular dominance, binocular interaction and baseline conditions. *J. Neurosci.* 8:

Tootell, R.B.H., Silverman, R.S., Hamilton, S.L., DeValois, R. L. & Switkes, E. (1988c) Functional anatomy of macaque striate cortex. III. Color. *J. Neurosci.* 8: 1569-1593.

Tootell, Hamilton, S.L., Switkes, E. & DeValois, R. L. (1988d) Functional anatomy of macaque striate cortex. V. Contrast and magno-parvo streams. *J. Neurosci.* 8: 1594-1609.

Tootell, R.B.H., Silverman, R.S., Hamilton, S.L., Switkes, E. & DeValois, R. L. (1988e) Functional anatomy of macaque striate cortex. V. Spatial Frequency. *J. Neurosci.* 8: 1610-1624.

T'so D.Y. & Gilbert C.D. (1988) The organization of chromatic and spatial interactions in the primate visual cortex. *J. Neurosci.* 8: 1712-1727.

Ueno, S. & Iramina, K. (1990) Models and source localization of MEG activites. *Brain Topog.* 3: 151-165.

Ungerleider, L.G. & Mishkin, M. (1979) The striate projection zone in the superior temporal sulcus of macaca mulatta: Location and topographic organization. *J. Comp. Neurol.* 188: 347-366.

Ungerleider, L.G., Galkin, T.W. & Mishkin, M. (1983) Visuotopic organization of projections from striate cortex to inferior and lateral pulvinar in rhesus monkey. *J. Comp. Neurol.* 217: 137-157.

Van der Tweel, L.H., Estévez, O. & Cavonius, C.R. (1979) Invariance of the contrst evoked potential with changes in retinal illuminance. *Vis. Res.* 19: 1283-1287.

Van Essen, D.C. (1985) Functional organisation of primate visual cortex. In A. Peters & E.G. Jones (eds) *Cerebral Cortex vol 3*. New York: Plenum Press. pp 259-330.

Van Essen, D.C., Newsome, W.T. & Maunsell, J.H.R. (1984) The visual representaion in striate cortex of macaque monkey: Asymmetries, anisotropies and individual variability. *Vision Res.* 24: 429-448.

Van Essen, D.C. & Zeki, S.M. (1978) The topographic organization of rhesus monkey prestriate cortex. *J. Physiol.* 277: 193-226.

Van Essen, D.C., Felleman, D.J., DeYoe, E.A. & Knierim, J. (1991) Probing the primate visual cortex: pathways and perspectives. In A. Valberg and B.B. Lee *From pigments to perception*. New York: Plenum Press. pp 227-239.

Verrey, L. (1888) Hemiachromatopsie droite absolue. *Archs. Ophthalmol. (Paris)* 8: 281-301.

Von der Haydt, R, Peterhans, E. & Baumgartner, G. (1984) Illusory contours and cortical neuron responses. *Science* 224: 1260-1262.

Vvedensky, V., Hari, R., Ilmoniemi, R. & Reinikainen, K. (1985) Physical basis of the generation of neuromagnetic fields. *Biophysics*. 30: 154-158.

Wässle H., Piechl L. & Boycott B.B. (1983) A spatial analysis of on and off ganglion cells in the cat retina. *Vision Res.* 23: 1151-1160.

Wiesel, T.N. & Hubel, D.H. (1966) Spatial and chromatic interactions in the lateral geniculate body of the rhesus monkey. *J. Neurophysiol.* 29: 1115.

Williamson, S.J., Lü, Z.L., Karron, D. & Kaufman, L. (1991) *Brain Topography* 4; 2: 169-179.

Wong-Riley M.T.T., Hevner R.F., Cutlan M.E., Egan R., Frost J., Nguyen T. (1993) Cytochrome oxidase in the human visual cortex: Distribution in the developing and adult brain. *Visual Neuroscience* 10: 41-58.

Yamamoto, T., Williamson, S.J., Kaurman, L., Nicholson, C. & Llinas, R. (1988) Localization of neuronal activity in the human brain. *Proc. Natl. Acad. Sci. USA* 85: 8732-8736.

Zeki S.M. (1969) Representation of central visual fields in prestriate cortex of monkey. *Brain Research* 14: 271-291.

Zeki, S.M. (1974) Functional organization of a visual area in the posterior bank of the superior temporal sulcus of the rhesus monkey. *J. Physiol.* 236: 549-473.

Zeki, S.M. (1977) Colour coding in the superior temporal sulcus of rhesus monkey visual cortex. *Proc. R. Soc. Lond. B.* 197: 195-223.

Zeki, S.M. (1978a) Uniformity and diversity of structure and function of rhesus monkey prestriate visual cortex. *J. Physiol.* 277: 273-290.

Zeki, S.M. (1978b) Functional specialisation in the visual cortex of the rhesus monkey. Nature 274: 423-428.

Zeki, S.M. (1980a) The response properties of cells in the middle temporal area (area MT) of owl monkey visual cortex. *Proc. R. Soc. Lond.* (B), 207: 239-248.

Zeki, S.M. (1983a) Colour coding in the cerebral cortex: The reaction of cells in monkey visual cortex to wavelengths and colours. *Neurosci.* 9:741-765.

Zeki, S.M. (1983b) Colour coding in the cerebral cortex: The responses of wavelength selective and colour-coded cells in monkey visual cortex to changes in wavelength composition. *Neurosci.* 9:767-781.

Zeki, S.M. (1983c) The distribution of wavelength and orientation selective cells in different areas of monkey visual cortex. *Proc. R. Soc. Lond. B.* 217: 449-470.

Zeki, S.M. (1990) Parallelism and functional specialization in human visual cortex. *Cold Spring Harbour on Quantitative Biology, Volume LV.* Cold Spring Harbour: Laboratory Press.

Zeki, S.M. (1993) *A Vision of the Brain.* Oxford: Blackwell Scientific Publications.

Zeki, S., Watson, J.D.G., Lueck, C.J., Friston, K.J., Kennard, C. & Trackowiak, R.S.J. (1991) A direct demonstration of functional specialisation in human visual cortex. *J. Neurosci.* 11: 641-649.

Zeki, S. & Shipp, S. (1988) The functional logic of cortical connections. *Nature* 355: 313-317.

Zihl, J., Von Cramon, D. & Mai, N. (1983) Selective disturbance of movement vision after bilateral brain damage. *Brain* 106: 313-340.

Zimmerman, J.E., Thiene, P. & Harding, J.T. (1970) Design and operation of stable rf-biased superconducting point-contact quantum devices, and a note on the properties of perfectly clean metal contacts. *J. Appl. Phys.* 41: 1572-1580.

Zrenner E. (1983b) *Neurophsysiological aspects of color vision in primates.* Berlin: Springer-Verlag.

Zrenner E., Abaramov I., Akita M., Cowey A., Livingstone M. & Valberg A. (1990) Color perception retina to cortex. In L. Spillman and J. Werne (eds) *Visual Perception: The Neurophysiological Foundations.* San Diego: Academic Press. pp